

**PALEOMAGNETISM OF MIOCENE SEDIMENTARY ROCKS  
IN THE TRANSVERSE RANGES:  
THE IMPLICATIONS FOR TECTONIC HISTORY**

*Thesis by*

**Wei Liu**

**In Partial Fulfillment of the Requirements**

*for the Degree of*

**Doctor of Philosophy**

**California Institute of Technology**

**Pasadena, California**

**1990**

**(Submitted February 26, 1990)**

© 1990

Wei Liu

All rights Reserved



## ACKNOWLEDGEMENTS

I would like to thank Joe Kirschvink and Ray Weldon for their guidance, suggestions, support and understanding. I am indebted to them, especially to Joe Kirschvink, for their time, effort and patience in critically reading this thesis. Mike Woodburne also considerately and critically reviewed my thesis; his helpful and important comments and suggestions are greatly appreciated. I also thank Bob Reynolds for his productive collaboration and suggestions. All of their efforts have made this thesis a better production.

I also extend my great appreciation to Kerry Sieh. Without his encouragement and support at the beginning, it would have been impossible for me to start my study at Caltech. Kerry Sieh also acted as my academic advisor and provided me with very helpful guidance, acknowledgement and support.

I thank Leon Silver, Clarence Allen, and Hiroo Kanamori, both for reviewing this thesis and serving on the examination committee and for advice and guidance while I have been at Caltech. Leon Silver and Clarence Allen also provided inexhaustible sources of knowledge and valuable discussions on the tectonics and geology of southern California.

In addition to these individuals, I appreciate the discussions, ideas, and suggestions from Robin Chang, Rob Ripperdan, Marcus Bursik, Carol Prentice, Steve Salyards, Sally McGill and Janet Boley. Rob Ripperdan and Marcus Bursik also helped me revise some of my manuscripts. Many other students have contributed to my study by helping collect samples; their efforts are appreciated.

Finally, I thank my family for all of their love and support. My parents, Zongxian

and Erfen Liu, were understanding and their love is appreciated. Most importantly, I want to acknowledge my wife Xuehua and my son Han for their help with sample collection, data measurement and illustration preparation. I thank them for their love, understanding, patience, and support.

In addition, I would like to emphasize particularly the efforts of several geologists, upon which my study relies heavily. Among them are Levi Noble's pioneering work (1926; 1954) in Cajon Pass area and Tom Dibblee's maps (1967). The map and detailed late Cenozoic stratigraphy of Mike Woodburne and Dave Golz (1972), and John Foster (1980) were crucial foundations upon which much of my work in Cajon Pass was built. Particularly, the most important base for this study was the magnificent work of Weldon (1986) in the Cajon Pass area. Weldon's (1986) results and geological maps were extensively used in this study, and questions raised from his study initially stimulated me to conduct this study. In addition, combined paleomagnetic work on the Crowder Formation of Ray Weldon and Doug Winston (Weldon et al., 1984; Winston, 1985; this thesis, chapter 2), and collaborative efforts by Ray Weldon and Joe Kirschvink on paleomagnetic work of the Cajon Formation (Liu et al., 1988; this thesis, chapter 2, submitted to JGR), and paleontology by Bob Reynolds at the San Bernardino County Museum all led to many of the insights in this dissertation.

## ABSTRACT

Reconstructions of the offset history of the San Andreas fault in southern California have relied mainly on the correlation of rocks and structures within the Central Transverse Ranges. Only a few Miocene basins exposed along the fault zone in this area are associated closely with the early activity of the San Andreas system. The age of these sedimentary rocks is therefore critical for constraining the early activity, and helping understand the history, of the San Andreas fault. This study refines the ages of three Miocene sedimentary rock units, the Cajon, Crowder, and type Punchbowl, and Mill Creek formations, along the San Andreas fault in the Central Transverse Ranges by paleomagnetic methods, in order to provide age constraints on structures and tectonic events in the area. In addition, these data can be used to determine the magnitude of net tectonic rotations that may have occurred in these rocks.

Magnetic polarity stratigraphies have been developed for the top three units of the Cajon Formation and for the entire Crowder Formation in the Cajon Valley. By matching the magnetic polarity stratigraphies with the standard magnetic polarity time scale, the ages of the Cajon and the Crowder formations are constrained to range from at least 17 Ma to 12.7 Ma and from 17 Ma to 9 Ma, respectively. Although deposition of these two formations began at nearly the same time (about 17 Ma), the youngest rocks preserved in each unit differ in age by nearly 4 million years. In conjunction with their distinct sedimentary features, source areas, and geographic extent, this indicates that they were deposited in different basins. Hence, the offset along the Squaw Peak fault that now separates the units was probably on the order of at least several tens of

kilometers.

Because unit 6 of the Cajon Formation (ca. 13 Ma) and unit 5 of the Crowder Formation (9.0 Ma) are the youngest units obviously truncated by the Cajon Valley and Squaw Peak faults, respectively, and the 4.2 Ma Phelan Peak Formation is not offset by these faults, these two faults were active sometime between 13 and 9 Ma, respectively and 4.2 Ma. As the San Gabriel and Liebre Mountain faults were also active during these intervals of time, our results are compatible with the theory that the Cajon Valley and the Squaw Peak faults are the offset extensions of the San Gabriel and Liebre Mountain faults, respectively. This further supports the proposal that the total offset along the modern San Andreas fault during Pliocene and Pleistocene time has been 150 - 160 kilometers.

A similar paleomagnetic stratigraphic study was conducted on the late Miocene Punchbowl Formation at the Devil's Punchbowl County Park of California. The magnetic polarity pattern obtained from the Punchbowl Formation can be matched unambiguously to the geomagnetic reversal time scale from chrons 5Ar to 4Br, which implies that the formation was deposited from about 12.5 to 8.5 Ma. Combined with our age constraints on the Cajon Formation, this demonstrates that the Cajon and Punchbowl formations were deposited during completely different periods of time. This confirms the interpretation of Woodburne and Golz (1972) that the two formations do not correlate. Hence, the distance between these two formations cannot be used to constrain the total offset along the San Andreas fault.

The age of the Punchbowl Formation also constrains the activity of the Fenner fault, which may be an old strand of the early San Andreas system. The Punchbowl Formation is the oldest unit that is not offset by the Fenner fault. Although the Paleocene San Francisquito Formation is the youngest unit offset by the fault at Devil's

Punchbowl, early Miocene rocks were offset by the San Francisquito and Clemens Well faults, which were suggested as offset portions of the Fenner fault (Powell, 1980). Hence, the Fenner fault was probably active between early Miocene time and 12.5 Ma. Timing of another strand of the early San Andreas system, the Punchbowl fault, is also constrained by our result. Based on the geologic data, the Punchbowl fault has had two episodes of activity, one immediately before the deposition of the Punchbowl Formation, another after its deposition. Therefore, our results constrain these two episodes to start at about 12.5 Ma and after 8.5 Ma, respectively.

Tectonic rotations determined by anomalies in the paleomagnetic declination of these formations are quite different. In Cajon Valley, the Cajon Formation shows clockwise rotations of up to  $26^\circ$ , whereas rotation in the Crowder Formation is much less (at most  $4^\circ$  clockwise). Rotations in the Cajon Formation were probably caused by differential thrusting along the Squaw Peak thrust system, complicated further by small contributions from drag on "tear" segment of the Squaw Peak and the San Andreas faults.

Abnormal counterclockwise rotations ( $27.5^\circ \pm 4.3^\circ$ ) were found in the Punchbowl Formation, which are compatible with those interpreted in the Mint Canyon Formation ( $13^\circ \pm 30^\circ$ ) 40 to 50 km to the west. This suggests that the entire San Gabriel block between the San Andreas and San Gabriel faults may have been rotated counterclockwise. The rotation probably occurred as the San Gabriel block moved adjacent to the preexisting bent segment of the San Andreas fault, aided by the Mojave Desert block acting as a "backstop." After correcting for this rotation, the Punchbowl and Fenner faults would be parallel to the San Andreas fault in this area. This supports the proposal that the Fenner and Punchbowl faults were strands of the early San Andreas system during Miocene time.

There is little or no rotation in the Mill Creek Formation, which was exposed in an elongated block between two (or three) strands of the San Andreas fault. As the Mill Creek block is a long sliver in, and parallel to the strike of, the fault zone, it is thus difficult to rotate.

Our results do not agree with the prediction that the entire Transverse Ranges have been rotated clockwise in Neogene time. They also suggest that the geometry of major faults along which rigid blocks move is critical for producing the rotation and for determining the sense of the rotation. If our interpretation is correct, it implies that the San Andreas fault has had its abnormal geometry since it formed, and that the fault itself and the San Bernardino Mountains have not been rotated since Miocene time.

TABLE OF CONTENTS

ACKNOWLEDGEMENTS ..... iii

ABSTRACT ..... v

TABLE OF CONTENTS ..... ix

LIST OF FIGURES ..... xiii

LIST OF TABLES ..... xv

**Chapter One: Introduction: Purpose and Organization ..... 1**

    Introduction ..... 2

    Purposes ..... 2

    Organization ..... 6

**Chapter Two: Paleomagnetism of Miocene Sedimentary Rocks in Cajon Pass  
Area, Southern California ..... 11**

    Abstract ..... 12

    Introduction ..... 13

|   |     |
|---|-----|
| Setting and Previous Work .....                   | 18  |
| Physical Stratigraphy .....                       | 26  |
| I. The Cajon Formation .....                      | 26  |
| II. The Crowder Formation .....                   | 29  |
| Magnetostratigraphy .....                         | 31  |
| Techniques .....                                  | 31  |
| I. Cajon Formation .....                          | 53  |
| Sampling Sections .....                           | 53  |
| Magnetic Mineralogy and Origin of Remanence ..... | 57  |
| Microfossil Age Constraints .....                 | 76  |
| Stratigraphic Correlation .....                   | 77  |
| Depositional Rate .....                           | 85  |
| Rotations .....                                   | 90  |
| II. Crowder Formation .....                       | 96  |
| Sampling .....                                    | 96  |
| Stability Tests .....                             | 97  |
| Stratigraphic Correlation .....                   | 102 |
| Sedimentation Rate .....                          | 105 |
| Rotation .....                                    | 110 |
| Discussion .....                                  | 113 |
| Conclusions .....                                 | 120 |
| Acknowledgments .....                             | 121 |
| References .....                                  | 121 |



|   |     |
|---|-----|
| <b>Chapter Three. Paleomagnetism of the Punchbowl Formation at Devil's<br/>Punchbowl, southern California</b> ..... | 127 |
| <b>Abstract</b> .....   | 128 |
| <b>Introduction</b> .....   | 129 |
| <b>Geological Setting</b> .....   | 131 |
| <b>The Punchbowl Formation</b> .....  | 135 |
| <b>Paleomagnetic Procedures</b> .....   | 140 |
| <b>Sampling</b> .....   | 140 |
| <b>Measurements</b> .....   | 141 |
| <b>Magnetic Mineralogy</b> .....  | 151 |
| <b>Test of Data Reliability</b> .....   | 151 |
| <b>Magnetic Polarity Stratigraphy</b> .....   | 161 |
| <b>Sedimentation Rate</b> .....   | 165 |
| <b>Rotation</b> .....   | 165 |
| <b>Discussion</b> .....   | 174 |
| <b>Summary and Conclusions</b> .....  | 181 |
| <b>Acknowledgements</b> .....   | 181 |
| <b>References</b> .....   | 182 |

|   |     |
|---|-----|
| <b>Chapter Four: Paleomagnetic Study of the Mill Creek Formation, Mill Creek,<br/>Southern California</b> ..... | 186 |
| <b>Introduction</b> .....   | 187 |
| <b>Geologic Background</b> .....  | 187 |
| <b>Paleomagnetic Procedures</b> .....   | 191 |
| <b>Implications</b> .....   | 204 |
| <b>Acknowledgements</b> .....   | 205 |
| <b>References</b> .....   | 205 |
| <br>  |     |
| <b>Chapter Five: Summary</b> .....  | 208 |
| <b>Introduction</b> .....   | 209 |
| <b>Magnetostratigraphy and Its Tectonic implications</b> .....  | 209 |
| <b>Tectonic rotations</b> .....   | 212 |
| <b>References</b> .....   | 215 |

## LIST OF FIGURES

**Chapter Two:**

|   |    |
|---|----|
| Figure 1. Geologic setting map of the Cajon Pass area . . . . .           | 14 |
| Figure 2. Simplified lithologic column diagram . . . . .                  | 19 |
| Figure 3. Typical demagnetization results of Cajon samples . . . . .      | 33 |
| Figure 4. Great circle or stable "end point" . . . . .                    | 37 |
| Figure 5. Typical demagnetization behavior of Cajon samples . . . . .     | 40 |
| Figure 6. Typical normal sample of the Crowder samples . . . . .          | 45 |
| Figure 7. Typical reversed sample of the Crowder samples . . . . .        | 47 |
| Figure 8. Comparison of different analysis methods . . . . .              | 50 |
| Figure 9. Geological map and the sampling locations . . . . .             | 54 |
| Figure 10. Thermal demagnetization curve . . . . .                        | 59 |
| Figure 11. Equal-area plots of each unit of the Cajon Formation . . . . . | 61 |
| Figure 12. Reversal test of unit 5 of the Cajon Formation . . . . .       | 70 |
| Figures 13 and 14. Fold tests of the Cajon Formation . . . . .            | 72 |
| Figure 15. Magnetostratigraphy of the upper Cajon Formation . . . . .     | 78 |
| Figure 16. Magnetostratigraphy of unit 3 . . . . .                        | 80 |
| Figure 17. Magnetostratigraphy of unit 5 . . . . .                        | 82 |
| Figure 18. Magnetostratigraphy of unit 6 . . . . .                        | 86 |
| Figure 19. Sedimentation rate curve of the Cajon Formation . . . . .      | 88 |
| Figure 20. Mean directions of different localities . . . . .              | 92 |
| Figure 21. Fold test of the Crowder Formation samples . . . . .           | 98 |

|   |     |
|---|-----|
| Figure 22. Reversal test of the Crowder Formation samples . . . . . | 100 |
| Figure 23. Magnetostratigraphy of the lower Crowder Formation       | 103 |
| Figure 24. Magnetostratigraphy of the Crowder Formation . . . . .   | 106 |
| Figure 25. Depositional rate variation with time . . . . .          | 108 |
| Figure 26. Mean direction of the Crowder Formation . . . . .        | 111 |
| Figure 27. Tectonic rotation model of the Cajon Pass area . . . . . | 118 |

### Chapter Three:

|   |     |
|---|-----|
| Figure 1. Geological map of the Devil's Punchbowl area . . . . .                  | 132 |
| Figure 2. Geological map and sampling localities . . . . .                        | 137 |
| Figure 3. Typical demagnetization paths -- the first type . . . . .               | 143 |
| Figure 4. Typical demagnetization paths of the second type . . . . .              | 147 |
| Figure 5. Typical demagnetization paths of the third type . . . . .               | 149 |
| Figure 6. Rock magnetism experiment plot . . . . .                                | 152 |
| Figure 7. Thermal demagnetization curves . . . . .                                | 154 |
| Figure 8. Fold test of the Punchbowl samples . . . . .                            | 157 |
| Figure 9. Plot of conglomerate test results . . . . .                             | 159 |
| Figure 10. Magnetostratigraphy of the Punchbowl Formation . . .                   | 162 |
| Figure 11. Mean of the Lower Punchbowl Formation . . . . .                        | 167 |
| Figure 12. Mean of the Upper Punchbowl Formation . . . . .                        | 169 |
| Figure 13. Mean of the Punchbowl Formation . . . . .                              | 171 |
| Figure 14. Magnetostratigraphy of the Punchbowl and Cajon<br>formations . . . . . | 175 |

**Chapter Four:**

Figure 1. Geological map of the Mill Creek area ..... 188

Figure 2. Typical demagnetization paths ..... 193

Figure 3. Typical demagnetization paths ..... 195

Figure 4. Typical demagnetization paths ..... 197

Figure 5. Fold test of the Mill Creek samples ..... 199

Figure 6. Mean direction of the Mill Creek Formation ..... 202

**LIST OF TABLES**

**Chapter Two:**

Table 1. Results from Fisher and VGP calculation ..... 44

Table 2. Results of fold test from the Cajon Formation ..... 75

Table 3. Results of Fisher and Bingham statistics ..... 91

Table 4. Mean directions of sections ..... 95

**Chapter Three:**

Table 1. Results of Fisher and Bingham statistics ..... 166

CHAPTER ONE

**INTRODUCTION:  
PURPOSE AND ORGANIZATION**

## Chapter 1

### Introduction

This thesis was undertaken to address two basic problems in the geology of the Transverse Ranges: The first is to refine the stratigraphic correlations and age constraints for late Cenozoic sedimentary rocks in the Transverse Ranges that were offset by faults of the San Andreas system; the second is to determine tectonic rotations that constrain models for deformation along the San Andreas fault zone. Both of these problems are important for understanding the structural evolution and tectonic history of the San Andreas fault and the Transverse Ranges. My contribution to the understanding of these problems involves the use of paleomagnetic methods.

### Purposes

Age control on Late Cenozoic sedimentary rocks offset by the San Andreas fault in the Transverse Ranges are important because they constrain the timing of tectonic events, including motion along faults of the San Andreas system. During the last several decades, late Cenozoic reconstructions of the San Andreas system have relied heavily on correlations of rocks and structures in the central and eastern Transverse Ranges (Hill and Dibblee, 1953; Crowell, 1962, 1982; Powell, 1981; Matti et al., 1985; Weldon, 1986; Meisling and Weldon, 1989). Although it is believed generally that the San Andreas fault in southern California formed between 4 and 5 (or at most 8) million years ago, and about 240 km offset has been accumulated since then (Crowell, 1981; Ehlig, 1981), this model is not consistent with the displacement history recorded by the

rocks of the central Transverse Ranges (Weldon et al., 1990).

This inconsistency has led to various speculations that a right-lateral deformation system predated the modern San Andreas fault in southern California, and that it is responsible for about 100 km of offset during Miocene time (Crowell, 1962; Powell, 1981; Weldon et al., 1990). In various scenarios for reconstruction of this "pre" San Andreas system, the age range of the Miocene sedimentary rocks is critical because it constrains the possible correlations of the offset units, as well as the timing of activity of individual faults in the system. However, the nonmarine, late Tertiary sedimentary rocks in the Transverse Ranges are very difficult to date because they lack marine fossils and commonly lack materials amenable to isotopic dating, and also because it is commonly difficult to find sufficient and usable fossils from these rocks even for roughly assessing their age. One of the possible and promising techniques for dating these sediments utilizes the polarity of natural remanent magnetism, which is often preserved in these sediments and is relatively easy to identify.

The Tertiary geomagnetic field is known to change polarity every few  $10^5$  years or so in a quasi-random fashion (Harland et al., 1982), and as the sequence of polarity zones (or chrons) has been preserved in the sea-floor magnetic stripes (Vine, 1966), the calibration of the reversal pattern provides a reference magnetic-polarity time scale (e.g., Harland et al., 1982) of great use for stratigraphic correlation. In magnetostratigraphic study, a measured pattern of rock magnetic polarity is thus matched with this reference magnetic-polarity time scale to determine the age of the rocks. On the average, the resolution of Tertiary magnetostratigraphic dating is generally on the order of  $10^5$  to  $10^6$  years. However, in order to provide a match to the reversal time scale, it is necessary to have some other independent age estimate of the age of the rocks, provided by another method such as paleontologic or radiometric dating. From this



start, it is often possible to make a unique match to the reversal sequence for an entire formation.

There are only a few Miocene sedimentary basins along the San Andreas fault in the central Transverse Ranges which record evidence of the early activity of the San Andreas system, including: the Ridge, Devil's Punchbowl, Cajon Valley, and Mill Creek basins. My work focused mainly on the "Punchbowl Formation" of Noble (1954), including both the type formation at Devil's Punchbowl and the "Cajon beds," called Cajon Formation in this thesis, in Cajon Valley. The two formations were thought to be the same terrestrial rock unit offset by the San Andreas fault (Noble, 1926, 1954). Woodburne and Golz (1972) indicated that the two formations are mainly of different ages and have no important lithologic similarities, thus they do not fit a close correlation. However, Woodburne and Golz (1972) also suggested that the two rock units were deposited in a large, continuous basin and close to where they are today, implying a small offset along the San Andreas fault. Although virtually no one believes this correlation today, it is still not clear whether or not whether the two units overlap in age with one another (Woodburne and Golz, 1972; Woodburne, 1975), which would be permissive of the proposal of Woodburne and Golz (1972). In this study I attempt to test these hypotheses by refining the age constraints for both of these sedimentary rock units.

Refining the age of the Mill Creek Formation by magnetostratigraphic study was one of my initial goals, although I found it later to be unsuitable for this kind of study. The Mill Creek formation, and the type Punchbowl Formation at Devil's Punchbowl, are the only two "pull-apart" basins completely within the San Andreas fault zone in the Transverse Ranges, deposition of which is associated closely with the early phase of the San Andreas system. Weldon et al. (1990) noticed that the similarity between the two

formations, and Weldon (personal communication, 1987, 1990) tentatively proposed that the two formations may have been deposited in the same basin. Hence, refining the ages for the type Punchbowl and Mill Creek formations is important for constraining the early phase of the San Andreas system and for testing Weldon's proposal.

Apart from the use of paleomagnetism to determine the age range of sedimentary rocks, the determination of rotation by paleomagnetic methods has provided useful tests of models concerning deformation at plate margins and in continental blocks. Many geoscientists have speculated on rotations of fault-bounded blocks (Garfunkel, 1974; Freund, 1974; Bird and Rosenstock, 1984). While rotations around a horizontal axis can be determined by measuring geological markers such as tilted beds and folds, rotation about a vertical axis is much more difficult to determine by geological and other geophysical methods. Paleomagnetic methods, however, can provide substantial estimates for the magnitude of such rotation. Large paleodeclination anomalies are found usually in regions of strike-slip faulting, and have led to the suggestion that lateral displacement is the principal mechanism for crustal rotation (Beck, 1976; Freund, 1974; Luyendyk et al., 1980, 1985; Garfunkel and Ron, 1985). Specifically, Luyendyk and others (1980, 1985) have predicted that the central and eastern Transverse Ranges of southern California have been rotated clockwise up to 90°, as have the western Transverse Ranges during the Neogene period. On the other hand, Garfunkel (1974) proposed that the Mojave Desert block and the San Andreas fault next to it have been rotated counterclockwise about 30°, producing the "big bend." Both models of Luyendyk et al. (1980, 1985) and that of Garfunkel (1974) imply rotation of the San Andreas fault and a decrease of its slip rate. Hence, measuring the magnitude of vertical-axis rotation in the central Transverse Ranges and the Mojave block is also important for understanding the history of the San Andreas system.

All three rock units included in my study are bounded by two or three lateral-slip and thrust faults and are in the central and eastern Transverse Ranges next to the Mojave Desert, which provide excellent geologic settings for the study of tectonic rotation. Also, these are basically the only exposures of Tertiary sediments in the central Transverse Ranges. Older rocks may be rotated by other events and younger Quaternary rocks may not have seen the total impact of San Andreas deformation. In addition to the rotation difference, the timing of the rotations is also different in different crustal blocks. One of my goals is thus to test those rotation models by placing constraints on the tectonic rotations that have occurred in these particular sites and also on the timing of the rotations.

### Organization

My thesis is organized into five chapters, which include this introduction, the studies of Cajon, Punchbowl, and Mill Creek formations in chapters 2, 3 and 4, respectively, and a final summary. Chapters 2 through 4 are presented here as individual papers that have separate abstracts, introductions, bibliographies, and multiple authors as appropriate.

In chapter 2 the magnetostratigraphies of the Cajon ("Cajon Facies" of Noble) and Crowder formations are presented as a multi-author paper with my main contribution being the work on the Cajon Formation. Unpublished studies of the Crowder formation are combined in this paper, which were conducted by Winston (1985) and Weldon (1984, published; 1986). By comparing these sediments of similar age, I also discuss their implications to the geologic structures and tectonic evolution of the Cajon Pass area. The different rotations between these two formations are

discussed in this chapter 2 which has been submitted recently to the Journal of Geophysical Research.

In chapter 3, the magnetic stratigraphy of the Punchbowl Formation at the type location in the Devil's Punchbowl was established in order to evaluate the correlations between it and the Cajon Formation in Cajon Pass. Abnormal counterclockwise rotations were found from the Punchbowl Formation, which provide a different view of the tectonic rotations that may have occurred in the Transverse Ranges. I also plan to submit chapter 3 to the Journal of Geophysical Research.

In chapter 4, I discuss the tectonic rotations found in the Mill Creek Formation, which lies between the north and south branches of the San Andreas fault east of city of San Bernardino. Because it is relatively short, chapter 4 is in preparation for Geophysical Research Letters.

Although most chapters in this dissertation are written as independent papers, development of interpretations and ideas in some chapters are more or less dependent on data and conclusions presented in other chapters. Chapter 5 is thus an overall summary, in which I discuss the geologic history of tectonic rotation found in these fault bounded blocks.

## REFERENCES

- Bird, P., and Rosenstock, R.W., 1984. Kinematics of present crust and mantle flow in southern California: Geological Society of America Bulletin, v. 95, p. 946 - 957.
- Beck, M.E. Jr., 1976. Discordant paleomagnetic pole positions as evidence of regional shear in the western Cordillera of North America, Am. J. Sci., v. 276, p. 694 -

712.

- Crowell, J.C., 1962. Displacement along the San Andreas fault, California: Geological Society of America Special Paper 71, 62 p.
- Crowell, J.C., 1981. An outline of the tectonic history of southeastern California: in Ernst, W.G., ed., the geotectonic development of California (Rubey Volume 1), Englewood Cliffs, New Jersey, Prentice-Hall, p. 583 - 600.
- Crowell, J.C., 1982. The tectonics of the Ridge Basin, southern California, in J.C. Crowell and M.H. Link, eds., Geologic history of Ridge Basin, southern California, Los Angeles, California, Society of Economic Paleontologists and Mineralogists, Pacific Section, p. 143 - 149.
- Ehlig, P.L., 1981. Origin and tectonic history of the basement terrane of the San Gabriel Mountains, central Transverse Ranges, in Ernst, W.G., ed., The geotectonic development of California (Rubey Volume 1), Prentice-Hall, New Jersey, p. 253 - 283.
- Freund, R., 1974. Kinematics of transform and transcurrent faults: Tectonophysics, v. 21, p. 93 - 134.
- Garfunkel, Z., 1974. Model for the late Cenozoic tectonic history of the Mojave Desert, California, and its relation to adjacent regions: Geological Society of America Bulletin, v. 85, p. 1931 -1944.
- Garfunkel, Z., and Ron, H., 1985. Block rotation and deformation by strike-slip faults 2. the properties of a type of microscopic discontinuous deformation: J. G. R., v. 90, p. 8589 - 8602.
- Harland, W.B., Cox, A.V., Llewellyn, P.G., Pickton, C.A.G., Smith, A.G, and Walters, R., 1982. A Geological Time Scale. Cambridge Univ. Press, London/New York.
- Hill, M.L., and Dibblee, T.W., Jr., 1953. San Andreas, Garlock, and Big Pine faults,

California - A study of the character, history, and tectonic significance of their displacement: Geological Society of America Bulletin, v. 64, p. 443 - 458.

Liu, W., Weldon, R.J., and Kirschvink, J.L., 1988. Paleomagnetism of sedimentary rocks from and near the DOSECC Cajon Pass well, southern California: Geophysical Research Letters, v. 15, p. 1065 - 1068.

Luyendyk, B.P., Kamerling, M.J., and Terres, R.R., 1980. Geometric models for Neogene crustal rotations in southern California. Geol. Soc. Amer. Bull., v. 91, p. 211-217.

Luyendyk, B.P., Kamerling, M.J., Terres R.R., and Hornafius, J.S., 1985. Simple shear of southern California during Neogene time suggested by paleomagnetic declinations. Jour. Geophys. Res., v.90, p. 12,454-12,466.

Matti, J.C., Morton, D.M., and Cox, B.F., 1985. Distribution and geological relations of fault systems in the vicinity of the central Transverse Ranges, southern California. U.S. Geol. Surv. Open File Report. 85-365, 37 p.

Meisling, K.E., and Weldon, R.J., 1989. Late Cenozoic tectonics of the northwestern San Bernardino Mountains, southern California: Geological Society of America Bulletin, v. 101, p. 106 - 128.

Noble, L.F., 1926. The San Andreas rift and some other active faults in the desert region of southeastern California. Carnegie Institute of Washington, Yearbook no. 25, p. 415-422.

Noble, L.F., 1954. Geology of the Valyermo Quadrangle and vicinity, California. U.S. Geological Survey Quadrangle Map Series, Washington D.C.

Powell, R. E, 1981. Geology of the crystalline basement complex, eastern Transverse Ranges, southern California: Constraints on regional tectonic interpretations: Ph. D. thesis, California Institute of Technology, Pasadena, California, 441 p.

- Vine, F.J., 1966. Spreading of the ocean floor: new evidence: *Science*, v. 154, 1405 - 1415.
- Weldon, R.J., II, 1984. Implications of the age and distribution of the late Cenozoic stratigraphy in Cajon Pass, southern California: in *San Andreas fault -- Cajon Pass to Wrightwood*, Hester, R.L. and Hallinger, D.E., eds., Pacific Sect., AAPG, Volume and Guidebook, 55, p. 9-15.
- Weldon, R. J., II, 1986. The late Cenozoic geology of Cajon Pass: Implications for tectonics and sedimentation along the San Andreas fault, Ph.D. thesis, California Institute of Technology, Pasadena, California. 400 p.
- Weldon, R.J., Meisling, K.E., and Alexander, J., 1990. A speculative history of the San Andreas fault system in the central Transverse Ranges: in Powell, R.E. and Weldon, R.J. eds., *Palinspastic reconstruction of the San Andreas fault zone*, Geological Society of America Special Paper (in press).
- Winston, D.S., 1985. Magnetic stratigraphy of the Crowder Formation, southern California, M.S. Thesis, University of Southern California, Los Angeles, California, 100 p.
- Woodburne, M.O. and Golz, D., 1972. Stratigraphy of the Punchbowl Formation, Cajon Valley, southern California. *University of California Publications in Geological Sciences*, Vol. 92, 73 p.
- Woodburne, M.O., 1975. Late Tertiary nonmarine rocks, Devil's Punchbowl and Cajon Valley, southern California: in Crowell, J.C., ed., *San Andreas fault in southern California*, California Division of Mines and Geology, special report 118, p. 187 - 196.

CHAPTER 2

**PALEOMAGNETISM OF MIOCENE SEDIMENTARY ROCKS;  
IMPLICATIONS FOR TECTONIC EVOLUTION  
OF THE CAJON PASS AREA, SOUTHERN CALIFORNIA**

by

W. Liu<sup>1</sup>, R.J. Weldon<sup>2</sup>, D.S. Winston<sup>3</sup>, J.L. Kirschvink<sup>1</sup>, and D.W. Burbank<sup>3</sup>

1 - California Institute of Technology

2 - University of Oregon

3 - University of Southern California



**Chapter 2****ABSTRACT**

Late Miocene sedimentary rocks in Cajon Valley provide a record of the tectonic evolution of the Transverse Ranges and the San Andreas fault. Magnetic-polarity stratigraphies have been developed for the top three units of the Cajon Formation and the entire Crowder Formation in the Cajon Valley of southern California in order to constrain the ages of these two formations and to help interpret the geological history of the Cajon Pass area. By matching the magnetic-polarity stratigraphies with the Magnetic Polarity Time Scale, the ages of the upper part of the Cajon and the Crowder formations are constrained to range from slightly younger than 17 Ma to 12.7 Ma and from 17 Ma to 9 Ma, respectively.

While deposition of the Crowder and the upper part of the Cajon formations began at nearly the same time (about 17 Ma), the youngest rocks preserved in each unit differ by nearly 4 million years. In conjunction with their distinctly different sedimentary features, source areas, and geographic extent, this indicates that they were deposited in different basins. Hence, the offset along the Squaw Peak fault that now separates the units was probably on the order of several tens of kilometers since 9.5 million years ago.

The Cajon Valley and the Squaw Peak faults have been suggested to be the offset extensions of the San Gabriel and Liebre Mountain faults, respectively. Because unit 6 of the Cajon Formation is the youngest unit obviously truncated by the Squaw Peak and Cajon Valley faults, and the 4.2 Ma old Phelan Peak Formation is not offset by these faults, these two faults were active sometime between 13 and 4.2 Ma. As the San Gabriel and Liebre Mountain faults were also active during this interval of time,

our results are compatible with the above theory.

Tectonic rotations determined by anomalies in the paleomagnetic declination of these two formations are quite different: the Cajon Formation showing variable clockwise rotations of up to 27°, whereas rotation in the Crowder is much less (clockwise about 4°). These observations further confirm that the two formations had distinct tectonic histories before they were brought together by the Squaw Peak fault. Although there may be some other possibilities considering the complexity of rotation, rotations in the Cajon Formation were probably caused by uneven compression of the thrusting along the Squaw Peak thrust system, further complicated by small contributions of drag on the "tear-apart" segment of the Squaw Peak and the San Andreas faults.

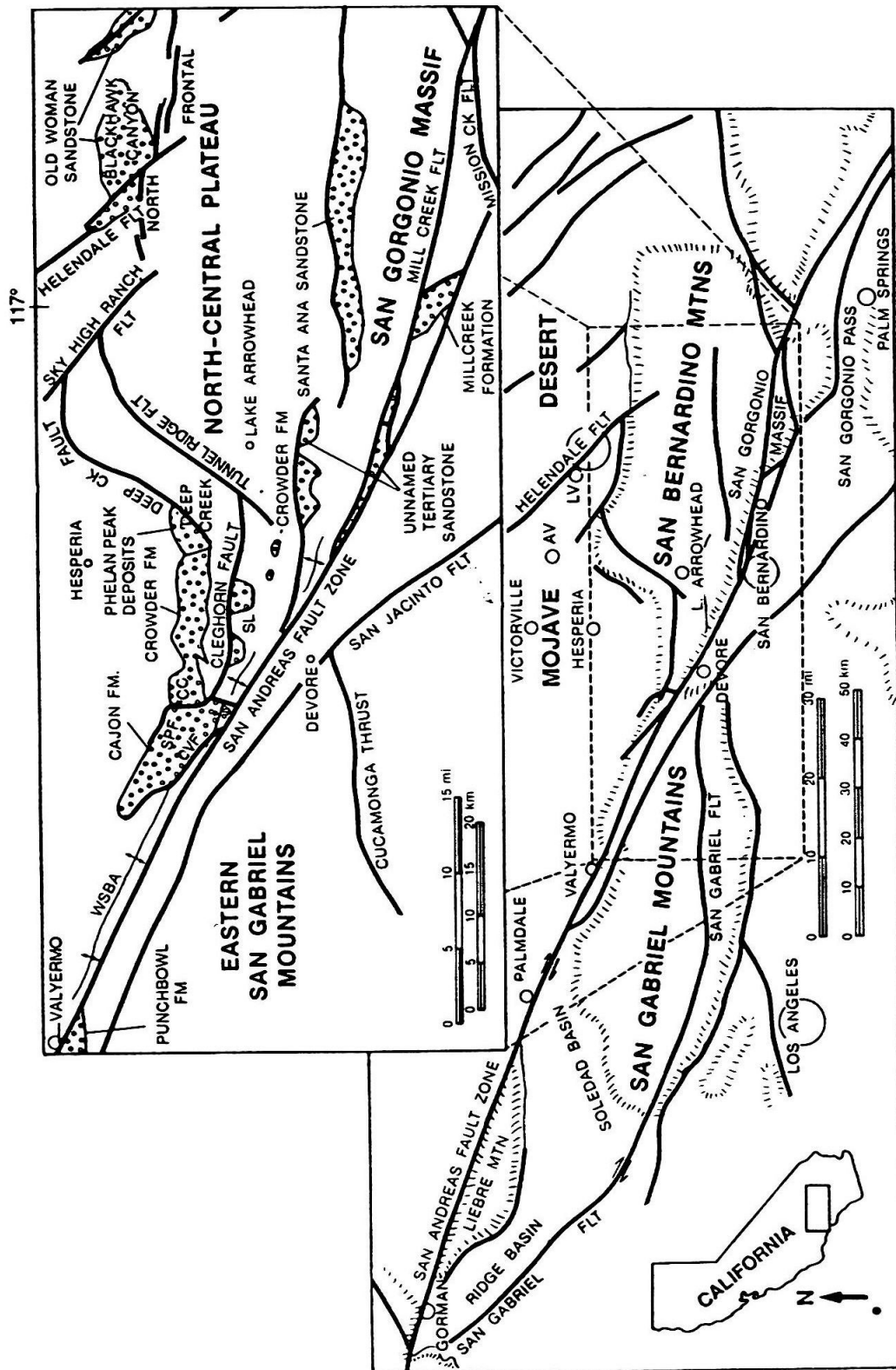
## INTRODUCTION

Cajon Pass, an area that connects the San Bernardino and the San Gabriel Mountains, is a tectonically active region in Southern California. The geologic history of the area has been influenced by the evolution of the central Transverse Ranges and by the development of the San Andreas fault. Two late Miocene sedimentary rock units, the Cajon and Crowder formations, crop out prominently in this area. Their position within the late Cenozoic stratigraphy of the Cajon Valley, and vicinity, is thus of special interest to geologists because they constrain the timing of major tectonic events and provide important clues to major structures in this area.

As early as 1926, Levi Noble proposed that the Cajon Formation (his "Cajon beds" of the Punchbowl Formation) was offset from similar rocks in the Devil's Punchbowl, about 35 km to the northwest, by the San Andreas fault (Figure 1). Woodburne and Golz (1972) demonstrated that the "Cajon beds" of the Punchbowl

**Figure 1. Geologic setting map of the Cajon Pass area.**

Modified from Meisling and Weldon (1989).



Formation differ from the type Punchbowl Formation in stratigraphic detail, provenance and likely, but not certainly, their age. On these bases, Woodburne and Golz (1972) suggested that the two formations did not fit a close correlation. Fossils from the base of the Punchbowl and middle part of the Cajon formations suggested that the Punchbowl was younger than the Cajon Formation. At that time, no fossils had been found from the top of the Cajon Formation whereas the bottom of the Punchbowl Formation was loosely constrained by insufficient fossils. It was not possible to determine whether or not the two formations had overlapping ages. Hence, Woodburne and Golz (1972) suggested that they were deposited in the same continuous depositional basin although probably at different times. For this reason, the name Punchbowl Formation is still used widely for these rocks, despite the recommendation of the USGS Geologic Names Committee that the formation in Cajon Valley be called the Cajon Formation.

The Crowder Formation is the only late Miocene sedimentary rock unit that overlies depositionally the eroded basement of the San Bernardino Mountains in Cajon Pass. Therefore, its age of onset marks the time that the area switched from erosion to deposition. Previously the age of the Crowder Formation was loosely constrained by its structural affinity with formations of known age (Meisling and Weldon, 1982). Foster (1980) interpreted the Crowder Formation (his "western facies") as unconformably overlying the Cajon Formation and unconformably overlain by the Harold Formation. At that time, the Cajon and Harold formations were thought to be Hemingfordian - Barstovian (Woodburne and Golz, 1972) and Rancholabrean age (Noble, 1954), respectively. Hence, the Crowder Formation was thought to be any age from Barstovian to Rancholabrean. Foster suggested that the Crowder was closer in age to the Harold Formation (2 - 4 Ma), because he recognized only minor structural differences

separating the Crowder and Harold formations whereas a significant angular unconformity separated the Crowder and Cajon formations. This is consistent with a fission-track age of less than 4 Ma in what was thought to be the eastern facies of the Crowder Formation near Silverwood Lake (Meisling and Weldon, 1982).

This Pliocene age became questionable when new mammalian fossil data suggested an early Miocene age for the Crowder Formation (Reynolds, 1983). Weldon (1984, 1986) realized that the type Crowder Formation was separated from the Cajon Formation by the Squaw Peak fault, and that the sediment overlying both the Cajon and Crowder formations is another distinct unit of early Pliocene age that he named the Phelan Peak Formation. Age of the upper part of the Crowder Formation was refined by magnetostratigraphic study of Weldon (1984) to be between 11.5 and 9.5 Ma. The Crowder Formation on the northeast side of the Squaw Peak fault is thus mostly the same age as the Cajon Formation (Weldon, 1986), which implies that the Squaw Peak fault must have had large movements to bring these two units together. This hypothesis could not be proven until the ages of the two units were better constrained. In this study, we develop magnetic polarity stratigraphies for the Crowder and Cajon formations, which, by correlation to the Geomagnetic Reversal Time Scale, can evaluate these questions.

In addition to the stratigraphic implications, the results of this magnetic study can be used to determine the magnitude of any tectonic rotation that may have occurred in these units. Based on the shape of the San Andreas fault through the Transverse Ranges and the geometry displayed by the frontal fault systems of the San Bernardino and San Gabriel Mountains, several geologists have proposed hypotheses suggesting that the entire Transverse Ranges province has been rotated counterclockwise about a central vertical axis (Garfunkel, 1974; Baird et al., 1974). Terres and

Luyendyk (1985) and Weldon and Humphreys (1986) proposed that only the San Gabriel Mountains have been rotated counterclockwise. Alternatively, Luyendyk et al. (1980, 1985) proposed a clockwise "block rotation" model of the entire Transverse Ranges based on their paleomagnetic studies mainly on the western Transverse Ranges. They predicted (Luyendyk et al., 1980, 1985) that the central and eastern Transverse Ranges may have also been rotated clockwise by about the same amount (up to 90°) as that of the western Transverse Ranges. However, paleomagnetic data in the central and eastern Transverse Ranges display far less rotation than was found in the western area where the hypothesis was formulated (Ensley and Verosub, 1982; Luyendyk et al., 1985; Terres and Luyendyk, 1985, Liu et al., 1988). More measurements of the tectonic rotations that have occurred in the Central Transverse Ranges are provided by this study, which can help our understanding of the origin and extent of the tectonic rotation in the Transverse Ranges.

## SETTING AND PREVIOUS WORK

Based on studies by Woodburne and Golz (1972), Foster (1980), Weldon (1986), and Meisling and Weldon (1989), rock units exposed in and adjacent to Cajon Valley include pre-Cenozoic basement crystalline rocks, the Paleocene and Eocene San Francisquito Formation (?), the lower Miocene Vaqueros Formation, the upper Miocene Cajon and Crowder formations, the Pliocene Phelan Peak Formation, the upper Pliocene and lower Pleistocene Harold Formation and Shoemaker Gravels, as well as older and younger alluviums (Figure 2). The pre-Cenozoic basement rocks and the Cajon Formation are the dominant units in and along the Cajon Valley. The Crowder Formation is exposed mainly in the northeastern part of Cajon Valley and

**Figure 2. Simplified lithologic column diagram of the Cajon and Crowder formations, and their relationships with other rock units in Cajon Pass area.**

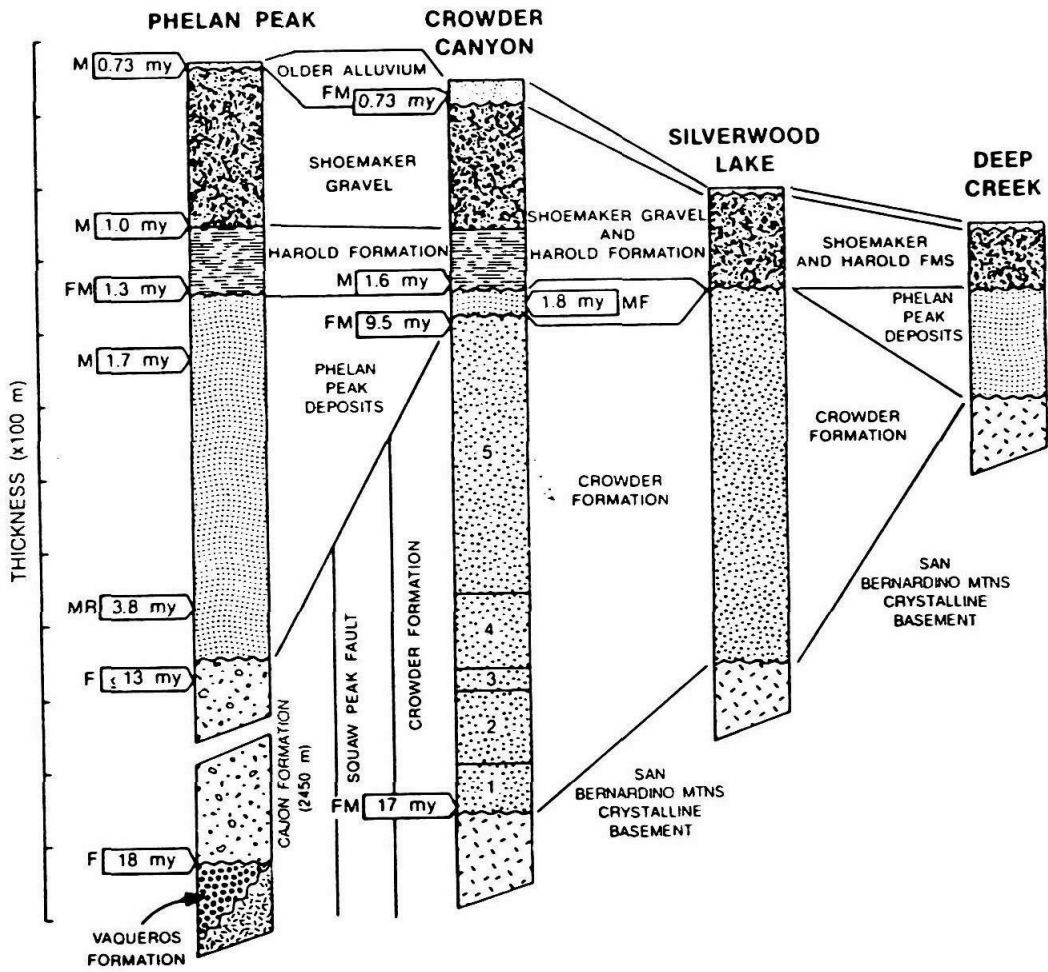
Modified from Meisling and Weldon (1989). See Figure 1 for locations of columns. Units in the Cajon Formation have not been shown, whereas numbered units in the Crowder Formation are from Foster (1980). Columns are composite, and thicknesses shown are maximum values. All units are highly variable in thickness.

F -- dated by vertebrate and microvertebrate fossils;

M -- dated by magnetostratigraphy;

R -- based on fission-track data on ash.





extends northeastward along the northern flank of the San Bernardino Mountains. Pleistocene deposits occur primarily along the northern and eastern boundaries of the valley. All these rock units have been described and summarized by Woodburne and Golz (1972), Foster (1980), Meisling and Weldon (1982,1989), and Weldon (1984, 1986). This paper therefore will focus only on the Cajon and Crowder formations.

Noble (1926) first mapped and described the stratigraphy of Cajon Valley. In 1954, he published a summary of his work in this region, including geological information from the vicinity of Cajon Pass. The name "Cajon Facies of the Punchbowl Formation" was given to what is now called the Cajon Formation (Noble, 1932, 1954) because of the general similarity in lithologies of these two formations. Noble (1926, 1954) suggested that the 36 kilometers between these two similar rock units may represent the offset of the San Andreas fault since late Miocene time. Although most geologists do not accept this correlation, the name Punchbowl Formation is still used for the rocks underlying Cajon Valley (Dibblee, 1967; Woodburne and Golz, 1972; Foster, 1982).

Additional geological information in the northwest-trending Cajon Valley was provided by other geologists, including Yerkes (1951), Swinehart (1965), Tamura (1961), and Dibblee (1967). These studies are important to the understanding of the geologic history of the area. Particularly, the stratigraphy of Cajon Valley was described in greater detail by Dibblee (1967), and he also named the Crowder Formation.

Woodburne and Golz (1972) revised the stratigraphy of Cajon Valley, specifically that of the Cajon Formation. They divided it into seven stratigraphic units, two of them (units 4 and 5a) are probably lateral equivalents. Mammalian fauna were collected by them and were used to constrain the age of the Cajon and also the Punchbowl formations. Although the fossils were only collected from the middle part (units 2, 3,

and 5) of the formation and were not sufficient to determine the age of the entire formation, Woodburne and Golz (1972) suggested it to be between late Hemingfordian and Barstovian in age. Woodburne and Golz (1972) concluded in their study that the Punchbowl Formation at Devil's Punchbowl is younger than the sediments in Cajon Valley and that they do not correlate. Woodburne and Golz (1972) also suggested that both of these formations formed close to where they are today, which implies small lateral displacements on the San Andreas fault. Based on the fossils collected from the lower and middle portions of the Cajon Formation, Woodburne and Golz (1972) estimated the depositional age of the formation to be middle to late Miocene. However, no fossils were found in the upper portion of the Cajon Formation so its youngest age of deposition was unknown. Whether or not this portion of the Cajon Formation overlaps in age with the lower portion of the type Punchbowl Formation was therefore unresolved by their work.

Foster (1980) mapped in Cajon Valley and collected paleocurrent and mineralogical data from clasts in the Crowder Formation. He also divided the Crowder Formation into five lithostratigraphic units, and divided the upper Crowder Formation into western and eastern facies. Foster developed a model for the tectonic evolution of the Cajon Valley region from these data. More recently, Meisling and Weldon (1982, 1989) and Weldon (1984, 1986) studied and synthesized the important aspects of the late Cenozoic stratigraphy and structure in the northwestern San Bernardino Mountains and the Cajon Valley area. New age constraints provided by magnetostratigraphic studies were used by Weldon (1986) and Meisling and Weldon (1989) in conjunction with structure and other geologic data to divide the late Cenozoic strata in the Cajon Pass area into three tectonostratigraphic groups of Miocene, Pliocene, and Quaternary age. These three packages bracket two distinct episodes of uplift, in late Miocene to

earliest Pliocene and Quaternary time, which are related to movements on low-angle structures beneath the range (Meisling and Weldon, 1989).

Providing age constraints on the Crowder Formation was one of Meisling and Weldon's (1984) main goals because the formation appears to predate the uplift of the western San Bernardino Mountains and activity of the Squaw Peak fault. A Pliocene age for the Crowder Formation was suggested by Dibblee (1967) and later by Woodburne and Golz (1972). The age estimate was based mainly on the hypothesis that the Foster's western facies of the Crowder overlies the Cajon Formation, which was believed to be late Miocene in age (Woodburne and Golz 1972). Woodburne and Golz (1972) thus thought it impossible for the Crowder to be of middle to late Miocene age even though they had discovered middle to late Miocene fossils from the basal part. They concluded that the fossils were reworked. A tentative fission-track age of less than 4 Ma was obtained (Meisling and Weldon, 1982) from what was considered to be part of the eastern facies of the Crowder Formation. This facies is now designated as part of the Phelan Peak Formation (Weldon, 1984). Based on the structural affinity and the fission-track date, Foster (1982) concluded that the Crowder Formation was probably deposited between 1 and 4 m.y. ago. In 1983 and 1985, Reynolds again discovered middle Miocene fossils from the base of the Crowder Formation, suggesting that it was much older than was previously thought. Paleomagnetic data from the Crowder Formation also support this contention (Weldon, 1984, 1986; Winston, 1985). In addition, the sedimentary rocks overlying the Cajon and also the Crowder formations, the "western Crowder" of Foster (1980), are now mapped as a separate unit and have been named the Phelan Peak Formation based on magnetostratigraphic and fission track dating (Weldon, 1984, 1986). The Crowder Formation is therefore in fault contact, and is partially contemporaneous with, the Cajon Formation.

At least three major faults cut through the Cajon Valley area, including the San Andreas fault at the southwest end subparallel to the axis of the valley, the Cajon Valley fault at the west end, and the Squaw Peak fault at the north and east ends of the Cajon Valley. These faults bound the Cajon Formation and separate it from the Crowder Formation and basement rocks. Part of another late Cenozoic active fault, the Cleghorn fault, cuts the Squaw Peak fault and extends into the Cajon Valley.

The most active fault that cuts through the Cajon Pass area is the modern San Andreas fault. Although the relative displacements have been occurring between the North America and Pacific plate system during the past thirty million years, the modern San Andreas fault was probably not started until about 5 million years ago (Atwater, 1970; Crowell, 1981, Weldon, 1986). As it is much younger than the Cajon and Crowder formations, it will not be discussed further here.

The Squaw Peak Fault is a large, low-angle thrust fault in this area, separating the basement of the San Bernardino Mountains and the overlying Crowder Formation from the basement of unknown affinity and the overlying Cajon Formation (Weldon, 1986; Meisling and Weldon, 1989). A portion of this fault had been previously mapped by Foster (1980) as the Squaw Peak fault, which is the name given to the entire structure. Foster thought that the Squaw Peak fault was a minor normal fault, which dropped the lower Crowder against the Cajon Formation, and was overlain by the upper Crowder (the Phelan Peak Formation of Weldon, 1984, 1986). On the other hand, Weldon (1984, 1986) suggested that the Squaw Peak fault is a major structure, probably the offset extension of the Liebre Mountain fault, which would postdate both the Cajon and the Crowder formations and is overlain by the Phelan Peak Formation. Therefore, the active period of motion along the Squaw Peak fault is bracketed by the Phelan Peak Formation at the top, and the Cajon and/or Crowder formations at the bottom. If the

Cajon and Crowder formations were indeed deposited in different basins, the movements along the Squaw Peak fault can be roughly estimated based on the geometries and original sizes of depositional basins.

According to Weldon (1986), the main trace of the Squaw Peak fault generally trends northwesterly and dips at low angles to the east. North of Squaw Peak, the fault trends north, whereas further north it trends northwesterly, and separates the Crowder and Cajon formations. It is offset left-laterally by the Cleghorn fault, and continues southward separating the Cajon Formation from the San Bernardino Mountains basement. The north-trending segment is interpreted by Weldon (1986), Meisling and Weldon (1989), and Miller and Weldon (1989) as a high-angle tear fault in an otherwise northwest-southeast trending low-angle thrust system. This interpretation was questioned (Ehlig, 1988) because no surface exposure of the north-trending segment of the fault has been found.

Another fault, the Cajon Valley fault, separates the sedimentary rocks in Cajon Valley from the basement rocks. It was proposed to be a reverse fault that joins the San Andreas fault obliquely, dropping the Cajon Formation against the pre-Cenozoic basement rocks (Noble, 1932; Dibblee, 1967; Woodburne and Golz, 1972; Foster 1982). The offset of the Cajon Valley fault is not yet known. Woodburne and Golz (1972) suggested that unit 5a of the Cajon Formation is a clastic wedge and was derived from tectonic activity west of the Cajon Valley fault. Accordingly, the activity of the Cajon Valley fault would start after the deposition of unit 5a of the Cajon Formation. Based on Weldon's map (1986) and spatial relationships between unit 5a and the fault, however, the activity of the Cajon Valley fault more likely started after deposition of the Cajon Formation. In 1984 and 1986, Weldon proposed that the Cajon Valley fault is a right-lateral strike-slip fault and that it may have been an earlier strand of the San

Andreas system. Subsequently, Matti et al. (1985) proposed that it is an offset continuation of the San Gabriel fault. Again, the youngest rock unit cut by this fault is the Cajon Formation, and the oldest unit that it does not cut is the Phelan Peak Formation. So the ages of these units are critical for verifying these hypotheses.

The Cleghorn fault has been active mainly during Quaternary time. The fault was originally named by Noble (1932) for its exposures in Cleghorn Valley. It cuts the Squaw Peak fault near the center of Cajon Valley, and extends about 25 km through the Silverwood Lake area to the Tunnel Ridge fault west of Lake Arrowhead (Meisling and Weldon, 1989). Over most of its length the Cleghorn fault dips between vertical and  $85^\circ$  to the north. It cannot be traced west of the Squaw Peak fault, but may extend an unknown distance beneath the alluvium of Cajon Valley (Meisling and Weldon, 1989). Meisling and Weldon (1989) suggested that the cumulative left-lateral motion on the Cleghorn fault is between 3.5 and 4.0 km. Based on the offsets of terraces, they also suggested an average slip-rate for the Cleghorn fault of 2 to 3 mm/yr (Meisling, 1984; Meisling and Weldon, 1982, 1989).

## PHYSICAL STRATIGRAPHY

### I. The Cajon Formation

The stratigraphy and lithology of the Cajon Formation has been discussed in detail by Woodburne and Golz (1972). In this paper, we will concentrate only on the magnetostratigraphy of this formation, its tectonic rotation, and their implications for the tectonic evolution of the Cajon Valley area. Therefore, the following paragraphs provide a general summary of the lithologic characteristics of the formation mainly



based on Woodburne and Golz's study (1972). For a more detailed description of the Cajon units, and in particular stratigraphic position of the fossil locations, readers are directed to the appendix of Woodburne and Golz' paper (1972).

The Cajon Formation is described by Woodburne and Golz (1972) as an assemblage of non-marine, moderately to strongly deformed strata, which is extensively exposed in Cajon Valley between the Squaw Peak and the San Andreas faults (Figure 1). It is unconformably overlying the basement rocks and the Early Miocene Vaqueros Formation, and overlain by the Pliocene Phelan Peak Formation. The formation is about 2700 meters thick and mainly consists of arkosic conglomerate and conglomeratic sandstone in the lower portion, and fine-grained sand- and siltstone interbedded with conglomeratic sandstone in the upper portion. Based on cross-bedding, pebble imbrication, and lamination of granule layers in the formation, Woodburne and Golz (1972) suggested that the Cajon Formation was deposited by southwestward flowing streams in a basin with somewhat irregular original surface. The lower part of the formation (units 1, 2, and 3) is best characterized as a periodic, fluvial deposit, while the upper half (units 5 and 6) was mainly accumulated under relatively continuous, low energy depositional condition (Woodburne and Golz, 1972) as most of the fine-grained sediments in the upper part of the formation apparently were deposited in temporary lakes or ponds. The uniformity of lithology over a wide area and the long depositional duration of the Cajon Formation imply that it was deposited in a basin of considerable size.

Although the conglomerates and conglomeratic sandstones are predominant, fine-grained sandstone and siltstone interbeds can be found very often through the entire formation, particularly in the upper half of the formation. Based on the detailed lithological variations, this formation has been divided into seven units by Woodburne



and Golz (1972), named units 1 to 6 plus a lateral unit, unit 5a. Each of these has a distinctive feature, including the hogbacks of units 2 and 4, the weathered red beds of unit 3, the variegated beds of unit 5 and its lateral face of unit 5a, and the unusual volcanic and red sandstone clast suite of unit 6. These different features probably reflect basin-wide variations in sediment source and depositional environments through time.

The contacts between all the main units, except unit 4, of the Cajon Formation are all comfortable and gradational. There is no major unconformity within the formation except short disruptions of deposition indicated by abundant paleosols in units 3 and 6, and also in unit 2. Unit 4 is probably a lateral equivalent of unit 5, as is unit 5a, based on its stratigraphic relationship with unit 5 (Woodburne and Golz, 1972). Mammalian fossils were only found from units 2, 3, and 5, which range from late Hemingfordian to Barstovian in age (Woodburne and Golz, 1972). Microvertebrate fossils were found later (Reynolds, 1985) from units 5 and 6, which are all of Barstovian age. The ages and stratigraphic levels of these fossils are described in the following.

Woodburne and Golz (1972) collected a fossil from the uppermost part of unit 2, about 3.3 meters below the contact with unit 3 in central Cajon Valley. It is predominantly represented in late Hemingfordian faunas. Therefore, a late middle Miocene age was suggested for the upper part of unit 2.

Fossils of late Hemingfordian age were found from 80 meters above the base to within 17 meters of the top of unit 3 in the southern part of the Cajon Valley, west of Cajon Junction. Fossils of early Barstovian age were also collected from unit 3, about 270 meters above its base (Woodburne and Golz, 1972). Based on these fossils and their stratigraphic position, the boundary between the Hemingfordian and Barstovian biochrons is probably within unit 3 of the Cajon Formation.

Relatively abundant vertebrate fossils were recovered from unit 5, although most of them were not sufficient to determine the age of the unit (Woodburne and Golz, 1972). Fossils were collected from about 40 meters above the base, and also about 100 meters below the top and about 600 meters above its base. These fossils are of late Barstovian age. Considering their stratigraphic positions, Woodburne and Golz (1972) suggested unit 5 to be of "late, but not latest Barstovian" age. In 1984 and 1985, microvertebrate fossils of the Barstovian assemble age were also collected from unit 5 by Reynolds (1984, 1985).

No fossils had been found in unit 6 prior to 1985, except for a few gastropods in the middle part of the sequence east of Alray (Woodburne and Golz, 1972). In 1985, Reynolds reported a microvertebrate fossil, *Copemys tenuis*, which occurs in the Barstow Formation dated between 15 and 13.7 or more precisely, 13.4 Ma (MacFadden et al., 1990), from the bottom of unit 6 of the Cajon Formation. This suggests that the upper age of the formation was late early to middle Miocene (Reynolds, 1985; Weldon 1986).

## II. The Crowder Formation

The Crowder Formation was named first by Dibblee (1967), who described it as a sequence of fluvial sediment resting on the Cajon Formation and pre-Tertiary crystalline rock, and overlain conformably by older (Quaternary) alluvium. In the type area near Crowder Canyon, the formation is nearly 1,000 meters thick and consists of nonmarine arkosic sandstone and conglomerate, which are generally pinkish-gray in color and cemented by carbonate. Trough cross-stratification, channel scour, and paleosols suggest that the Crowder is mainly a fluvial unit. Based on imbrication of cobbles and crossbedding, the sediments were laid down by braided streams flowing

from northeast to southwest (Foster, 1980; Winston, 1985; Weldon, 1986). The Crowder Formation is exposed west of Lake Arrowhead as far as the edge of the San Bernardino plateau and the Tunnel Ridge lineament (Figure 1). The original geometry and extent of the Crowder Formation are not known, but lithologic similarity of remnants preserved throughout the western San Bernardino Mountains suggests that it was deposited in a large, continuous, homogeneous basin that was uplifted and largely removed by erosion.

The Crowder Formation has been divided into five units in Crowder Canyon (Foster, 1980). The thickest section of the formation lies just east of the Squaw Peak fault, which is of unknown displacement. The type section of Crowder in Crowder Canyon, 1 kilometer to the east of the Squaw Peak fault is 884 m thick.

There is no evidence of any unconformities within the Crowder Formation, and all contacts between units of the formation appear conformable. Hemingfordian and Barstovian fossils were collected by Reynolds (1985) from unit 1, approximately from the 86- through the 130-meter stratigraphic levels. An age of about 16 Ma has been assigned to this fossil locality. Hence, the upper unit 1 of the Crowder Formation must be about 16 million years in age.

Woodburne and Golz (1972) collected fossils from unit 2. However, these fossils were in inverse stratigraphical order, with Barstovian below Hemingfordian. Hence, they considered the Cajon Formation to be a source of Crowder sediment and the fossils to represent progressive erosion of Cajon sediments. This theory is not supported by either the paleocurrent data or the structural and temporal relationships, however, whereas a fluvial reworking of the deposit would be (Reynolds, 1985). The reversed order of fossil ages may be due to this reworking within the formation, overlap of fossil ages, or the sampling techniques used. Subsequent paleontology (Reynolds and Weldon, 1988)

shows no indication of significant stratigraphic inconsistency.

Fossils collected from the base of unit 4 (Reynolds, 1984) are representative of the middle Clarendonian land mammal age, implying ages of about 11 m.y. for the Crowder 3-4 boundary.

## MAGNETOSTRATIGRAPHY

### Techniques

As most sediments of the Cajon and Crowder formations are poorly- or unconsolidated, drilling is not suitable. Hence, we used a new impact-coring technique first described by Weldon (1986) to collect magnetic samples from the Cajon Formation and also from the upper part of the Crowder Formation. A nonmagnetic stainless-steel tube with a beveled edge and 2.5 cm inner diameter was pounded gently into the sediments. The orientation of the tube then was measured using standard techniques prior to removal from the outcrop. After removal, the end of the sample (sticking out of the tube) was smoothed and scratched with an orientation mark. The sample was then extruded into a quartz glass sample holder of the same diameter as the steel tube, and sealed with wax film to prevent loss of the moisture, which helps maintain the sample's integrity. The samples were cemented into their quartz tubes in a magnetically shielded environment with a solution of sodium silicate and processed like rock cores. In the test study, samples were collected both by the impact-coring technique and by hand carving of oriented samples and were measured by the same process. Comparisons of these two sets of samples demonstrated that the impact-coring technique did not cause any measurable realignment of the magnetic remanence. The results of this test

are included as the data for member 4 (see later section, Figure 23) of the Crowder Formation. The middle part of unit 5 in section MS - Ca (see later section, Figure 17) was also sampled by using both drilling and the impact-coring technique. These two sets of samples were all combined together in our analysis. Our results indicate again that there is no difference between these two sampling methods.

Two different strategies for sample collection in the field were used in this combined study, and these deserve detailed discussion and comparison herein. The first technique, used largely by the Caltech group, was developed during the last two decades for the high resolution study of sedimentary rocks. A more "standard" method that has been used mainly for study of volcanic rocks since it was developed in early 1950's is employed by the USC group.

The Caltech procedure is as follows. For the upper parts of the Cajon and Crowder formations, one sample was taken from closely-spaced stratigraphic horizons in order to obtain better coverage of magnetozone. Both alternating field and thermal demagnetization techniques were employed to isolate a characteristic component of remanence from each sample. Instead of blanket demagnetization, each of the samples was subjected to detailed demagnetization analysis. Most of the samples were progressively demagnetized in weak alternating magnetic fields (AF) of 2.5, 5.0, 7.5, and 10 mT to remove soft magnetic components. They were then subjected to stepwise thermal demagnetization from 100 °C up to 575 or 600 °C at 25, 50, and/or 100 °C intervals, and measured using a SQUID magnetometer controlled by a microcomputer. Progressive demagnetization plots (Figure 3) generally reveal characteristic components for each sample, and directions for the lines and planes of best least-squares fit were found using principle component analysis (Kirschvink, 1980). Only directions with maximum angular deviations of less than 10° were accepted. Almost all

**Figure 3. Typical results of alternating and thermal demagnetization of the Cajon Formation samples.**

LEFT -- orthogonal plots:

Solid circles are projected on a horizontal plane; Open circles are projected on a vertical plane;

The initial direction (NRM) were showing by the box symbols.

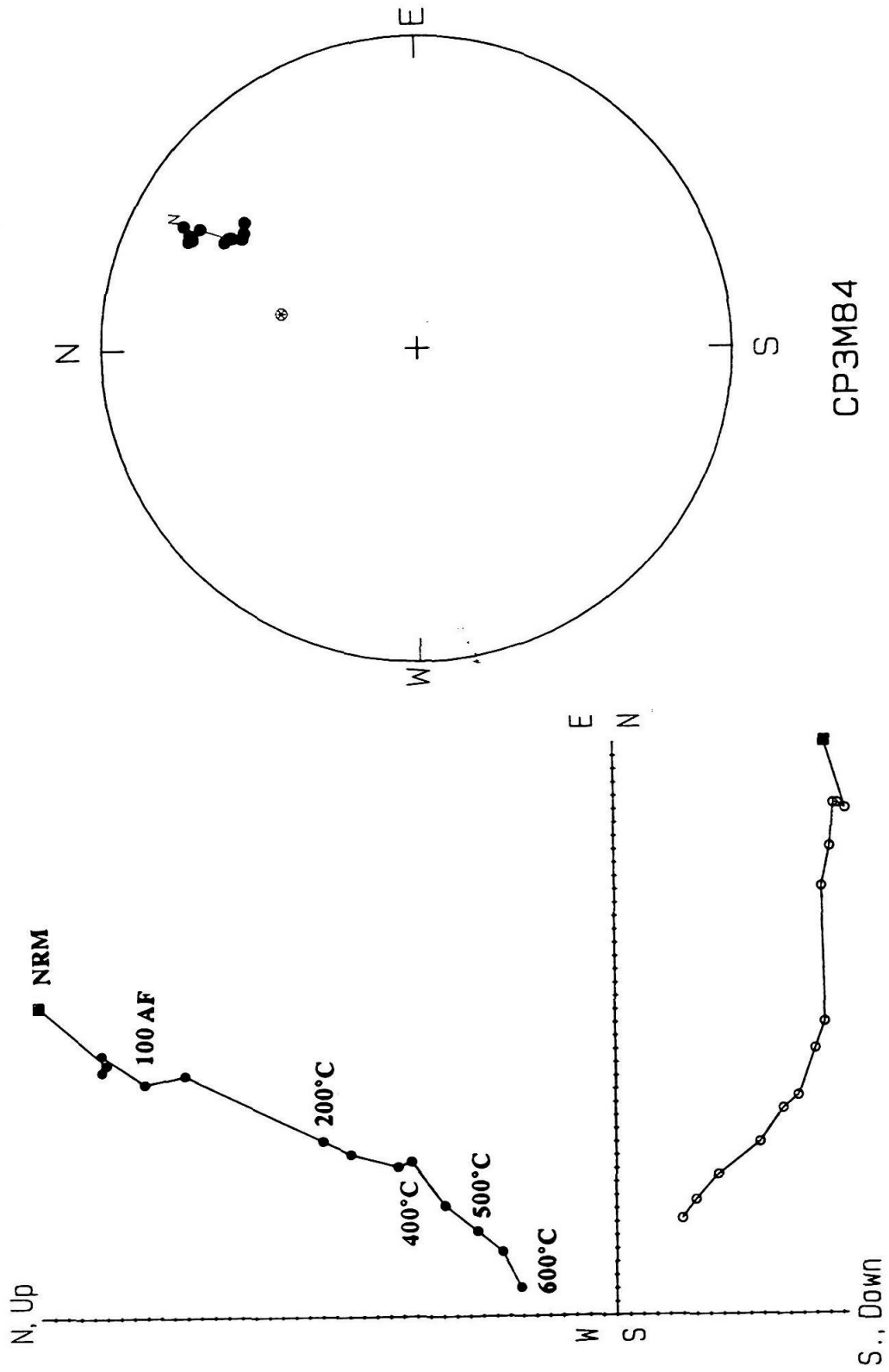
RIGHT -- equal-area stereographic projection:

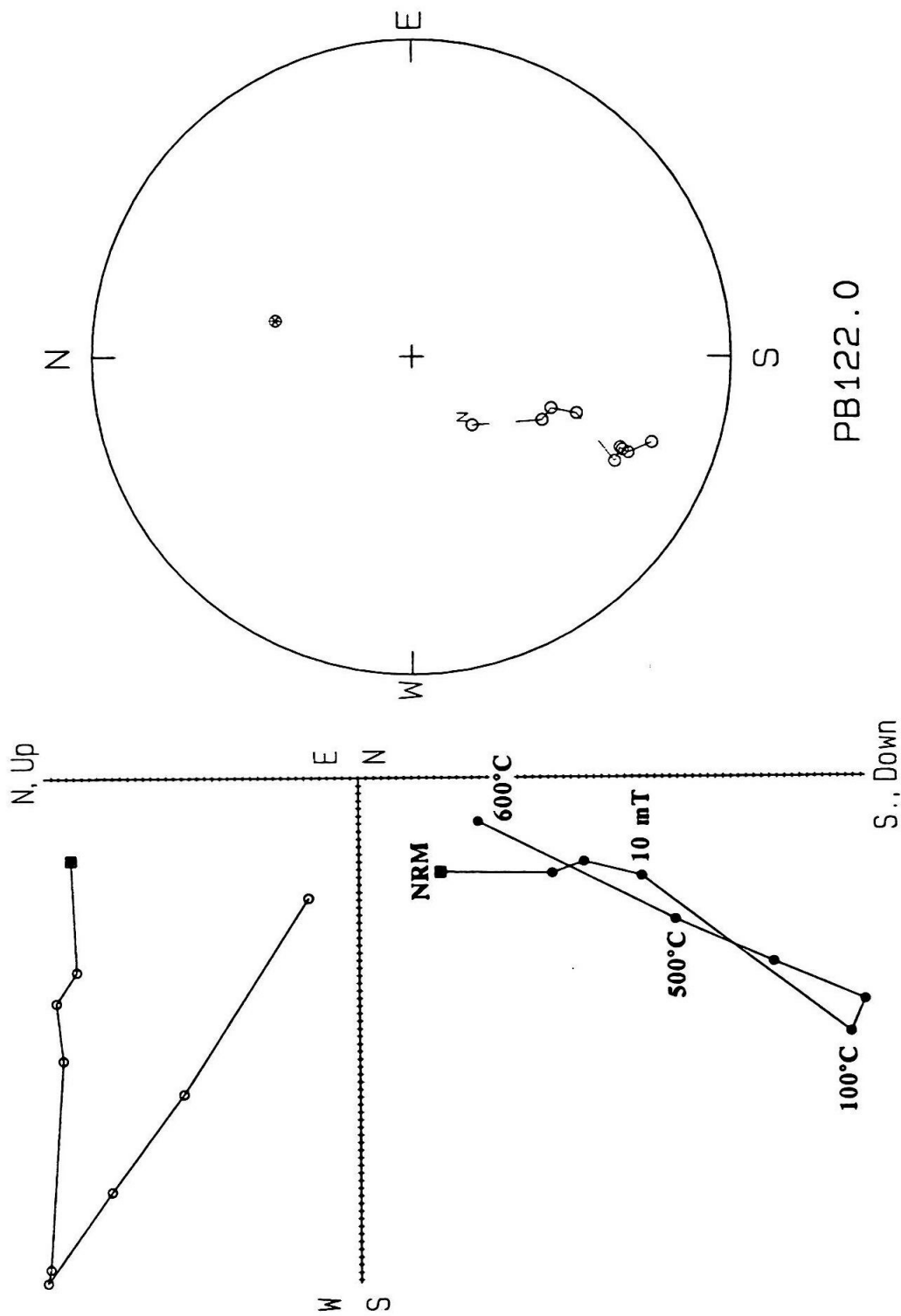
Open circles are the plots on the upper hemisphere, and solid circles are the plots on the lower hemisphere.

The NRM directions are marked by letter N next to the vector.

Circled star is the present geomagnetic field direction.

The Characteristic component of sample CP3M84 is of a normal polarity, whereas that of sample PB122.0 has a reversed polarity.







samples have an overprint of the present field direction that was often removed at low demagnetization steps (Figure 3). In some samples the overprint could not be completely removed, but their demagnetization paths typically produce great circles on a stereograph, which could be fitted to a plane (Figure 4). Thus, the polarity of a primary component of higher stability can usually be inferred from the trajectory of the path toward either normal or reversed directions.

The demagnetization paths for the high temperature steps exhibited linear trajectories towards the origin on orthogonal projections, which corresponds on a stereo net plot as a cluster of demagnetized directions (Figure 3 and 4b). Although the majority of the samples display either normal or reversed magnetic direction, some of the samples pass an indeterminate polarity (Figure 5). A few samples showed erratic demagnetization behavior, indicating a general magnetic instability. Others, however, followed great-circle trajectories (Figure 4), which could be used for magnetostratigraphy. Only the samples that were cleaned up to reveal a stable primary component were used for calculating mean directions of units for rotation studies.

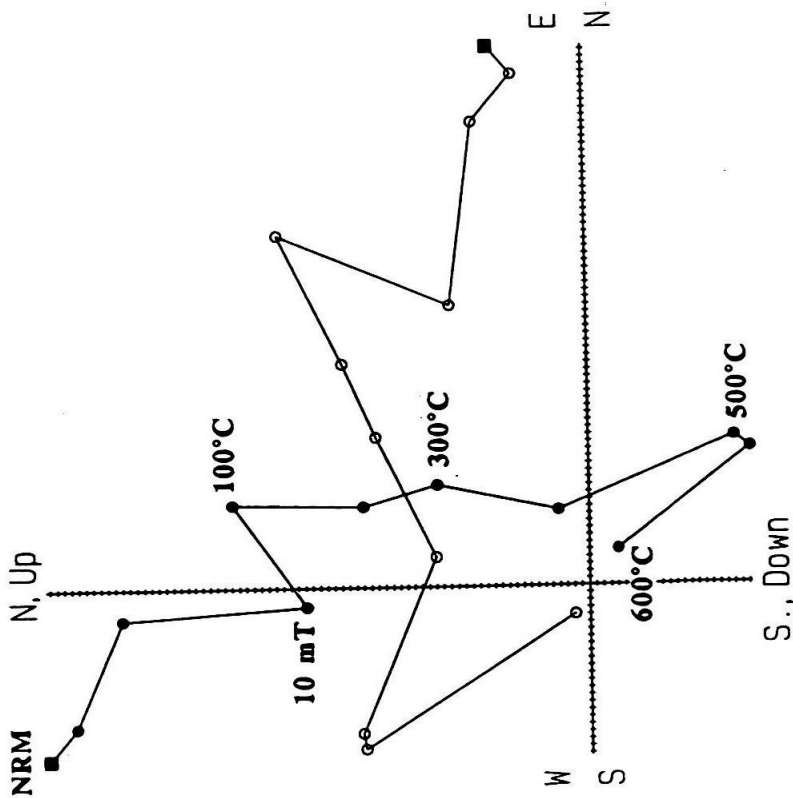
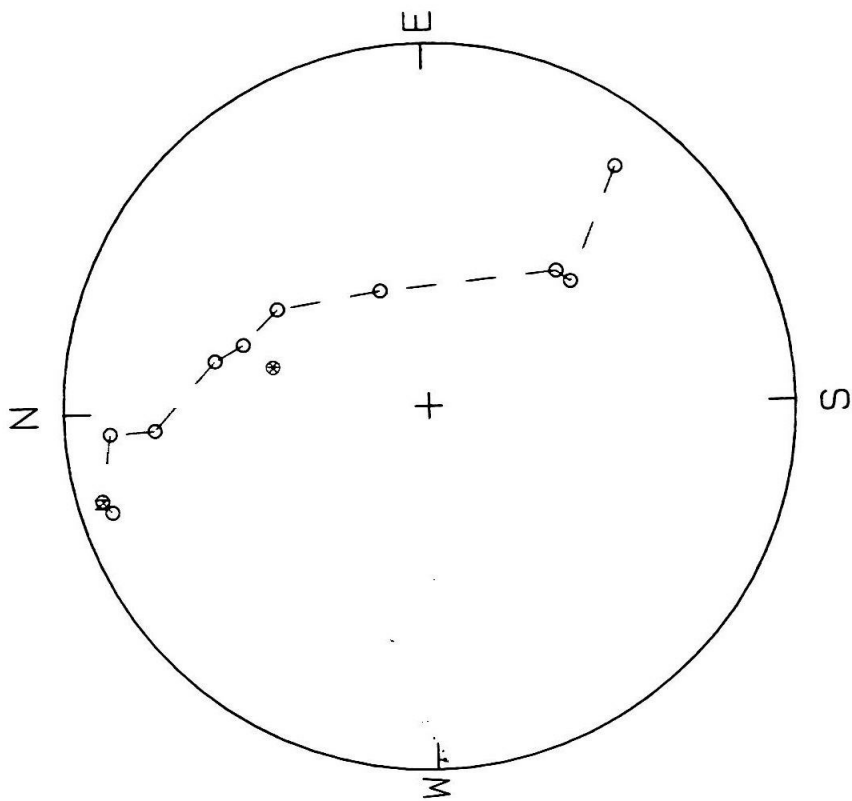
In another method that was used at USC for the lower part of the Crowder Formation (Winston, 1985), three samples were taken from each horizon with relatively large stratigraphic intervals. Representative samples were measured first to determine optimum temperatures useful in revealing the primary remnant magnetization. After measuring NRM (Natural Remanent Magnetization), they were heated to 200, 400, or 450, 500, 550, or 600 and in some cases, 650 °C with a magnetometer measurement subsequent to each step. Figures 6 and 7 illustrate some representative results obtained from these samples. Although secondary overprints are present in samples from the Crowder Formation, they are removed readily by thermal demagnetization. Most samples revealed whether they were of normal or reversed polarity without demagneti-

**Figure 4. Typical plots of the demagnetization path for the samples that fit a great circle or reach a stable "end point."**

Plotting conventions are the same as for Figure 3.

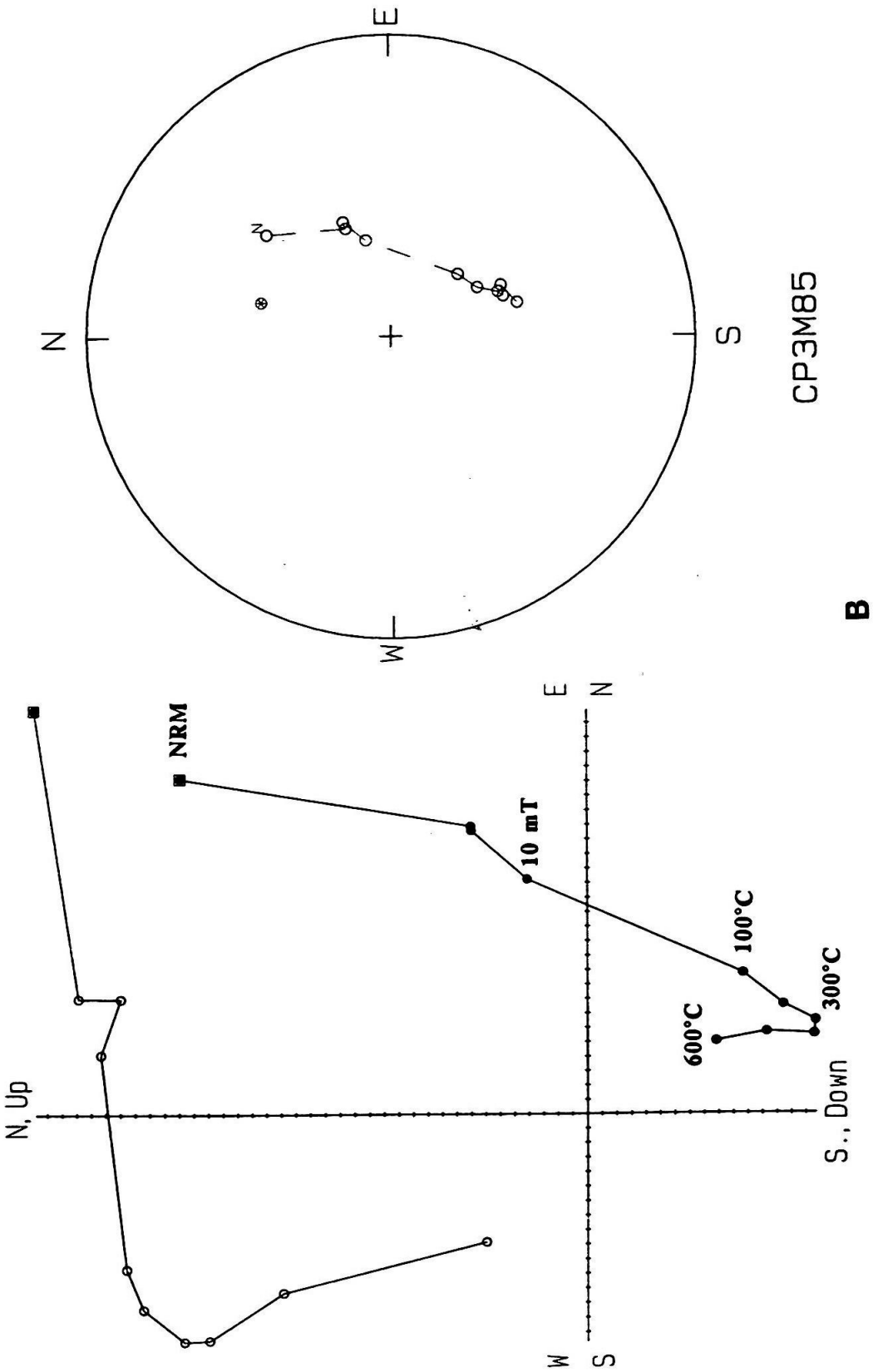
A -- sample for which demagnetization path fits with a great circle.

B -- sample reaches a stable "end point."



TP667.0

A



CP3M85

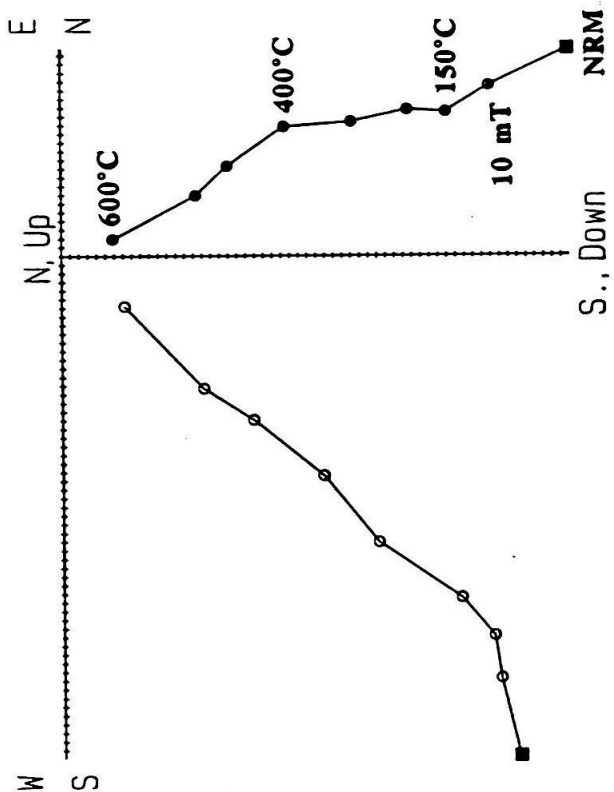
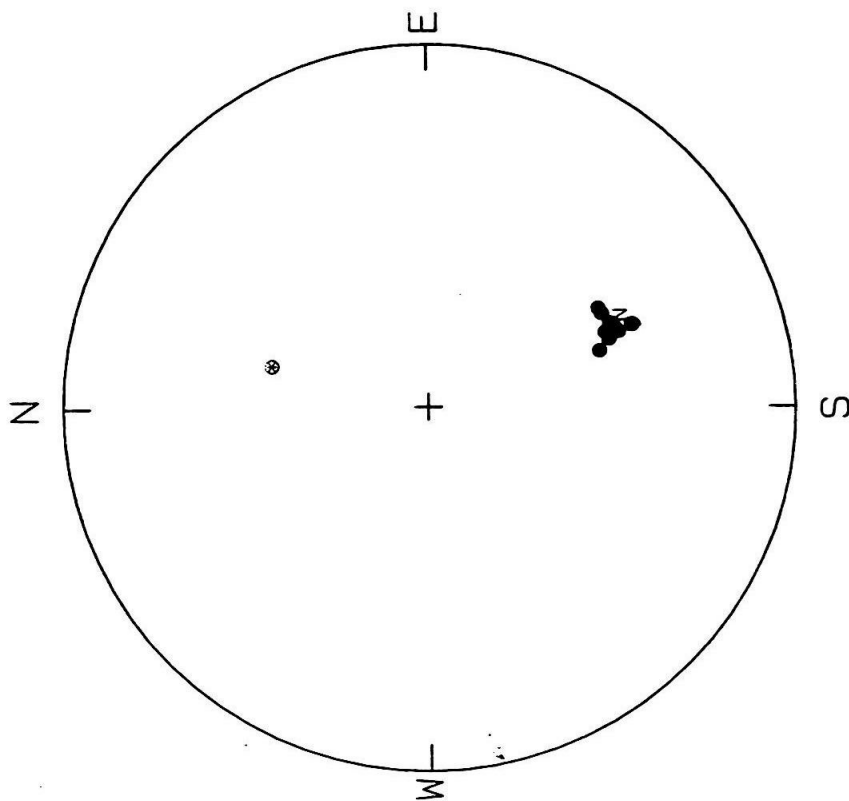
B

**Figure 5. Types of demagnetization behavior of the Cajon Formation samples.**

Plotting conventions are the same as for Figure 3.

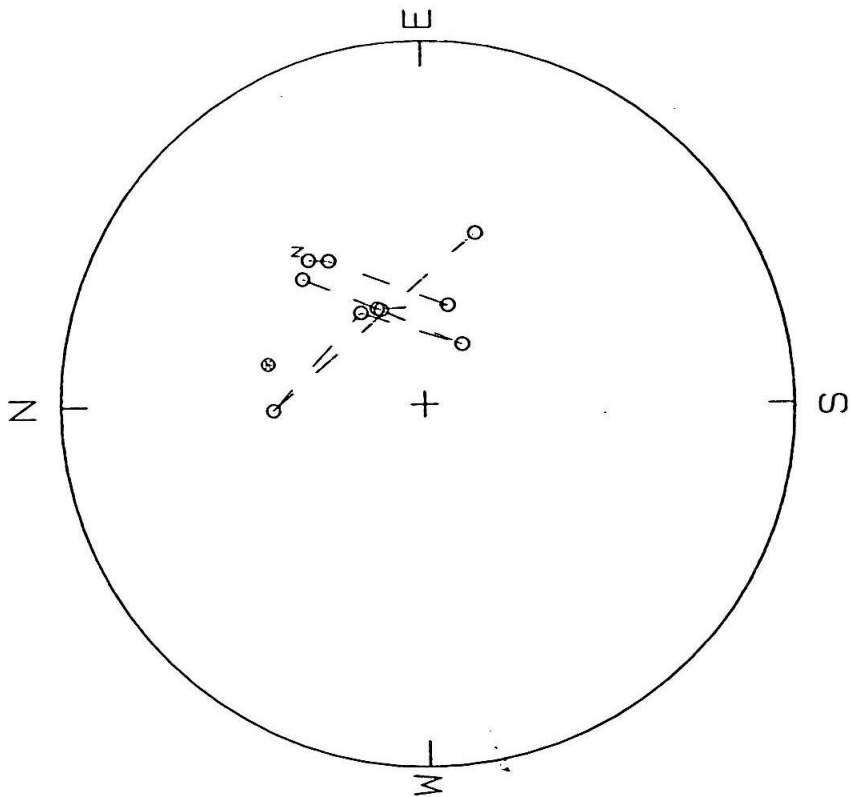
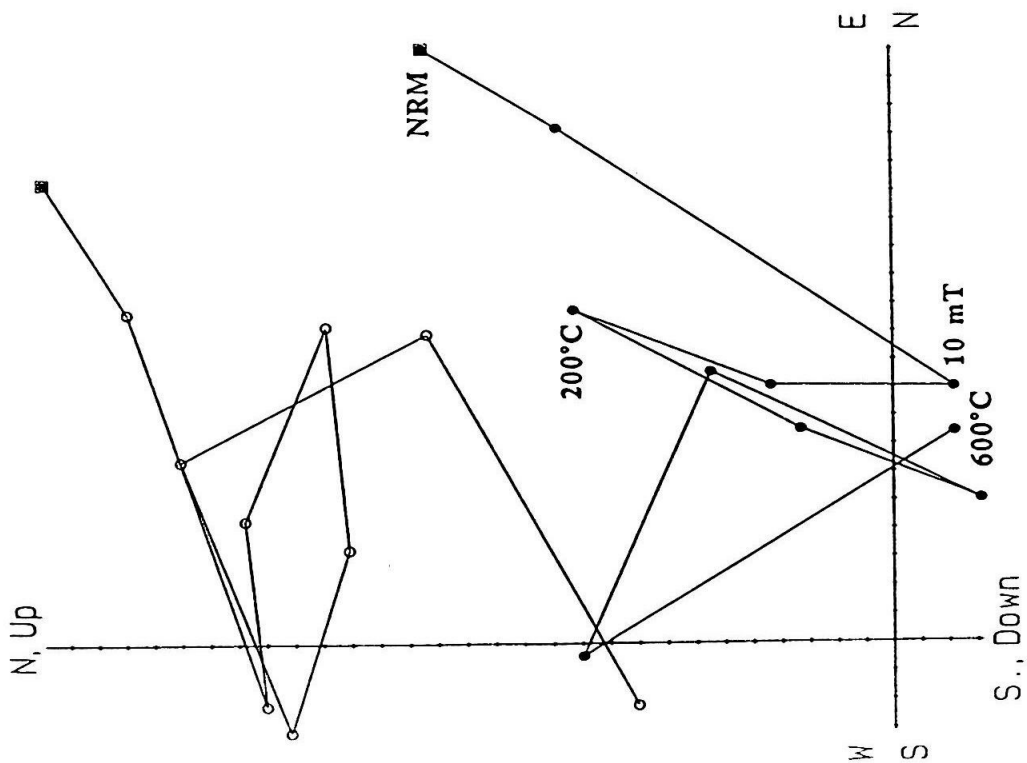
A -- Sample showing stable, linear demagnetization path corresponding to an indeterminable direction;

B -- Samples showing an unstable magnetization.



PB15.0

A



CP3M96

**B**

zation.

Subsequently, the remaining samples were subjected to "blanket" demagnetization at 450, 500, and 550 °C, and results from the 500 °C steps were used to represent the stable primary direction. In general, obvious overprinting had been removed by the 500 °C step and heating the samples to higher temperatures would only reduce the intensity of the remanence with minor changes in direction, implying a stable direction had been reached. Samples that did not behave in this manner, i.e., wild fluctuations in magnetic vector direction between thermal demagnetization steps, generally did not satisfy statistical requirements essential for their use in the study and were rejected.

The magnetic vectors at each site were averaged to determine the site mean, on the assumption that they represent one, instantaneous reading of the ancient field direction (an assumption rarely true in sediments). The inclination and declination of the site mean are then used to determine a virtual geomagnetic pole (VGP) position. The paleolatitude of the VGP of the site mean determines whether the site is of normal or reversed polarity. The three magnetic vectors were then analyzed using Fisher statistics (1953). If a site yields a precision value ( $k$ ) greater than 10, the data at this site is considered "Class I". If  $k$  value is less than 10, but two of the vectors are in close agreement, the data are "Class II", and the errant vector is not used in the VGP calculations. Data is termed "Class III" when there is little correlation between the three vectors. Class three are deemed unreliable and are not used to calculate VGP's. Table 1 summarizes the results of these statistical calculations. The site means were then used for developing magnetostratigraphy of the lower part of the Crowder Formation.



Table 1. Results for each site from Fisher and VGP calculations.

Class 2 sites used the 2 best samples for the calculations, hence, the high k values for these sites from the new calculations.

| Site<br>(meters) | Kappa  | $\alpha$ -95 | VGP<br>Latitude | VGP (East)<br>Longitude | Class |
|------------------|--------|--------------|-----------------|-------------------------|-------|
| 0                | 58.14  | 16.32        | 81.50           | 26.74                   | 1     |
| 7                | 46.12  | 18.36        | 73.39           | 14.67                   | 1     |
| 17               | 304.91 | 7.07         | 63.74           | 320.11                  | 1     |
| 27               | 18.89  | 29.20        | 67.64           | 11.12                   | 1     |
| 47               | 29.29  | 47.93        | -76.73          | 210.78                  | 2     |
| 55               | 84.26  | 13.52        | 69.24           | 354.66                  | 1     |
| 65               | 29.30  | 47.92        | 75.50           | 94.19                   | 2     |
| 72               | 370.85 | 6.41         | -72.36          | 241.39                  | 1     |
| 80               | 34.72  | 21.25        | -62.96          | 259.12                  | 1     |
| 86               | 33.16  | 21.76        | -66.39          | 209.25                  | 1     |
| 100              | 17.78  | 30.14        | -75.69          | 153.17                  | 1     |
| 109              | 12.95  | 76.29        | 56.64           | 1.95                    | 2     |
| 123              | 77.46  | 14.10        | 61.67           | 164.99                  | 1     |
| 131              | 47.92  | 36.90        | -75.27          | 158.63                  | 2     |
| 151              | 31.36  | 22.39        | 71.20           | 120.63                  | 1     |
| 161              | -      | -            | -               | -                       | 3     |
| 165              | 10.77  | 29.57        | 69.74           | 301.27                  | 1     |
| 170              | -      | -            | -               | -                       | 3     |
| 180              | 56.    | 16.53        | -73.04          | 166.52                  | 1     |
| 190              | 27.83  | 49.27        | -67.84          | 337.91                  | 2     |
| 199              | 9.89   | 90.70        | -71.34          | 47.51                   | 2     |
| 208              | 20.46  | 58.40        | -25.15          | 315.97                  | 2     |
| 219              | 17.50  | 30.40        | 80.78           | 131.24                  | 1     |
| 231              | 31.62  | 22.30        | -2.27           | 147.04                  | 1     |
| 241              | 51.30  | 35.61        | 44.98           | 16.63                   | 2     |
| 253              | -      | -            | -               | -                       | 3     |
| 268              | 31.56  | 22.32        | 77.37           | 184.17                  | 1     |
| 277              | 18.01  | 29.94        | 81.18           | 151.59                  | 1     |
| 283              | 293.45 | 7.21         | -78.57          | 108.63                  | 1     |
| 305              | 14.31  | 33.87        | 34.86           | 49.93                   | 1     |
| 313              | 13.40  | 35.09        | 48.50           | 333.07                  | 1     |
| 314              | -      | -            | -               | -                       | 3     |
| 322              | 108.58 | 11.89        | 74.69           | 20.53                   | 1     |

**Figure 6. Typical normal sample of the Crowder samples.**

Orthogonal and equal-area plots for a typical normal (CW 25.3) sample from the Lower Crowder Formation. Each circle represents a magnetic vector obtained after a demagnetization step. The plotting conventions are the same as for Figure 3. All directions are corrected for tilt of bedding. NRM is the initial sample vector.

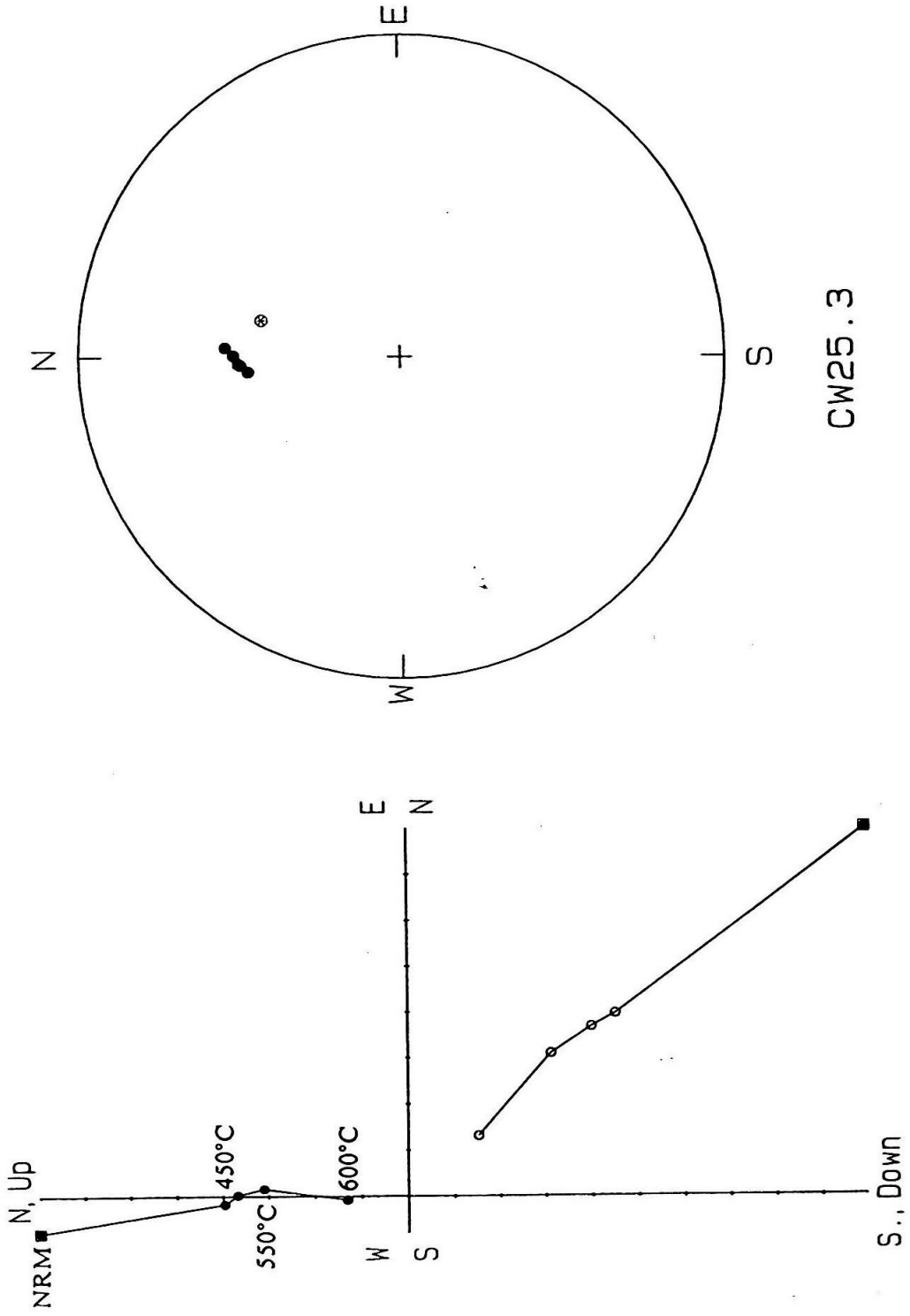
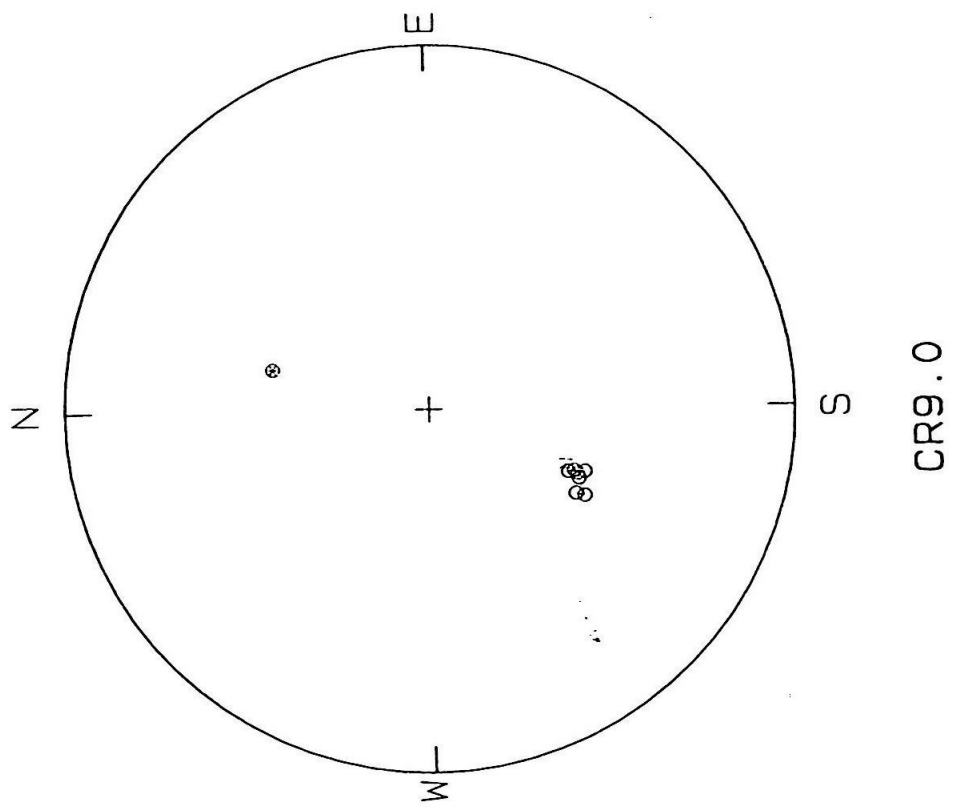
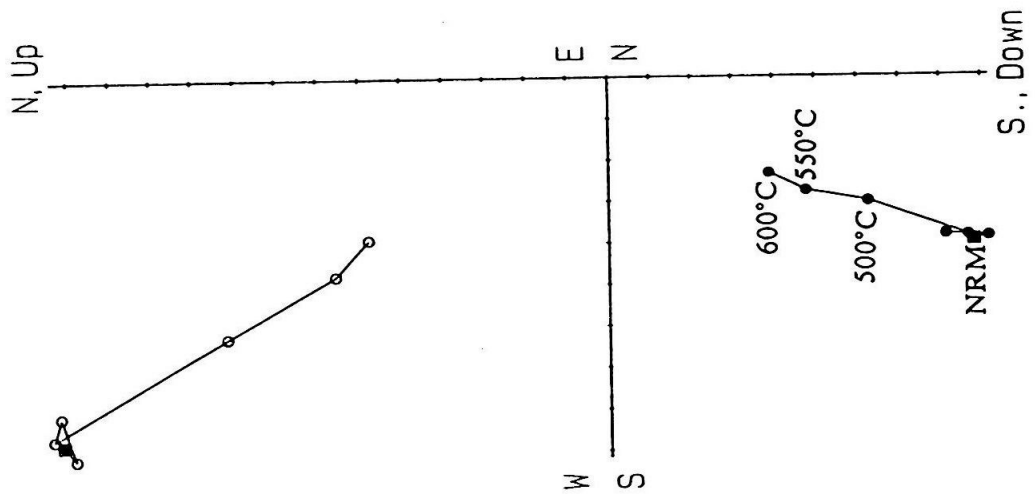


**Figure 7. Typical reversed sample of the Crowder samples.**

Orthogonal and equal-area plots from the reversed (CR 9.0) sample. The plotting convention is the same as Figure 3.



CR9.0



### Comparison of different techniques:

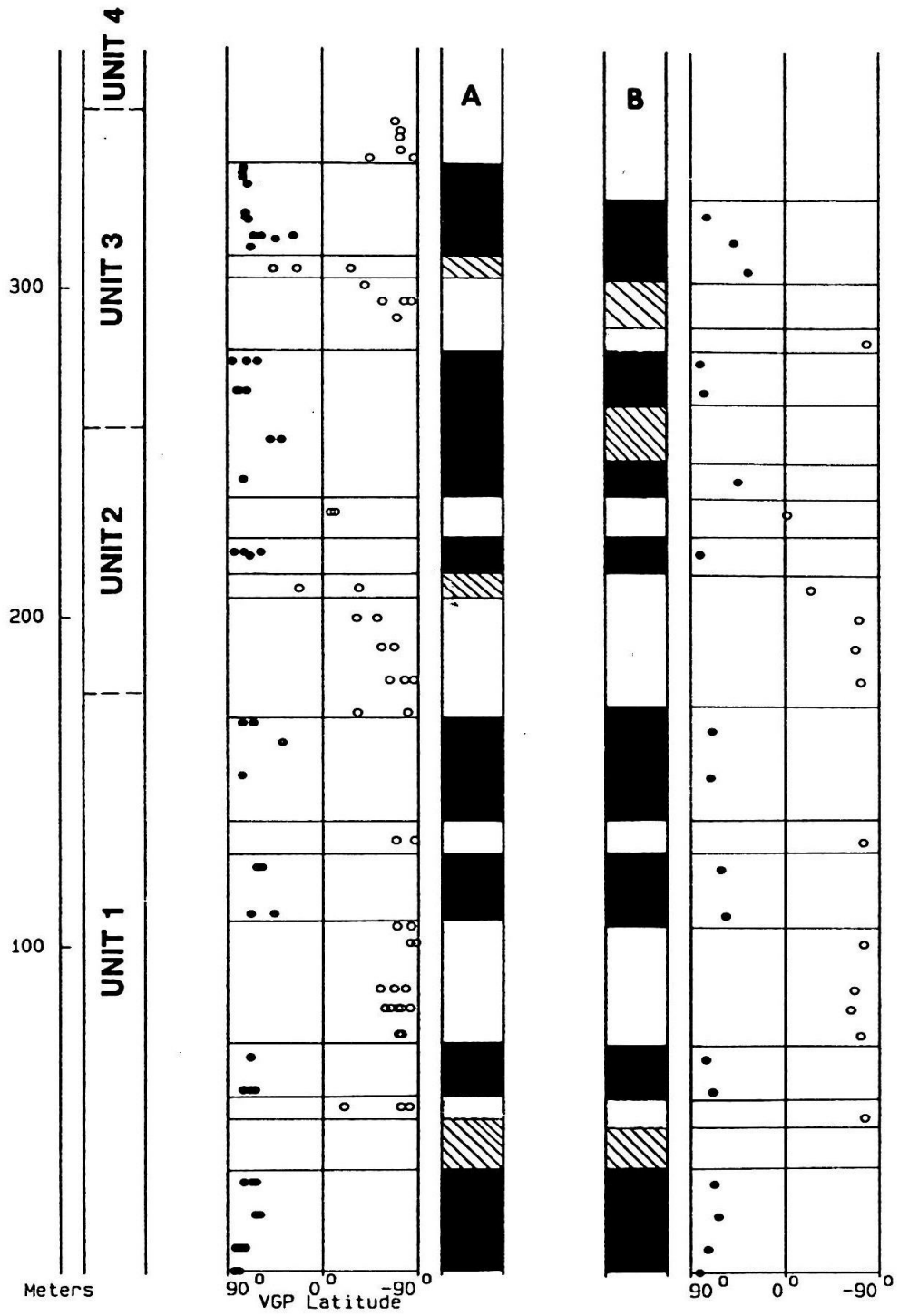
Both magnetic polarity stratigraphies obtained using the two different statistical methods for the lower part of the Crowder Formation were illustrated in Figure 8. Although apparently the two resulting magnetic polarity stratigraphies are almost same, they are obviously not as good as the magnetostratigraphies obtained using the different method for the upper parts of the Cajon and Crowder formations (see Figure 15 and 24). If we collected one sample per site, for those class I and II sites used in the standard method, it would have hardly any difference in final result (magnetic polarity stratigraphy). In fact, there are several disadvantages in using this USC method for the study of sedimentary rocks. First, multiple samples collected from individual stratigraphic horizons give no better statistical results than one sample per bed. As sedimentary rocks generally obtain magnetization (detrital remanent magnetization, DRM or pDRM) in a much different way from that of volcanic rocks (thermal remanent magnetization, TRM) (McElhinny, 1973; Tarling, 1983), it is difficult to obtain a site mean from a particular bed which has Fisherian distribution as in volcanic rocks. It is also not appropriate to use Fisher statistics for such purpose because Fisher statistics requires samples being uniformly distributed (i.e. uniformly magnetized) (Onscott, 1983) whereas DRM is generally not as uniformly distributed as TRM. Weldon (1986) concluded that multiple samples from the same horizon and processed in this manner generally yielded either good or bad results, which is further supported by our results from the lower and upper parts of the Crowder, and also, from the upper part of unit 6 of the Cajon Formation. Hence, multiple samples per horizon actually give little additional information for the additional work.

**Figure 8. Comparison of magnetic polarity stratigraphies developed using different statistical analysis.**

The VGP latitude of the primary component of each sample is plotted against stratigraphic position. Solid and white columns of magnetic polarity stratigraphy represent normal and reversed magnetic polarities, respectively. The ambiguities (indeterminable polarity) are represented by hachured zones and may be of either normal or reversed polarity.

A -- developed without using Fisher statistics. The characteristic component of each sample, obtained using principal component analysis (Kirschvink, 1980), is plotted against its stratigraphic position. Obviously, samples collected from the same horizon generally have same polarity and similar directions. For the top part (the uppermost of unit 3 and the bottom of unit 4), the Caltech methodology was used and higher resolution and reliability appears to be provided.

B -- developed using the USC method. Presumably primary component was obtained from each sample at 550 °C thermal demagnetization step. Site mean directions were then calculated using Fisher statistics on samples from the same horizon, and were plotted against the stratigraphic thickness. Only those class I and II site means (Table 1) were used. The resulting magnetic polarity stratigraphy is almost the same as that in part A. As multiple samples were collected from individual horizons with a large interval between samples, this methodology obviously provides lower resolution of magnetic polarity, no better results for individual sites, and less information for the same amount of effort, than the alternate procedure.





Second, large sampling intervals often used in the USC method results in a low resolution of the magnetic polarity stratigraphy (Figure 8). On the other hand, as only one sample is collected from individual strata, more beds can be sampled in a small stratigraphic distance, which provides higher resolution of magnetic polarity for the same amount of work (Figure 8, top of part A). Hence, it can be concluded that individual samples from many beds were more efficient than multiple samples from few beds. Because we still require more than one sample to define a consistent magnetozone, interpretation of an individual magnetozone is also more reliable than that which relies on one site mean obtained from multiple samples. Also, secular variations of geomagnetic field were efficiently averaged as long enough stratigraphic sections were sampled in small sampling interval. Therefore, only one sample was collected in most part of this study from each stratigraphic horizon or site in shorter intervals.

Finally, Kirschvink (1980) has indicated that detailed analysis of demagnetization history of each sample using principal component analysis is necessary for isolating the direction of a primary remanent magnetization from each sample. It is more important for study of sedimentary rocks because magnetic and lithologic characteristics of sedimentary rocks vary more rapidly than those of volcanic and igneous rocks. Therefore, we feel justified for using our methodology in study of these coarse-grained sedimentary rocks. Although the standard methods were used previously for study of the lower part of the Crowder Formation (Winston, 1985), the same statistical analyses as used for the upper parts of the Crowder and Cajon formations were also conducted for samples from the lower part of the Crowder Formation. Characteristic components obtained in this method were used to develop the magnetic polarity stratigraphy for all units included in this study.

## I. Cajon Formation

### Sampling Sections

Although deposits of the Cajon Formation are widely exposed in the Cajon Valley, it is difficult to sample a continuous or complete stratigraphic section that includes all units of the formation. Units 4 and 5a of the formation are probably lateral facies equivalents, and are composed of sediments too coarse to sample for magnetic studies. Unit 1 was not studied also because it is not suitable for paleomagnetic study in terms of exposure and magnetic features (too coarse sediments and poorly bedded). Although unit 2 is generally well exposed and forms distinct "hogback" features, there are fewer fine-grained interbeds in the unit, and those that exist are more deeply weathered. Therefore, this study only included units 3, 5, and 6, and a little of unit 2 of the Cajon Formation. This probably represents 70% of the entire formation and probably most of its age range.

A relatively continuous stratigraphic section of units 3 and 5 that includes a small part of units 2 and 6 has been sampled near the center of the Cajon Valley (Figure 9, section b). The exposure in this area is relatively fresh because most parts of it were quarried recently to build the railways and freeway. This is also the most complete section of the Cajon Formation because units 2, 3, 5, and 6 of the formation are stratigraphically continuous. The section, called MS - Ca, starts at near the boundary between units 2 and 3 of the Cajon Formation north of Highway 138 along a railway road-cut west of the Cajon Junction (Figure 9). Within this section a total of 160 samples was taken from units 3 and 5, covering adequately the two units, whereas only five samples were collected from unit 2 and fifteen from unit 6. As the intervals between fine-grained interbeds are irregular, we generally took one sample from each

**Figure 9. Geological map of the Cajon Pass area and the sampling locations.**

Geology is after Woodburne and Golz (1972) and Weldon (1986).

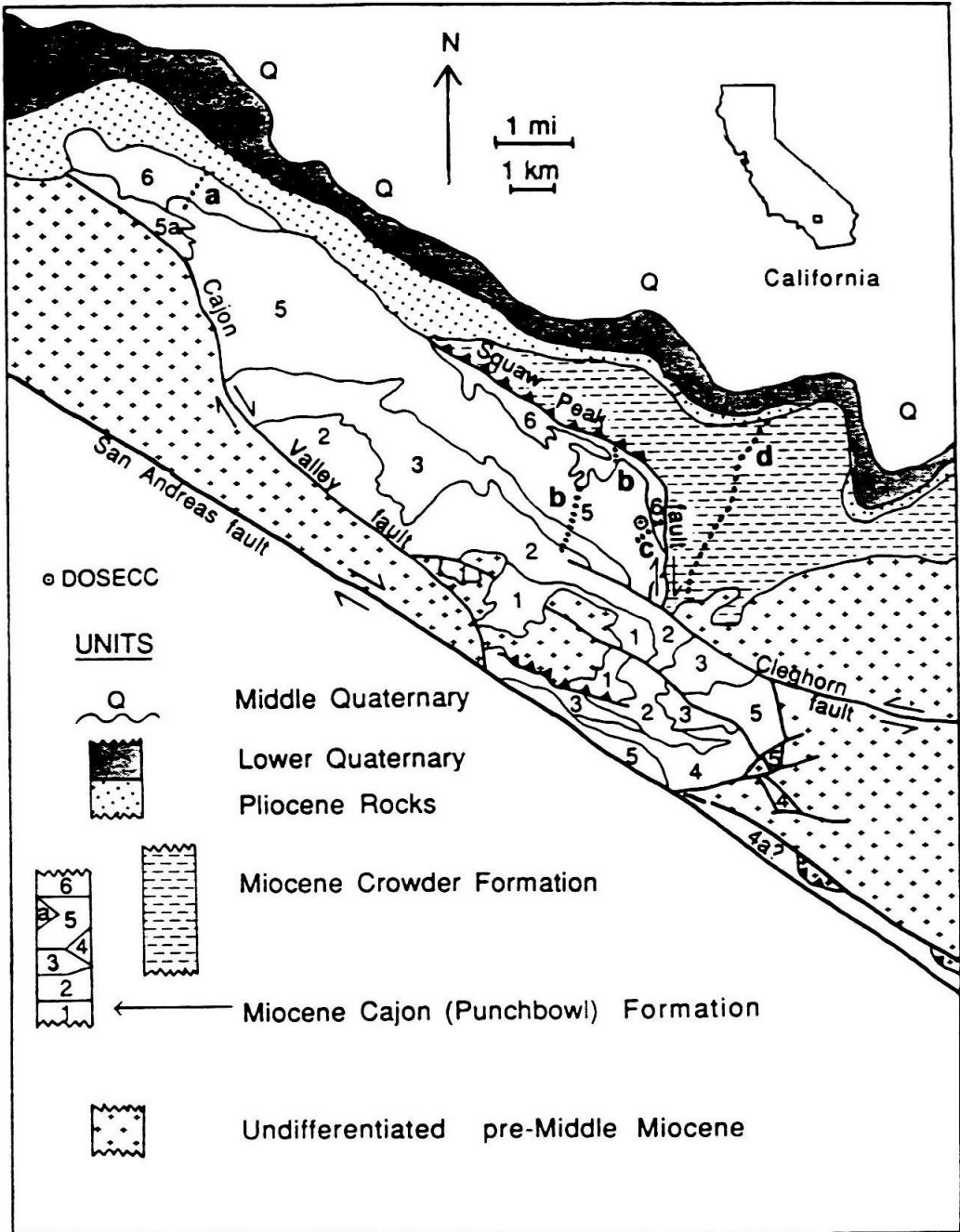
DOSECC -- Location of Cajon Pass deep drill hole;

a) Section NW - Ca, including entire unit 6 and small portion of upper unit 5;

b) Section MS - Ca, including entire units 3 and 5, part of unit 6 and small portion of upper unit 2;

c) Section NE - Ca, including parts of unit 5 and unit 6;

d) Section of Lower Crowder Formation.



site at 1 to 10 meter intervals.

The beds of units 2, 3, and 5 dip homoclinally about  $45^{\circ}$  to  $70^{\circ}$  towards northeast. Near the north end of section MS-Ca (Figure 9), where the Squaw Peak fault separates the Cajon from the Crowder formations, unit 6 is deformed strongly and is exposed only locally on top of unit 5. Therefore, samples collected from unit 6 in MS - Ca are used only for the study of tectonic rotation.

Units 5 and 6 also crop out in the northeastern and northwestern parts of Cajon Valley (Figure 9). In the northwest, the sequence begins in the uppermost part of unit 5 and continues with excellent exposures of unit 6, where it reaches its maximum thickness (333 meters). Both units 5 and 6 are tilted homoclinally, although unit 5 dips more steeply (ca.  $80^{\circ}$ ) than unit 6 (ca.  $60^{\circ}$ ) because it is closer to the axis of folding. The two units at this locality are simple in structure. At the base, unit 5 is laterally gradational with unit 5a, which is cut by the Cajon Valley fault. At the top of the section, unit 6 is overlain unconformably by the younger Phelan Formation and generally dips steeply towards the north (Figure 9). Our second section for paleomagnetic sampling, (NW-Ca), was chosen in this locality (Figure 9), and it covers entire unit 6 and the upper part of unit 5. The upper part of this section terminates below the Phelan Peak magnetostratigraphic section of Weldon (1984).

The base of section NW-Ca is at the upper part of unit 5 about 50 meters below the boundary between units 5 and 6 (Figure 9). There is a 45 m gap in which no samples were recovered because there is no exposure. Eighty-three samples were collected from fifty-nine sites in this section, with 18 samples collected from the top of unit 5 in order to provide good stratigraphic control on the boundary between units 5 and 6, and to compare rotations in both units with those from other localities.

The third section was sampled near the northeastern end of the Cajon

Formation (NE-Ca, Figure 9). It covers part of unit 6 and is above the previously studied section of unit 5 (Liu et al., 1988). As it is next to the Squaw Peak fault, the beds are strongly deformed and folded. Thus, a fold test can be performed in this section in addition to determining local tectonic rotations. As our main purpose of studying this section was to compare the rotations at different localities in the same unit, only 20 samples were taken in a short stratigraphic distance.

Almost all of the samples were collected from fine-grained facies which are more magnetically stable than those coarse-grained sediments. Besides grain size, the weathering indicated by color also controls the stability of samples. Siltstones and silty fine-grained sandstones of light-color generally yield better results than other sediments of the Cajon Formation. Dark-color, e.g. brownish green and green, siltstones or fine-grained sandstones often produced aberrant directions, probably due to later weathering.

Although the spacing between sampling sites was controlled by the availability of fine-grained sediments and suitability for sampling, every effort was made to obtain continuous stratigraphic coverage of each section. Except where sediments are too coarse to be magnetically stable or appear to be weathered, the interval between sampling horizons generally ranged from 2 to 7 meters. The samples were oriented carefully in the field using both magnetic compass and sun-compass, when the use of the latter was possible. The sampling sites are easily and quickly eroded, but the stratigraphic distances between sample sites were measured carefully.

### Magnetic Mineralogy and Origin of Remanence

Identification of the minerals carrying the remanence is critical to paleomagnetic studies, because they often provide direct evidence for the timing of the magnetization

and for the mechanism by which such remanence was acquired. Two lines of evidence suggest that the major magnetic mineral phase in samples of the Cajon Formation is magnetite, although small amounts of hematite and goethite can also be found in some samples. First, magnetic minerals extracted from the fresh samples, using a method similar to that of Chang and Kirschvink (1985), are almost all magnetite crystals, with a few hematite grains that are wrapped within or adhere to quartz crystals. Second, only a small fraction of the NRM remains after the 570 °C demagnetization step for most samples, suggesting that the main remanence carrier of the samples is not hematite (Figure 10). By this temperature, all of the magnetic remanence carried by magnetite, maghemite, or goethite should be destroyed, leaving only that carried by hematite (Hargraves and Banerjee, 1973; Tarling, 1983).

Although examination of the magnetic extract shows that only a portion of the remanence carrier is probably hematite, the hematite grains show detrital features and are commonly wrapped in or adhere to quartz crystals, suggesting they are of detrital origin. It is also conceivable that the surface of magnetite grains could be oxidized to hematite at low-temperature after deposition. However, the magnetite grains extracted from these samples show detrital features such as rounding and fracture surfaces, which do not appear to be oxidized. Hence, the principal magnetic remanence of these samples is probably a primary detrital remanent magnetization (DRM) or an early post-detrital remanent magnetization (pDRM). This interpretation is supported by several observations. First, the in-situ cleaned magnetic mean directions of all sections have very steep inclinations, far greater than the inclination of the Tertiary geomagnetic field for this latitude in North America (Figure 11). Upon correction for the tilt of bedding, however, the inclination values shallow to a more consistent level. Furthermore, the mean directions of units 5 and 6 at different localities overlap each other after tilt

**Figure 10. Temperature vs. magnetization plot of the Cajon samples.**

Temperature is in degree of centigrade; the steps before 100 °C are those of alternating field demagnetization, and the units for them are 5.0, 7.5, and 10.0 mT, respectively;

Squares -- samples CP3-3 (A), CP5-89 (B);

Circles - samples CP3-18 (A), CP5-91 (B);

Triangles -- samples CP-25 (A), CP-99(B);

Diamond - samples CP-31 (A), CP-121 (B).



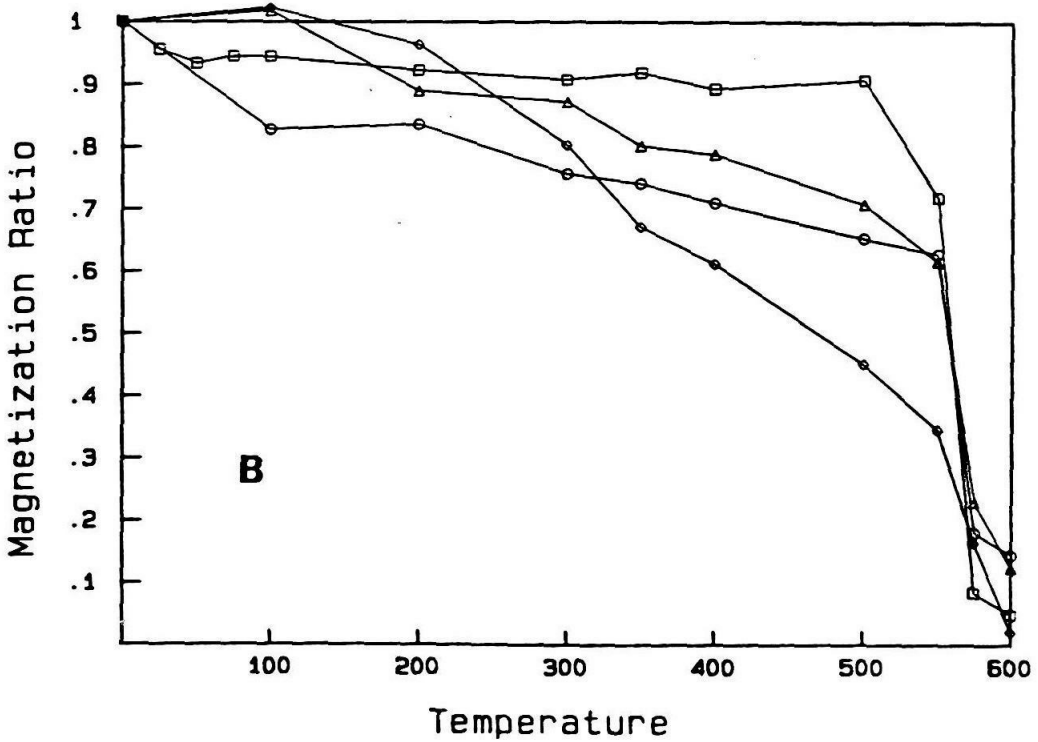
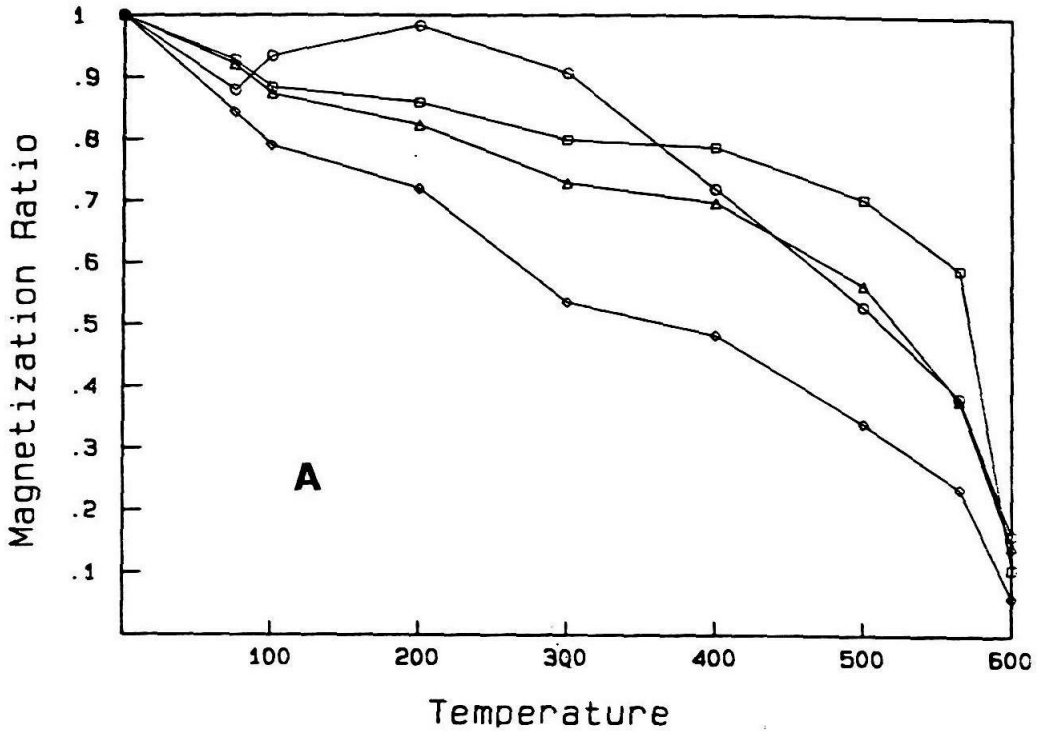


**Figure 11. Equal-area plots of all normal and reversed directions from each unit of the Cajon Formation.**

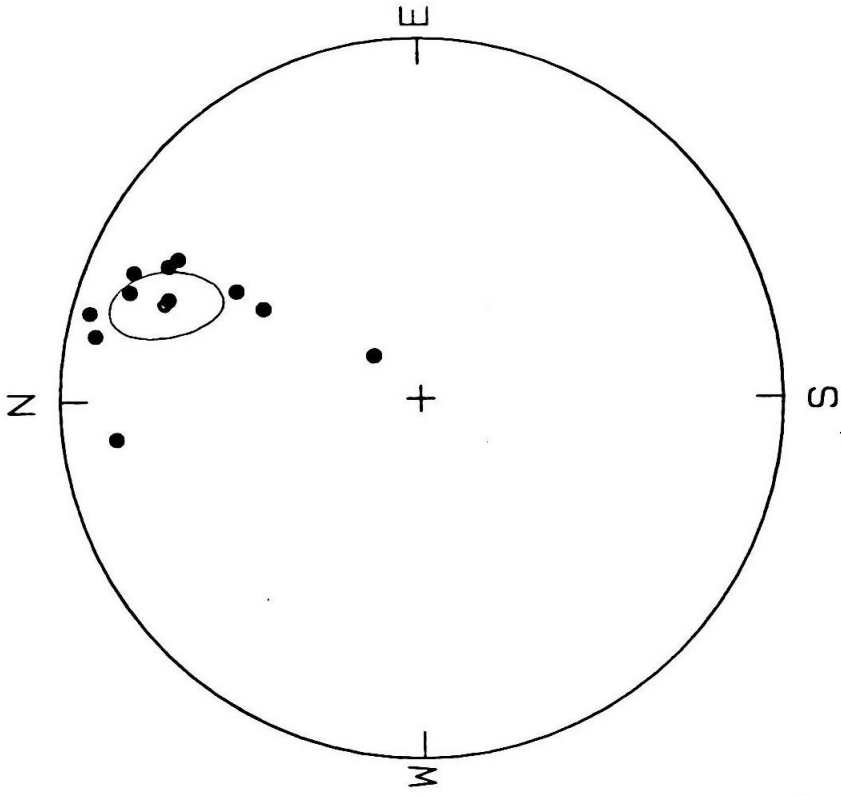
Directions plotted are all least-square characteristic components from each sample, obtained using principle component analysis (Kirschvink, 1980). Only those stable primary directions were used here.

A -- units 5 and 6 at the northeastern end of the formation (section NE-Ca);

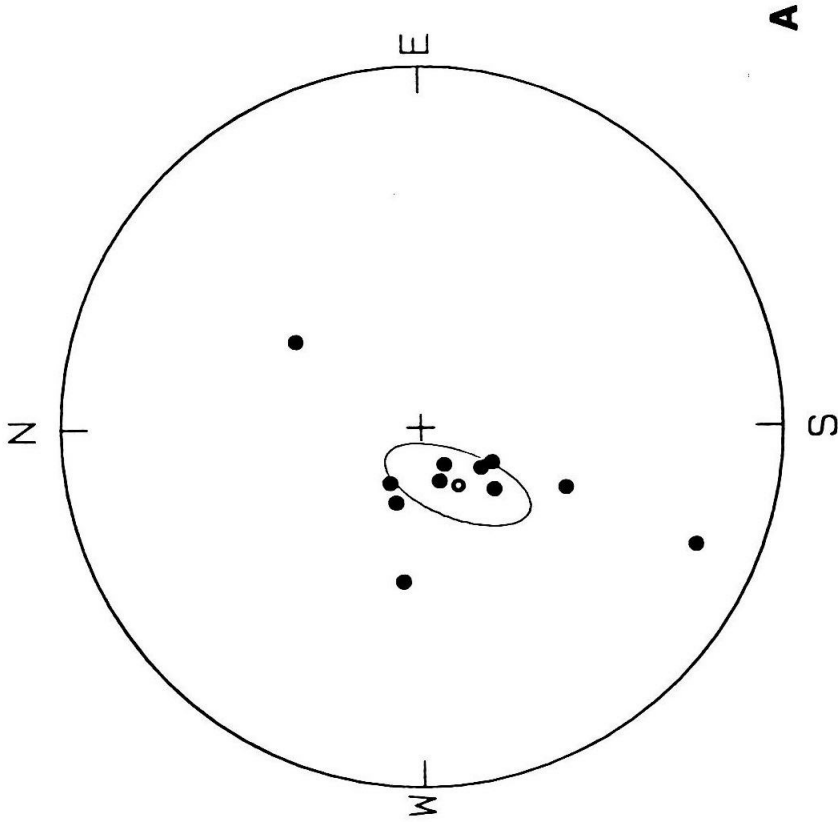
B -- units 3, 5, and 6 at the center of the formation (section MS-Ca);

C -- units 5 and 6 at the northwestern end of the formation (section NE-Ca).

Open circles are projected onto the upper hemisphere and solid ones are projected onto the lower hemisphere.



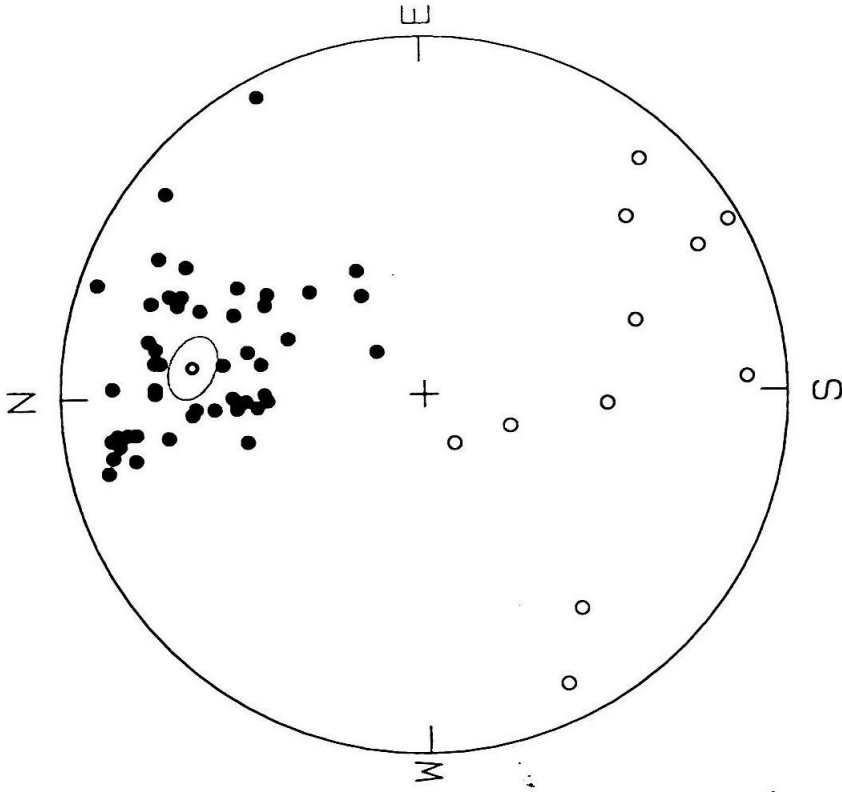
TILT-CORRECTED



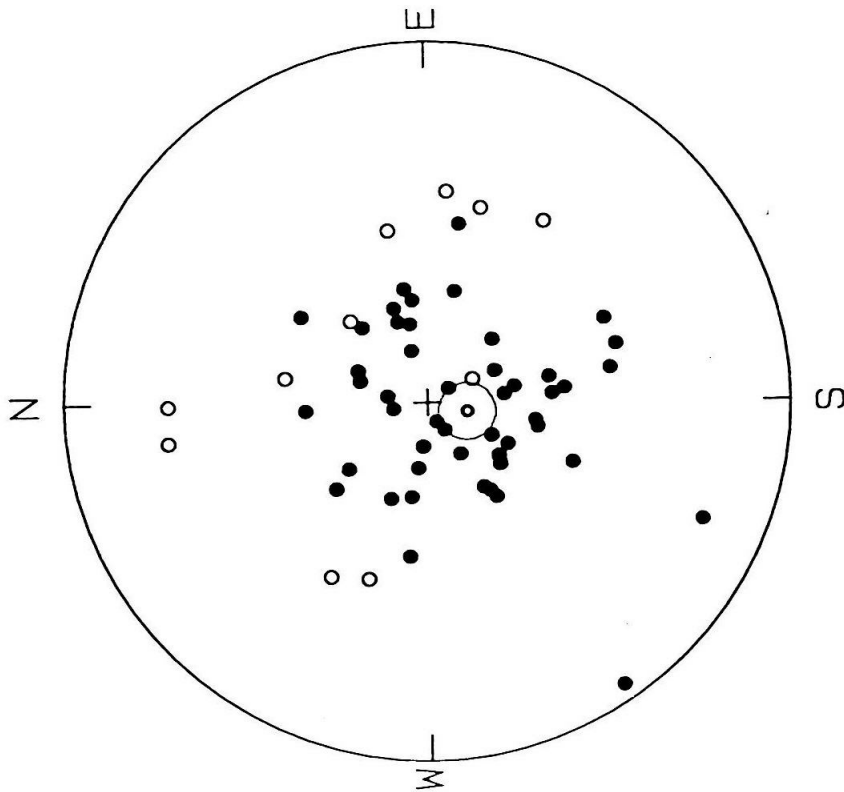
GEOGRAPHIC

**UNIT 5 (NORTHWESTERN)**

A



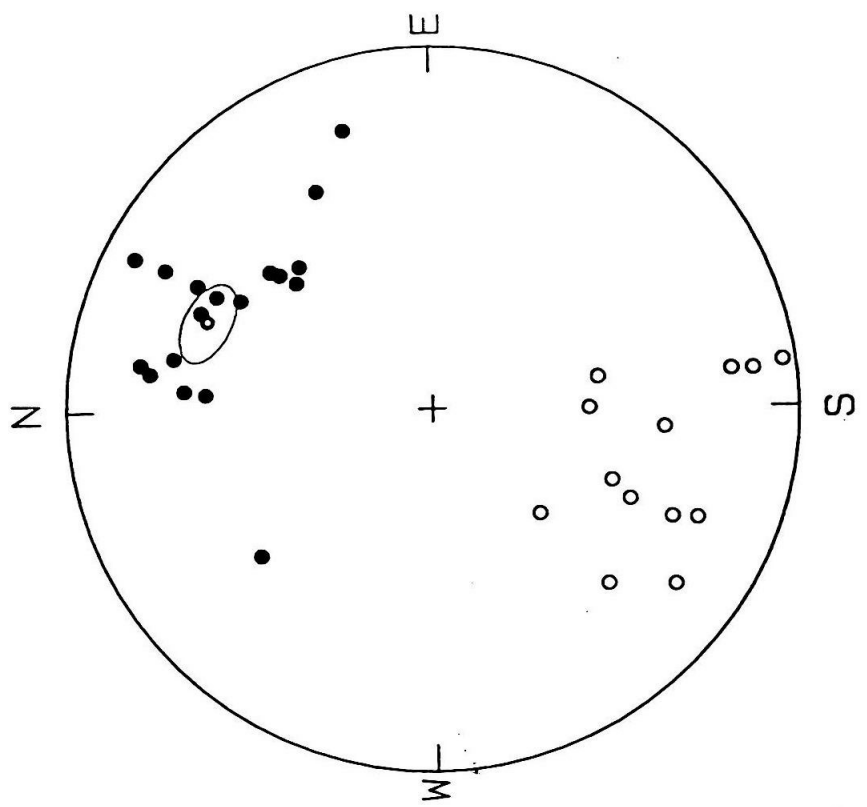
TILT-CORRECTED



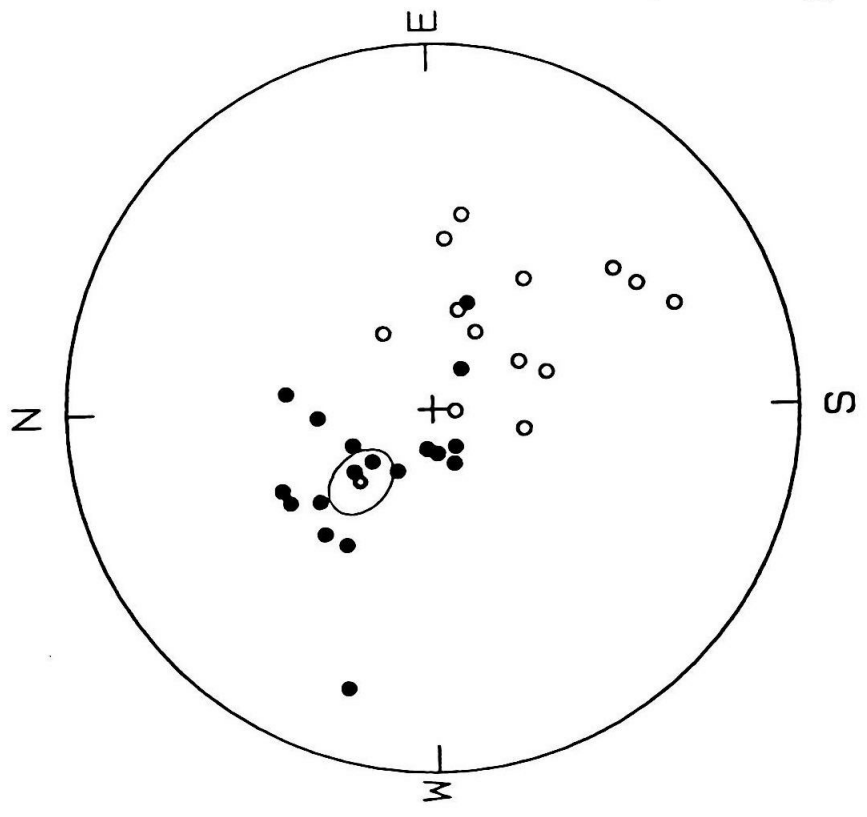
GEOGRAPHIC

UNIT 6 (NORTHWESTERN)

A



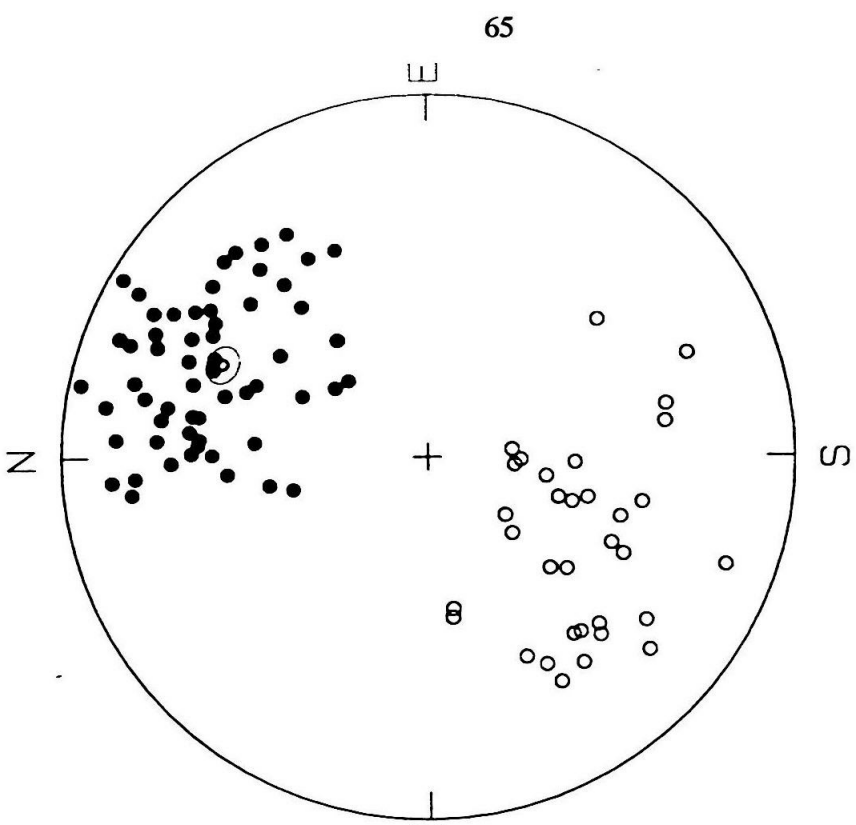
TILT-CORRECTED



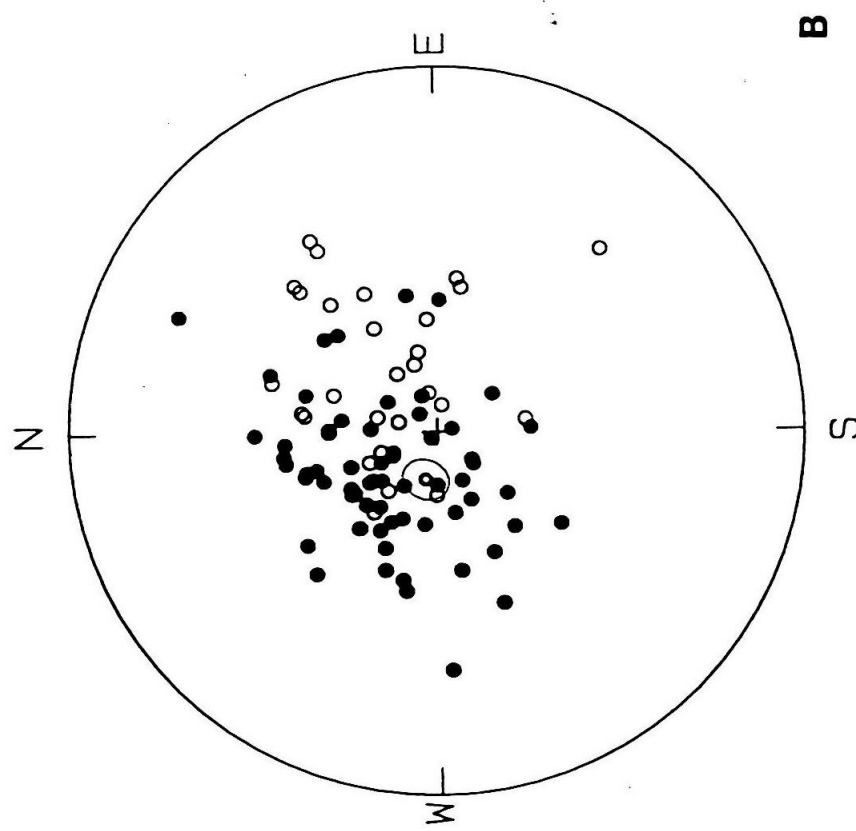
GEOGRAPHIC

**UNIT 3 (CENTRAL)**

**B**



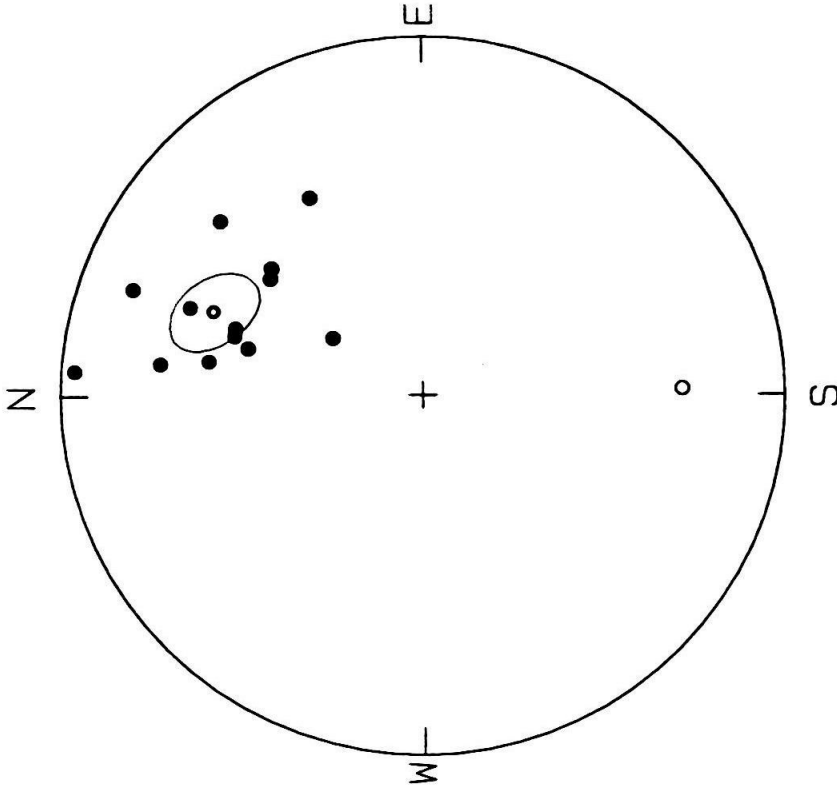
TILT-CORRECTED



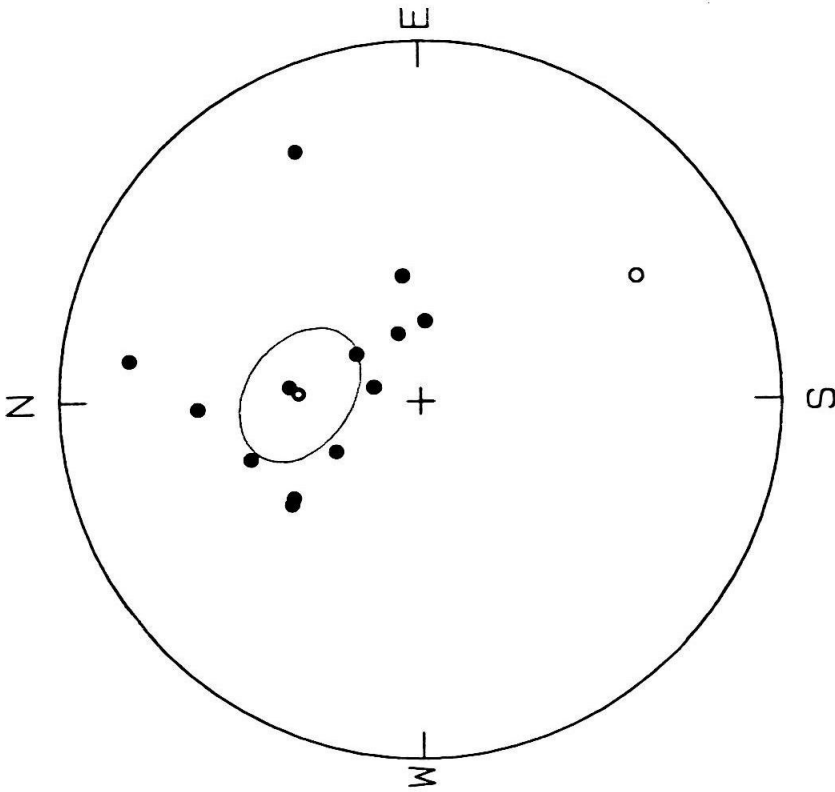
GEOGRAPHIC

**UNIT 5 (CENTRAL)**

**B**



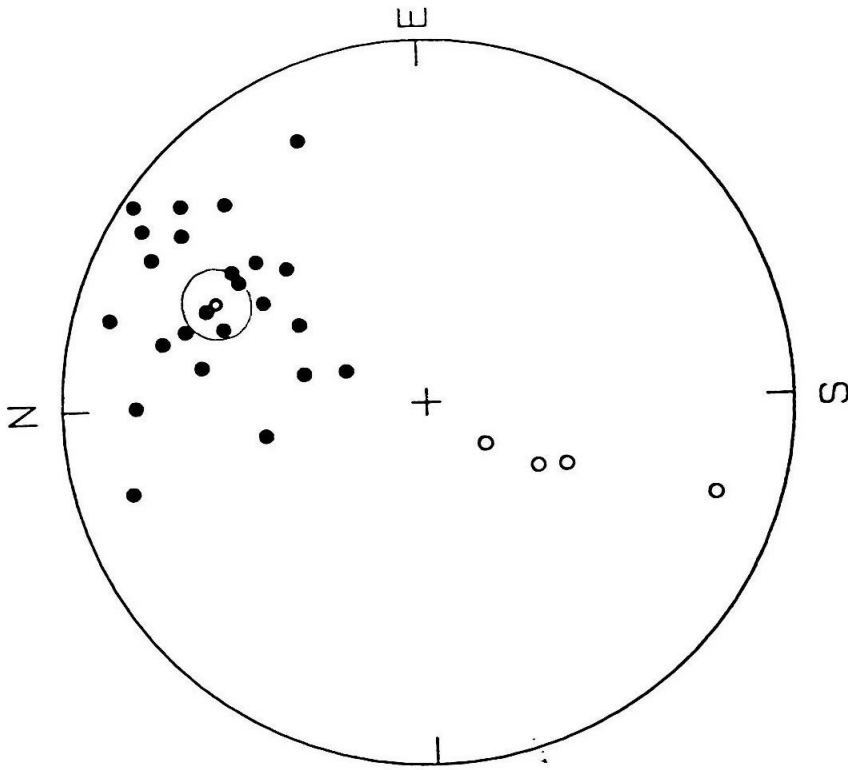
**TILT-CORRECTED**



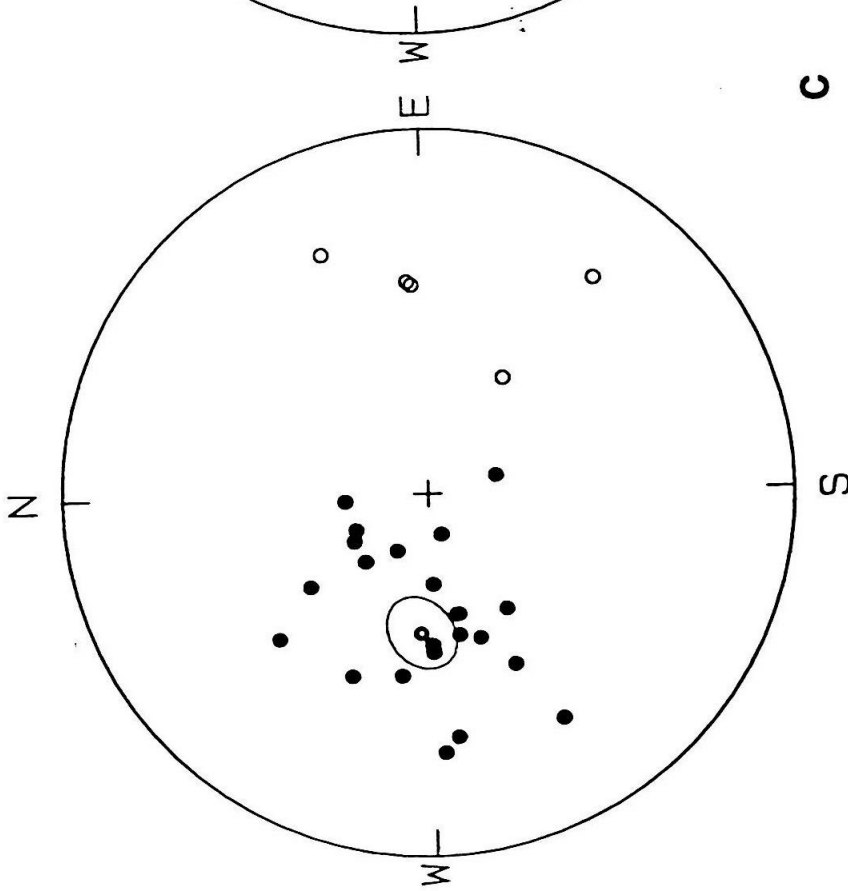
**GEOGRAPHIC**

**B**

**UNIT 6 (CENTRAL)**



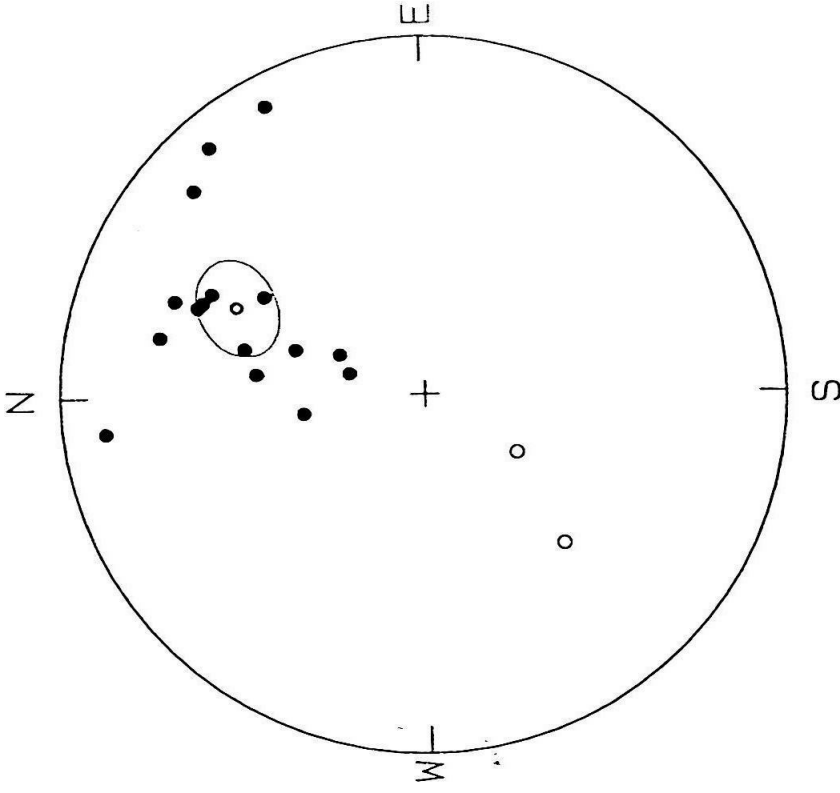
TILT-CORRECTED



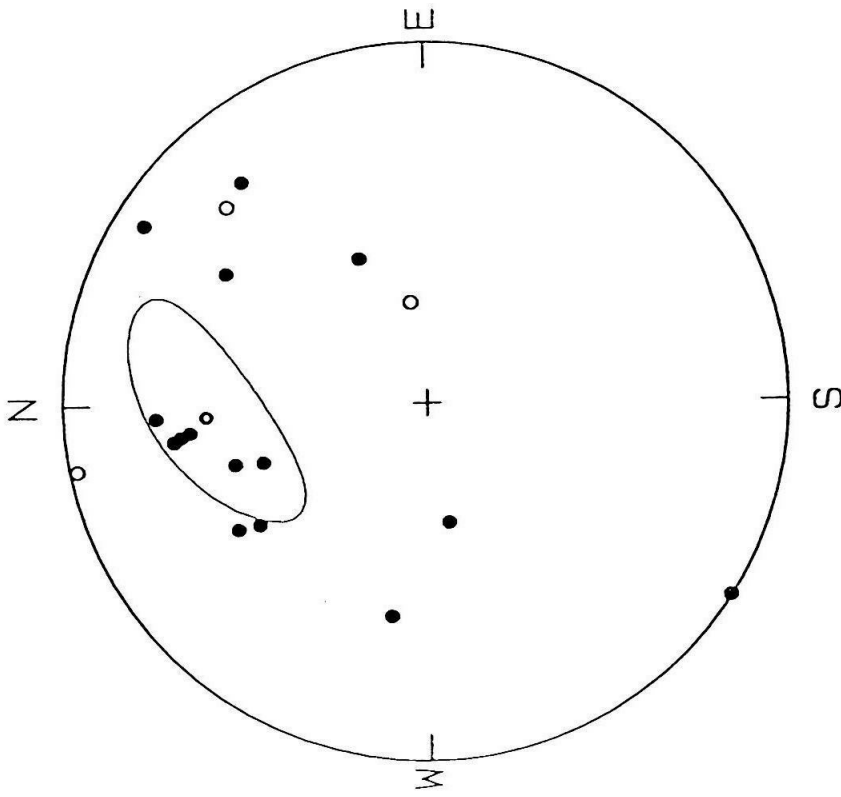
GEOGRAPHIC

UNIT 5 (SOUTHEASTERN)





TILT-CORRECTED



GEOGRAPHIC

UNIT 6 (SOUTHEASTERN)

C

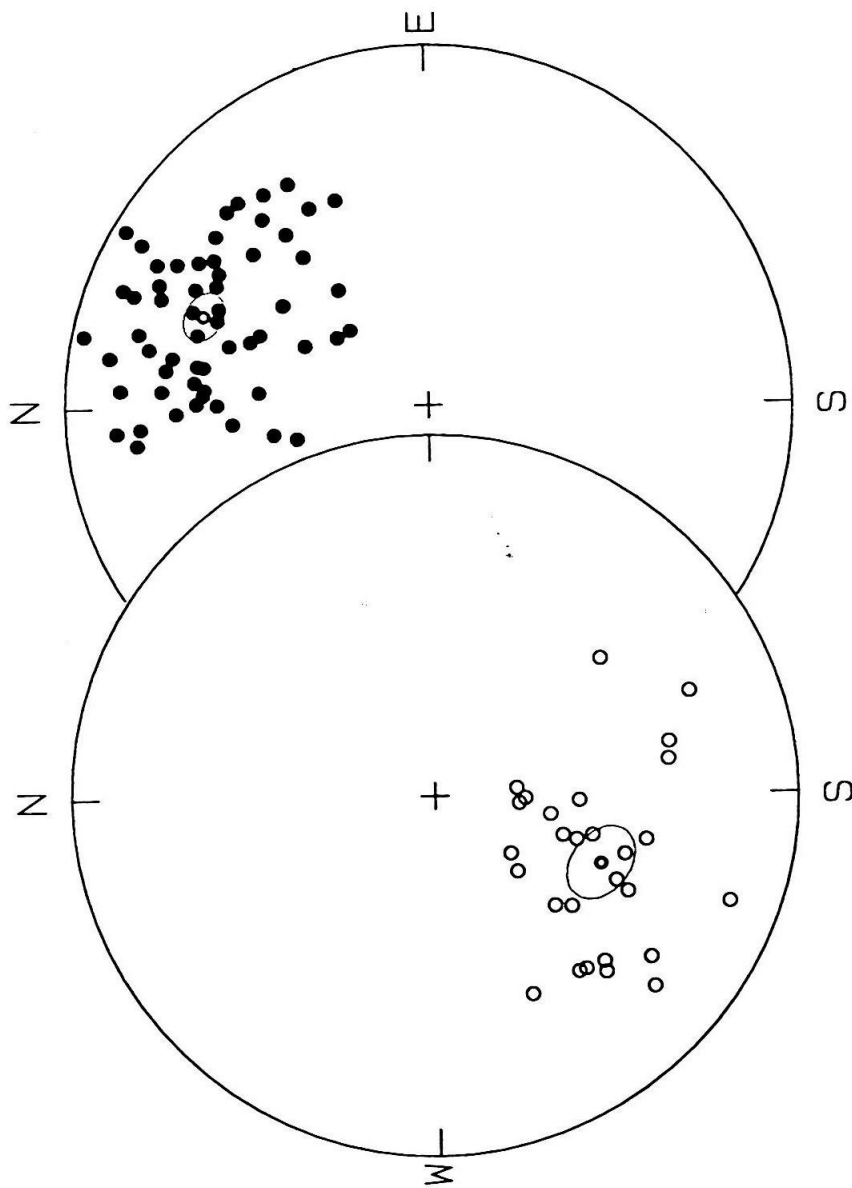
correction of bedding (Figure 11).

Second, plots of tilt-corrected directions for both normal and reversed sites (Figure 12) of unit 5 show that the means of all normal polarity samples ( $D = 22.5^\circ$ ,  $I = 34.0^\circ$ ,  $\alpha-95 = 5.0^\circ$ ) are antipodal to the means of all reversed polarity samples ( $D = 202.4^\circ$ ,  $I = 48.6^\circ$ ,  $\alpha-95 = 8.2^\circ$ ) within error limits. The positive reversal test indicates that any overprint of secondary fields is negligible.

Finally, several fold tests were conducted in unit 6 of the Cajon Formation to determine whether the magnetic vectors obtained are the DRM or some type of post-depositional remanent magnetization. At the eastern end and in the middle of the Cajon Formation, unit 6 is strongly deformed and folded by movements along the Squaw Peak fault (Figure 2), making it possible to perform fold tests for the sediments. Figures 13 and 14 show stereonet (equal-area) projection of these directions both before and after structural correction. In each case, the fold test is passed at the 95% confidence level (McElhinny, 1964) (Table 2), demonstrating conclusively that the characteristic magnetization was acquired before folding.

**Figure 12. Reversal test diagram of unit 5 of the Cajon Formation.**

The normal and reversed directions were all stable primary components that were obtained using the principle component analysis method (Kirschvink, 1980). Open circles are projected onto the upper hemisphere, and solid circles are on the lower hemisphere. The equal-area plots demonstrate that the average directions for the normal- and reversed-polarity samples are virtually antipodal to each other.



REVERSED DIRECTIONS    NORMAL DIRECTIONS

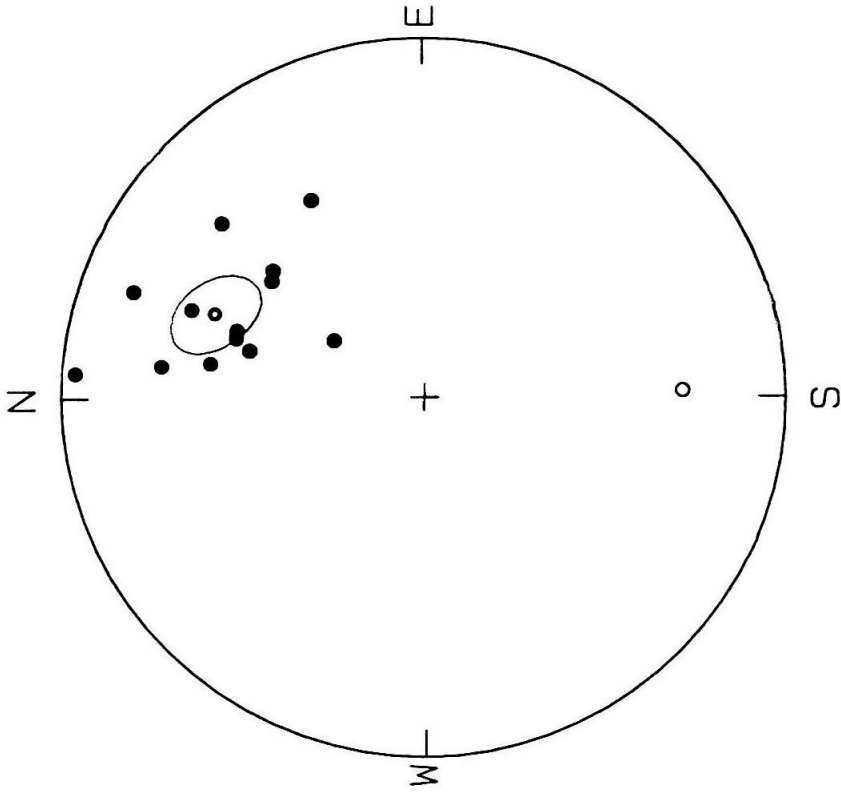
**CAJON (UNIT 5) REVERSAL TEST**

**Figures 13 and 14. Fold tests of unit 6 at the northeastern end and central parts of the Cajon Formation.**

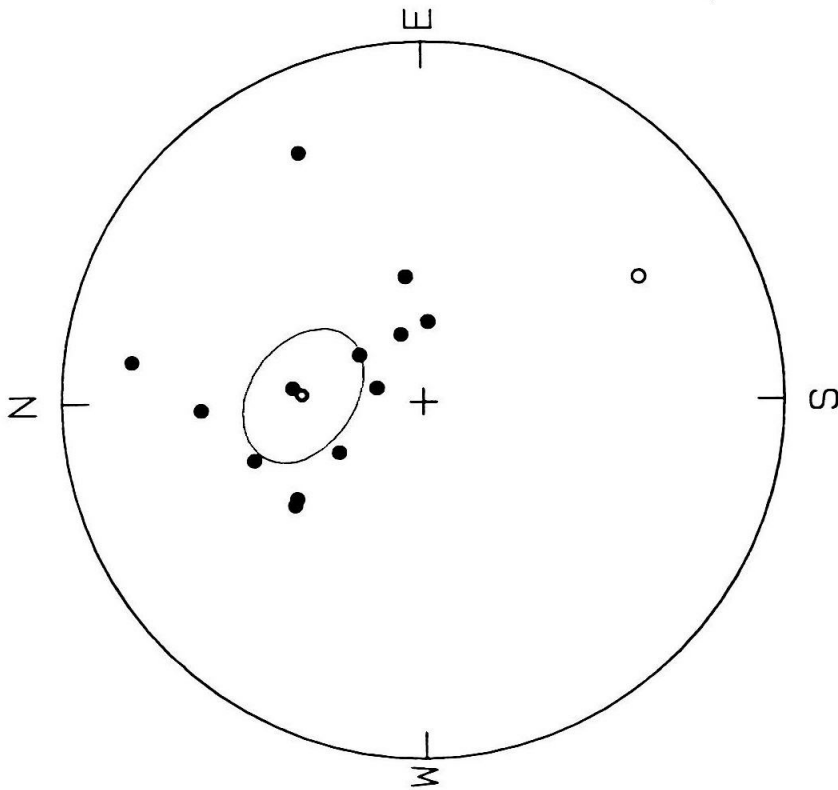
LEFT -- results obtained before tilt correction of bedding;

RIGHT -- results obtained after tilt correction of bedding.

Solid circle represents a vector directed onto the lower hemisphere, hollow circles represent vectors directed onto the upper hemisphere. The characteristic components of cleaned samples are scattered before tilt-correction for bedding. After correction for folding, they became relatively clustered, suggesting that a fold test is passed.

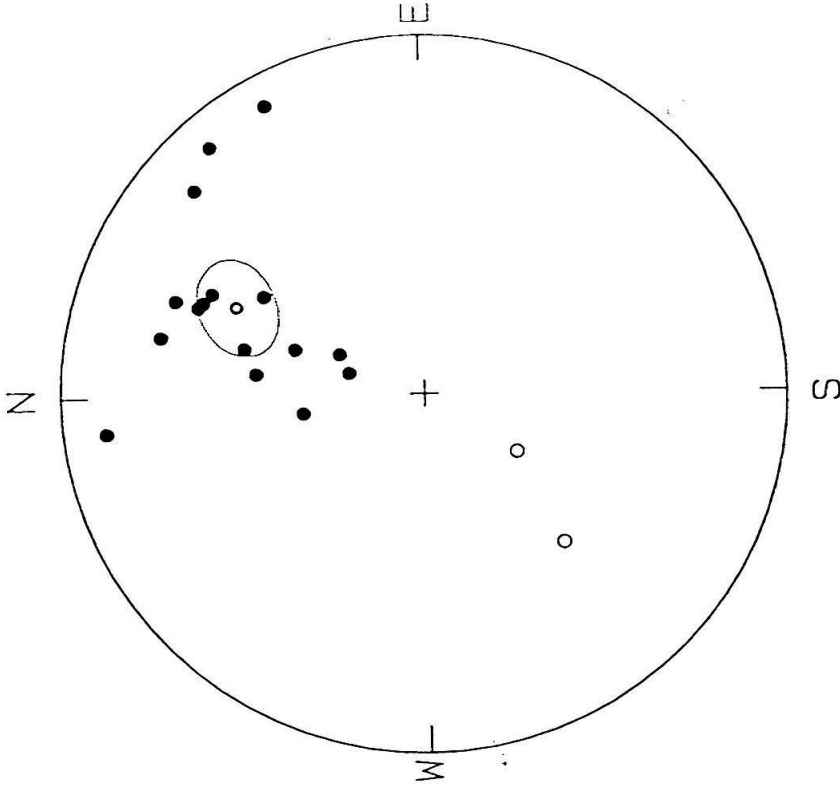


**TILT-CORRECTED**

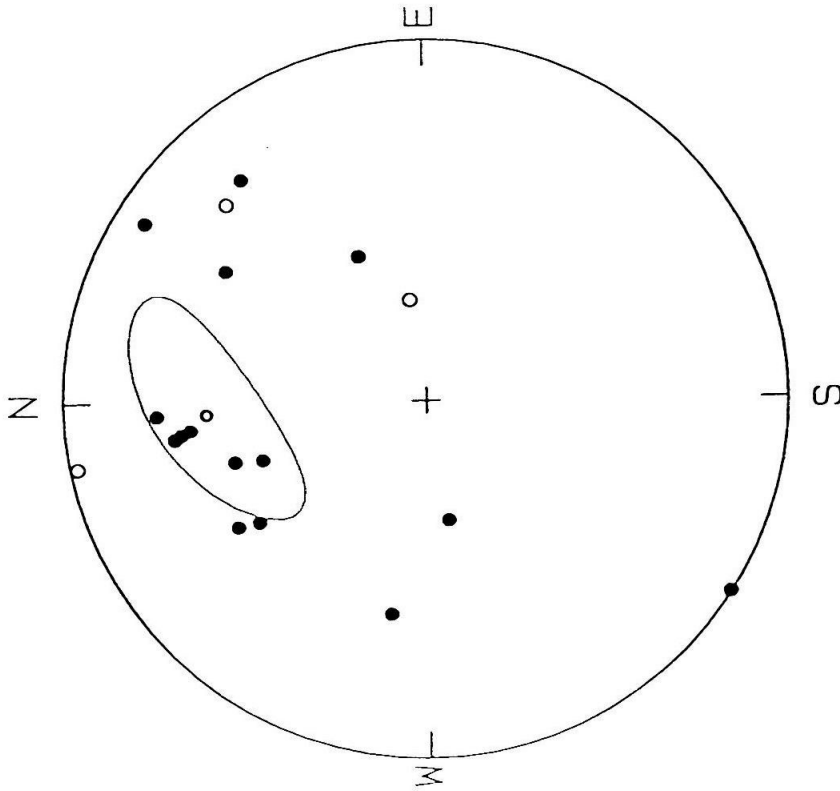


**GEOGRAPHIC**

**UNIT 6 (CENTRAL)**



TILT-CORRECTED



GEOGRAPHIC

UNIT 6 (SOUTHEASTERN)

**Table 2. Results of fold test from the Cajon Formation.**

| Section | N  | K1  | K2   | K2/K1 | Significance Level (McElhinny) |
|---------|----|-----|------|-------|--------------------------------|
| MS-Ca   | 18 | 3.0 | 11.1 | 3.7   | > 95%                          |
| SE-Ca   | 14 | 7.3 | 15.7 | 2.2   | > 95%                          |

K1 and K2 are the precision values calculated using Fisher statistics before, and after, respectively, correcting for folding.



### Microfossil Age Constraints

Additional time constraints are necessary for our study because there are several possible ways to match a sequence of geomagnetic polarity chrons to the standard time scale. One of the most promising techniques for dating the nonmarine late Tertiary sediments utilizes rodent teeth, which are often preserved in these sediments and are easily identified. In addition, many rodent microfossils have been dated by radiometric methods in the nearby Barstow basin, which has interbedded volcanics. Therefore, the correlation provides independent estimates of the age of the Cajon Formation.

In collaboration with R. Reynolds at the San Bernardino County Museum, we collected more than 2700 pounds of rock from a paleosol near the middle of unit 6 of the Cajon Formation. Using the technique described by Reynolds (1985), we obtained several microfossil fragments. Of these, the most useful fossils are the teeth identified as *Pseudadjidaumo stirtoni* and *Copemys tenuis* (Reynolds, personal communication, 1987). They range only through the *Pseudadjidaumo stirtoni* assemblage zone of the Barstovian land mammal age (Lindsay, 1972), which is bracketed by tuffs that are separately dated at  $15.5 - 14.8 \pm 0.3$  Ma and  $13.4 \pm 0.7$  Ma at the type locality near Barstow, California (Woodburne and Tedford, 1985). Therefore, the fossils we found support the conclusion that the middle of unit 6 of the Cajon Formation is between 15 and 13.4 Ma old.

Specimens of *Pseudadjidaumo stirtoni* were also found in unit 5 of the Cajon Formation at the level approximately 670 meters above the boundary between unit 5 and unit 3 and approximately 34 meters below the contact of unit 5 and unit 6 (Reynolds, 1985). Taxa of *Copemys tenuis* were also found in unit 6 about 16 meters above its contact with unit 5. By combining these microfossil results with Woodburne

and Golz's (1972) vertebrate fossil discoveries from the lower part of unit 5 of the Cajon Formation, unit 5 of the Cajon Formation may be of late, but not the latest, Barstovian age. As the top of unit 5 is at least 15 Ma old, the base of unit 6 cannot be older than 15 Ma, as suggested by fossils from both units.

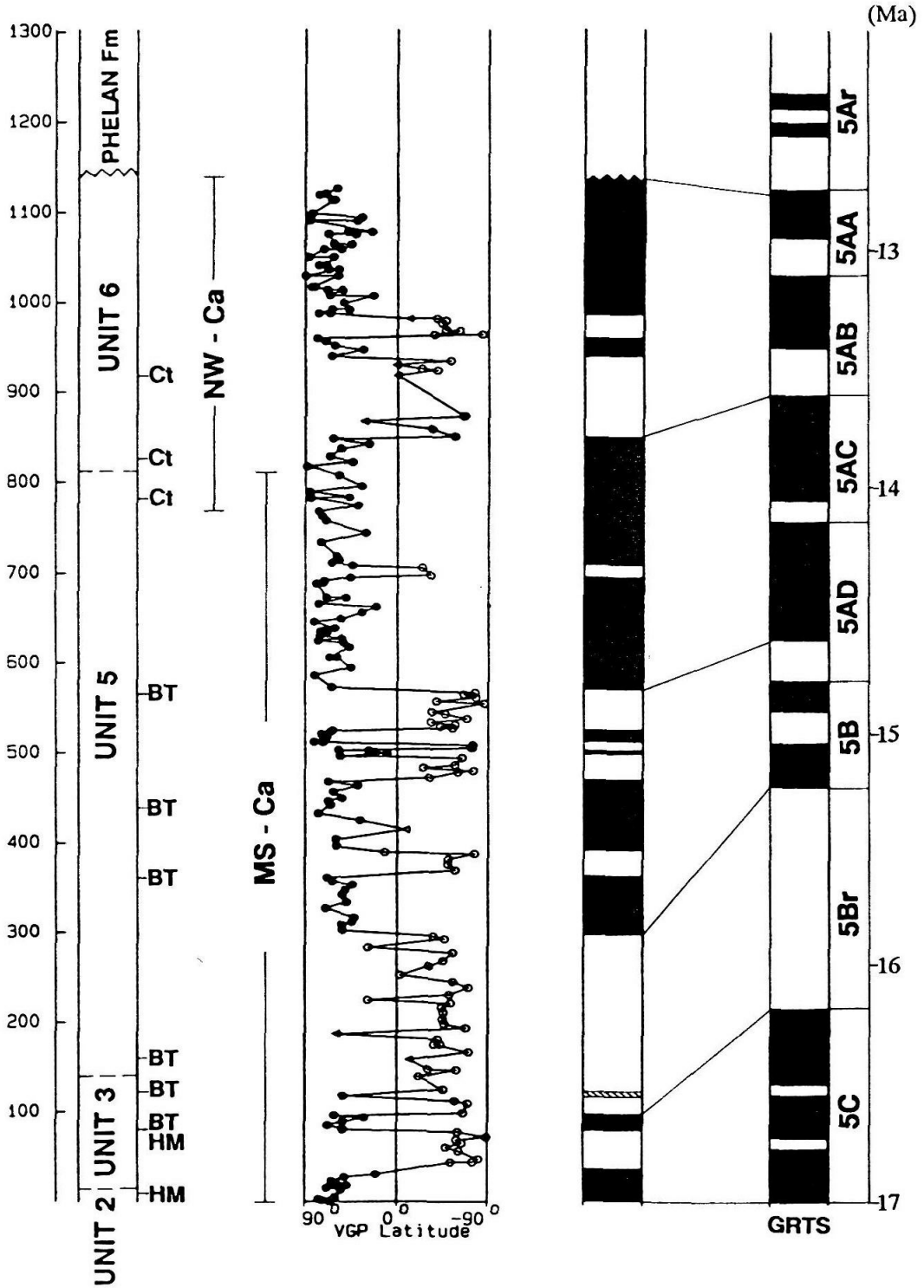
### Stratigraphic Correlation

Figure 15 shows our magnetic polarity interpretation for units 3, 5, and 6 of the Cajon Formation. The VGP latitudes, corrected for the tilt of the bedding, are plotted together with the stratigraphic column and the level at which fossils were reported. For those fossils that were not found from our sections, their stratigraphic level were roughly projected on to our sections. Most of them, therefore, are relative stratigraphic level at which fossils were found. The correlation of the magnetic stratigraphy of units 3, 5, and 6 of the Cajon Formation with the geomagnetic reversal time scale (GRTS) of Harland et al. (1980) constrains the age of the upper part of the formation to be from 17 Ma to 12.7 Ma.

From the continuous section MS-Ca northwest of Cajon Junction, unit 3 yields a good magnetic polarity stratigraphy (Figures 15 and 16), although it is not at its thickest here. This section covered both boundaries between units 2 and 3 at the bottom and units 3 and 5 at the top. The magnetic polarities of the section include two normal and two reversed chrons. Near the top, the spacing between stratigraphic sites is relatively large due to the lower abundance of fine-grained, unweathered sediments. A complete magnetic polarity stratigraphy of unit 5 was also obtained from the same section (MS-Ca), which shows long normal and reversed chrons at the top and bottom of the section, respectively, (Figures 15 and 17) and several shorter normal and reversed magnetozones in the middle of the section. The top of the section is about 1 to 2

**Figure 15. Magnetostratigraphy of units 3, 5, and 6 of the Cajon Formation and its correlation to the Standard Geomagnetic Reversal Time Scale (Harland et al., 1982).**

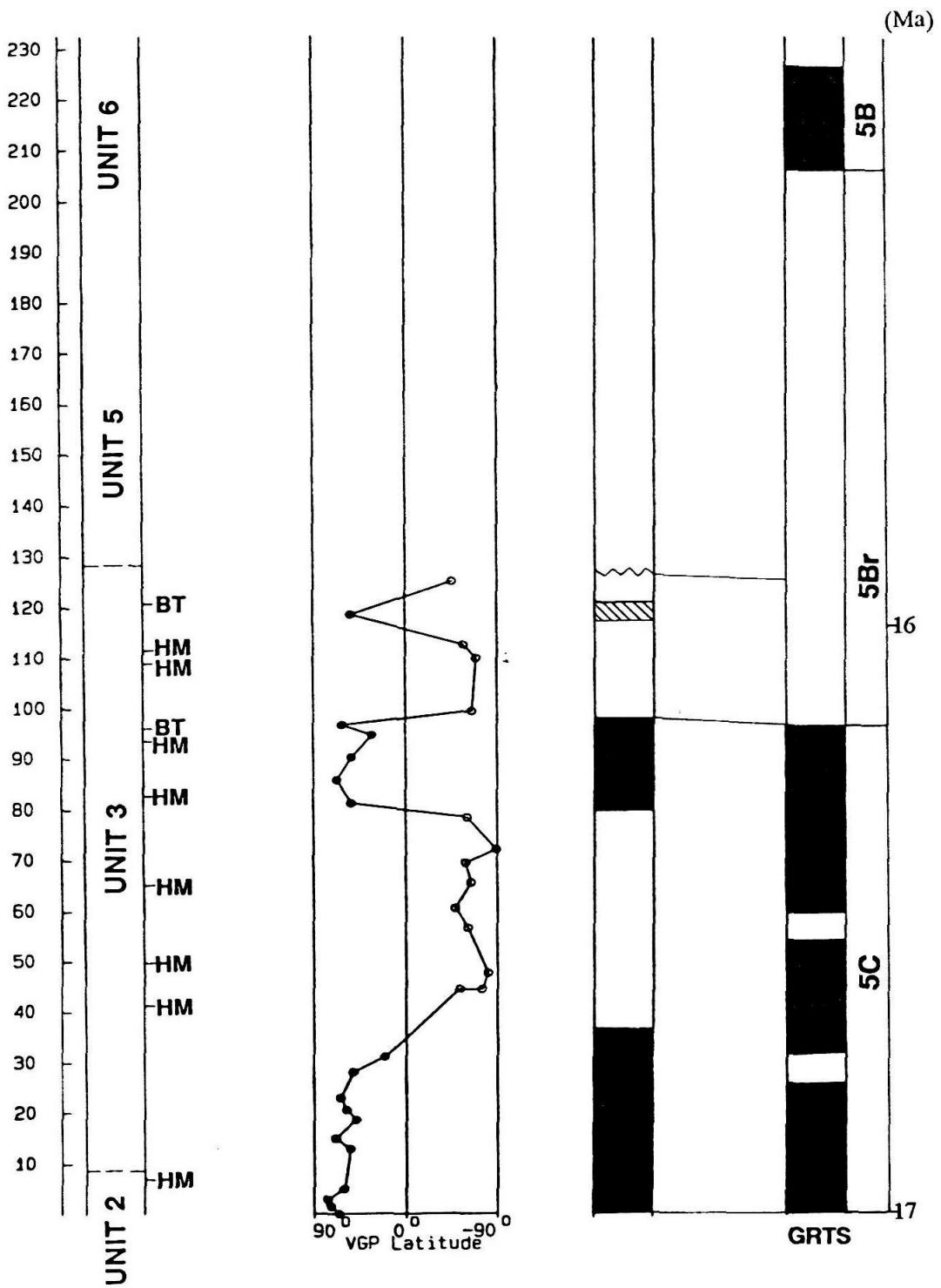
The VGP latitude of the characteristic component of each sample is plotted against stratigraphic thickness. Solid and white columns of magnetic polarity stratigraphy represent normal and reversed magnetic polarities, respectively. The boundaries of polarity magnetozone are placed at intermediate position between two successive sites having opposite polarities. The unit boundaries and the level of collected fossils are indicated in and next to the most left column. Stratigraphic levels of fossils are projected relatively on to these sections based on those of Woodburne and Golz (1972). Ages of the fossils are also shown at the bottom of the figure. The sampling sections are indicated next to the VGP latitude plots, and see Figure 9 for the locations.



**Fossil Ages:** Ct - *Copemys tenuis* (15 - 13.5 Ma);  
 BT - Barstovian (16 - 12 Ma);  
 HM - Hemingfordian (21 - 16 Ma)

**Figure 16. Magnetostratigraphy of unit 3 and its correlation to the Standard Magnetic Polarity Time Scale (Harland et al., 1982).**

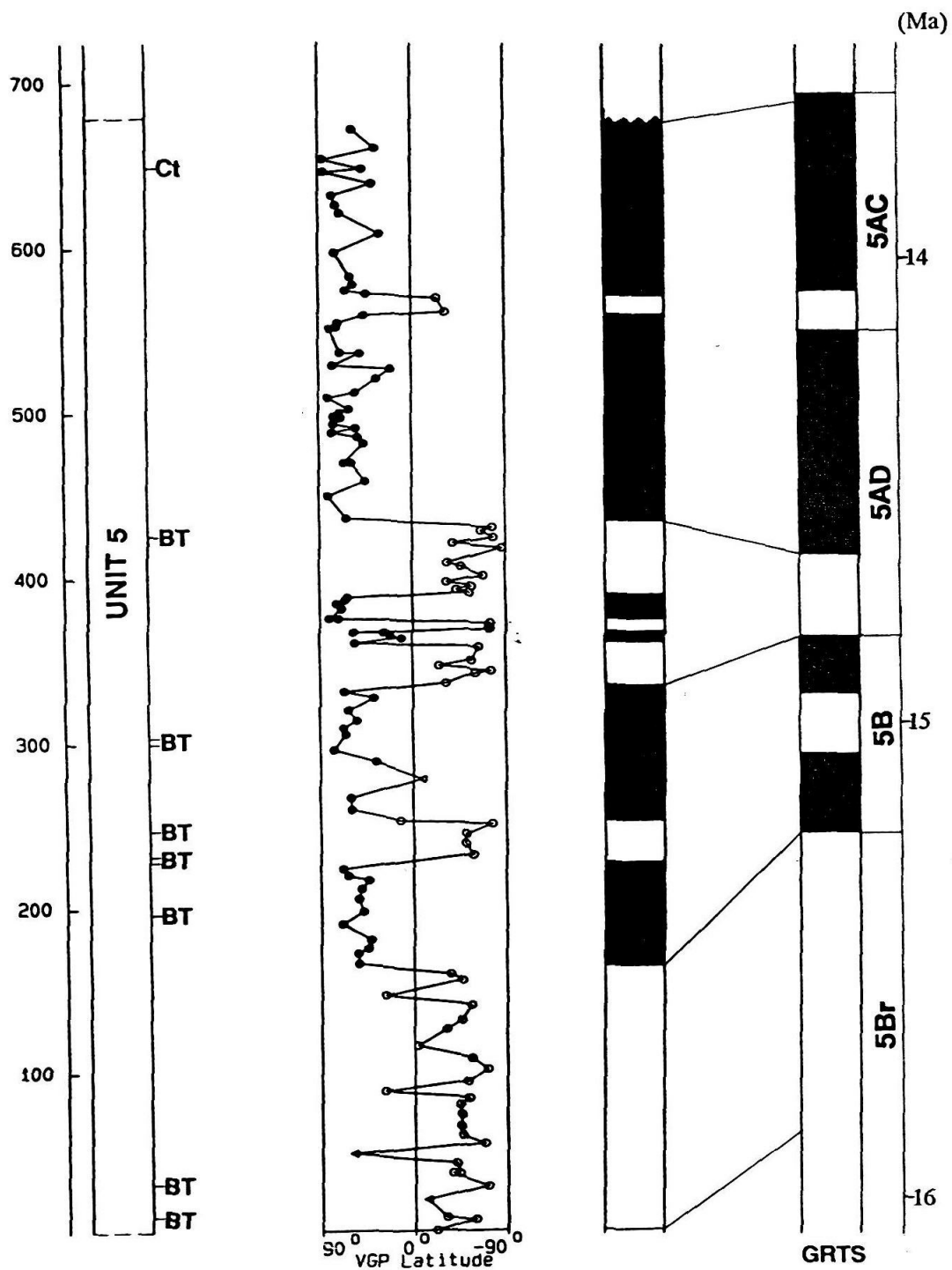
Plotting conventions are the same as for Figure 15. Samples are all collected in section MS - Ca (Figure 9, section b), central part of the formation. Fossil data are from Woodburne and Golz (1972). Barstovian (BT) fossils were collected from a different section (locality) from that were Hemingfordian fossils.



**Fossil Ages:** BT - Barstovian (16 - 12 Ma);  
 HM - Hemingfordian (21 - 16 Ma).

**Figure 17. Magnetostratigraphy of unit 5 and its correlation to the Standard Magnetic Polarity Time Scale (Harland et al., 1982).**

Plotting conventions are the same as Figure 15. Samples are all from section MS - Ca (Figure 9, section b), central part of the formation.



**Fossil Ages:** Ct - *Copemys tenuis* (15 - 13.5 Ma);  
 BT - Barstovian (16 - 12 Ma).



meters below the units 5 - 6 boundary of the Cajon Formation. The bottom of the section is also just a few meters above the units 3 - 5 boundary; this section therefore covers unit 5 entirely with average intersample distances of less than 10 meters.

The magnetic polarity zonation of unit 6 obtained from the northwestern exposures of the Cajon Formation (section NW - Ca) contains two long intervals of normal polarity at its top, and one at the bottom (Figures 15 and 18). Two shorter normal and reversed intervals are present in between, with what appears to be a long reversed polarity chron that is partially obscured by a 45-meter thick gap covered by Quaternary sediments. The boundary between units 5 and 6 is traversed and shown on the magnetic polarity stratigraphy. The location of our paleosol horizon with *P. stirtoni* and *C. tenuis* is shown by the arrow in Figure 18.

As discussed above, previous biostratigraphic studies imply that the age of unit 6 is younger than 15 Ma, and the middle should not be much younger than 13.5 Ma. It must also predate the Phelan Peak Formation, which overlies it. Therefore, the top of unit 6 of the Cajon Formation should have been deposited sometime between 14 and 5 Ma ago. Based on the depositional style of units 3, 5, and 6, we feel justified in assuming no major time break occurs within these units or at the boundaries between them. Therefore, unit 5 must be at least 14 Ma or older, and unit 3 would be about 16 Ma (at the Hemingfordian - Barstovian boundary) in age.

Based on above proximate age constraints, the magnetic polarity stratigraphy of units 3, 5, and 6 of the Cajon Formation can be matched well with the geomagnetic reversal time scale (GRTS) of Harland et al. (1982) as follows: as both Hemingfordian (21 - 16 Ma) and Barstovian fossils were found from unit 3 of the formation, the depositional time period of unit 3, probably the uppermost part, should contain this mammalian age boundary at about 16 Ma. Therefore, the top normal magnetozone of

unit 3 should match with the top normal chron of Chron 5C of the GRTS, while its bottom probably matches the bottom of the Chron 5C (Figure 16). This constrains the age of unit 3 at this locality to be from about 16.9 to 15.9 Ma.

With proximate age constraints between 14 and 16 Ma, the magnetic polarity stratigraphy of unit 5 can be matched easily with the chrons of GRTS from 5Br to 5AC (Figure 17). There are two very short normal magnetozones in the middle of the section, which add some ambiguity. Compared with other magnetozones, however, their much shorter duration suggests that they might be some short term disturbance of the geomagnetic field or they may not be recognized by GRTS. Hence, the otherwise good match between the magnetic polarity stratigraphy of unit 5 with GRTS suggests that unit 5 was deposited in a time period range from 16.1 Ma to 13.8 Ma.

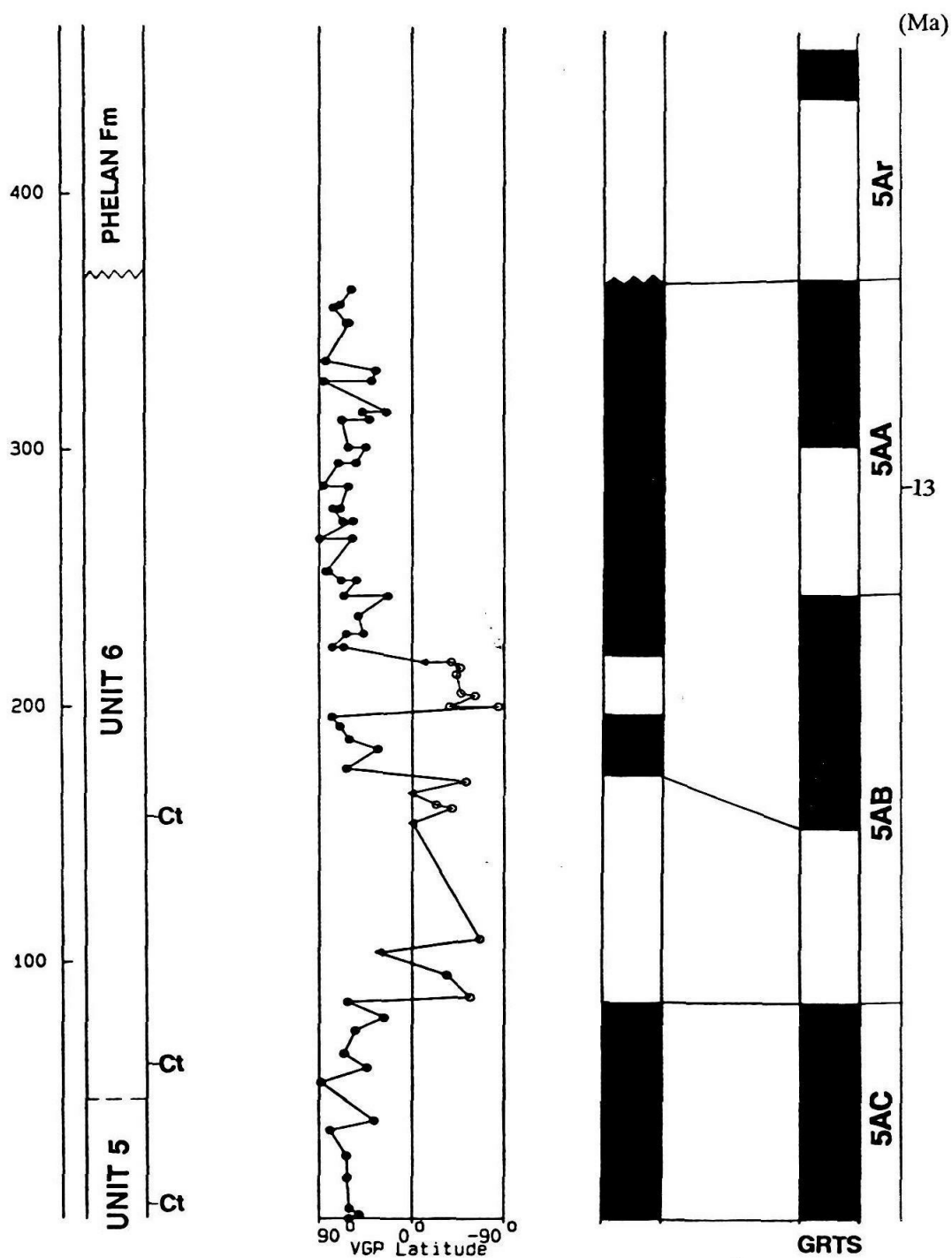
Based on the microfossil age and magnetostratigraphic age constraints of units 5 and 3, the magnetic zonation of unit 6 appears to match the chrons from the top of 5AC to 5AA of the GRTS (Figure 18). The uppermost unit of the Cajon Formation was thus deposited during the time period from 13.8 to 12.7 Ma.

### Depositional Rate

Magnetostratigraphic results from this study imply that the 1200 meters of the upper Cajon Formation were deposited over a period of about 4 million years, yielding an average sedimentation rate of 295 meters per million years ( $0.3 \pm 0.19$  m / k.y.). Average sedimentation rates of units 5 and 6 are almost the same ( $0.34 \pm 0.18$  m / k.y. and  $0.35 \pm 0.26$  m / k.y., respectively), while the rate of unit 3 ( $0.15 \pm 0.07$  m / k.y.) is almost half of units 5 and 6 (Figure 19). The relatively smaller variation of, and lower depositional rate of unit 3 are probably due to its regular and intermittent deposition, suggested by the regular occurrence of weathered red beds within the unit. Hence, the

**Figure 18. Magnetostratigraphy of unit 6 of the Cajon Formation and its correlation with the Standard Magnetic Polarity Time Scale of Harland et al. (1982).**

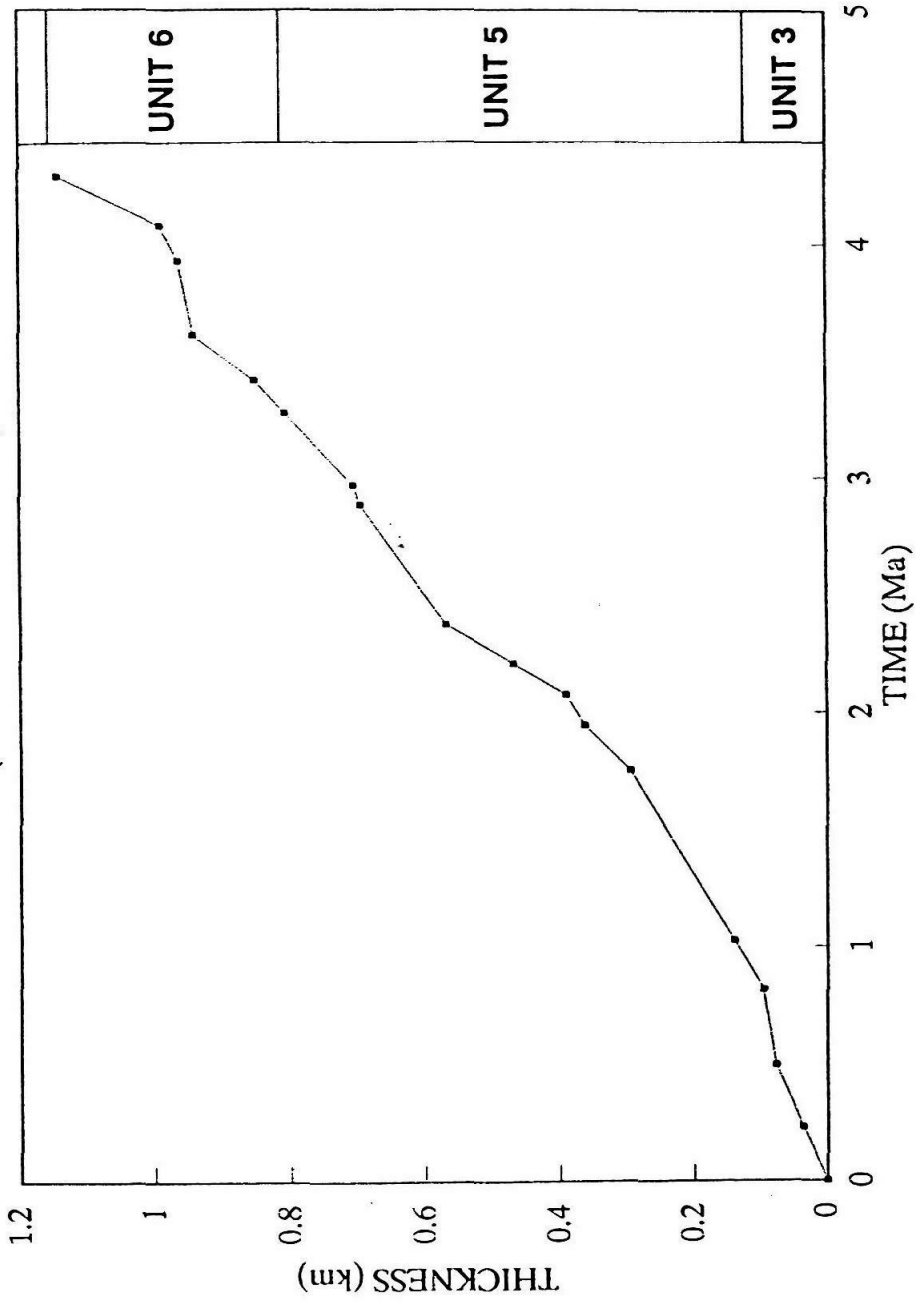
Plotting conventions are the same as for Figure 15. Section is located at the northwestern part of the formation, section NW - Ca (Figure 9). The approximately stratigraphic level at which microvertebrate fossils were found by collaboration with Reynolds is indicated by an arrow.



Fossil Ages: Ct - *Copemys tenuis* (15 - 13.5 Ma);

**Figure 19. Sedimentation rate curve of the Cajon Formation.**

# SEDIMENTATION RATE (CAJON FORMATION)



sedimentation rates of units 5 and 6 are higher but also irregular even though their sediments are finer whereas the lower units are more conglomeratic.

### Rotations

All stable or primary directions of individual units of the Cajon Formation at different localities were analyzed using both Fisher (1953) and Bingham (1974) statistics. The results are shown in Table 3. Rotations that occurred in the upper part of the Cajon Formation were found at different localities along the long axis of the formation (and of the valley). Table 3 and Figure 20 show average paleomagnetic results for units of the Cajon Formation at different places, based only on those samples with clean separation of the magnetic components using Principal Component Analysis (Kirschvink, 1980). Some shallowing of the magnetic inclination appears to be present, similar to that typically seen for the DRM carried by sedimentary rocks. At the northwest end of the formation, the mean stratigraphic declination for unit 6 of the Cajon Formation is  $8.0^{\circ} \pm 6.5^{\circ}$  at the 95% confidence level. Hence, little rotation appears to have occurred in unit 6 of the Cajon Formation at this locality. Unit 5 at this locality shows about  $20^{\circ}$  clockwise rotations, which are similar to the rotations of other localities of the formation. However, the larger rotation in unit 5 at this locality is probably due to secular variation that may not be averaged out by short stratigraphic section (about 50 meters) and/or relatively insufficient samples (11 cleaned ones).

Units 3, 5, and 6 near the central part of the Cajon Formation all show rotations between 22 and 26 degrees clockwise rotation (Table 3 and Figure 20) compared with expected mid-Miocene directions for North America ( $D = 1.9^{\circ}$ ,  $I = 47.5^{\circ}$ , Irving and Irving, 1982).

At the northeastern end of the Cajon Formation next to the Squaw Peak fault

**Table 3. Results of Fisher (upper part) and Bingham (lower part) statistics.**  
 For all units of the Cajon Formation at different places. Only those samples that reached stable primary directions were used for calculations.

| Unit                     | N  | Geographic |      |              |             | Tilt-corrected |      |              |              |        |  |
|--------------------------|----|------------|------|--------------|-------------|----------------|------|--------------|--------------|--------|--|
|                          |    | Dec        | Inc  | $\alpha$ -95 | K           | Dec            | Inc  | $\alpha$ -95 | K            |        |  |
| <b>Southeastern Part</b> |    |            |      |              |             |                |      |              |              |        |  |
| 5                        | 28 | 274.4      | 58.2 | 8.3          | 11.8        | 26.6           | 36.7 | 8.3          | 11.7         |        |  |
| 6                        | 18 | 359.7      | 39.1 | 19.7         | 4.1         | 26.5           | 42.3 | 11.1         | 10.7         |        |  |
| <b>Central Part</b>      |    |            |      |              |             |                |      |              |              |        |  |
| 3                        | 31 | 315.3      | 66.7 | 7.8          | 12.0        | 21.4           | 34.5 | 7.8          | 12.0         |        |  |
| 5                        | 92 | 284.9      | 78.9 | 4.9          | 10.1        | 24.7           | 39.1 | 4.5          | 11.9         |        |  |
| 6                        | 14 | 6.8        | 61.4 | 15.8         | 7.3         | 22.2           | 37.7 | 10.4         | 15.7         |        |  |
| <b>Northwestern Part</b> |    |            |      |              |             |                |      |              |              |        |  |
| 5                        | 11 | 234.8      | 73.7 | 16.1         | 9.0         | 20.7           | 27.0 | 13.4         | 12.6         |        |  |
| 6                        | 59 | 197.0      | 79.7 | 7.4          | 7.2         | 8.0            | 36.1 | 6.5          | 9.2          |        |  |
| Unit                     | N  | Dec        | Inc  | $\alpha$ -95 | K1, K2      |                | Dec  | Inc          | $\alpha$ -95 | K1, K2 |  |
| <b>Southeastern Part</b> |    |            |      |              |             |                |      |              |              |        |  |
| 5                        | 28 | 274.2      | 58.2 | 6.8, 8.3     | -9.4, -6.0  | 26.6           | 36.7 | 6.8, 8.9     | -9.5, -5.9   |        |  |
| 6                        | 18 | 356.7      | 39.2 | 12.5, 28.9   | -6.4, -1.8  | 25.9           | 42.9 | 8.4, 11.8    | -9.9, -5.4   |        |  |
| <b>Central Part</b>      |    |            |      |              |             |                |      |              |              |        |  |
| 3                        | 31 | 315.5      | 67.0 | 5.8, 8.5     | -11.6, -5.8 | 21.8           | 34.5 | 5.8, 8.5     | -11.6, -5.8  |        |  |
| 5                        | 92 | 283.8      | 78.9 | 4.4, 5.2     | -7.5, -5.6  | 24.8           | 39.0 | 3.8, 3.9     | -9.5, -9.1   |        |  |
| 6                        | 14 | 3.4        | 62.5 | 11.9, 16.5   | -7.2, -4.1  | 22.2           | 38.0 | 7.5, 11.1    | -14.5, -7.1  |        |  |
| <b>Northwestern Part</b> |    |            |      |              |             |                |      |              |              |        |  |
| 5                        | 11 | 238.3      | 74.4 | 7.5, 17.3    | -19.7, -4.3 | 20.7           | 25.4 | 6.6, 14.7    | -24.3, -5.5  |        |  |
| 6                        | 52 | 193.6      | 81.0 | 6.4, 6.4     | -6.3, -6.3  | 7.4            | 36.0 | 5.5, 7.0     | -7.6, -5.0   |        |  |

N -- number of the samples used for calculation;

Dec -- declination;

Inc -- inclination;

$\alpha$ -95 -- error angle of mean at 95% confidence level;

K, K1, and K2 - precision value.

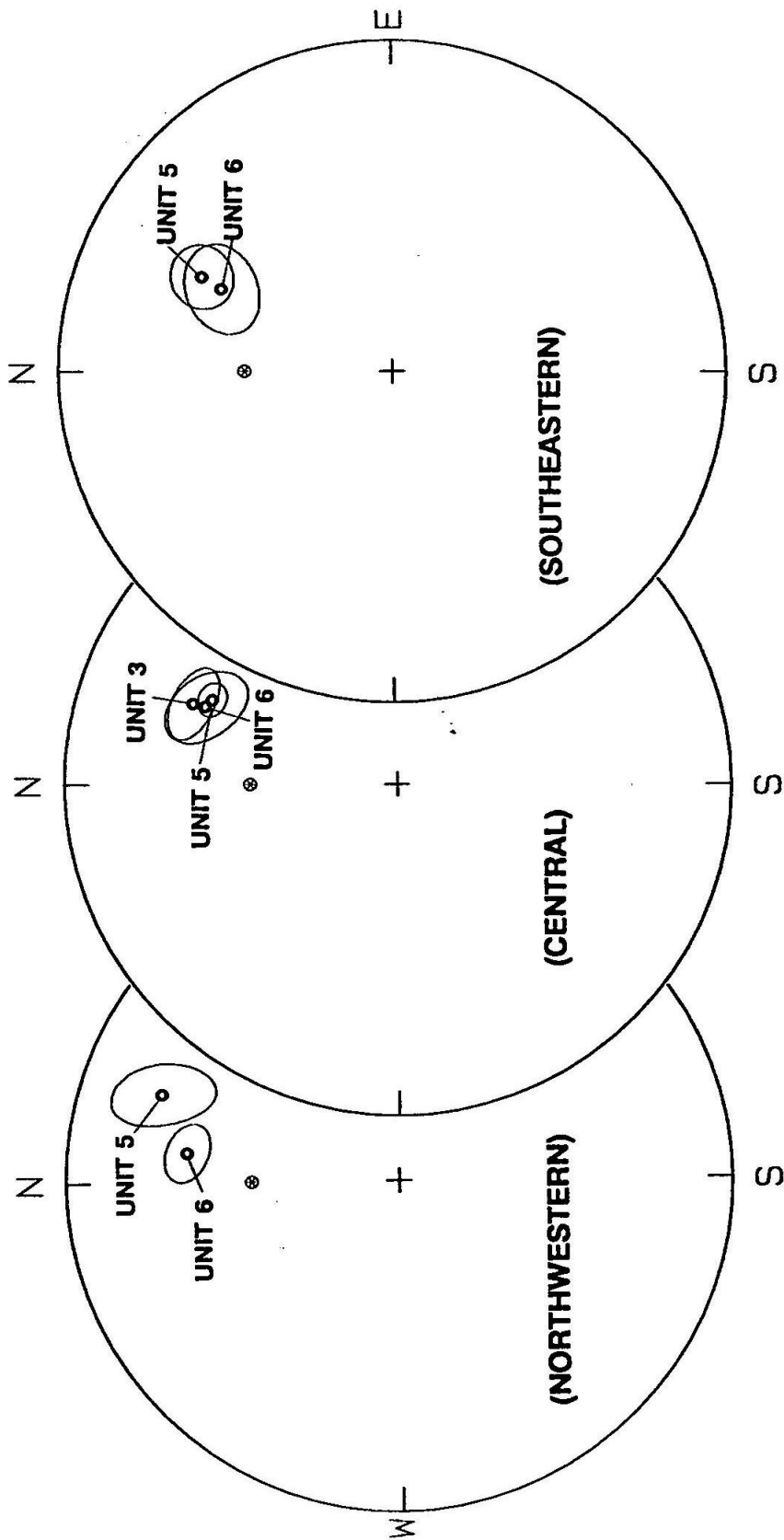
Geographic -- the values calculated before correction for tilt of bedding;

Tilt-corrected -- the values after structural correction.



**Figure 20. Mean directions of all units at different localities.**

The error ovals are from Bingham (1974) statistics; the reference Miocene geomagnetic field direction (Irving and Irving, 1982) is represented by circled star.



**CAJON FORMATION**

and the DOSECC deep hole, the rotations found in units 5 and 6 are also about 26° in clockwise sense (Table 3 and Figure 20). Results reported earlier from unit 5 (Liu et al., 1988) were augmented in this study with several additional samples. The new results are similar to the previous results, but with higher precision.

Averaged directions, from all cleaned samples at each locality, are shown in Table 4. The units at each individual locality have similar amounts of rotation, indicating that the rotation occurred after the deposition of the Cajon Formation. Another feature of the rotation in Cajon Formation is the apparent difference between the northwestern and northeastern parts of the formation, which is probably due to differential thrusting that caused the rotations of the Cajon Formation (see discussion).

**Table 4. Mean directions of sections.**

Calculated from all studied units at each locality using both Fisher (1953, the upper part) and Bingham (1974, the lower part) statistics.

| Loc. | N   | Dec   | Geographic<br>Inc | $\alpha$ -95 | K   | Dec  | Tilt-corrected<br>Inc | $\alpha$ -95 | K    |
|------|-----|-------|-------------------|--------------|-----|------|-----------------------|--------------|------|
| NE   | 46  | 148.8 | 59.0              | 15.7         | 2.8 | 26.5 | 38.9                  | 6.5          | 11.4 |
| CENT | 137 | 308.4 | 76.3              | 4.3          | 8.9 | 23.6 | 37.9                  | 3.6          | 12.3 |
| NW   | 65  | 202.7 | 79.9              | 6.8          | 7.8 | 9.6  | 34.1                  | 6.1          | 9.3  |

| Loc. | N   | Dec   | Inc  | $\alpha$ -95 | K1, K2     | Dec  | Inc  | $\alpha$ -95 | K1, K2     |
|------|-----|-------|------|--------------|------------|------|------|--------------|------------|
| NE   | 46  | 111.0 | 59.2 | 7.1, 14.3    | -7.1, -2.4 | 26.5 | 39.1 | 5.3, 7.1     | -9.5, -5.7 |
| CENT | 137 | 307.0 | 76.4 | 3.9, 4.4     | -6.6, -5.4 | 24.0 | 37.0 | 3.2, 3.8     | -8.7, -6.6 |
| NW   | 65  | 202.0 | 81.1 | 6.3, 6.6     | -5.6, -5.2 | 9.2  | 33.9 | 5.4, 6.4     | -7.1, -5.3 |

Dec -- declination;

Inc -- inclination;

$\alpha$ -95 -- error angle of mean at 95% confidence level;

K, K1 and K2 -- concentration value;

Geographic -- the values calculated before correction for tilt of bedding;

Tilt-corrected -- the values after structural correction.

(See Figure 9 for section localities.)

## II. Crowder Formation

### Sampling

Samples were taken from both lower (units 1, 2, and 3) and upper parts (units 4 and 5) of the Crowder Formation. The methodology used for the upper part of the Crowder Formation is the same as that for the upper part of the Cajon Formation, results of the paleomagnetic study has been also published (Weldon, 1984). Thus, in the following section, only the study of the lower part of the Crowder Formation, based mainly on the paleomagnetic study of Winston (1985), will be discussed in detail.

The thickest, most representative section of the lower part of the Crowder Formation was found to be adjacent to the Squaw Peak fault (Figure 9). This section was also selected for its continuous exposures, accessibility, and location with respect to section of upper Crowder Formation. Another section was measured, described, and sampled along Crowder Creek about 1 km to the east in the early parts of the study. This section provides a basis for examining lateral variations and similarities in lithology.

Stratigraphic thickness was measured with a combination of tape measure and Brunton Compass. Occasionally, poor exposure of strata or difficult terrain required the extrapolation of some measurements. For the lower part of the Crowder Formation, paleomagnetic samples were collected during and after description and measurement of the section using a hand-held, water-cooling drill, and oriented by standard methods. Samples in the aforementioned secondary section at Crowder Creek were taken every 10 meters from suitable and unsuitable strata. Very coarse sandstones to fine sandstones were sampled and poor paleomagnetic results were obtained from most of these strata.

In the primary section near the Squaw Peak fault, samples were taken at intervals of no less than 6 m and no more than 30 m with supplementary samples taken to fill in the larger intervals where possible. Three oriented samples were taken at each location in both sections. Strata that had been affected by pedogenetic alternate, i.e., white mottling, altered depositional fabrics and discoloration (mostly shades of green and violet), were avoided except where there were no other suitable strata. There appears to be correlation between the aforementioned pedogenetic characteristics and poor paleomagnetic results. This was true especially in Crowder units 2 and 3 where pedogenetic mottling and discoloration of siltstones and mudstones becomes more prominent.

### Stability Tests

A fold test was conducted for the Crowder samples to determine whether the magnetic vectors obtained were acquired close to the time of deposition. Action along the Squaw Peak fault has provided a number of ideal opportunities within the Crowder Formation to conduct fold tests. For each individual test, samples were taken from these folded beds at the same stratigraphic level. The results of a typical fold test are illustrated by the equal-area plots on Figure 21. The geographic directions are scattered, while the tilt-corrected directions are clustered in a reversed polarity direction, indicating that the magnetic remanence in the Crowder Formation was acquired prior to folding. A reversal test further supports the reliability of these magnetic data, as the mean of all normal samples ( $D = 6.0^\circ$ ,  $I = 46.1^\circ$ ) is antiparallel to the mean of all reversed samples ( $D = 185.6^\circ$ ,  $I = -45.9^\circ$ ) within  $1^\circ$  (Figure 22).

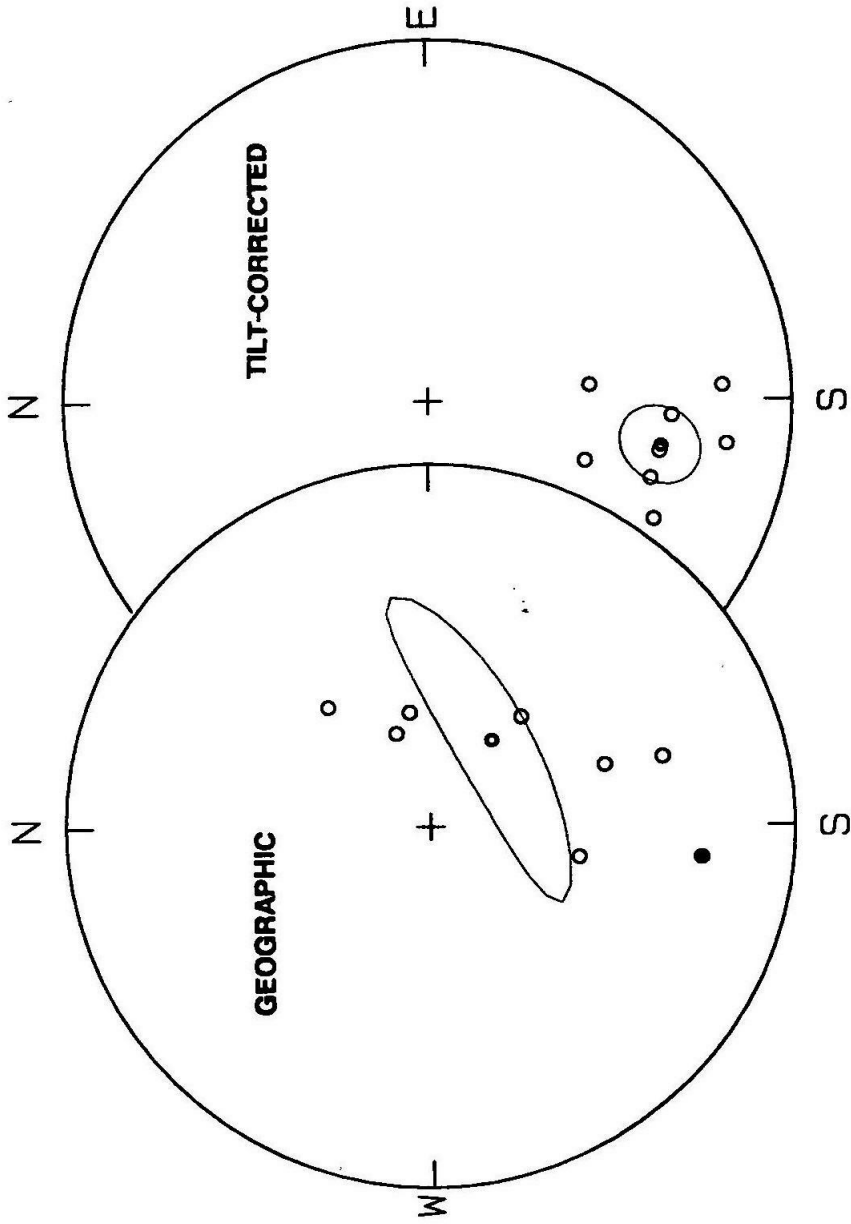
**Figure 21. Fold test of the Crowder Formation samples.**

Stereographic projection for eight samples from a fold test in Crowder Unit 4.

LEFT -- results obtained before tilt corrections of bedding;

RIGHT - results obtained after tilt corrections of bedding.

Plotting conventions are the same as for Figure 3.

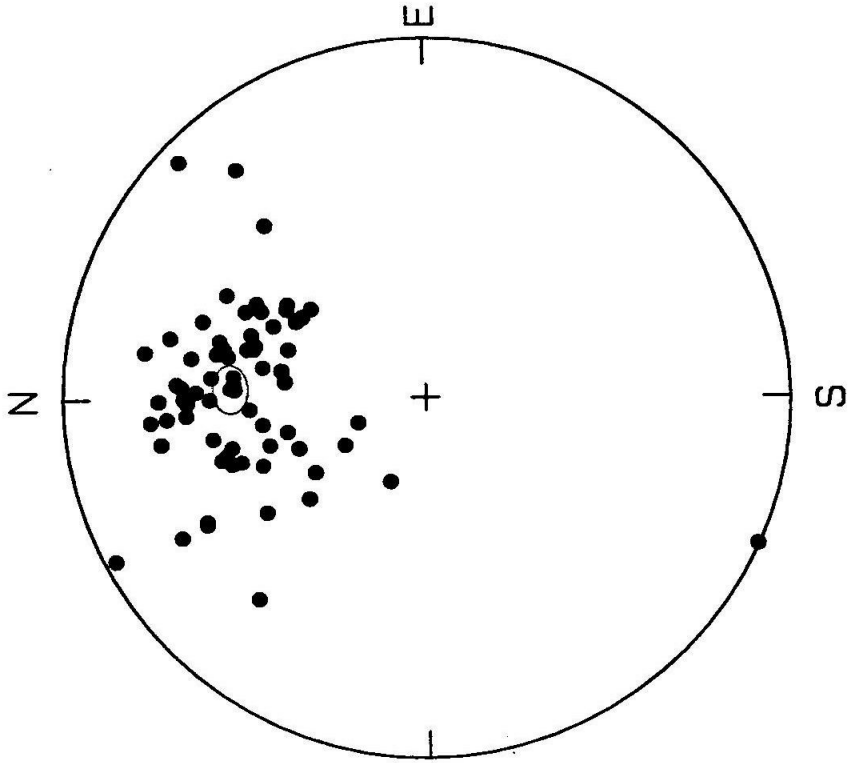


**CROWDER FORMATION FOLD TEST**



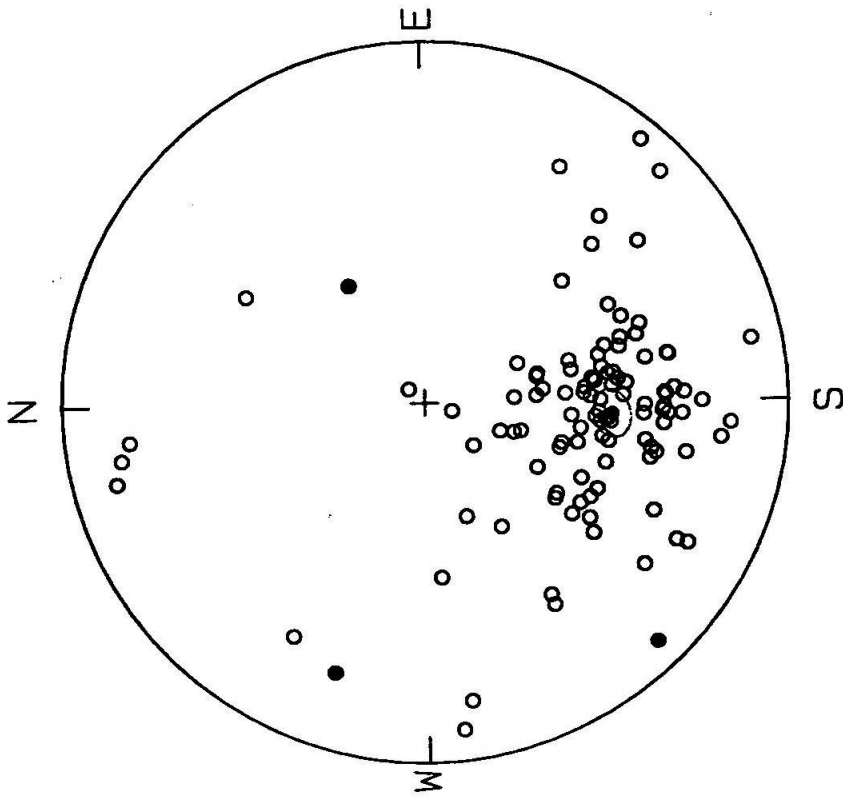
**Figure 22. Reversal test of the Crowder Formation samples.**

**Plotting convention is the same as Figure 12.**



NORMAL DIRECTIONS

Tilt Corrected



REVERSE DIRECTIONS

Tilt Corrected

### Stratigraphic Correlation

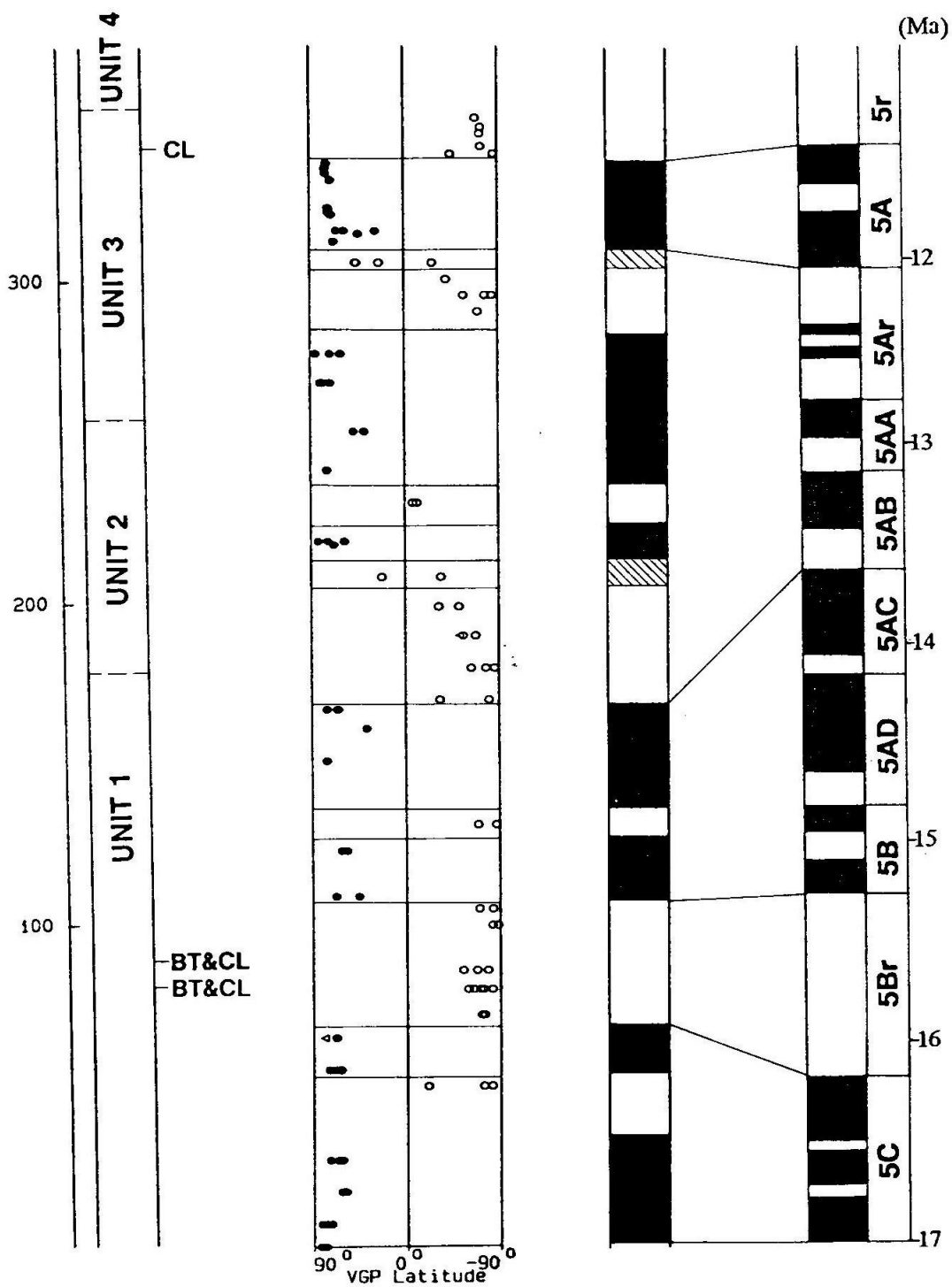
Correlation of the magnetic polarity stratigraphy of the Lower Crowder Formation to the Standard Magnetic Time Scale (Harland et al., 1982) is difficult. There are 13 distinct magnetozones and 2 hachured areas that represent magnetozones of indeterminable polarity. Additional magnetozones may be present within the normal, reversed, and ambiguous zones because of the sampling interval and the nature of the fluvial deposit.

The Lower Crowder magnetic polarity stratigraphy has two relatively long reversed zones. The lower zone covers the location of the Hemingfordian-Barstovian (approximately 16 Ma) fossils collected by Reynolds (1985). Assuming that the fossils have been dated correctly, the reversed zone in which they are located is polarity Chron 5Br (Figure 23). It appears that the base of the Crowder Formation is about 17 Ma old. Due to the relatively low resolution of the polarity stratigraphy, it is difficult to calibrate the upper age of the lower part of the formation. The boundary between units 3 and 4 might range in age from 13 Ma to 11.5 Ma, depending on the correlation made to the GRTS. The latter correlation is illustrated in Figure 23. This correlation discounts the short subchrons of the Standard Time Scale because of the relatively low resolution of our polarity stratigraphy. The only problem with this correlation is that the magnetozones of our polarity stratigraphy and the Standard Scale do not match in relative length (time) to one another. There are two possible explanations for this: 1) deposition rate was extremely variable during deposition of Crowder sediments or 2) the correlation is wrong. The first explanation, of course, is the preferred one in this case, because other correlations are just as bad.

The magnetic polarity stratigraphy of the entire Crowder Formation is illustrated

**Figure 23. Magnetostratigraphy of the lower part of the Crowder Formation and its correlation with GRTS.**

The figure illustrates stratigraphic level (in meters), lithology, sedimentary structures, fossils, (from Reynolds, 1985) and unit boundaries. Characteristic components of all samples are shown by solid (normal) and open (reversed) circles, and triangles (samples that were statistically bad or gave ambiguous results). The geomagnetic reversal time scale (GRTS) is adapted from Harland et al. (1982). Microfossils collected from unit 1 have been dated as encompassing Hemingfordian and Barstovian land mammal age (Reynolds, 1983, 1984, 1985). The fossil levels are thus designated as BT&CL (ca. 16 Ma).



**Fossil Ages:** CL - Clarendonian (12 - 10 Ma);  
 BT - Barstovian (16 - 12 Ma);

in Figure 24. The correlation of the Upper Crowder magnetostratigraphy is more straightforward than the Lower Crowder, because it is dominated by a long reversed interval. Based on middle Clarendonian (approximately 11 Ma) fossils collected by Reynolds (1985) within the long reversed zone, the Crowder 3-4 boundary is at about 11.5 Ma and the top of the Crowder Formation ranges from 10.3 Ma to about 9.0 Ma.

From these correlations, the age for the entire Crowder Formation illustrated in Figure 24 was derived. The base of the Crowder Formation at Cajon Junction is younger than about 17 Ma and lies somewhere within Chron 5C. The unit 1-2 boundary lies at about 13.5 Ma within the 5ABr polarity chron. The unit 2-3 boundary lies at about 12.5 Ma within the 5Ar polarity chron. The unit 3-4 boundary lies just below the 11.5 Ma fossil locality, at the boundary between the 5A and 5r polarity chrons. The unit 4-5 boundary lies at about 11 Ma within the relatively long 5r polarity chron. The top of the Crowder Formation, which is unconformably overlain by Phelan Peak Formation (Weldon, 1984,1986), is approximately 9.0 Ma old and lies within the Chron 5.

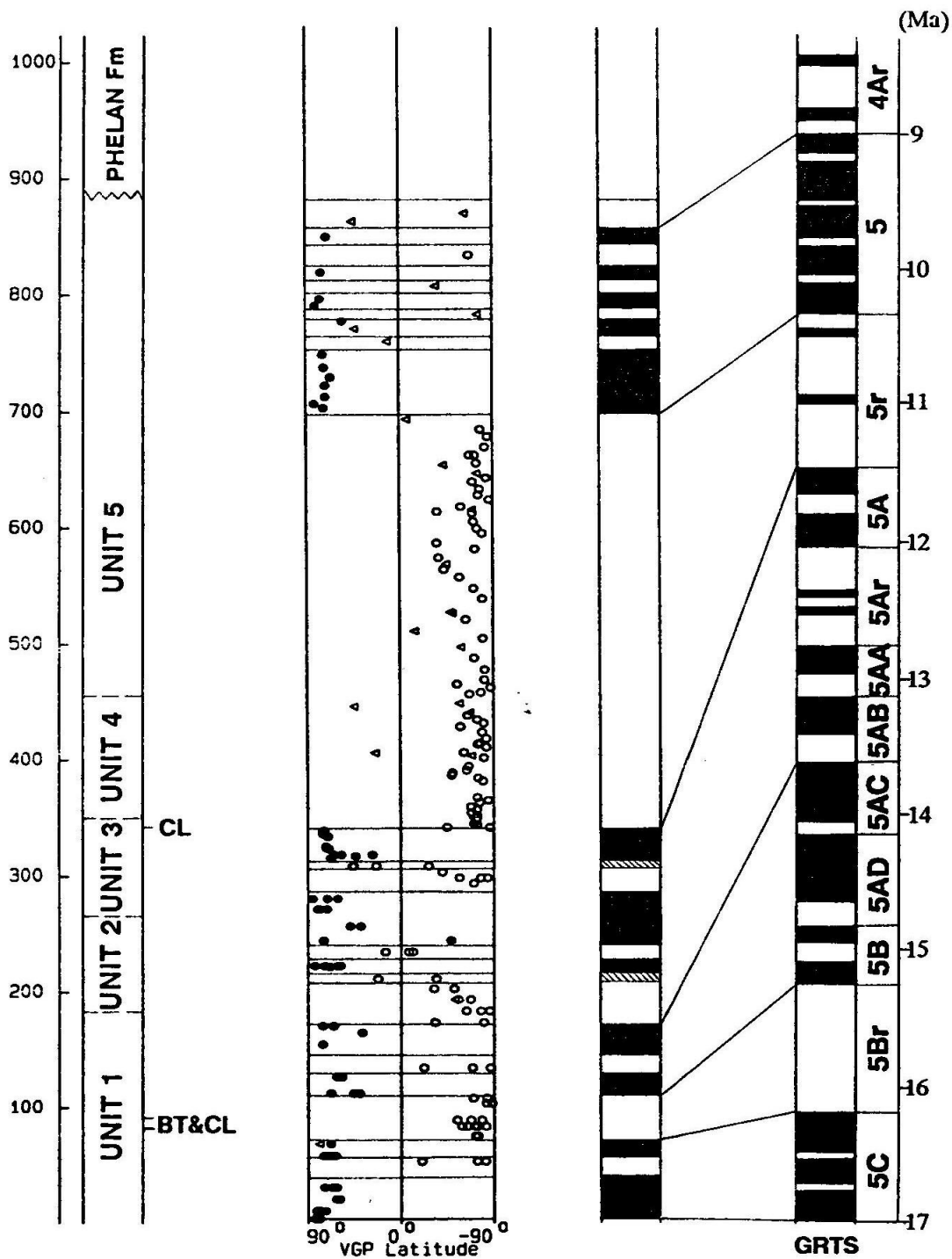
### Sedimentation Rate

Based on above results, the 800 meters of the Crowder Formation were deposited over a period of about 7.5 million years. This yields an average sedimentation rate of 107 meters per million years, which translates to about 0.1 meters every 1,000 years.

The variability of sedimentation rate is illustrated in Figures 23, 24, and 25. The finer-grained units of the Crowder Formation appear to have a higher sedimentation rate than the coarse-grained units. Perhaps the coarse-grained material was being transported largely down a slope towards the center of the basin, inhibiting its deposition. As the basin filled, fine-grained sediments reached the area, resulting in a

**Figure 24. Magnetic polarity stratigraphy of the Crowder Formation.**

Magnetic-polarity stratigraphy from the Crowder Formation. The match between the MPS and GRTS is made using least-squares data. Plotting convection and fossil level designation are the same as Figure 23.



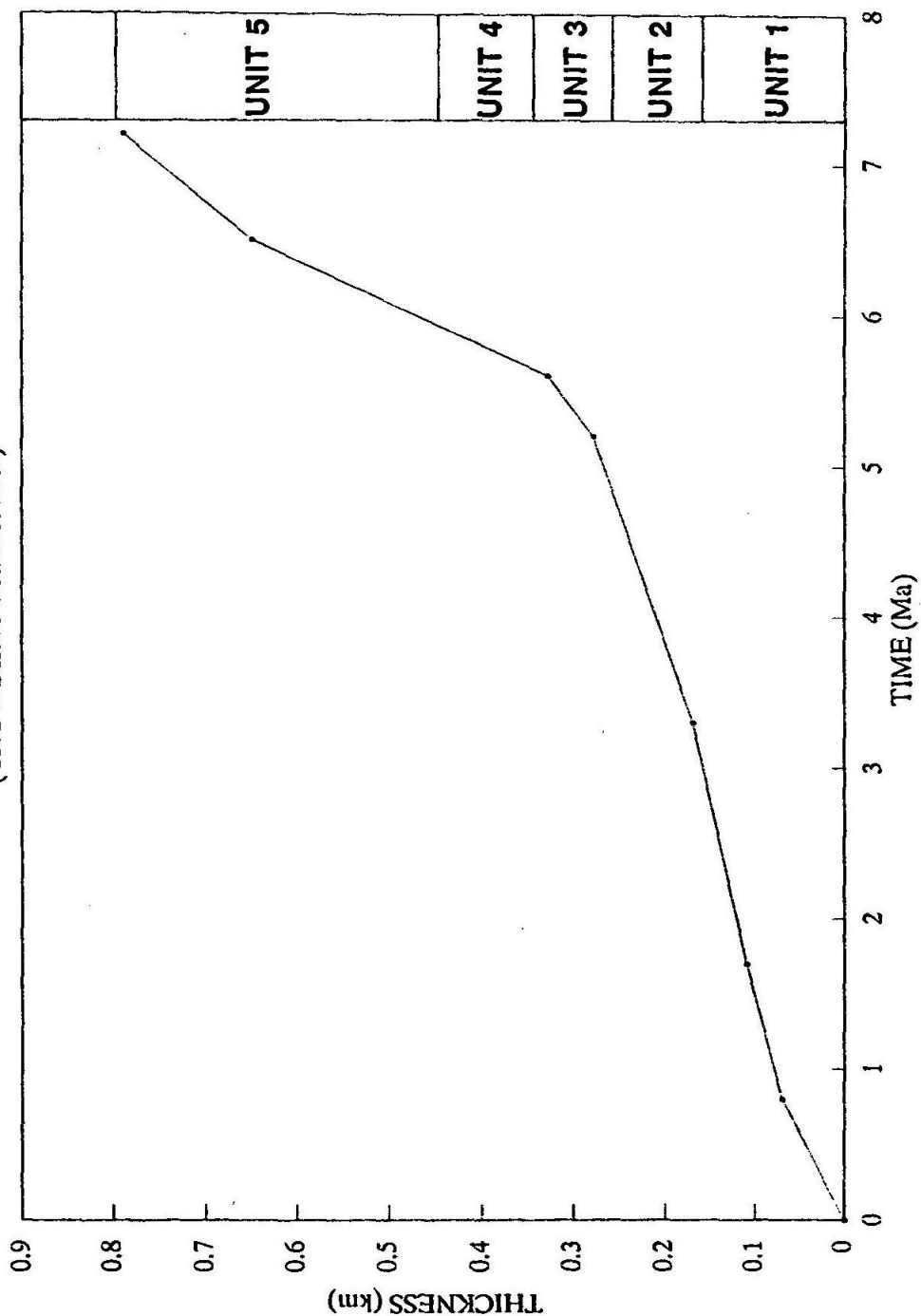
Fossil Ages: CL - Clarendonian (12 - 10 Ma);  
 BT - Barstovian (16 - 12 Ma);



**Figure 25. Depositional rate variation with time.**

Graph of thickness vs. age. This illustrates the variability of the sedimentation rate of the Crowder Formation. The Upper Crowder Formation was deposited more quickly than the Lower Crowder Formation.

# SEDIMENTATION RATE (CROWDER FORMATION)



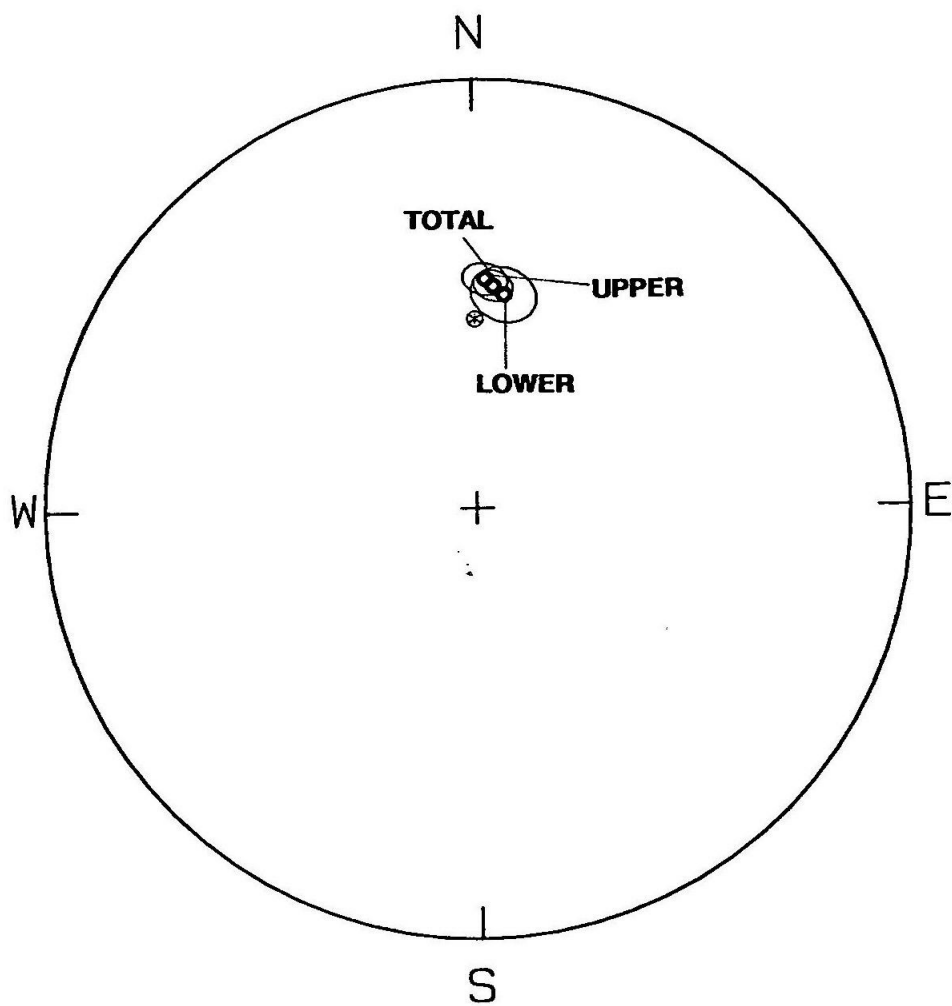
higher deposition rate. This would explain the difficulty in matching the chron lengths of our magnetic polarity scale with the standard time scale. Assuming this to be the case, the match between measured polarities with the standard ones is perhaps not so bad.

### Rotation

Figure 26 illustrates the results obtained by treating samples from both the Lower and Upper Crowder Formation with Bingham statistics. The mean direction of the lower part of the Crowder Formation is slightly different from that of the upper part. Although the difference is not statistically significant, it might be caused by drag on closer lower part of the formation along the Squaw Peak fault (discussed next). In contrast to the Cajon Formation, these results suggest there has been very little, if any, clockwise rotation of the Crowder Formation.

**Figure 26. Mean of all directions obtained from the Crowder Formation.**

Equal-area plot revealing the result of Bingham statistics on Upper and Lower Crowder data. This plot shows that the Lower Crowder Formation may have been rotated  $7.6^\circ$  and the Upper Crowder rotated  $2.6^\circ$  for an average of  $4.7$  degrees for the Crowder. The error oval for each of these averages is shown. The rotation is statistically insignificant.



### CROWDER FORMATION

Tilt Corrected

## DISCUSSION

The magnetostratigraphies of the Cajon and Crowder formations reveal important information regarding the geologic history of the Central Transverse Ranges and the southwestern Mojave Desert. The deposition of the Crowder Formation began at least 17 million years ago on an eroded surface of igneous basement rock. The approximately 800 meter-thick formation was deposited by a braided fluvial system that flowed from north to south until at least 9.0 Ma. The topography over which this system flowed did not have the mountainous relief that is now present. Any southern and western extension of the Crowder Basin has been long since removed by subsequent faulting, orogenesis, and erosion. The relatively undisturbed presence of what is left of the Crowder Formation is strong evidence that the area where it lies has been relatively immune to the tectonic activity displayed just a few kilometers to the south and west.

In contrast, the deposition of the Cajon Formation may have begun at about 18 Ma on an initially irregular surface by southwestward fluvial streams (Woodburne and Golz, 1972). The depositional condition changed considerably into a low energy environment about 16 million years ago, which may coincide with the boundary between the Hemingfordian and Barstovian mammal age. After this change, about 2000 meters of sediment were deposited in a quite large and relatively stable basin. A considerable part of the Cajon sediments was removed by subsequent faulting and erosion by an alluvial system beginning 12.7 million years ago.

Although the ages refined by this study indicate that the Cajon and Crowder formations overlap in age, they were obviously deposited in different geological and tectonic settings as indicated by large differences in sedimentation style, rate, and

**lithologies. If the Cajon Formation was deposited from about 18 to 12.7 m.y. ago as our data suggest, then the top of the Crowder Formation (with an age of up to 9.0 Ma) is 3.7 Ma younger than the top of the Cajon Formation. This difference and the obvious contrast of depositional characteristics between these two formations seem not to support the proposal (Ehlig, 1988) that the Cajon and the Crowder formations were deposited in the same basin but in different geologic settings. Instead, these two formations must have been deposited in different basins that were located in different geologic and tectonic settings. Considering the original geometries and sizes (more than ten kilometers) of the basins in which the Cajon and Crowder sediments were deposited, and the overlap of their ages, the Squaw Peak fault that separates them must have a minimum displacement on the order of tens of kilometers.**

**Our refined age of the upper Cajon Formation suggests that activity of the Cajon Valley and the Squaw Peak faults started after 12.7 million years ago. As discussed before, unit 5a of the Cajon Formation is probably not related to the activity of the Cajon Valley, because of its wedge shape, presumably narrow source, and truncation of fold pairs that almost perpendicular to the Cajon Valley fault. Hence, unit 6 of the Cajon Formation would be the youngest unit offset by the Cajon Valley fault, which more likely started its activity after deposition of unit 6 of the Cajon Formation. The Squaw Peak fault may have formed after 9.0 Ma, as suggested by the age of the Crowder, the uppermost part of which is apparently offset by the Squaw Peak fault. This suggests that the activities of these two faults (between 12.7 and 4.2 Ma as bracketed by ages of the Cajon Formation and the Phelan Peak Formation) overlap in time with that of the San Gabriel (from 12 to 4 Ma, Woodburne, 1975) and the Liebre Mountain faults (from 8 to 4 Ma, Ensley and Verosub, 1982) as shown in Figure 1. Thus it is consistent with the proposal of Matti et al. (1985) and Weldon (1986) that**

the Squaw Peak and the Cajon Valley faults are the offset extensions of the Liebre Mountain and the San Gabriel faults, respectively.

Luyendyk et al. (1980, 1985) suggested that the Transverse Ranges area has undergone extreme clockwise block rotation. Our results of this study, however, show a contradictory pattern: units in the eastern and central part of the Cajon Formation have been rotated clockwise  $22^\circ$  to  $26^\circ$ , with the magnitude of rotation possibly decreasing northwestwards, away from the Squaw Peak and San Andreas faults. On the other hand, results from the northwestern part of the Cajon Formation and from the entire Crowder Formation (Weldon et al. 1984; Winston, 1985; Weldon, 1986) show little or no significant rotation. In our earlier study (Liu et al., 1988) of the Cajon Formation, we proposed that the rotation of the Cajon Formation decreased either with time or with the distance from the Squaw Peak fault, and the rotations were suggested to be a result of drag along the Squaw Peak fault. However, the similar rotations in different units of the Cajon Formation at the same locality exclude the possibility of progressive rotation during its deposition. The plausible differential rotations between the northwestern and northeastern parts of the Cajon Formation are probably due to non-brittle block rotation caused by drag on the San Andreas and Squaw Peak faults, but the magnitudes and the distributions of the rotations in the Cajon Formation also imply this drag may cause only small local rotations.

Luyendyk et al. (1980, 1985) proposed that the rotation observed in the Western Transverse Ranges occurred between 16 and 10 m.y. ago. Terres and Luyendyk (1985) also suggested that the San Gabriel block between the San Gabriel and San Andreas faults has been rotated clockwise by  $37.1^\circ \pm 12.2^\circ$  or up to  $53^\circ$  (considering  $16^\circ \pm 30^\circ$  counterclockwise rotations in the younger Mint Canyon Formation). It is possible that the Cajon Formation was attached to the San Gabriel block and rotated clockwise



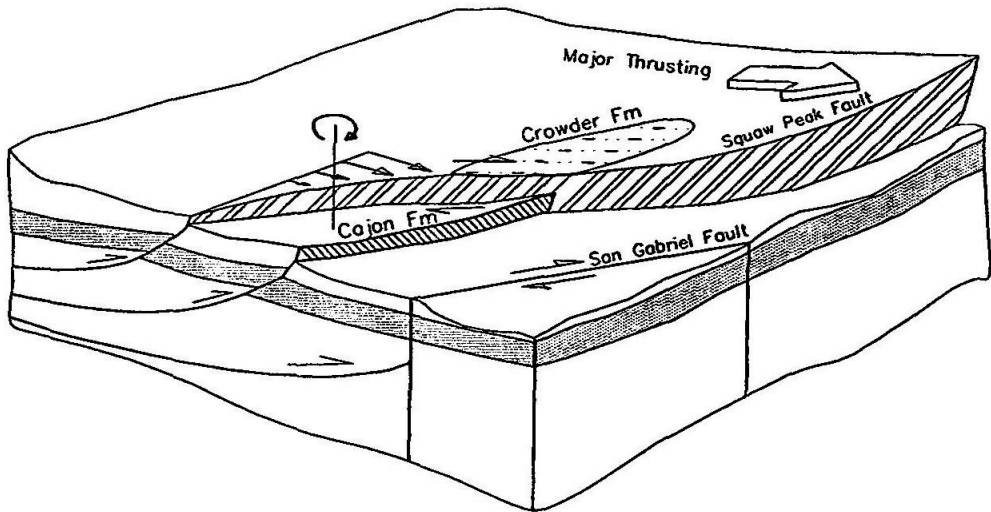
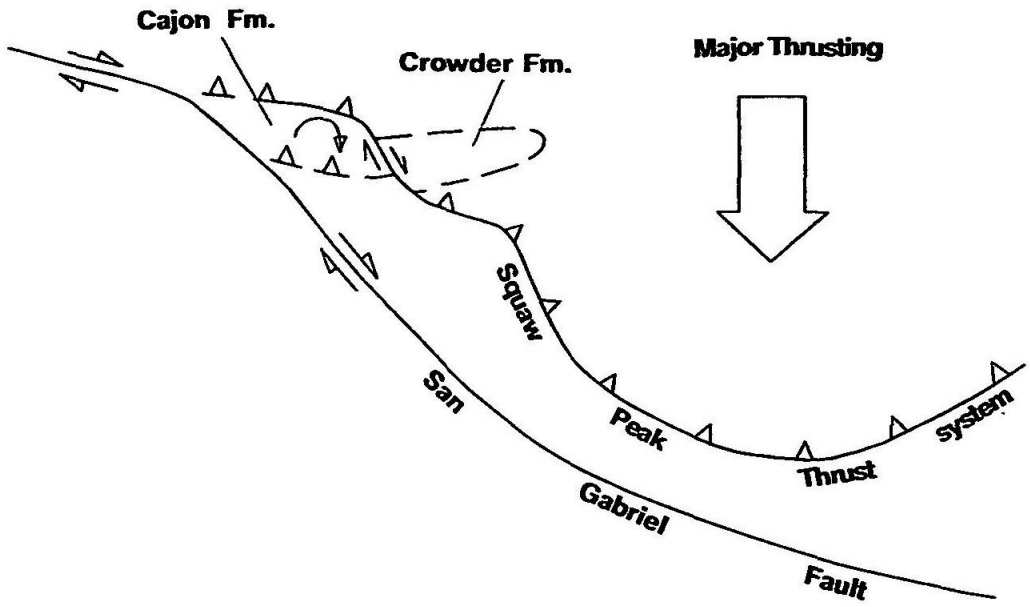
together with it. Afterwards, this part was cut off from the San Gabriel block by the right-lateral offset of the modern San Andreas fault (Weldon, 1986; Matti et al., 1985) and has not been rotated since. In contrast, the San Gabriel block was subsequently rotated counterclockwise (Terres and Luyendyk 1985; Liu et al., in preparation, this thesis, chapter 3). At the same time that the Cajon Formation was being rotated, the Crowder Formation was not affected, presumably because it was deposited in a different region and belonged to a different unit. Subsequent motion along the Squaw Peak fault brought the Crowder into its present position against the rotated Cajon Formation. However, a main problem of this model is the inconsistency of timing for the rotations of both the San Gabriel and Cajon blocks. According to Terres and Luyendyk (1985) and Luyendyk et al (1980, 1985), clockwise rotation occurred in San Gabriel block would stopped at about 12 Ma due to the starting of activity of the San Gabriel fault. This is also suggested by paleomagnetic studies of the San Gabriel block, which show that there seemed no rotation occurred from 12 to 8.5 Ma, whereas counterclockwise rotations have occurred after 8.5 Ma, in the San Gabriel block (Terres and Luyendyk, 1985; Liu et al., 1988, chapter 3, this thesis). On the other hand, the consistency of the rotations in different units of the Cajon Formation indicates that the rotation must occur after the deposition of the formation, i. e., after 12 Ma. If the Cajon Formation was attached to the San Gabriel block as suggested by the proposal of Matti (1985) and Weldon (1986), it would be more likely that the Cajon block rotated counterclockwise than clockwise. Therefore, the rotations of Cajon Valley area cannot be explained by the model of Terres and Luyendyk (1985) and Luyendyk et al. (1980, 1985).

In addition, the displacements along the lateral-slip bounding faults of the Cajon block would cause rotations of opposite sense according to the models of Luyendyk et al. (1980, 1985), Garfunkel and Ron (1985), and Nur et al. (1986). Hence, none of

these models are capable of explaining the rotations in the Cajon Pass area. Although the rotations of the Cajon Formation could occur after deposition of the formation (12.7 Ma) and prior to the movement on the Squaw Peak fault (9.5 Ma), considering that there was no any documented structures responsible for the rotations, it is very unlikely the case.

The obvious difference in rotations of the Cajon and Crowder formations suggests that the rotation must be related mainly to thrusting on the Squaw Peak fault system. The presence of many low angle faults below the Cajon Formation encountered by the DOSECC deep-drilling program (Silver and James, 1988; Silver, personal communication, 1990) suggest that both formations are probably sitting on the top of the Squaw Peak thrust system (Silver, personal communication, 1990) or related low-angle fault system. The Squaw Peak fault, which separates the two formations at the surface, is probably one of the surface faults in this entire system. In addition, the Cajon sediments were folded much more strongly than were those of the Crowder Formation, suggesting that the Cajon experienced more compression than the Crowder. As the Cajon Formation is located at the northwestern end of the Squaw Peak thrust system and deformation was largest east of the Cajon block, it was subjected possibly to uneven compressional stresses (Figure 27). This is also suggested by the "tear" segment of the surface Squaw Peak fault near the eastern end of the Cajon Formation (Weldon, 1986; Meisling and Weldon, 1989). Under the influence of this stress, the Cajon block rotated clockwise above the low angle fault(s) related to the Squaw Peak thrust system, which acted as a decollement to accommodate the shear stress near the surface (Figure 27). On the other hand, the Crowder Formation is on the uppermost part of the upper-plate of the thrust system, and was moving together with the main block of the upper-plate. The dextral shear caused by the southward movement of the

**Figure 27. Tectonic rotation of the Cajon Pass area.**



**ROTATIONS OF CAJON VALLEY AREA**

upper block would thus have little effect on the Crowder as suggested by its relatively gentle deformation. Hence, it does not show significant rotations (Figure 27). It is also possible, however, that the Crowder had been rotated first clockwise, and thereafter counterclockwise, in response to the changing direction of the fault displacement.

## CONCLUSIONS

Combined with fossil data and regional geological information, the magnetic polarity zonation of the top three units of the Cajon Formation can be correlated unambiguously with the Magnetic Polarity Time Scale from above chrons 5C-2 to 5AA. The magnetostratigraphy of the Crowder Formation can also be matched from the bottom of Chron 5C to the top of Chron 5. These correlations suggest that most of the Cajon sediments were deposited from about 17 Ma to no later than 12.7 Ma, while the Crowder Formation was deposited from 17 Ma until 9.0 Ma.

The new age constraints on the Cajon and Crowder formations indicate that they mostly overlap in age. However, the considerable differences in the youngest age of the deposition, sedimentational features, and tectonic histories of these two formations suggest that they were deposited in distinctively different basins. Consequently, this supports the suggestion that the Squaw Peak thrust system separating them probably has had movements on the order of tens of kilometers.

Tectonic rotations determined by magnetic declination anomalies of these two formations are distinctly different: the Cajon Formation was rotated clockwise about 25 degrees, but the Crowder was not rotated. Tectonic rotations of the Cajon Formation probably have been generated by uneven compressional stresses caused by the south-south-westward thrusting of the Squaw Peak thrust system, the low angle faults of which

provided a decollement to accommodate this motion. On the other hand, the smaller rotation of the Cajon and nonrotation of the Crowder formations also imply that the prediction of Luyendyk and others (1980, 1985) is not valid for both the eastern and possibly the central Transverse Ranges.

### ACKNOWLEDGMENTS

Discussions with Lee Silver are greatly appreciated and very helpful. This study was supported partially by NSF DOSECC Cajon Pass Deep Drilling Program and NSF grants EAR83-51370, by matching grants of the Chevron Oil Field Research Company, and by the Arco Foundation.

### REFERENCES

- Atwater, T., 1970. *Implications of plate tectonics for the Cenozoic tectonic evolution of western North America*, Geological Society of America Bulletin, v. 81, p. 3513 - 3536.
- Baird A.K., Morton, D.M., Woodford, A.O., and Baird, K.W., 1974. *Transverse Ranges province: A unique structural-petrochemical belt across the San Andreas fault system*: Geological Society of America Bulletin, v. 85, p. 163 - 174.
- Bingham, C., 1974. *An antipodally symmetric distribution on the sphere*: Ann. Stat., v. 2, p. 1201 - 1225.
- Chang, S.R., and Kirschvink, J.L., 1985. *Possible biogenic magnetite fossils from the Miocene marine clay of Crete*: in Magnetite Biomineralization and magnetore-

- ception in Organisms. Kirschvink, J.L., Jones, D.S., and McFadden, B.J. ed., Plenum Press, New York, p. 647-669.
- Crowell, J.C., 1981. An outline of the tectonic history of southern California: in Ernst, W.G., ed., *The geotectonic development of California (Rubey Volume)*, Englewood Cliffs, New Jersey, Prentice-Hall, Inc., p. 583 - 600.
- Crowell, J.C., 1982. The tectonics of the Ridge Basin, southern California, in *Geologic history of Ridge Basin, southern California*, Crowell, J.C., and Link, M.H. eds., Pac. Sect. S.E.P.M. Guidebook, p. 25-42.
- Dibblee, T.W., Jr., 1967. *Areal geology of the western Mojave Desert, California*: U. S. Geological Survey Professional Paper 522, 153 p.
- Ehlig, P.L., 1988. Geologic structure near the Cajon Pass scientific drill hole: *Geophysical Research Letters*, v. 15, p. 949 -952.
- Ensley, R.A., and Verosub, K.L., 1982. Biostratigraphy and magnetostratigraphy of southern Ridge basin, central Transverse Ranges, California, in *Geologic history of Ridge Basin, southern California*, Crowell, J.C., and Link, M.H. eds., Pac. Sect. S.E.P.M. Guidebook, p. 13-24.
- Fisher, R.A., 1953. Dispersion on a sphere: *Proc. Roy. Soc. Lond.*, v. A217, p. 295 - 305.
- Foster, J.H., 1980. Late Cenozoic tectonic evolution of Cajon Valley: Unpublished Ph. D. Dissertation, University of California, Riverside, 242 p.
- Foster, J.H., 1982. Late Cenozoic tectonic evolution of Cajon Valley, southern California: in Sadler, P.M., and Kooser, M.A., eds.: *Late Cenozoic stratigraphy and structure of the San Bernardino Mountains*. Geol. Soc. Amer., Cordilleran Section Field Trip Guide, 6, p. 67-73.
- Garfunkel, Z., 1974. Model for the late Cenozoic tectonic history of the Mojave Desert,

California, and its relation to adjacent regions: Geological Society of America Bulletin, v. 85, p. 1931 -1944.

Garfunkel, Z. and Ron H, 1985. Block rotation and deformation by strike-slip faults, 2: The properties of a type of macroscopic continuous deformation. J. G. R., v. 90, p. 8589 - 8602.

Hargraves, R.B., and Banerjee, S.K., 1973. Theory and nature of magnetism in rocks: in Annual Review of Earth and Planetary Science, vol. 1, p. 269 - 296.

Harland, W.B., Cox, A.V., Llewellyn, P.G., Pickton, C.A.G., Smith, A.G., and Walters, R., 1982. A Geological Time Scale. Cambridge Univ. Press, London/New York.

Irving, E., and Irving, G.A., 1982. Apparent polar wander paths carboniferous through Cenozoic and the assembly of Gondwana: Geophysical Surveys, v. 5, p. 141 - 188.

Kirschvink, J. L., 1980. The least-squares line and plane and the analysis of the paleomagnetic data: examples from Siberia and Morocco. Geophysical Journal of the Royal Astronomical Society, v. 62, p. 699-718.

Lindsay, E.H., 1972. Small mammal fossils from the Barstow Formation, California. University of California Publications in Geological Science. v. 93, 104 p.

Liu, W., Weldon, R.J., and Kirschvink, J.L., 1988. Paleomagnetism of sedimentary rocks from and near the DOSECC Cajon Pass well, southern California: Geophysical Research Letters, v. 15, p. 1065 - 1068.

Luyendyk, B.P., Kamerling, M.J., and Terres, R.R., 1980. Geometric models for Neogene crustal rotations in southern California. Geol. Soc. Amer. Bull., v. 91, p. 211-217.

Luyendyk, B.P., Kamerling, M.J., Terres R.R., and Hornafius, J.S., 1985. Simple shear of southern California during Neogene time suggested by paleomagnetic declina-



- tions. *Jour. Geophys. Res.*, v.90, p. 12,454-12,466.
- Matti, J.C., Morton, D.M., and Cox, B.F., 1985. Distribution and geological relations of fault systems in the vicinity of the central Transverse Ranges, southern California. U.S. Geol. Surv. Open File Report. 85-365, 37 p.
- McElhinny, M.W., 1964. Statistical significance of the fold test in paleomagnetism. *Geophys. J. R. Astr. Soc.* v. 8, p. 338 - 340.
- Meisling, K.E., 1984. Neotectonics of the north frontal fault system of the San Bernardino Mountains: Cajon Pass to Lucerne Valley, California: Ph. D. thesis, California Institute of Technology, 394 p.
- Meisling K.E., and Weldon, R.J., 1982. The late Cenozoic structure and stratigraphy of the western San Bernardino Mountains: in *Geologic excursions in the Transverse Ranges*, Cooper, J. D. ed., p. 75 - 81.
- Meisling, K.E., and Weldon, R.J., 1989. Late Cenozoic tectonics of the northwestern San Bernardino Mountains, southern California: *Geological Society of America Bulletin*, v. 101, p. 106 - 128.
- Noble, L.F., 1926. The San Andreas rift and some other active faults in the desert region of southeastern California. *Carnegie Institute of Washington, Yearbook no. 25*, p. 415-422.
- Noble, L. F., 1932. The San Andreas rift in the desert region of southern California: *Carnegie Institute of Washington Yearbook*, no. 31, p. 355 - 363.
- Noble, L.F., 1954. *Geology of the Valyermo Quadrangle and vicinity, California*. U.S. Geological Survey Quadrangle Map Series, Washington D.C.
- Nur, A., Ron, H., and Scotti, O., 1986. Fault mechanics and the kinematics of block rotations: *Geology*, v. 14, p. 746 - 749.
- Reynolds, R.E., 1983. Paleontologic salvage, Highway 138 borrow cut, Cajon Pass, San

Bernardino County, California: San Bernardino County Museum Association, Redlands for state of California Department of Transportation District VIII, San Bernardino, 205 p.

Reynolds, R.E., 1984. Miocene faunas in the Lower Crowder Formation, Cajon Pass, California: a preliminary discussion, in Guidebook for the San Andreas fault - Cajon Pass to Wrightwood, Hester, R.L., and Hallinger, D.E. eds., Pacific Sect., AAPG, Volume and Guidebook, 55, p. 9-15.

Reynolds, R.E., 1985. Tertiary small mammals in the Cajon Valley, San Bernardino County, California, in Geologic investigations along interstate 15 - Cajon Pass to Manix Lake, California, Reynolds, R.E., ed., Field Trip Guide for 60th meeting, Western Assoc. Verte. Paleon., p. 49-58.

Reynolds, R.E. and Weldon, R.J., 1988. Vertebrate paleontologic investigation, DOSECC "Deep Hole" Project Cajon Pass, San Bernardino County, California: Geophysical Research Letters, v. 15, p.

Silver, L.T., and James, E.W., 1988. Geological setting and lithologic column of the Cajon Pass deep drillhole: Geophysical Research Letters, v. 15, p. 941 - 944.

Swinehart, J.B., 1965. Geology of a portion of the lower Cajon Valley, San Bernardino County, California: Unpublished senior thesis, University of California, Riverside.

Tamura, A.Y., 1961. Stratigraphy of a portion of the upper Cajon Valley, California: Unpublished senior thesis, University of California, Riverside.

Tarling, D.H., 1983. Paleomagnetism. Chapman and Hall, 379 p.

Terres, R.R., and Luyendyk, B.P., 1985. Neogene tectonic rotation of the San Gabriel region, California, suggested by paleomagnetic vectors: Journal of Geophysical Research, v. 90, p. 2467 - 2484.

- Weldon, R.J., II, 1984. Implications of the age and distribution of the late Cenozoic stratigraphy in Cajon Pass, southern California: in San Andreas fault -- Cajon Pass to Wrightwood, Hester, R.L. and Hallinger, D.E., eds., Pacific Sect., AAPG, Volume and Guidebook, 55, p. 9-15.
- Weldon, R.J., II, 1986. The late Cenozoic geology of Cajon Pass: Implications for tectonics and sedimentation along the San Andreas fault, Ph.D. thesis, California Institute of Technology, Pasadena, California. 400 p.
- Weldon, R.J., and Humphreys, E., 1986. A kinematic model of southern California: *Tectonics*, v. 5, p. 33 - 48.
- Weldon, R.J., and Sieh, K.E., 1985. Holocene rate of slip and tentative recurrence interval for large earthquakes on the San Andreas fault in Cajon Pass, southern California: *Geological society of America Bulletin*, v. 96, p. 793 - 812.
- Weldon, R.J., Winston, D.S., Kirschvink, J.L. and Burbank, D.W., 1984. Magnetic stratigraphy of the Crowder Formation, Cajon Pass, so. California. Abstracts with Programs, 97th Annual Meeting, Geol. Soc. Amer., Vol. 16, p. 689.
- Winston, D.S., 1985. Magnetic stratigraphy of the Crowder Formation, southern California, M.S. thesis, University of Southern California, Los Angeles, California, 100 p.
- Woodburne, M.O., and Golz, D., 1972. Stratigraphy of the Punchbowl Formation, Cajon Valley, southern California. *University of California Publications in Geological Sciences*, Vol. 92, 73 p.
- Woodburne, M.O., and Tedford, R.H., 1985. Litho- and Bio-stratigraphy of the Barstow Formation, Mojave Desert, California: in *Geologic investigations along interstate 15 - Cajon Pass to Manix Lake, California*, Reynolds, R.E. ed., Field Trip Guide for 60th meeting, Western Assoc. Verte. Paleon.

CHAPTER THREE

**PALEOMAGNETISM OF THE PUNCHBOWL FORMATION  
AT DEVIL'S PUNCHBOWL, SOUTHERN CALIFORNIA**

by

**Wei Liu<sup>1</sup>, Joseph L. Kirschvink<sup>1</sup> and Ray J. Weldon<sup>2</sup>**

**1 - California Institute of Technology**

**2 - University of Oregon**

## ABSTRACT

We conducted a paleomagnetic magnetostratigraphic study of the late Miocene Punchbowl Formation at Devil's Punchbowl. One hundred and sixty-four samples were collected from the entire formation, covering a stratigraphic thickness of about 1200 meters. The magnetic polarity pattern obtained from the Punchbowl Formation can be matched unambiguously to the geomagnetic reversal time scale from the chrons 5Ar to 4Br, which implies that the formation was deposited from about 12.5 to 8.5 million years ago. These refined age constraints, combined with a similar study on the Cajon Formation, demonstrate that they were deposited during different periods of time. Hence, the two formations do not correlate and the distance between them cannot be used to constrain the total offset along the San Andreas fault.

The age of the Punchbowl Formation also constrains the activity of the Punchbowl fault, which is an old strand of the early San Andreas system. Based on the geologic data, the Punchbowl fault has had two episodes of activity, one was immediately before the deposition of the Punchbowl Formation, another was after its deposition. Therefore, our results constrain these two episodes to be about 12.5 Ma and after 8.5 Ma, respectively. Timing of another strand of the early San Andreas system, the Fenner fault, is also constrained by our result. Because the basal unit of the Punchbowl Formation is the oldest unit that is not offset by the Fenner fault, activity of the Fenner fault must end before 12.5 Ma. In conjunction with the dating of the Paleocene San Francisquito Formation that is the youngest unit offset by the fault, the Fenner fault was active between Paleocene time and before 12.5 Ma.

Abnormal counterclockwise rotations ( $27.5^\circ \pm 4.3^\circ$ ) found in the Punchbowl

Formation are compatible with those found in the Mint Canyon Formation 40 to 50 km to the west ( $13^\circ \pm 30^\circ$ ). This suggests that the San Gabriel block between the San Andreas and San Gabriel faults may have been rotated counterclockwise. The rotation probably occurred as the San Gabriel block moved into the preexisting bent segment of the San Andreas fault, aided by the Mojave Desert block acting as a "backstop." After taking the rotation back, the Punchbowl and Fenner faults would be parallel to the bent segment, and to the segment south of the bend, of the San Andreas fault, respectively. This supports the proposal that the Fenner and Punchbowl faults are strands of the early San Andreas system, and that the bend of the San Andreas fault probably has existed since Paleocene time.

## INTRODUCTION

This study has been undertaken to help unravel the complex depositional and deformational history of the Transverse Ranges in the vicinity of the San Andreas Fault Zone. The late Miocene Punchbowl Formation, including its type locality at the Devil's Punchbowl and the "Cajon Facies" in the Cajon Valley, have attracted the attention of various workers for the past half century (Noble, 1932, 1954; Dibblee, 1967; Woodburne and Golz, 1972; Foster, 1980, 1982; Weldon, 1986) because of their distinctive appearance, easy accessibility, and most importantly, because of the information carried by these rocks for the tectonic history of the Transverse Ranges province.

The exposures of the Punchbowl Formation at Devil's Punchbowl and of the Cajon Formation in Cajon Valley are so similar that they were once thought to be the same rock formation separated by the San Andreas Fault (Noble, 1926, 1954).

Therefore, the distance between these two formations (about 35 km) was suggested as the indication of the total offset along the fault system. This proposal was criticized severely in the 1930's. Noble withdrew the idea eventually because at that time no one believed that large lateral motions across faults were possible. Subsequently, Woodburne and Golz (1972) demonstrated that these sediments did not record the amount of offset along the San Andreas fault because they are different in stratigraphic detail and probably in age. However, as the ages of the bottom of the Punchbowl and the top of the Cajon formations were assessed only loosely or not dated at that time, it was not clear whether or not these two formations overlapped in age or were deposited in a continuous basin (Woodburne, 1975).

Similarly, John Matti (1985), Ray Weldon (1986), and others proposed tentatively that the Mill Creek Formation had been deposited in the same basin in which the Punchbowl Formation had been deposited, and that they were offset subsequently by the San Andreas fault. However, the age of the Mill Creek Formation is constrained only by a few poorly-preserved plant fossils found in it. In addition, the Punchbowl and Fenner faults were proposed to be strands of the early San Andreas system (Weldon et al., 1990), and an accurate age for the Punchbowl Formation would constrain the timing of their activity. Therefore, it was necessary to develop better age constraints on these sedimentary formations in order to help evaluate the above proposals and to help understand the history of the San Andreas fault system.

The Punchbowl Formation is bounded by the San Andreas and Punchbowl faults, covers the Fenner fault with its basal breccia unit, and is exposed on the northern front of the San Gabriel Mountains (Figure 1). Terres and Luyendyk (1985) carried out a paleomagnetic study of the Oligocene Vasquez and late Miocene Mint Canyon formations in the San Gabriel Mountains, and concluded that the "San Gabriel block"

between the San Andreas and the San Gabriel faults had first been rotated clockwise about  $37^\circ$  (and possibly as much as  $50^\circ$ ), then rotated counterclockwise about  $13^\circ$ . In our preliminary study (Liu et al., 1988), counterclockwise rotation was also found in the Punchbowl Formation. This was apparently different from the rotation found in the Western Transverse Ranges and conflicts somewhat with Luyendyk and other's proposal (1980, 1985) that the entire Transverse Ranges have been rotated clockwise about  $90^\circ$  from a previous north-south direction to their present position.

These results and the unresolved problems stimulated us to carry out this study. Magnetostratigraphy is utilized to constrain the age, sedimentation rate, and span of time encompassed by the Punchbowl Formation. Paleomagnetic directions from the Punchbowl Formation are used to delineate the tectonic rotations that have occurred in this rock unit in order to address the discordance between rotations observed in rocks from the western and central Transverse Ranges.

## GEOLOGICAL SETTING

The Punchbowl Formation is a moderately to strongly deformed and folded unit of coarse- to fine-grained sedimentary rocks lying upon the Paleocene San Francisquito Formation. The beds of the formation are folded, forming the Punchbowl Syncline (Figure 1). The section of Punchbowl Formation used in this study is located near the Devil's Punchbowl Los Angeles County Park and is mainly on the northern limb of the Punchbowl Syncline. At this location, the Punchbowl Formation is well-exposed and folded.










The San Francisquito Formation in the Devil's Punchbowl rests unconformably on top of basement rocks, and in turn, is overlain unconformably by the Punchbowl

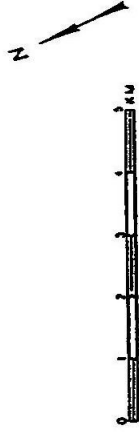


**Figure 1. Geological map of the Devil's Punchbowl area and its vicinity.**

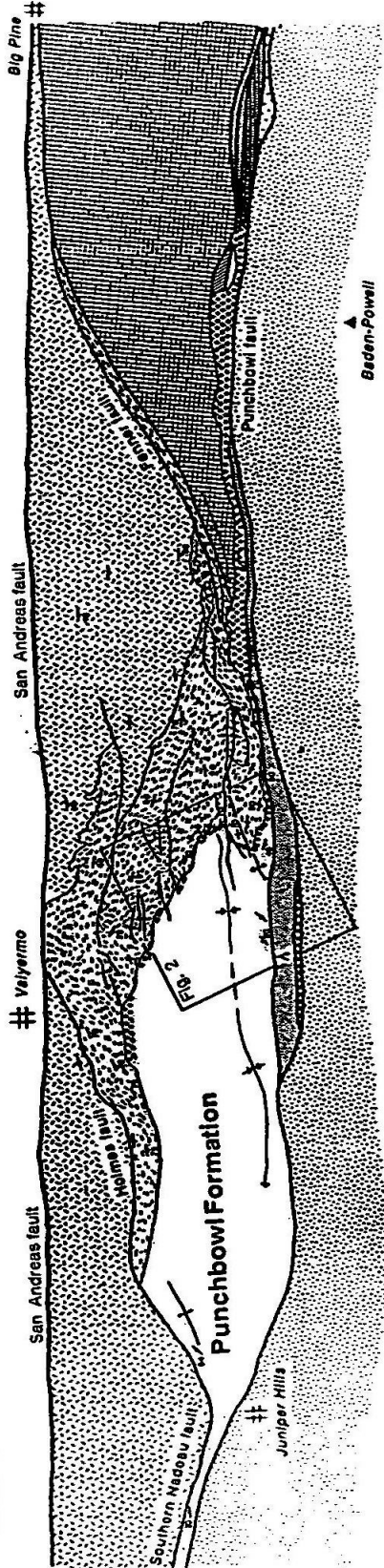
Modified from Weldon et al. (1990).

**Legend**

- |   |  |   |                                       |   |                       |
|---|--|---|---------------------------------------|---|-----------------------|
|  | granodiorite                                   |  | Palms Schist                          |  | sandstone (Vasquez ?) |
|  | gneisses and plutonics of the San Gabriel Mtns |  | San Francisco Formation               |  | leucocratic plutonics |
|  | basal breccia                                  |  | littered gneisses and mafic plutonics |  | volcanics (Vasquez ?) |



Rocks younger than the Punchbowl Fm not shown



Formation. It is the only sedimentary rock unit in this area of pre-Miocene age. The formation is composed of dark colored conglomerate and bedded arkosic sandstone and siltstone. The clasts in the formation are mainly granodiorite and gneiss, as well as porphyritic volcanic rocks (Woodburne and Golz, 1972). Its age is considered as Paleocene based on invertebrate fossils found from these rocks (Dibblee, 1967; Woodburne and Golz, 1972; Barrows, 1985).

The Punchbowl and San Francisquito formations are bounded by the present active trace of the San Andreas fault on the north and by the Punchbowl fault on the south. The Punchbowl fault is probably an abandoned strand of the San Andreas fault system (Ehlig, 1968, 1975), and is located one to two kilometers south of and parallel to the San Andreas fault. The Punchbowl fault offsets both the San Francisquito Formation and the Pelona Schist (of late Cretaceous age), which are juxtaposed together by the Fenner - San Francisquito fault, a similar distance (Ehlig, 1968, 1975). Using the Fenner - San Francisquito fault as a piercing point, total offset along the Punchbowl fault can be constrained at about 44 kilometers (Barrows, 1985). The Punchbowl fault shows no evidence of Holocene activity (Dibblee, 1967; Ehlig, 1968). An unknown amount of the Punchbowl Formation has been removed by the Punchbowl fault. Although lacking any features suggestive of recent displacement, the fault offsets a Quaternary terrace in the Devil's Punchbowl area (Noble, 1954; C. Allen, 1990, personal communication), suggesting a Quaternary activity or re-activation. The history of the Punchbowl fault is poorly understood and its activity was loosely constrained as starting after Paleocene time (Dibblee, 1967, 1968) or after deposition of the Punchbowl Formation (Barrows, 1985).

### The Punchbowl Formation

The Punchbowl Formation occurs on the southwest side of the San Andreas fault at the Devil's Punchbowl near Valyermo, California. According to Noble (1953, 1954), the Punchbowl Formation is also exposed southwest of the San Andreas fault near Pearland, and both northeast and southwest of the fault near Valyermo. However, Woodburne (1975) suggested that the rocks in Pearland and north of the San Andreas fault in Valyermo are quite different from the sediments in the type area. Barrows (1985) named the rocks in Pearland and north of the San Andreas fault in Valyermo as the Little Rock Formation. Therefore, in this paper we will only discuss the type Punchbowl Formation on the southwest side of the San Andreas fault (Figure 1).

The nonmarine, generally coarse-grained Punchbowl sediments overlie unconformably the Paleocene marine San Francisquito Formation and in turn is overlain unconformably by the Pleistocene Harold Formation (Noble, 1954; Dibblee, 1967). The entire formation is about 1300 meters thick and exposed on the western front of the San Gabriel Mountains, in the central Transverse Ranges.

The Punchbowl Formation was divided into two members by Noble (1954). He described the lower part of the formation as white to light buff arkosic conglomerate and conglomeratic sandstone. Some of the conglomerate beds are locally very coarse-grained and the most abundant clasts in the formation are quartz diorite gneiss and granodiorite (Woodburne and Golz, 1972). The thickness of the Lower Punchbowl Formation was thought to be about 310 meters (Noble, 1954; Woodburne and Golz, 1972). In this study, we found that the Lower Punchbowl is about 480 meters thick, as another 200 meters were exposed near the plunging axis of the Punchbowl syncline

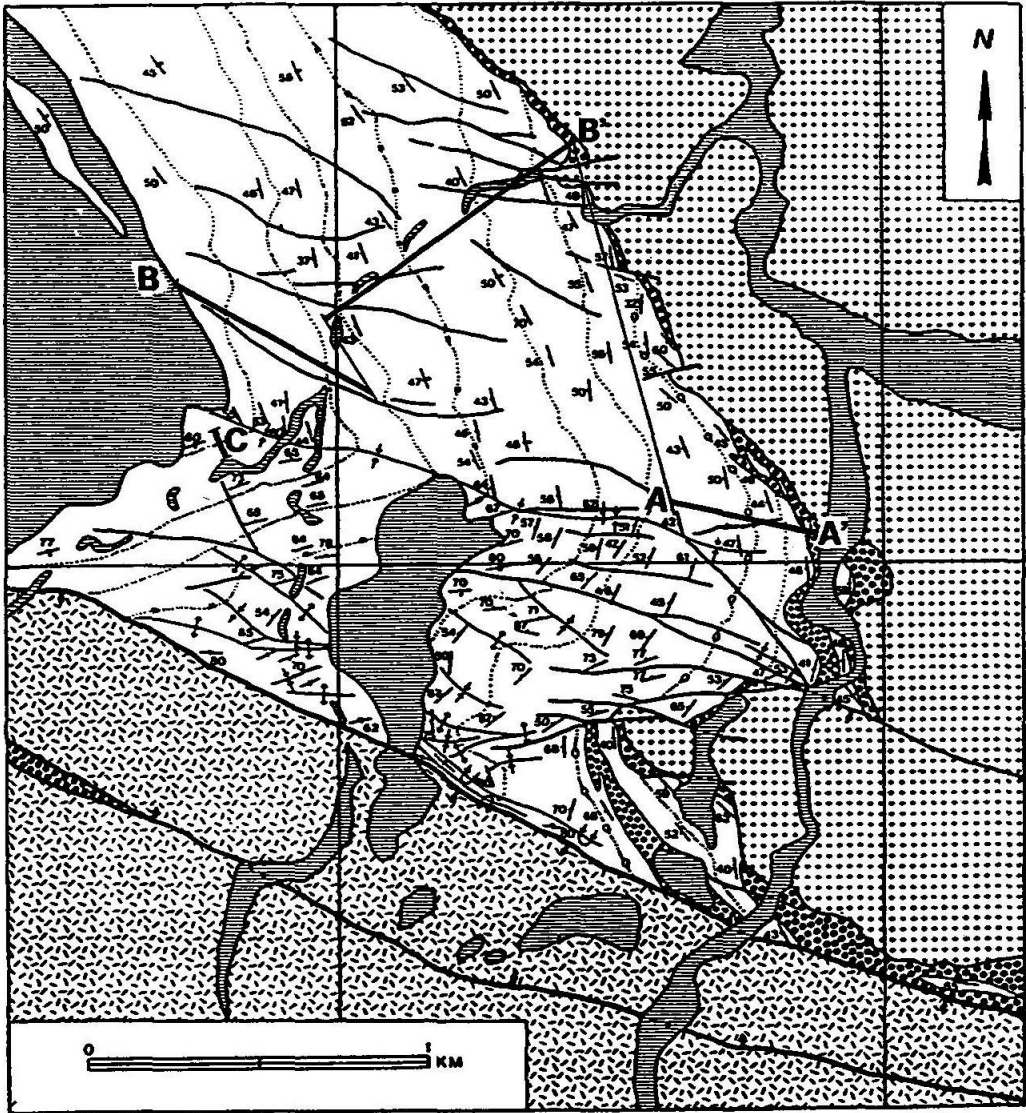
(Figure 2). Fine-grained interbeds are relatively more abundant in this part than that exposed on limbs of the fold.

A reddish-purple breccia unit occurs at the very base of the Punchbowl sediments and forms a narrow strip along the Punchbowl fault (Weldon et al., 1990) (Figure 1), which contains various clasts derived from the underlying slivers of different rocks. This unit is truncated on its southwestern margin by the Punchbowl fault, but there is no evidence that the fault was active during the deposition of the breccia. Near its southeastern end, the breccia overlies on the Fenner fault. Based on horse fossils recovered from this unit, the base of the Punchbowl Formation has been assigned a Clarendonian age (Tedford and Downs, 1965; Woodburne and Golz, 1972). Clarence Allen (personal communication, 1990) found a horse fossil from basal layers near the northeastern edge of the formation and our sample section B - B' (B', Figure 2), the age of which has been determined as Late Barstovian (?) or Early Clarendonian (?) (ca. 13 to 12 Ma, David Whistler, personal communication, 1990). The locality appears stratigraphically 200 meters higher than the base of the formation near the axis of the syncline (A', Figure 2). However, it is more likely located within the basal unit of the formation. If this is the case, the very base of the Punchbowl Formation should be close to the Barstovian-Clarendonian mammalian boundary or about 12 to 13 Ma in age. Other fossils were found by Woodburne and Golz at about 330 m above the base of the formation, near the boundary between the lower and upper members. These fossils belong to mammalian faunas of Hemphillian age, and the age of the Lower Punchbowl Formation thus was suggested to range from Clarendonian to about Hemphillian (Woodburne and Golz, 1972).

The Upper Punchbowl Formation gradationally overlies the lower member and is described as containing generally fewer beds of coarse-grained sandstone and more

**Figure 2. Geological map and sampling localities of the Punchbowl Formation.**

Modified from Weldon et al. (in press, 1990) that was based on both field mapping and air-photo interpretation. The illustrations are the same as for Figure 1.



interbedded layers of grayish-green to greenish-brown sandstones (Woodburne and Golz, 1972). The composition of clasts of this member is generally similar to that of the lower unit but with fewer clasts derived from the San Francisquito Formation and abundant felsitic to porphyritic volcanic rock clasts. The upper formation has been suggested by Woodburne and Golz (1972) to be about 830 meters thick although only about 700 meters were found in this study. Fossils found about 260 meters above its base from the upper member are also of Hemphillian age (Woodburne, 1975). The remaining stratigraphically higher parts of the Punchbowl Formation are undated. Nevertheless, the age range of the whole formation has been assigned roughly as from Clarendonian to at least Hemphillian so far.

Noble (1954) suggested that the clasts in the Punchbowl Formation were similar to basement rocks found southeast of the Punchbowl fault, but Pelka (1971) proposed that the Punchbowl clastic debris was derived from the east. As suggested by Woodburne and Golz (1972), the Punchbowl Formation appears to have been deposited by a highly competent, westward flowing stream or streams from the Mojave Desert across the San Andreas and Punchbowl faults.

The Punchbowl beds are folded to form an asymmetric west-plunging syncline, the Punchbowl syncline (Noble, 1954; Dibblee, 1967), with an axis plunging  $42^{\circ}$  towards the west. All of the beds exposed in the Devil's Punchbowl area are part of the syncline. Part of the southern limb of the Punchbowl Fold has been removed by the Nadeau-Punchbowl fault, whereas in the northern flank the entire Punchbowl Formation is continuously exposed by the fold.



## PALEOMAGNETIC PROCEDURES

### Sampling

Within the studied area, the Punchbowl Formation is well exposed and generally dips 40 to 60 degrees to the southwest. It is stratigraphically continuous and thicker near the plunging axis of the syncline than at either limb. Three sections appropriate for paleomagnetic sampling were chosen in this locality (Figure 2), which covered stratigraphically the entire formation (sections A - A' and B - B') and both sides of the syncline (section C). The main section of the Punchbowl Formation used in this study starts approximately 100 meters east of the parking lot of the Devil's Punchbowl Park and extends northeastward.

The base of section A - A' is at the boundary between the Punchbowl and San Francisquito formations in the reddish-brown basal unit. This section is about 200 m thick and lies within the lower member of the formation. It was a supplemental section, resulting from the observation that more layers are exposed near the plunging axis of the Punchbowl syncline. The section was located such that it was extrapolated to underlie directly section B - B' in order to obtain a complete stratigraphic section through the Punchbowl Formation. The extrapolation was based on both field mapping and air-photo interpretation (Figure 2). Section B - B' covered parts of both the lower and upper members of the Punchbowl Formation, with a total stratigraphic thickness for sections A - A' and B - B' of 1167 m. One hundred and fifty samples were taken from these sections, with every effort made to control the interval between sample sites to be less than 10 meters. In some instances, the stratigraphic intervals between some

sample sites were larger than 10 meters, especially in the middle part of the formation, because samples were taken only from the fine-grained sandstones and siltstones. Despite this, the Punchbowl Formation was still sampled sufficiently to detect magnetic polarity changes because in general the coarse- to very coarse-grained sediments were accumulated in a much shorter time period than the fine-grained sediments.

A standard water-cooled drill with 2.5 cm inner-diameter head was used for sampling the more consolidated sediments. All samples were oriented carefully using standard methods. The magnetic orientation was confirmed by Sun-compass, whenever possible.

The samples were cut into 2.5 cm high cylinders in the laboratory using a water-cooled saw with a non-magnetic blade. Some samples taken from near the bottom of the formation, which were poorly consolidated, were consolidated using a weak sodium-silicate solution. This procedure was carried out in a magnetically-shielded room to avoid acquisition of a spurious magnetic component.

### Measurements

All samples were subjected to progressive thermal demagnetization at temperatures ranging from 100 to 570 °C, in steps of 25 to 100 °C, following low field (up to 10 mT) alternating field (AF) demagnetization. Most samples were heated through the 570 °C step because the main magnetic mineral identified from these samples is magnetite (see below), and also because after 500 °C the magnetic direction of most samples did not change significantly.

Demagnetization behavior of the samples generally fell into one of three categories. Most of the samples exhibited either a normal (north and down) or a reverse

(south and up) magnetic direction (Figure 3) that did not change significantly during higher level demagnetization. Progressive demagnetization trajectories of these samples as viewed in orthogonal projection commonly have linear features and move towards the origin. Some samples appeared to reach a stable characteristic direction and had linear demagnetization paths during the last several steps, but with slight offset from the origin (Figure 4). A third type includes those samples that showed dramatic directional and intensity changes at low steps, but reached a stable end point (Figure 5) accompanied by very little directional and intensity change. As all samples were taken from carefully chosen sediments, very few magnetically unstable samples were in the collection.

A common feature of all of these samples is the existence of a strong secondary magnetic overprint, indicated by the dramatic changes after low AF or thermal demagnetization steps. Although the overprints are often removed after a few demagnetization steps, some of them are too persistent to be removed completely. This is especially prominent in the behavior of the second and third type of samples, and weakens their reliability (see below).

The demagnetization histories of each of these samples were analyzed using the principal component analysis method of Kirschvink (1980). In the first- and third-type samples, directions for lines of best least-square fit can be generally found from each sample. The polarity of a primary component of higher stability was then inferred from the trajectory of the linear path toward either a normal or reversed polarity. A few of the first-type samples showed an indeterminable polarity (Figure 3B), although their demagnetization paths appear to be stable. These directions were only used for plotting in the magnetic polarity zonation. For the second type samples whose trajectory did not move towards the origin, a line that was often forced to connect to the origin was fitted.

**Figure 3. Orthogonal and equal-area plots of the typical demagnetization paths -- the first type.**

A -- sample reached the stable primary direction of normal polarity.

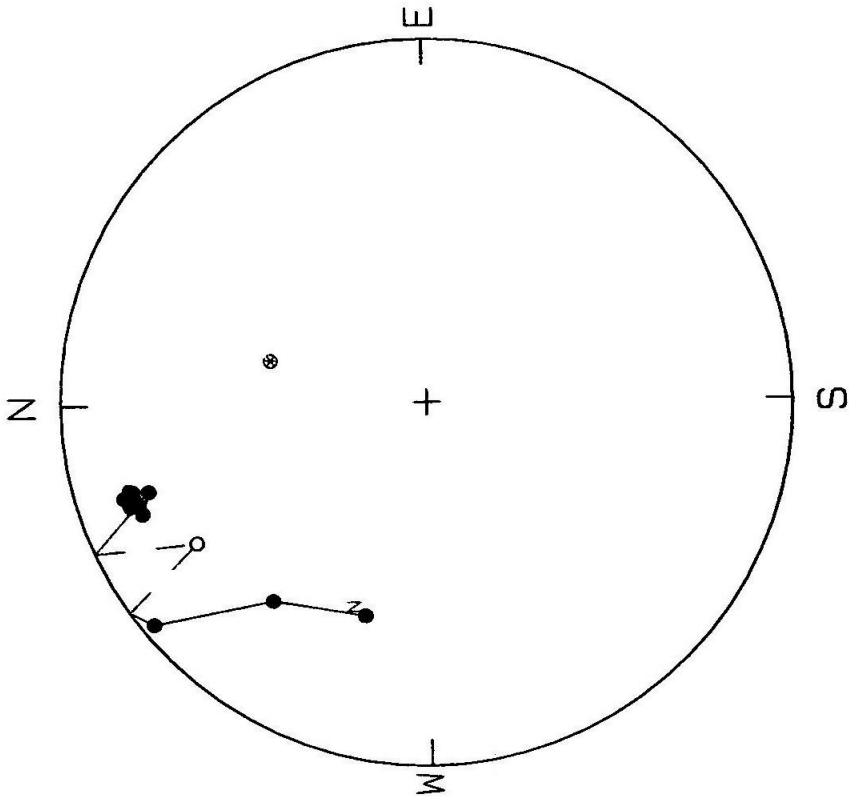
B -- sample has a stable characteristic component of reversed direction;

C -- sample reached a stable direction but with intermediate polarity.

LEFT - Orthogonal plot based on successive endpoints of demagnetization vectors. Solid circles are projected on a horizontal plane whereas open circles are on a vertical plane. Each division on axes represents remanent magnetization intensity of  $10^{-7}$  (A and C) and  $10^{-9}$  A·M<sup>2</sup>, respectively.

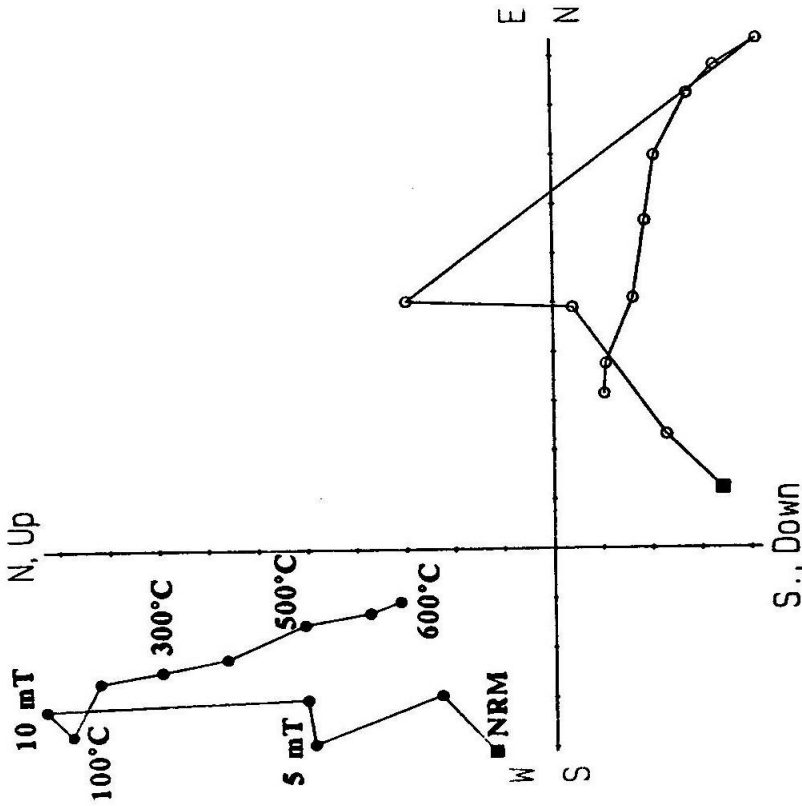
RIGHT - Equal-area stereographic projection of the same demagnetization vectors as in left. Solid circles are the vectors in the lower hemisphere and open ones are plotted on the upper hemisphere.

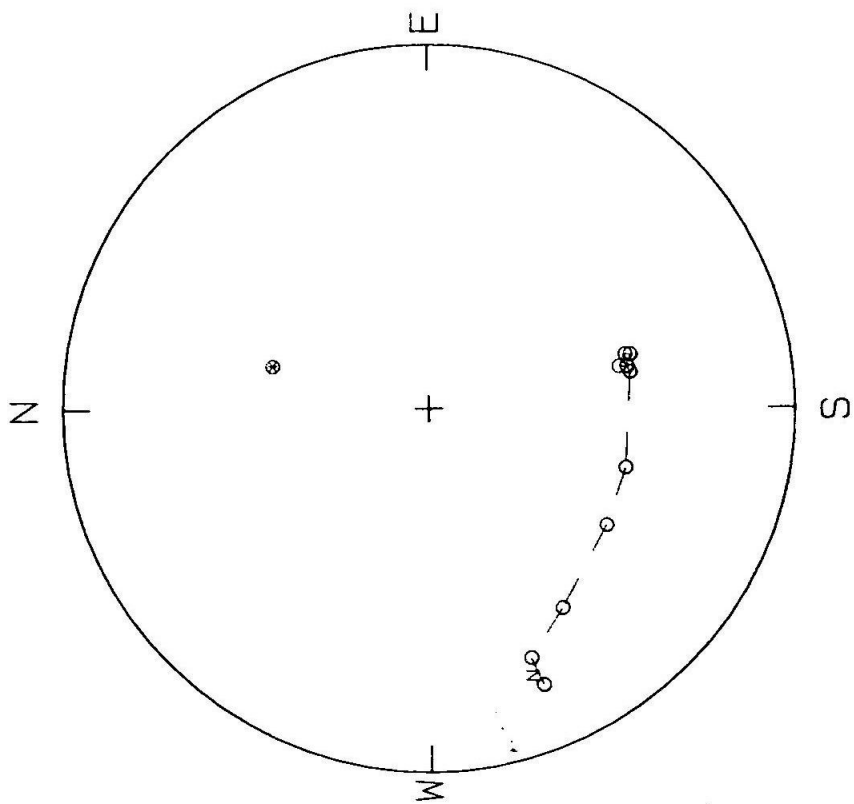
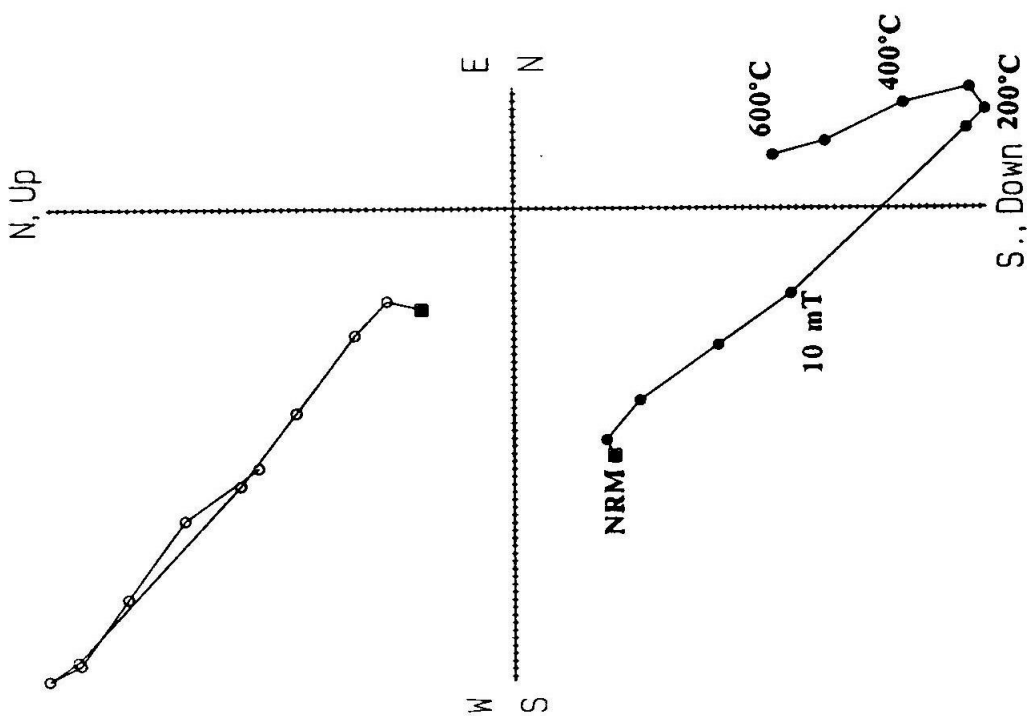
All of these plots are based on bedding-corrected directions of magnetization. The AF demagnetizing field is in millitesla and temperatures are in degree Celsius.



PDP20

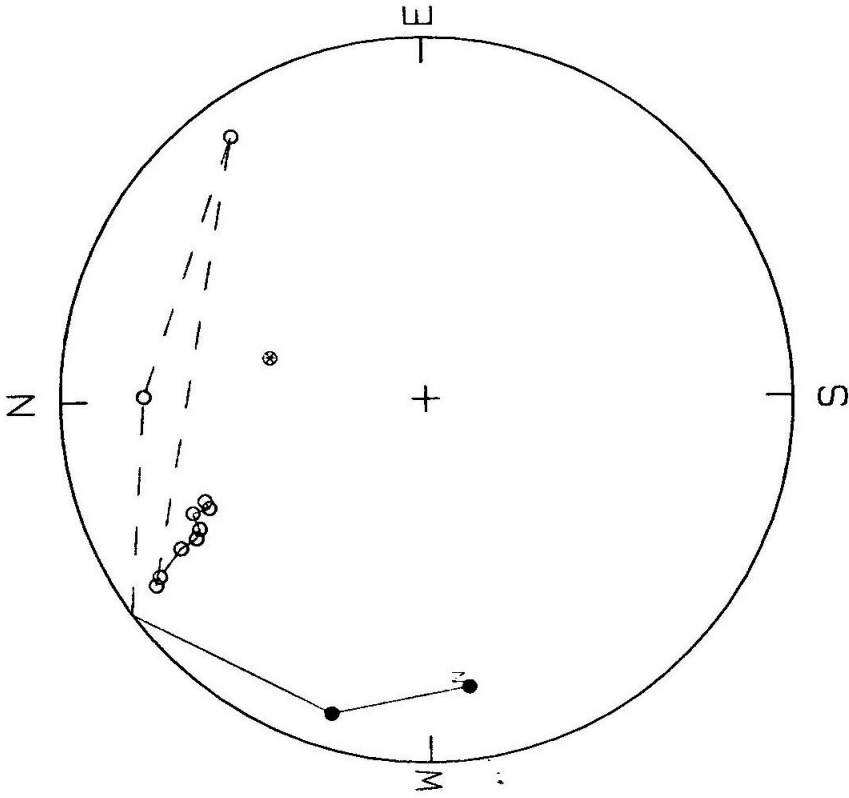
A





BPB43

B



PDP27

C

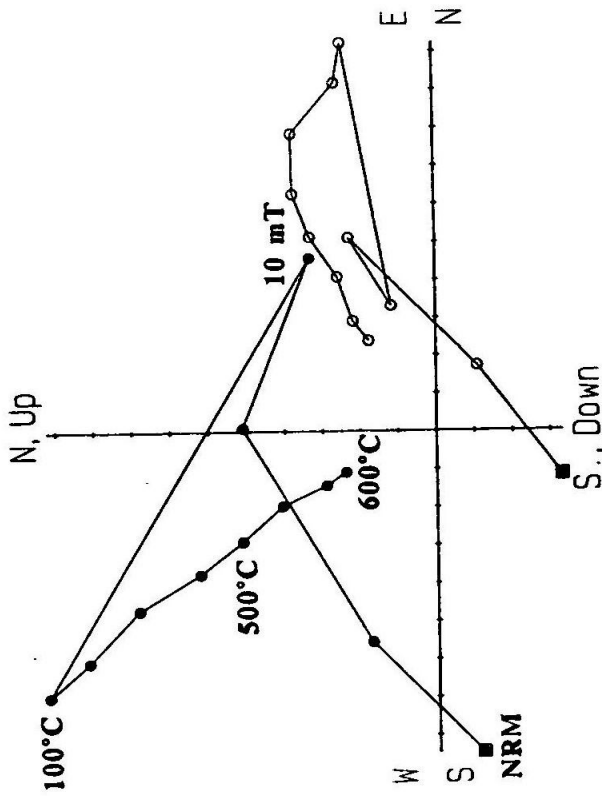


**Figure 4. Orthogonal and equal-area plots of the typical demagnetization paths of the second type.**

LEFT - Orthogonal plot;

RIGHT - Equal-area plot;

The sample appears to reach a stable characteristic direction but the trajectory is slightly offset from the origin, implying that the overprints of secondary fields may not be completely removed. Plotting conventions are the same as in Figure 3. Each division on the axes represents an intensity of  $10^{-8}$  A·M<sup>2</sup>.



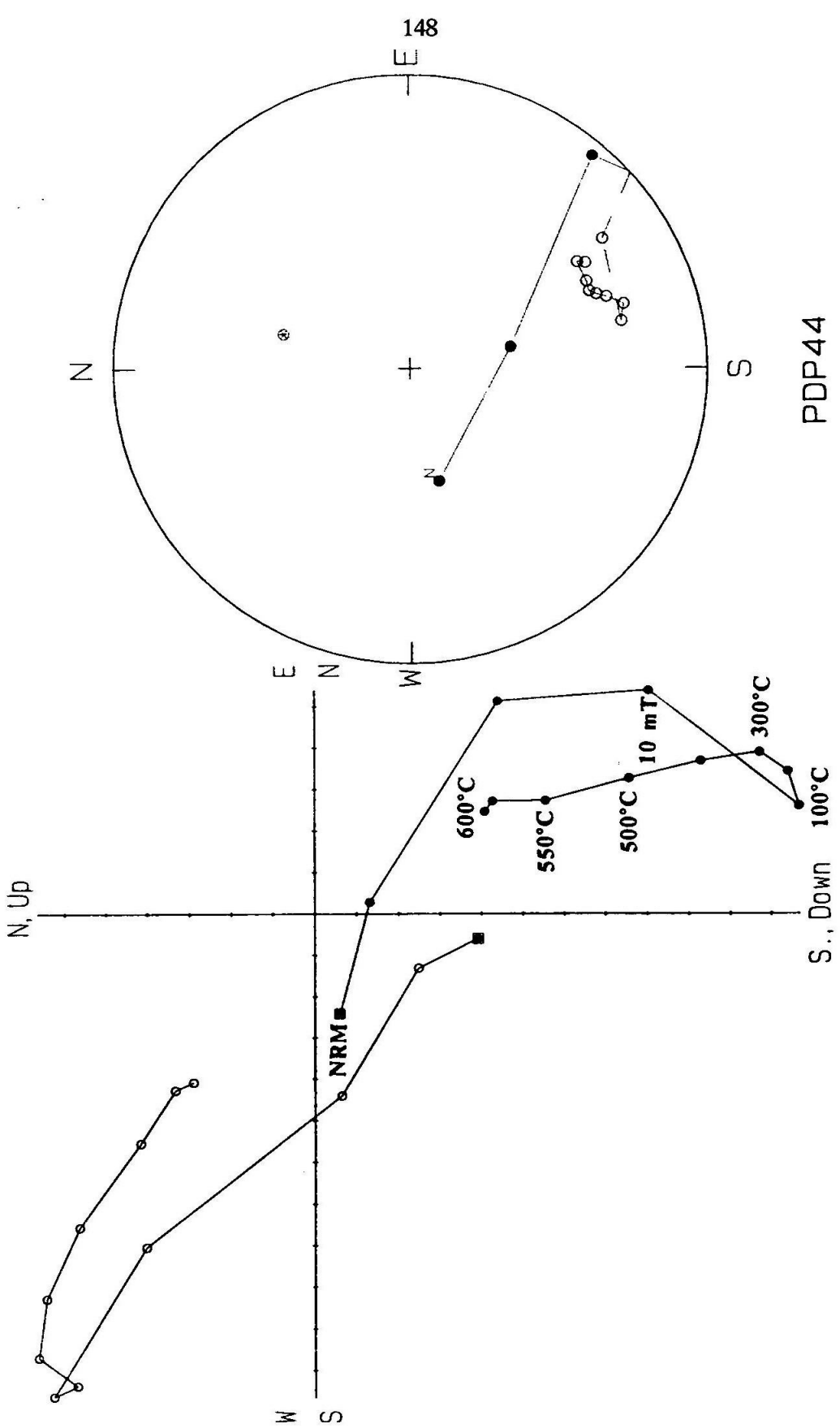
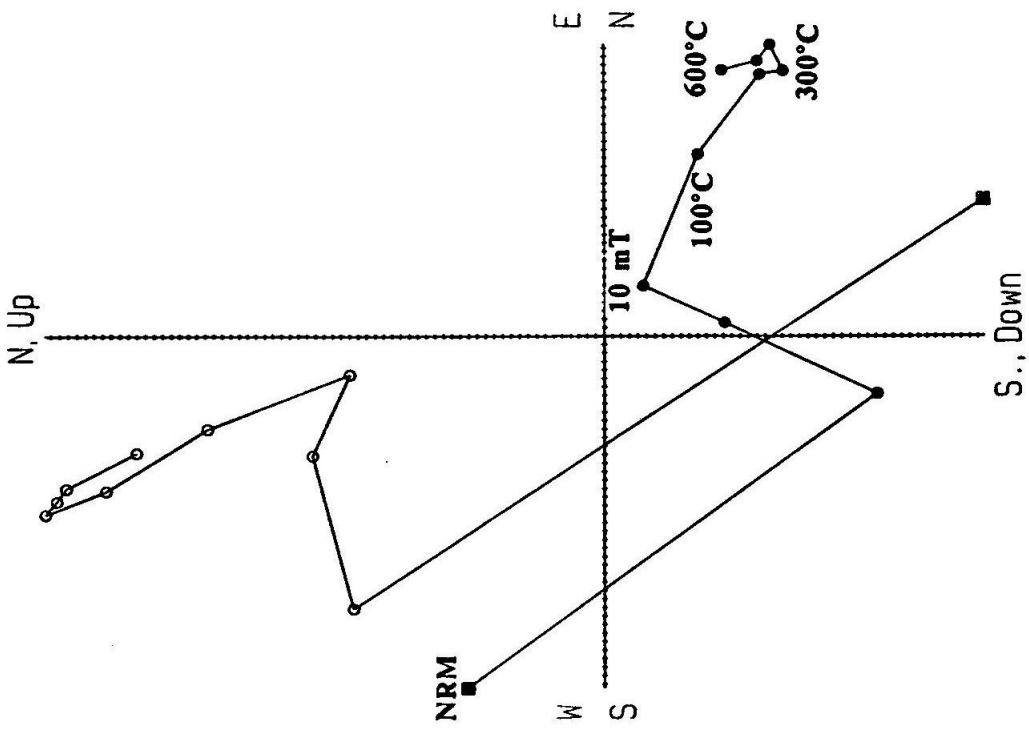
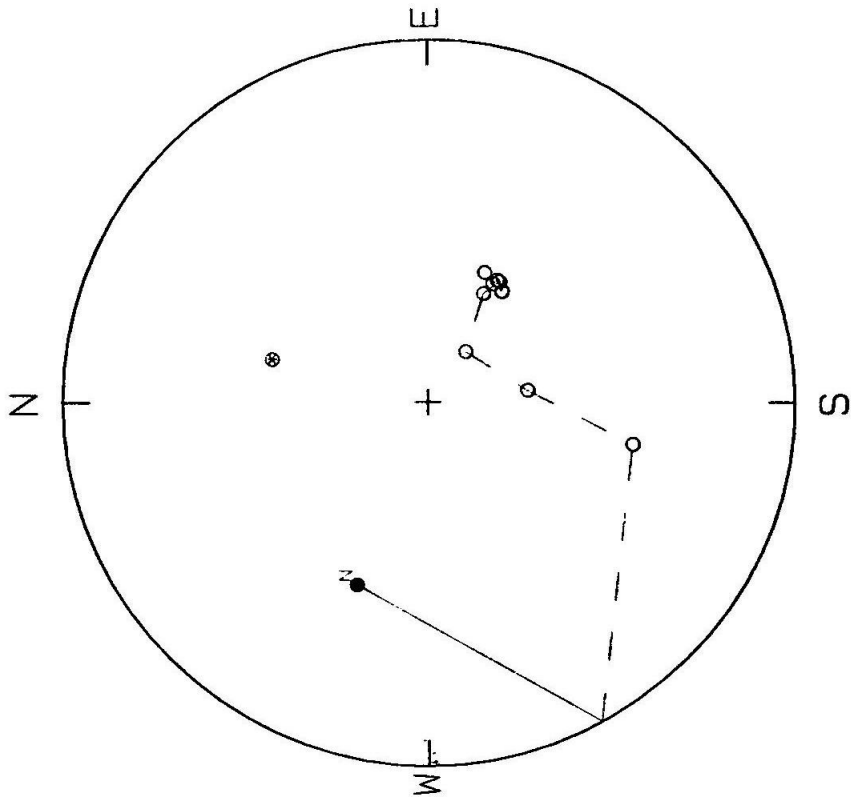


**Figure 5. Orthogonal and equal-area plots of the typical demagnetization paths of the third type.**

Sample reached a stable "end point" at which the directions and intensity no longer change significantly. The plotting conventions are the same as in Figure 3. Each division on the axes represents intensity of  $10^{-9}$  A·M<sup>2</sup>.

BPB8



Although the direction obtained from this line may differ from the primary one in some degree, it was still considered as a stable primary direction and used for magnetostratigraphic study because the effect of the overprinting field appears to be relatively weak. Only the type I samples with the highest stability were used for calculate mean directions and for rotation study. In all of these analyses, only those directions with maximum angular deviations less than  $10^\circ$  were accepted.

### Magnetic Mineralogy

We conducted rock magnetic experiments on representative samples of the Punchbowl Formation, including acquisition and alternating-field demagnetization of isothermal remanent magnetization (IRM). Most of the isothermal remanent magnetization of these samples is gained in fields below 100 mT (Figure 6), suggesting that magnetite or maghemite are the primary magnetic minerals present. A few other minerals, such as goethite or hematite may also exist in these samples, as the IRM curve does not completely saturate at 1000 mT. The median destructive fields of the samples are between 5 and 10 mT. All of these values fall within the range of single- or pseudo-single-domain magnetite (Bailey and Dunlop, 1983). Furthermore, the magnetic intensity of many samples changes dramatically between 450 and 500 °C and drops to a small percentage of the NRM intensity at 575 °C (Figure 7). This strengthens the conclusion that the primary magnetic minerals of the samples from the Punchbowl Formation are pseudo-single-domain magnetite, with minor amounts of maghemite.

### Test of Data Reliability

Our samples were collected from both flanks of the Punchbowl Syncline, making

**Figure 6. Rock magnetism experiment plot.**

Curve at left - demagnetization of isothermal magnetization (IRM);

Curve at right - acquisition of isothermal magnetization (IRM);

IRM gains in fields below 100 mT, tends to saturate at about 300 millitesla, and starts to be destructed between 5 and 10 millitesla. These values fall within the range of single- or pseudo-single-domain magnetite (Bailey and Dunlop, 1983).

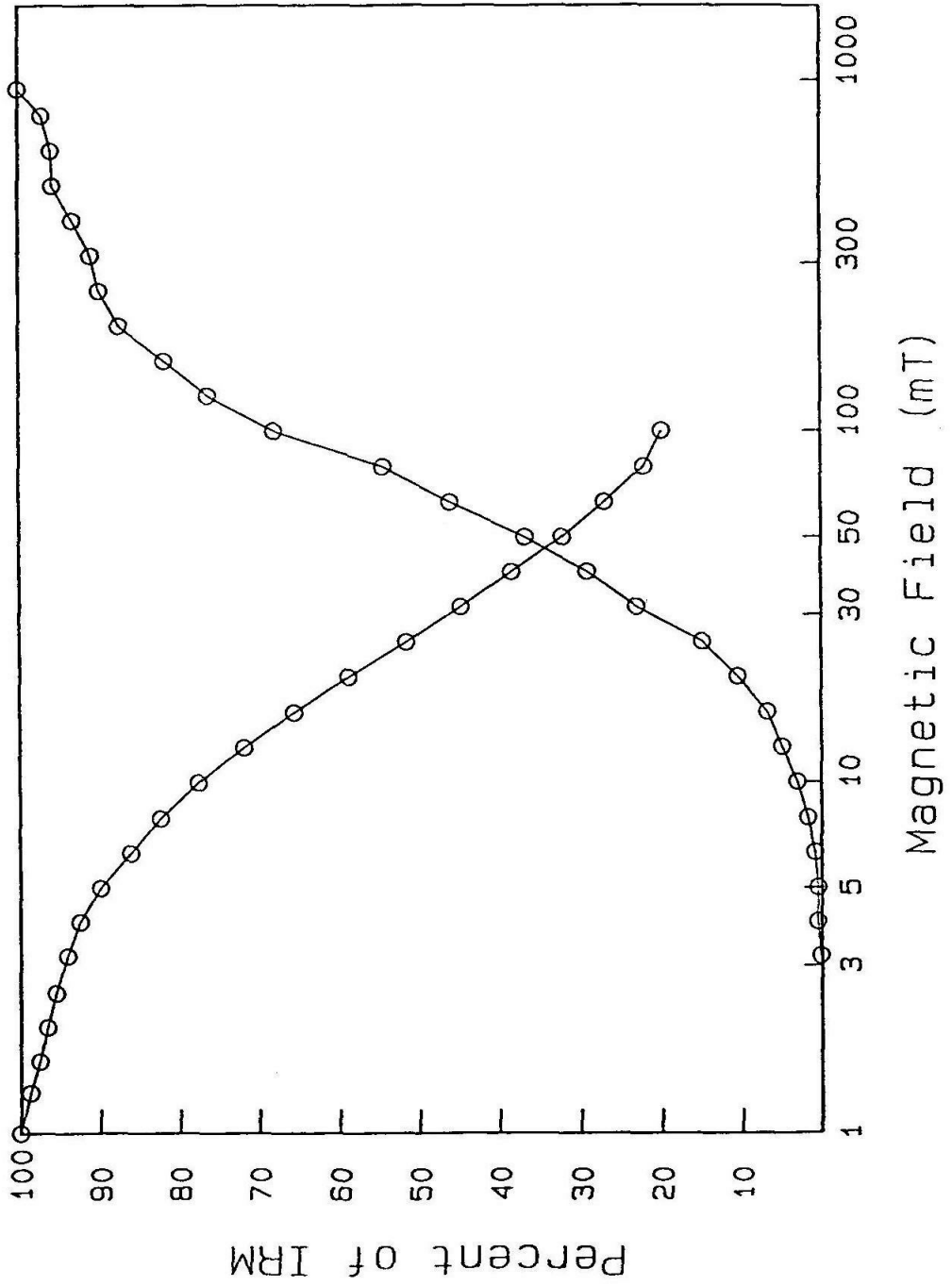


**Figure 7. Thermal demagnetization curves of magnetic samples from the Punchbowl Formation.**

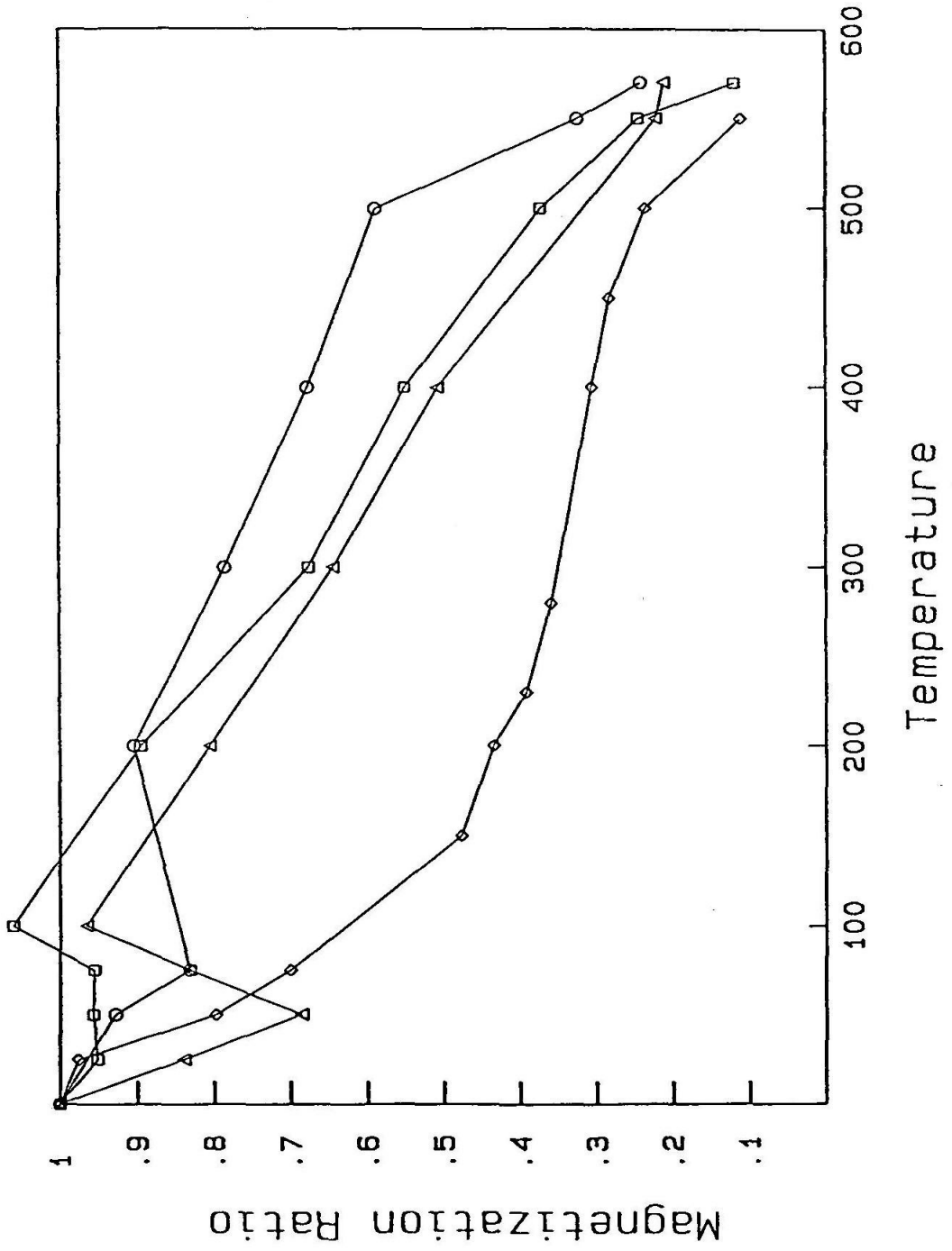
Squares -- sample BPB-3;

Circles - sample PDP-4;

Triangles -- sample PDP-46;

Diamond - sample PDP-115.

The magnetization ratio of the samples changes dramatically between 450 and 500 °C and drops to a small percentage of the NRM intensity at 575 °C, suggesting that main magnetic mineral are magnetite.





it possible to perform a fold test on the Punchbowl sediments. Samples from similar stratigraphic levels near the top of the formation on both sides of the syncline were used for averaging the mean direction. The Fisher (1953) precision parameter was calculated both before and after correction for tilt of bedding. The results are illustrated in Figure 8. The magnetic vectors are scattered and the precision value is relatively small ( $kappa1 = 9.3$ ) before bedding correction. After correction for tilt of bedding, the precision value increases dramatically ( $kappa2 = 34.3$ ). The fold test is passed at the 95% confidence level with a value of  $kappa1/kappa2 = 3.7$  (McElhinny, 1964). This fold test demonstrates conclusively that the characteristic magnetic component pre-dates the folding.

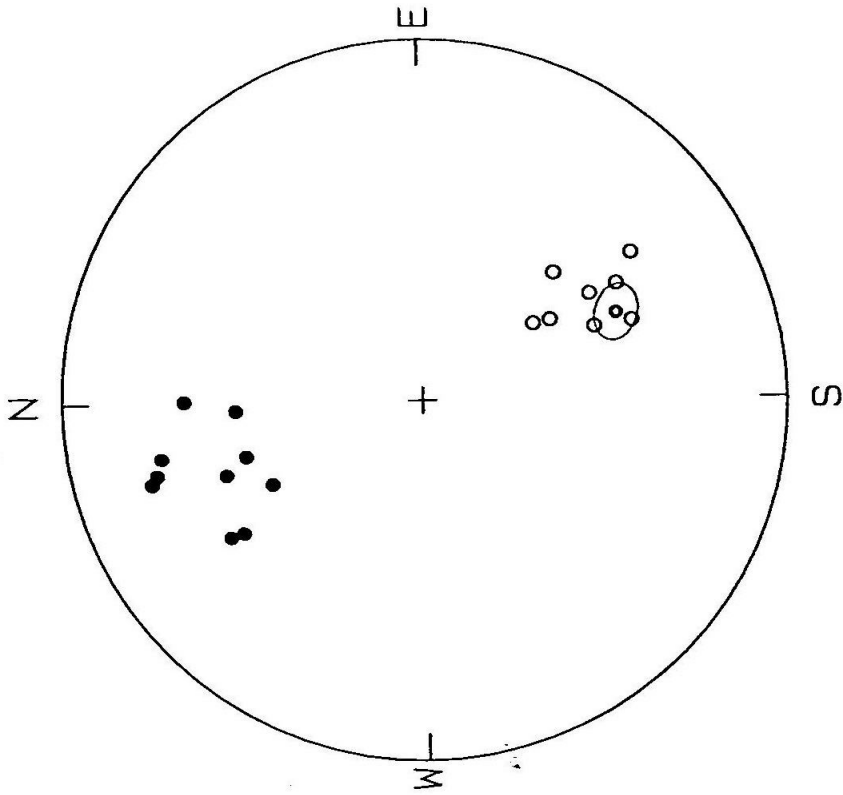
A positive conglomerate test conducted for the Lower Punchbowl Formation further confirms the above conclusion. Twelve samples were collected from reworked clasts of the Punchbowl Formation near the middle of the formation at section B - B'. The magnetic vectors obtained using the methods described above were illustrated in Figure 9. The resultant sum "R" of these vectors is 5.05. Using the randomness test of Fisher et al. (1987), we have  $3R^2/n = 6.38 < X^2_3 (0.05) = 7.81$ , ( $X^2_3$  is the upper probability percentage for 95% confidence with 3 degrees of freedom, n is the number of samples). The resultant R is also smaller than the 95% confidence level,  $R_0 (= 5.52)$ , of Irving (1964). Hence, the magnetic vectors of these samples are distributed randomly, implying that the clasts were magnetized prior to their local disruption and re-deposition. In conjunction with results from the positive fold test, we feel justified in interpreting most of the characteristic components isolated during demagnetization as primary.

**Figure 8. Fold test of the Punchbowl samples.**

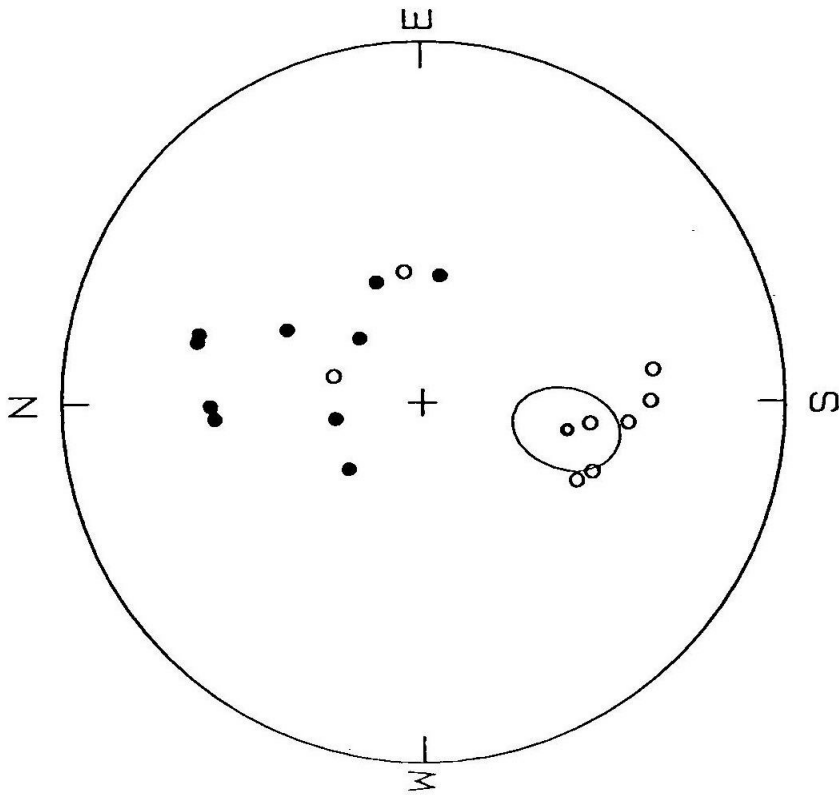
**LEFT -- results obtained before tilt correction of bedding;**

**RIGHT -- results obtained after tilt correction of bedding.**

Solid circle represents a vector directed onto the lower hemisphere, hollow circles represent vectors directed onto the upper hemisphere. Before correction of folding, the magnetic vectors are scattered. After correction of folding, they become much concentrated. This indicates that the magnetization of the samples were acquired before folding.



TILT-CORRECTED



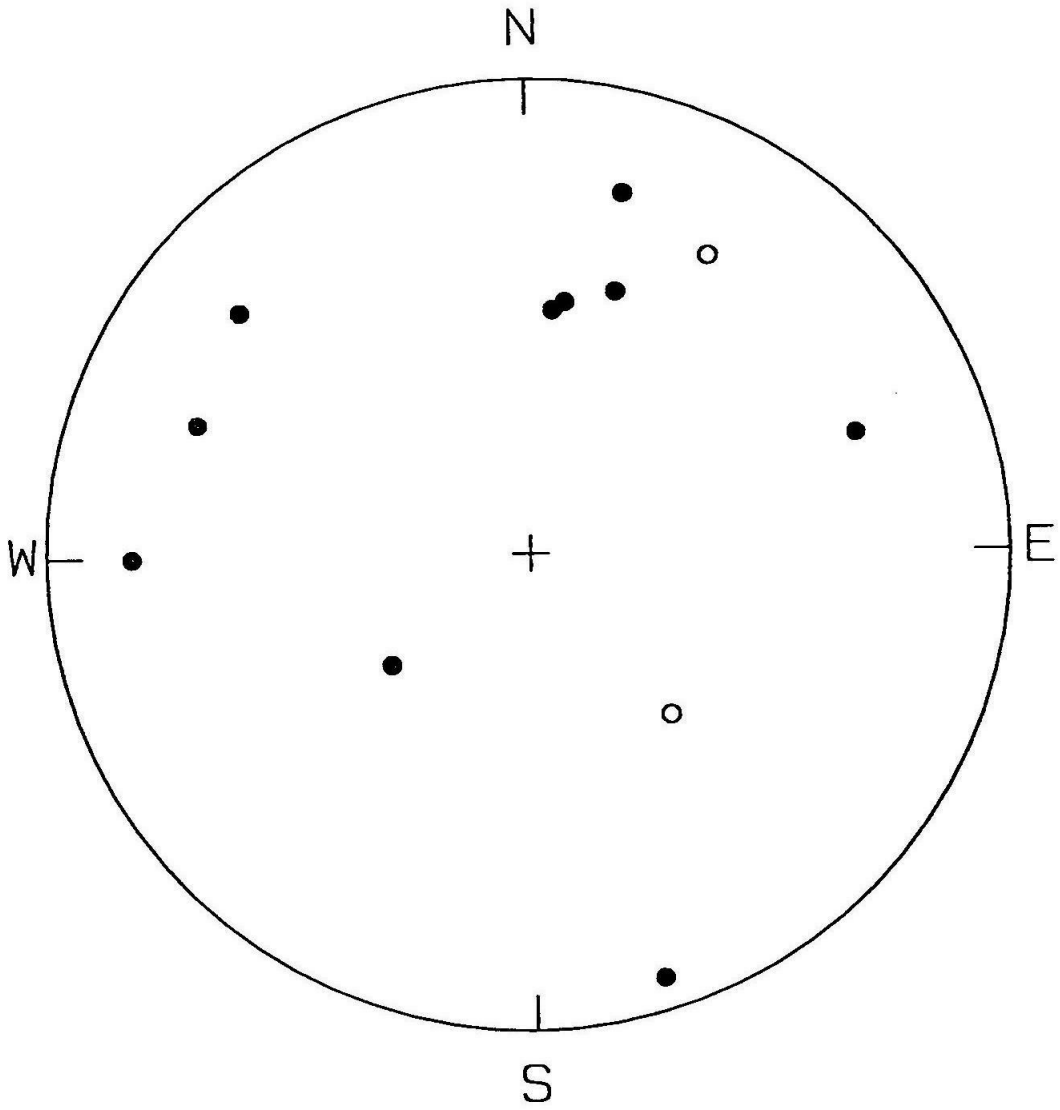
GEOGRAPHIC

**PUNCHBOWL FOLD TEST**

**Figure 9. Plot of conglomerate test results.**

Plot conventions are the same as those in Figure 8.

The directions are obviously scattered, indicating that the magnetization of the samples were acquired before the disruption or re-deposition of the clasts.



**PUNCHBOWL CONGLOMERATE TEST**

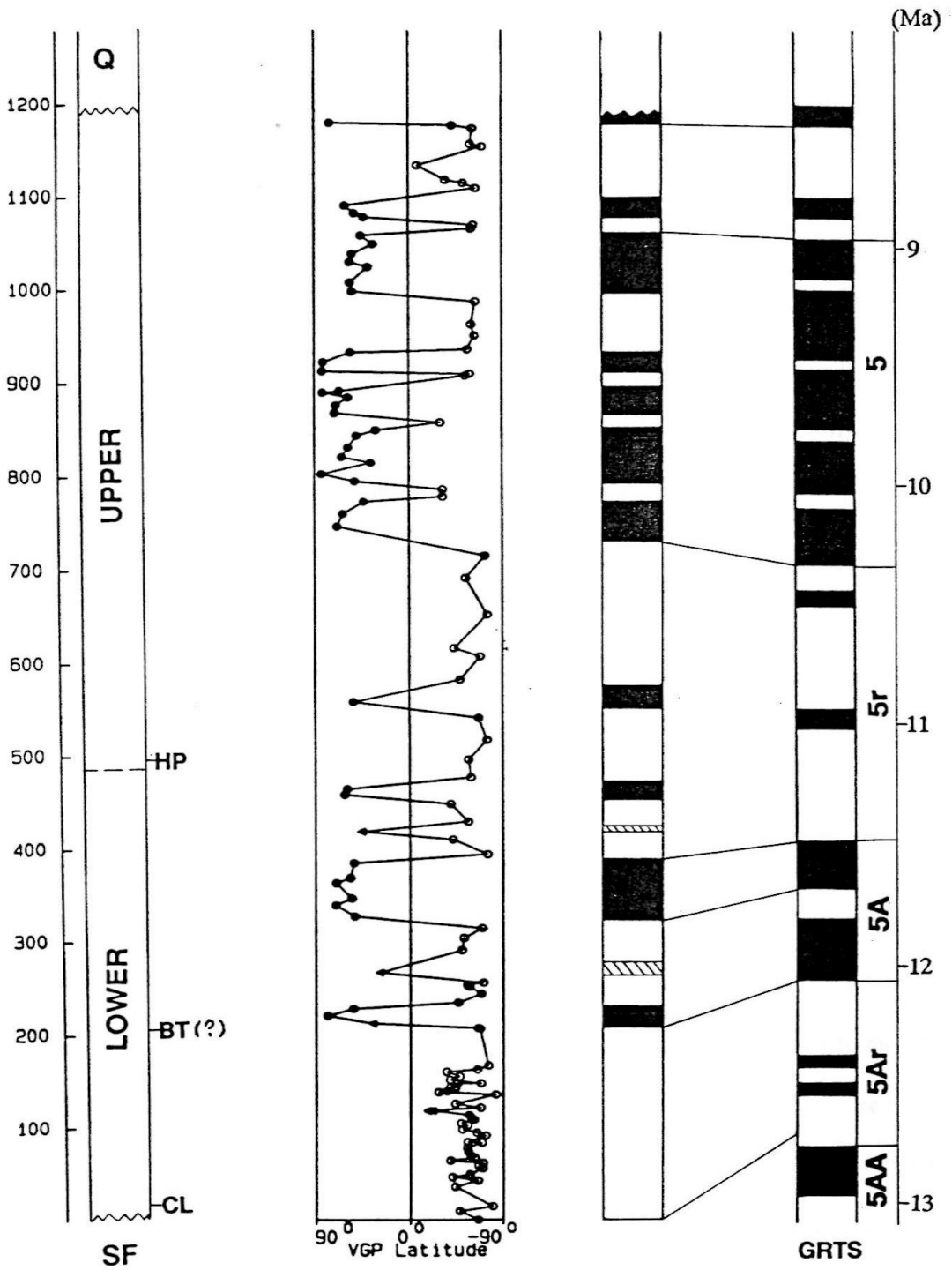
## MAGNETIC-POLARITY STRATIGRAPHY

Magnetic polarities were obtained after bedding correction using the above analysis. The north-seeking directions with positive (downwards) inclinations were interpreted as normal polarity, whereas the south-seeking sites with negative (upwards) inclinations were interpreted as reversed magnetic polarities. Polarities of the vectors with intermediate directions are generally referred to by their inclinations, which are more reliable than declination. These magnetic vectors are plotted against stratigraphic position in Figure 10. A series of horizons that have only normal polarities are interpreted as a normal magnetozone. On the other hand, a series of horizons with magnetic vectors of reverse polarities constitutes a reversed magnetozone. The boundary between a normal and a reversed magnetozone is arbitrarily placed midway between adjacent sites of opposite polarity. All magnetozones are based on more than one sample except two zones in which only one sample shows different polarity from adjacent zones. The latter are both type I samples and have very good linear decay paths.

The magnetic polarity stratigraphy of the Punchbowl Formation and our correlation with the GRTS are illustrated in Figure 10. The plot of magnetic vectors versus stratigraphic thickness of the Punchbowl Formation shows twenty-two magnetozones (Figure 10). A distinctive feature of this magnetic polarity stratigraphy is that, in the upper part, four to six short normal and shorter reversal magnetozones occur. Fossils found from the Upper Punchbowl Formation are of Hemphillian age (10 to 4 Ma, Woodburne, 1975), whereas the Lower Punchbowl may have been deposited during Clarendonian time (12 to 10 Ma) or slightly before. Given the fossil age constraints of

**Figure 10. Magnetostratigraphy of the Punchbowl Formation and its correlation to the Standard Magnetic Polarity Time Scale (Harland et al., 1982).**

The characteristic vector of each sample is plotted against stratigraphic thickness. Solid and open circles of magnetic vectors, and solid and white columns of magnetic polarity stratigraphy, represent normal and reverse magnetic polarities, respectively. Solid and open triangles are the samples with interminable direction. Reversal boundaries are placed half-way between two successive sites having opposite polarities. The unit boundaries and the level of collected fossils are indicated in the left-most column. The stratigraphic level of fossils are interpolated based on their relative position, i.e., projected on to the section.



Fossil Ages: HP - Hemphillian (10 - 4 Ma);  
 CL - Clarendonian (12 - 10 Ma);  
 BT - Barstovian (16 - 12 Ma).



between 12 to 4 Ma, only Chron 5 of the Standard Magnetic Polarity Time Scale (Harland et al., 1982) has the same distinctive features. Therefore, this part of the Punchbowl magnetic polarity pattern appears to correlate well with Chron 5 of the Harland et al.'s (1982) Magnetic Polarity Time Scale. The polarity pattern from the rest of the formation is relatively simple, predominantly having reverse polarities. Combining the fossil age constraints with the correlation of the upper magnetostratigraphy allows a relatively simple correlation of the lower magnetozones to the magnetic-polarity time scale (Figure 10). The oldest age is slightly uncertain because the lowest section (about 200 meter thick) has entirely reversed polarity with perhaps two indeterminable samples in it. In the event that we missed one or two short normal magnetozones, the lower limit of this long reversed magnetozone could be placed in the long reverse interval between either the normal chrons 5A-2 and 5Ar-1 or 5Ar-2 and 5AA of the magnetic polarity time scale (base of Figure 10). Considering the time period embraced by the section and the sedimentation rate (see below), the latter correlation seems more reasonable. In any case, however, the bottom age of the Punchbowl Formation would not be younger than 12.3 Ma or older than 12.7 Ma. Taking the average, the bottom age of the Punchbowl Formation is still well constrained to about 12.5 Ma.

Putting together the Upper and Lower Punchbowl Formation, the magnetostratigraphy is well matched from about Chron 5Ar-2 to just below Chron 4Ar-1 (Figure 10) of the magnetic-polarity time scale of Harland et al. (1982). The age of the entire Punchbowl Formation is thus constrained to be from 12.5 to 8.5 Ma. Although this age range is basically consistent with the paleontologic assessment, the age of the upper part of the formation appears slightly older than that suggested by the Hemphillian age fossils because they were found at and near the bottom of the Upper Punchbowl (Woodburne and Golz, 1972). Considering the following facts, however, we

believe that the magnetostratigraphic age constraints are correct: 1) the magnetic polarity pattern of the formation matches the time scale almost unambiguously and uniquely; 2) deposition in the irregular basin suggested by present exposures of the formation can cause the possible differences in stratigraphic level between the fossil localities and our sampling localities; 3) the fossil age ranges themselves may not be precisely evaluated.

### Sedimentation Rate

Rates of sediment accumulation were calculated for sediments of both the Lower and Upper Punchbowl Formation. The average sedimentation rate of the formation is 0.29 meter / 1000 years, and the Lower and Upper Punchbowl have average sedimentation rates of 0.28 meter / 1000 years and 0.21 meter / 1000 years, respectively.

### Rotation

The magnetic vectors obtained by using the above analyses were combined to calculate locality means using both Fisher (1953) and Bingham (1974) statistics. Only those magnetically stable samples, mainly the type I and some of type III, were used in these calculations. The results are illustrated in Table 1 and Figure 11 to 13.

The precision parameters (K1, K2, and kappa) in these calculations did not have large changes before and after structural correction because the samples were all collected from the same flank of the Punchbowl syncline. All values increase after correction for bedding. The mean directions for the Lower and Upper and for the entire formation are statistically the same (Table 1). The results for samples from both

**Table 1. Results of Fisher (upper part) and Bingham (lower part) statistics.**  
 Calculated using all magnetic vectors, except those with intermediate directions,  
 from the Punchbowl Formation.

| N                    | Geographic |      |              |      | Tilt-corrected |      |              |      |
|----------------------|------------|------|--------------|------|----------------|------|--------------|------|
|                      | Dec        | Inc  | $\alpha$ -95 | K    | Dec            | Inc  | $\alpha$ -95 | K    |
| Lower Part           |            |      |              |      |                |      |              |      |
| 45                   | 16.8       | 42.4 | 6.9          | 10.4 | 329.8          | 47.7 | 6.1          | 13.2 |
| Upper Part           |            |      |              |      |                |      |              |      |
| 38                   | 10.4       | 40.1 | 6.3          | 14.4 | 333.3          | 44.6 | 6.0          | 15.8 |
| The Entire Formation |            |      |              |      |                |      |              |      |
| 11                   | 13.8       | 41.4 | 4.7          | 11.9 | 331.5          | 46.3 | 4.3          | 14.4 |

| N                    | Geographic |      |              |             | Tilt-corrected |      |              |             |
|----------------------|------------|------|--------------|-------------|----------------|------|--------------|-------------|
|                      | Dec        | Inc  | $\alpha$ -95 | K1, K2      | Dec            | Inc  | $\alpha$ -95 | K1, K2      |
| Lower Part           |            |      |              |             |                |      |              |             |
| 45                   | 17.4       | 42.5 | 4.4, 8.3     | -14.3, -4.5 | 329.8          | 48.1 | 4.2, 7.3     | -15.0, -5.5 |
| Upper Part           |            |      |              |             |                |      |              |             |
| 38                   | 10.6       | 40.6 | 5.7, 6.7     | -9.9, -7.3  | 333.2          | 44.8 | 5.2, 6.3     | -11.6, -8.1 |
| The Entire Formation |            |      |              |             |                |      |              |             |
| 83                   | 14.0       | 41.5 | 3.8, 5.2     | -10.0, -5.8 | 331.4          | 46.5 | 3.5, 4.7     | -11.5, -6.9 |

N -- number of the samples used for calculation;

Dec -- declination;

Inc -- inclination;

$\alpha$ -95 -- error angle of mean at 95% confidence level;

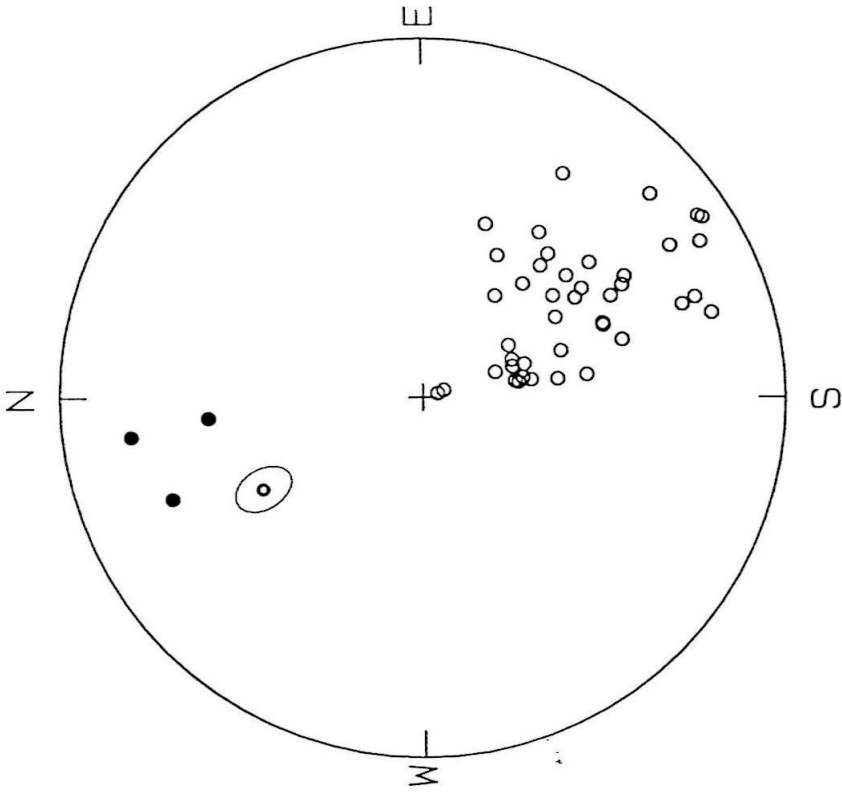
K, K1, and K2 -- precision value.

Geographic -- the values calculated before correction for tilt of bedding;

Tilt-corrected -- the values after structural correction.

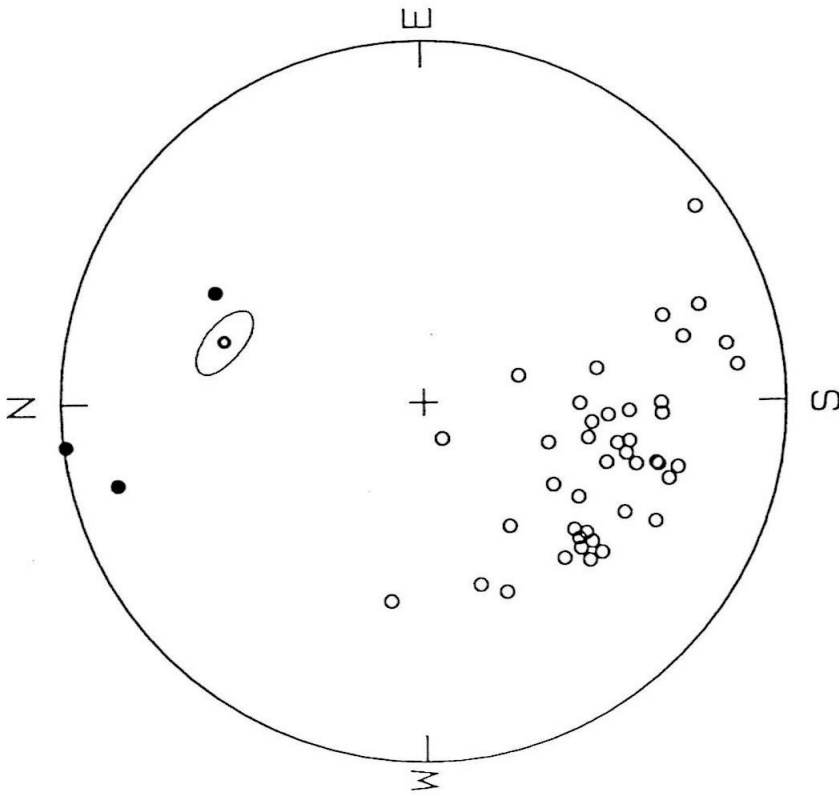
**Figure 11. Mean of the Lower Punchbowl Formation.**

Plotting convention is the same as Figure 8.



TILT-CORRECTED

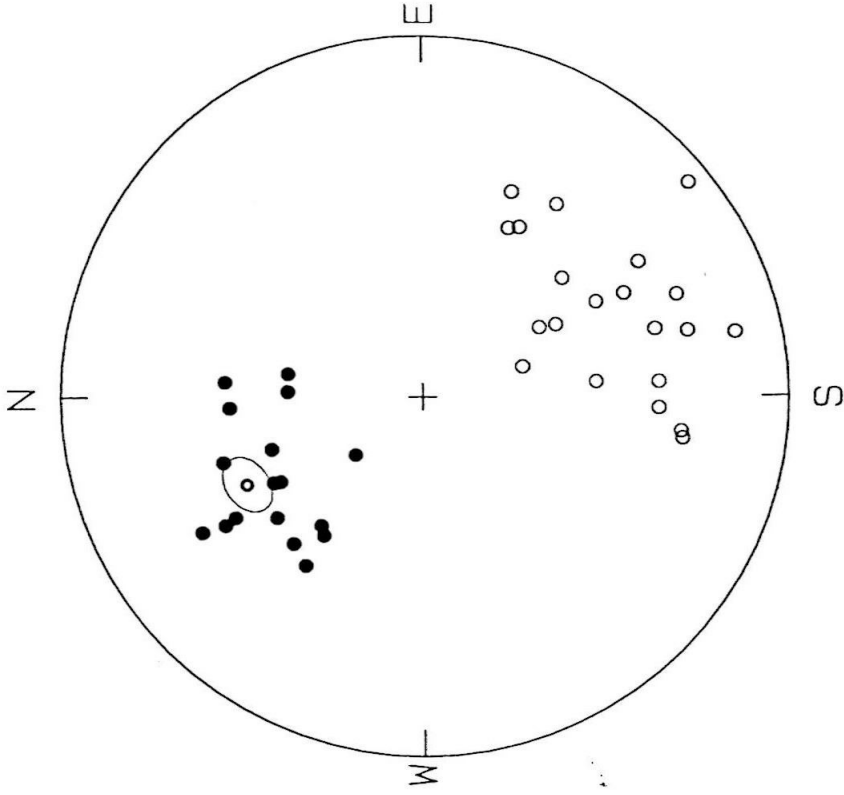
LOWER PUNCHBOWL



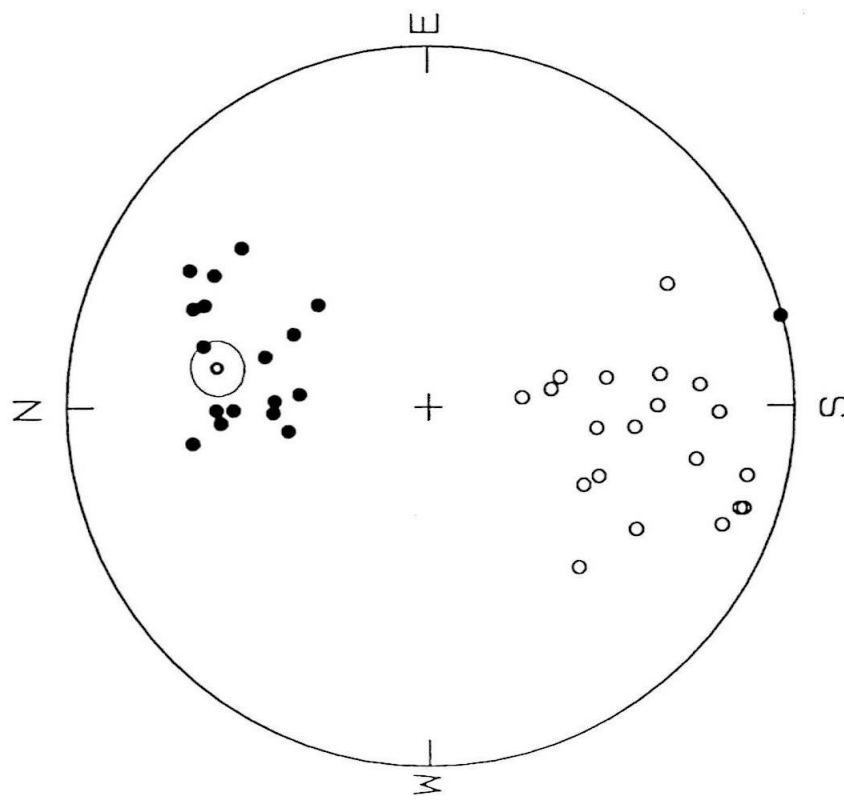
GEOGRAPHIC

**Figure 12. Mean of the Upper Punchbowl Formation.**

Plotting convention is the same as Figure 8.



TILT-CORRECTED



GEOGRAPHIC

UPPER PUNCHBOWL

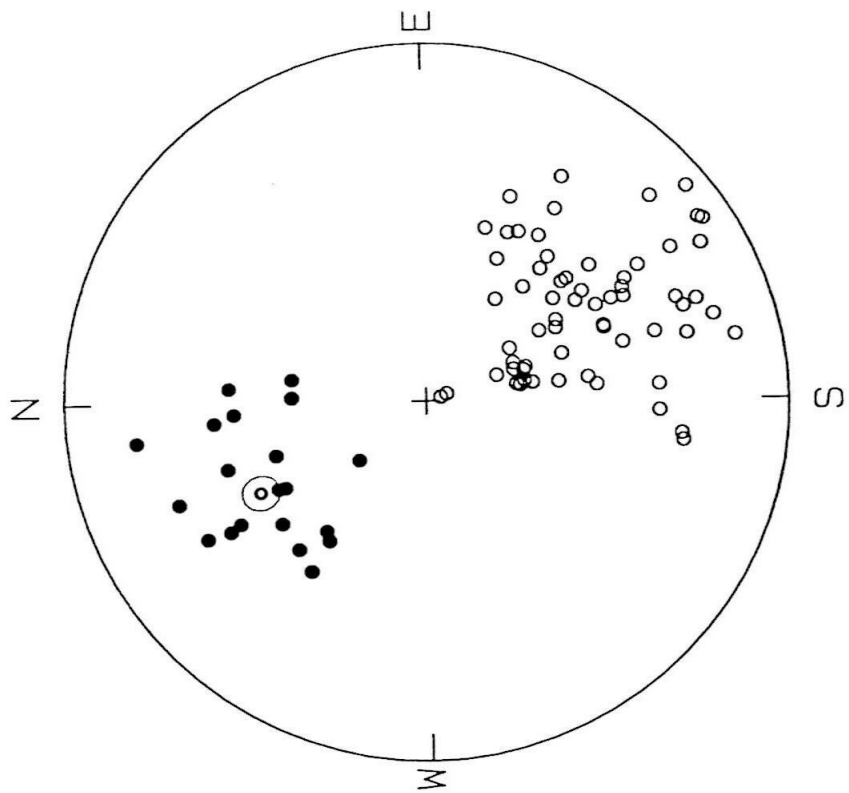
**Figure 13. Mean of the Punchbowl Formation.**

A - average of all cleaned samples;

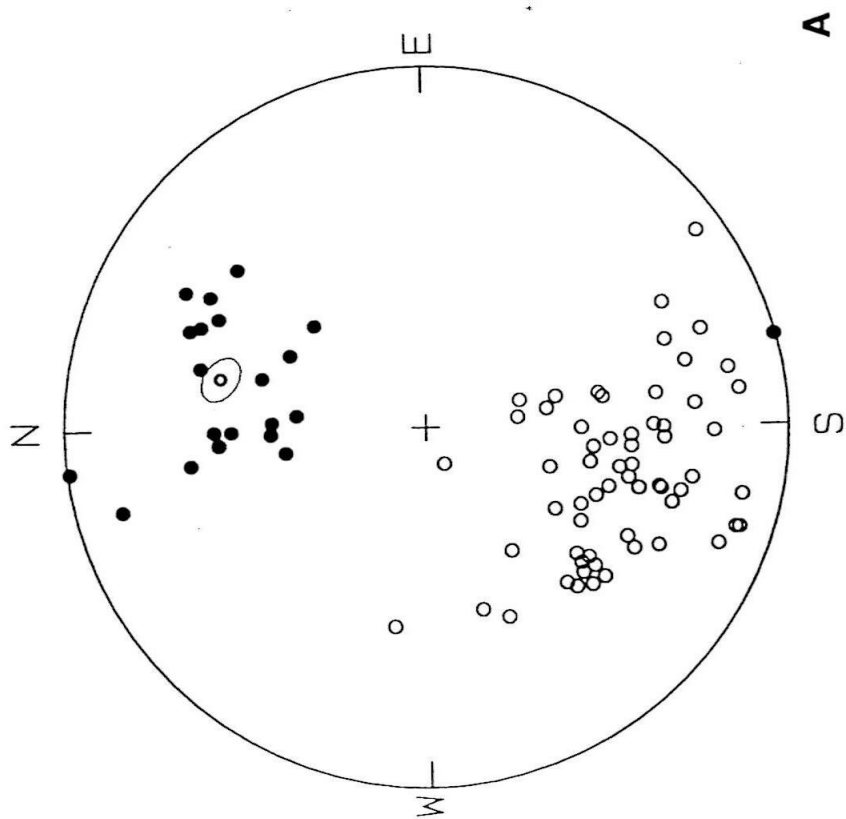
B - means of the Punchbowl Formation.

Plotting convention is the same as Figure 8.





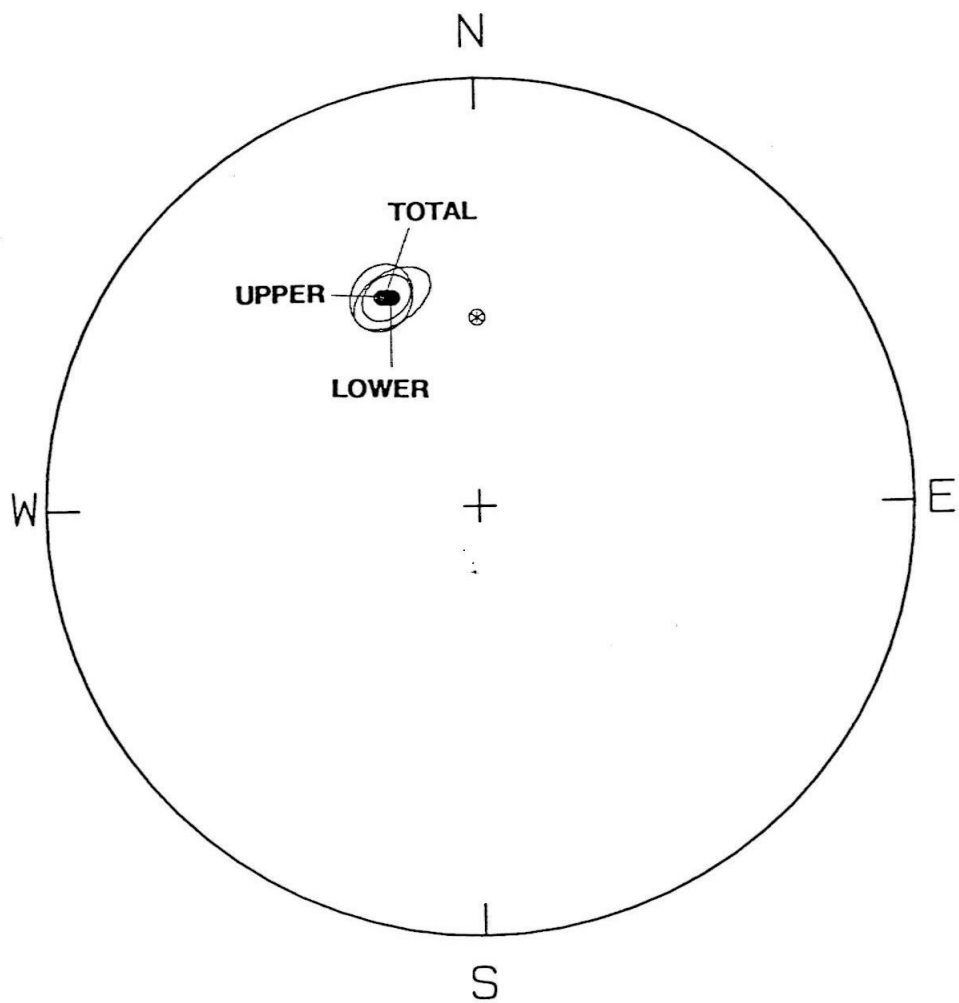
TILT-CORRECTED



GEOGRAPHIC

A

PUNCHBOWL FORMATION



# PUNCHBOWL FORMATION

Tilt Corrected

**B**

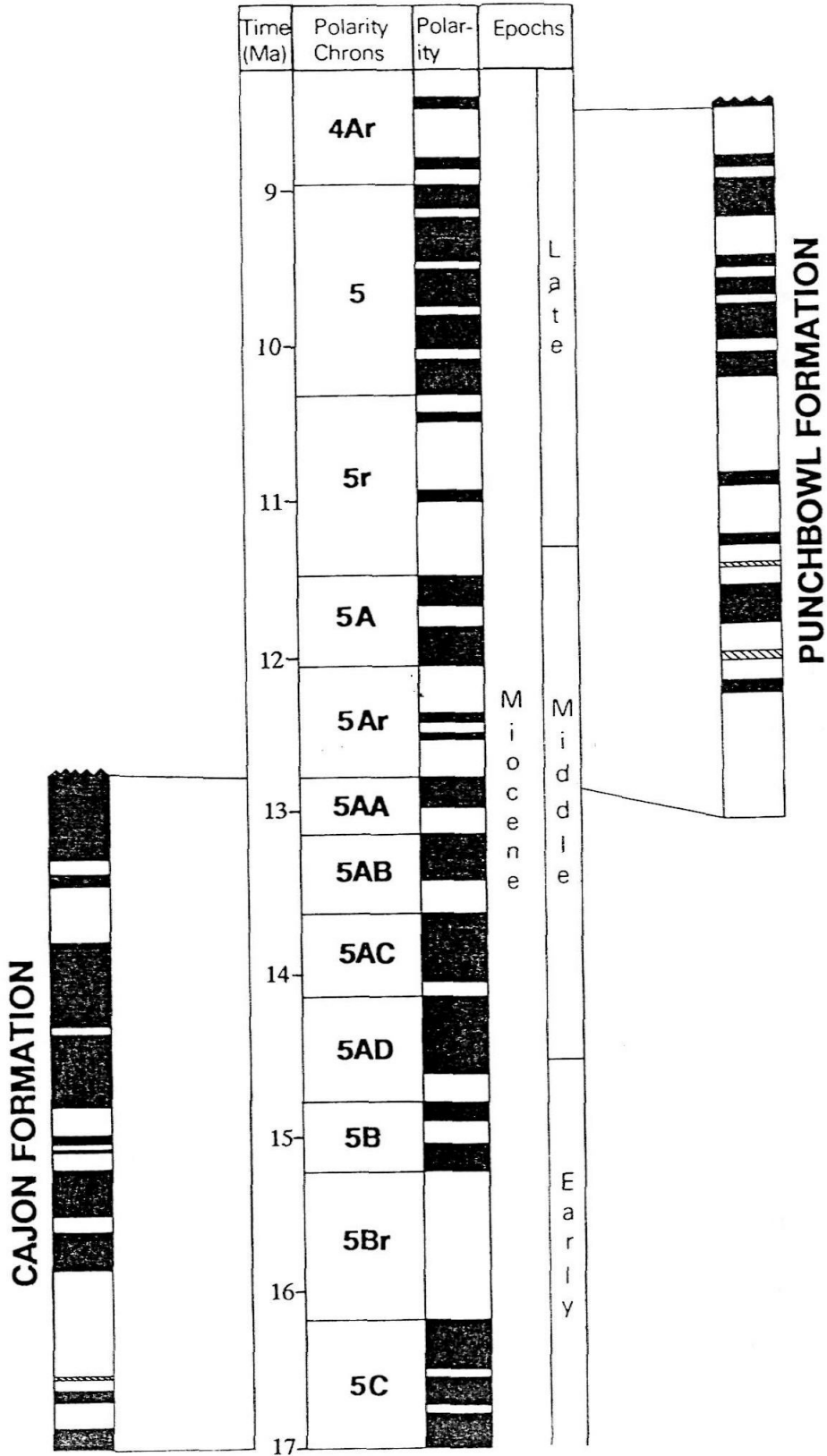
limbs of the Punchbowl syncline (Figure 8) are also consistent with those mean directions. It suggests that any remaining secondary components are very small and random, and that short-term secular variations have been averaged out. Thus the magnetic directions from the Punchbowl Formation are reliable and useful for tectonic interpretations.

## DISCUSSION

Figure 14 shows magnetostratigraphies of both the Cajon Formation in Cajon Valley and the Punchbowl Formation at Devil's Punchbowl, which were once thought either to be the same formation (Noble, 1954) or to be possibly to represent continuous deposits in the same basin (Woodburne and Golz, 1972; Woodburne, 1975). The upper part of the Cajon Formation was studied and presented in the last chapter. An obvious feature of the Devil's Punchbowl's section, which distinguishes it from the Cajon Formation in Cajon Valley, is that it is dominated by long intervals of reversed polarity at the lower part. The magnetostratigraphies of both formations suggest that the Punchbowl Formation was deposited during the period from 12.5 to 8.5 Ma, whereas the Cajon Formation has an age from at least 17 Ma to not younger than 12.7 Ma. Although the top age of the Cajon Formation is very close to the starting age for deposition of the Punchbowl Formation, they evidently do not overlap each other. In addition, the tectonic rotations preserved in these two formations are unquestionably different, implying they have distinct tectonic and geologic histories. Therefore, we can conclude that there is no correlation between the Cajon and the Punchbowl Formations. As a result, separation between these two formations cannot set constraints on the offset of the San Andreas fault.

**Figure 14. Magnetostratigraphies of the Punchbowl and Cajon formations.**

Solid and white columns of magnetic polarity stratigraphy, represent normal and reverse magnetic polarities, respectively.



The age constraint on the Punchbowl Formation also provides the base for correlation between this formation and the Mill Creek Formation. Although up to now the age of the Mill Creek Formation has not been constrained well, a correlation seems to be possible based on the new age of the Punchbowl and other tectonic and geologic correlations.

The timing of the Punchbowl fault was constrained loosely by the offset of the San Francisquito Formation and the Quaternary terrace as post-Paleocene (Dibblee, 1967, 1968) or post-Punchbowl (Barrows, 1985) to Quaternary. As the Quaternary terrace has been offset only tens of meters, compared with 44 kilometers of proposed offset (Barrows, 1985), it obviously cannot constrain the time of first motion along the Punchbowl fault even though it is the youngest offset unit. Except for this, the Punchbowl Formation is the youngest unit offset by the Punchbowl fault. Since the Paleocene San Francisquito Formation and older basement rocks (e. g., Pelona Schist) were both offset by the same amount (Dibblee, 1967, 1968; Sage, 1975), the maximum offset along the Punchbowl Formation might be 44 kilometers. Within this distance, one cannot find the counterpart of the Punchbowl Formation on the other side of the fault, with the possible exception of the Mint Canyon Formation in the Sierra Pelona region, 40 to 50 kilometers northwest of the Punchbowl (Figure 1). The geologic relationships between the Pelona Schist, San Francisquito and Vasquez formations, the Fenner fault, and the two formations are similar, which led to the correlation between these two regions (Dibblee, 1967; Ehlig, 1968). Based on fossils, the age of the Mint Canyon Formation is probably from Barstovian to Clarendonian (Dibblee, 1967, 1987) with a fission track date on the upper part suggesting 10 to 11.6 Ma (Terres and Luyendyk, 1985), and it is similar to that of the Punchbowl. Measured tectonic rotations in the two formations are also very similar (see below). Therefore, it is possible that the

Punchbowl and Mint Canyon formations were deposited, at least partially, in the same basin as suggested by Kew (1924) and Dibblee (1967), and separated subsequently by the Punchbowl fault. If this is the case, the Punchbowl fault could not be older than 13 million years, based on our dating of the Punchbowl Formation. On the other hand, based on the spatial relationship between the basal breccia of the formation that forms a narrow strip along the fault zone (Figure 2) and the Punchbowl fault, Weldon et al. (1990) concluded that the Punchbowl fault was active immediately before or during the beginning of deposition of the Punchbowl Formation, and also after its deposition. Hence, even if the Punchbowl does not correlate with the Mint Canyon, the age of the Punchbowl Formation still constrains the two episodes of activity to be 12.5 Ma and after 8.5 Ma, respectively.

Timing of another strand of the early San Andreas system, the Fenner fault, is also constrained by our result. Because the Punchbowl Formation is the oldest unit not offset by the Fenner fault whereas the youngest unit offset by the fault is the Paleocene San Francisquito Formation, the Fenner fault should be active between Paleocene time and before 12.5 Ma.

Rotations found in the Lower and Upper Punchbowl Formation are the same, suggesting that the rotation occurred after the deposition of the formation (8.5 Ma) and was coherent within the block. The mean direction of the Punchbowl Formation is rotated  $27.5^\circ \pm 4.3^\circ$  counterclockwise from the Late Miocene reference direction for stable North America ( $D = 1.9^\circ$ ,  $I = 47.5^\circ$ ,  $\alpha-95 = 3^\circ$ , Irving and Irving, 1982), and indicates a barely significant shallowing of the magnetic inclination, which is common in the sedimentary rocks. The declinations are similar to that from Terres and Luyendyk' study (1985) in the late Miocene Mint Canyon Formation from the San Gabriel Mountains, although their result is statistically uncertain ( $13^\circ \pm 30^\circ$ ). This might

suggest coherent counterclockwise rotation of the San Gabriel block between the San Andreas and the San Gabriel faults since Miocene time.

Early in 1974, Garfunkel proposed a kinematic model for the Mojave Desert, the bend of the San Andreas fault, and adjacent areas. In his model, the San Andreas fault was originally straight, but it has been bent progressively by differential crustal extension in the Basin and Range Province and the continental borderland in southern California. Simultaneously, the resultant north-south shortening, combined with right-lateral displacements along a set of closely spaced, parallel faults would lead to a net counterclockwise rotation and changes in over-all shape of the Mojave Desert and adjacent area, including the San Gabriel block and the San Gabriel and San Andreas faults themselves.

Offsets along the right-lateral faults in the Mojave Desert were later shown by Dokka (1983) to be much smaller than thought by Garfunkel (up to 30°, 1974), which implies that either smaller rotations within the Mojave block, or other effects and faults outside of the Mojave Desert, may be involved (Garfunkel and Ron, 1985). Our rotation results apparently agree with Garfunkel's model, which is close to his original estimate of the net rotation for the region. If we take his model and parameters, specifically the rotation gradient  $K$  ( $= 0.5$ ), and consider that the Punchbowl fault had been offset in response to north-south shortening, the offset along the Punchbowl fault needed for rotation and the bending would be only about 1 kilometer ( $D = K \times W = 0.5 \times 2$ , where  $D$  is offset on fault;  $W$  is width between faults). Based only on the Punchbowl fault having been active through Quaternary time, this amount of offset is plausible during the time period from Pliocene to Quaternary. However, Garfunkel's model (1974) requires a "reference boundary" across which the bounding faults do not extend, which seems not to be available in the San Gabriel block south of the San



Andreas fault. Also, the counterclockwise rotations of the Mint Canyon or the San Gabriel block cannot be explained by this model as the bounding faults are either inactive or have much less displacement during Pliocene and Quaternary time than that required by the model.

Alternatively, Terres and Luyendyk (1985) suggested (based on Garfunkel's model) that the San Gabriel block has been rotated counterclockwise about  $15^\circ$  as it moved into and along the bend of the San Andreas fault since Pliocene time. When the block moves into the preexisting bend of the San Andreas fault, with the Mojave Desert acting as a "backstop" (Weldon et al., 1990), the entire rigid block has to rotate to accommodate the stress and to continue the lateral movement. Considering the geometry of the San Andreas fault and the movements of the rigid San Gabriel block, this appears to be a better explanation for the rotations found in the Punchbowl Formation and the entire San Gabriel block.

The Punchbowl and Fenner (and San Francisquito) faults, which are proposed to be strands of an early San Andreas system (Weldon et al., 1990), now trend parallel to the bend of the San Andreas fault and oblique to it, respectively. However, if we rotate the entire block back according to our data, i. e., rotate the block  $28^\circ$  clockwise, the strike of the Fenner fault would be parallel to the bend of the San Andreas fault and the Punchbowl fault would trend along the San Andreas fault south of its bend. This appears to support the proposal (Weldon et al., 1990) that these faults are early strands of the San Andreas fault system, and implies that its bend has existed probably since Paleocene time.

## SUMMARY AND CONCLUSIONS

The paleomagnetic stratigraphy obtained from the Punchbowl Formation constrain the time of deposition of the formation to be from about 12.5 Ma to at least 8.5 Ma. In conjunction with the similar study of the Cajon Formation ("Cajon beds" of the Punchbowl Formation), our results suggest that these two units cannot be correlated and the distance between them cannot be used as the indication of offset along the San Andreas fault. The timing of the Punchbowl and the Fenner faults, which are proposed as strands of the early San Andreas system, is also constrained by our results: The two episodes of activity of the Punchbowl fault began at about 12.5 Ma and after 8.5 Ma, respectively, while the Fenner fault was active between Paleocene time and before 12.5 Ma.

About 28° of counterclockwise rotation was found in rocks of the Punchbowl Formation. While other rotation models seem not to be able to explain it, the rotation probably occurred as the San Gabriel block moved into the preexisting bent segment of the San Andreas fault. This rotation also supports the proposal that the Fenner and Punchbowl faults are strands of the early San Andreas system and that the bend of the San Andreas fault probably has existed since Paleocene time.

## ACKNOWLEDGEMENTS

The authors are thankful for very helpful discussions with Clarence Allen, and Lee Silver. This study was supported by NSF grants EAR83-51370; by the Chevron Oil Field Research Company; by the Arco Foundation; and by equipment grants from W. M. Keck and James Irving Foundations.

## REFERENCES

- Bailey, M.E., and Dunlop, D.J., 1983. Alternating field characteristics of pseudo-single-domain (2 - 14  $\mu\text{m}$ ) and multidomain magnetite: *Earth and Planetary Science Letters*, v. 63, p. 335 - 352.
- Bingham, C., 1974. An antipodally symmetric distribution on the sphere: *Ann. Stat.*, v. 2, p. 1201 - 1225.
- Dibblee, T.W., Jr., 1967. Areal geology of the western Mojave Desert, California. U. S. Geological Survey Professional Paper 522, 153 p.
- Dibblee, T.W., Jr., 1987. Geology of the Devil's Punchbowl, Los Angeles County, California: in Hill, M.L., ed., *Centennial Field Guide Volume #1, Cordilleran Section*, Geological Society of America, p. 207 - 210.
- Dokka, R.K., 1983. Displacements on late Cenozoic strike slip faults of the central Mojave Desert, California. *Geology*, v. 11, p. 305 -308.
- Ehlig, P.L., 1968. Causes of distribution of Pelona, Rand, and Orocopia schists. *Proceedings of Conference on Geologic Problems of San Andreas fault system*; Stanford University, p. 294 - 306.
- Ehlig, P.L., 1975. Basement rocks of the San Gabriel Mountains, south of the San Andreas fault, southern California. in Crowell, J.C., ed., *San Andreas fault in southern California*, California Division of Mines and Geology, special report 118, p. 177 -186.
- Fisher, N.I., Lewis, T., and Embleton, B.J.J., 1987. *Statistical analysis of spherical data*. Cambridge University Press, Cambridge, p. 329.
- Fisher, R.A., 1953. Dispersion on a sphere: *Proc. Roy. Soc. Lond.*, v. A217, p. 295 - 305.

- Foster, J.H., 1980. Late Cenozoic tectonic evolution of Cajon Valley: Unpublished Ph. D. Dissertation, University of California, Riverside, 242 p.
- Foster, J.H., 1982. Late Cenozoic tectonic evolution of Cajon Valley, southern California: in Sadler, P.M., and Kooser, M.A., eds.: Late Cenozoic stratigraphy and structure of the San Bernardino Mountains. Geol. Soc. Amer., Cordilleran Section Field Trip Guide, 6, p. 67-73.
- Garfunkel, Z., 1974. Model for the late Cenozoic tectonic history of the Mojave Desert, California, and its relation to adjacent regions: Geological Society of American Bulletin, v. 85, p. 1931 -1944.
- Garfunkel, Z., and Ron, H., 1985. Block rotation and deformation by strike-slip faults 2. The properties of a type of microscopic discontinuous deformation, Journal of Geophysical Research, v. 90, p. 8589 - 8602.
- Harland, W.B., Cox, A.V., Llewellyn, P.G., Pickton, C.A.G., Smith, A.G., and Walters, R., 1982. A Geological Time Scale. Cambridge Univ. Press, London/New York.
- Irving, E., 1964. Paleomagnetism and its application to geological and geophysical problems. John Wiley & Sons, Inc., 399 p.
- Irving, E., and Irving, G.A. 1982. Apparent polar wander paths carboniferous through Cenozoic and the assembly of Gondwana: Geophysical Surveys, v. 5, p. 141 - 188.
- Kew, W.S.W., 1924. Geology and oil resources of a part of Los Angeles and Ventura Counties, California. U. S. Geological Survey Bulletin, v. 753, 202 p.
- Kirschvink, J.L., 1980. The least-squares line and plane and the analysis of the paleomagnetic data: examples from Siberia and Morocco. Geophysical Journal of the Royal Astronomical Society, v. 62, p. 699-718.
- Liu, W., Weldon, R.J., and Kirschvink, J.L., 1988. Paleomagnetism of sedimentary rocks

from and near the DOSECC Cajon Pass well, southern California: *Geophysical Research Letters*, v. 15, p. 1065 - 1068.

Luyendyk, B.P., Kamerling, M.J., and Terres, R.R., 1980. Geometric models for Neogene crustal rotations in southern California. *Geol. Soc. Amer. Bull.*, v. 91, p. 211-217.

Luyendyk, B.P., Kamerling, M.J., Terres R.R., and Hornafius, J.S., 1985. Simple shear of southern California during Neogene time suggested by paleomagnetic declinations. *Jour. Geophys. Res.*, v.90, p. 12,454-12,466.

Matti, J.C., Morton, D.M., and Cox, B.F., 1985. Distribution and geological relations of fault systems in the vicinity of the central Transverse Ranges, southern California. *U.S. Geol. Surv. Open File Report*. 85-365, 37 p.

McElhinny, M.W., 1964. Statistical significance of the fold test in paleomagnetism. *Geophys. J. R. Astr. Soc.* v. 8, p. 338 - 340.

Noble, L.F., 1926. The San Andreas rift and some other active faults in the desert region of southeastern California. *Carnegie Institute of Washington, Yearbook* no. 25, p. 415-422.

Noble, L. F., 1932. The San Andreas rift in the desert region of southern California: *Carnegie Institute of Washington Yearbook*, no. 31, p. 355 - 363.

Noble, L.F., 1953. *Geology of the Pearland quadrangle, California: U. S. Geological Survey Geological Quadrangle Map GQ-24, scale 1:24,000.*

Noble, L.F., 1954. *Geology of the Valyermo Quadrangle and vicinity, California. U.S. Geological Survey Quadrangle Map Series, Washington D.C.*

Nur, A., Ron, H., and Scotti, O., 1986. Fault mechanics and the kinematics of block rotations: *Geology*, v. 14, p. 746 - 749.

Pelka, G.J., 1971. Paleocurrents of the Punchbowl Formation and their interpretation.

Geological Society of America, Abstracts with Programs, v. 3, p. 176.

- Sage, O., Jr., 1975. Sedimentological and tectonic implications of the Paleocene San Francisquito Formation, Los Angeles County, California. in Crowell, J.C., ed., San Andreas fault in southern California, California Division of Mines and Geology, special report 118, p. 162 -169.
- Tedford, R.H., and Downs, T., 1965. Age of the Punchbowl Formation, Los Angeles and San Bernardino Counties, California. Geological Society of America Special Paper 87, 239 p.
- Terres, R.R., and Luyendyk, B.P., 1985. Neogene tectonic rotation of the San Gabriel region, California, suggested by paleomagnetic vectors: *Journal of Geophysical Research*, v. 90, p. 2467 - 2484.
- Weldon, R.J., II, 1986. The late Cenozoic geology of Cajon Pass: Implications for tectonics and sedimentation along the San Andreas fault, Ph.D. thesis, California Institute of Technology, Pasadena, California. 400 p.
- Weldon R.J., Meisling, K.E., and Alexander, J., 1990. A speculative history of the San Andreas fault system in the Central Transverse Ranges: in Powell, R.E., and Weldon, R.J., eds., *Palinspastic Reconstruction of the San Andreas fault zone*, Geological Society of America Special Paper, (in press).
- Woodburne, M.O., 1975. Late Tertiary nonmarine rocks, Devil's Punchbowl and Cajon Valley, southern California: in Crowell, J.C., ed., *San Andreas fault in southern California*, California Division of Mines and Geology, special report 118, p. 187 - 196.
- Woodburne, M.O., and Golz, D., 1972. Stratigraphy of the Punchbowl Formation, Cajon Valley, southern California. *University of California Publications in Geological Sciences*, Vol. 92, 73 pp.

CHAPTER FOUR

**PALEOMAGNETIC ROTATION STUDY OF THE MILL  
CREEK FORMATION, SOUTHERN CALIFORNIA**

by

Wei Liu

California Institute of Technology

**Chapter 4****INTRODUCTION**

Large paleodeclination anomalies are often found in crustal blocks bounded by strike-slip faults, and have led to various kinematic models such as those of Garfunkel (1974), Beck (1976), Luyendyk et al. (1980, 1985), and McKenzie and Jackson (1983). Most of these models suggest that crustal rotations result from shear forces, and they commonly require another set(s) of faults perpendicular to or inclined to the direction of shear couple to accommodate stress (Garfunkel, 1974; Luyendyk et al., 1980, 1985, Nur et al., 1986). Since the phenomena have not been understood fully, these studies and results have generated new interest in the tectonic significance and kinematic history of crustal blocks, particularly of those within and near the San Andreas transform system.

In this study, I used paleomagnetic methods to determine whether or not tectonic rotations have occurred in the Mill Creek Formation, which is bounded by north and south branches of the San Andreas fault. This special tectonic position of the Mill Creek Formation provides a unique place for us to study the rotation of crustal blocks bounded by two large strike-slip faults, which may have been active during the past several million years.

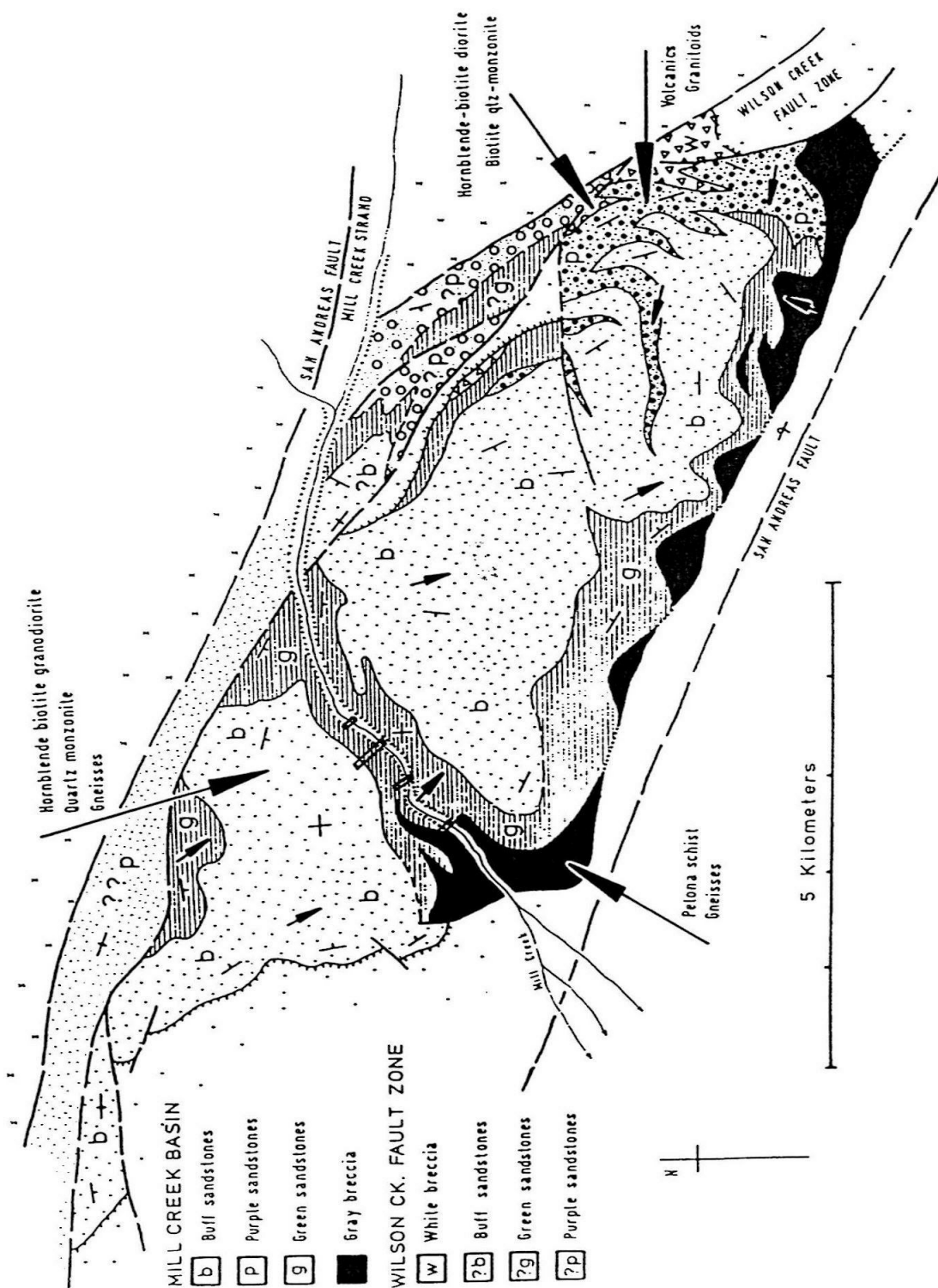
**GEOLOGIC BACKGROUND**

The Mill Creek Formation is located between two (or three) strike-slip faults, the modern San Andreas, Wilson and Mill Creek faults (Figure 1). A 50 km long



**Figure 1. Geological map of the Mill Creek area.**

Adopted from Sadler and Demirer (1986).



discontinuous sliver of similar rocks to the west between the Wilson Creek and Mill Creek faults has been included in the Mill Creek Formation by early workers (Owens, 1959; Gibson, 1971). It is separated from the main unit in the south by the Wilson Creek fault. Sadler and Demirer (1986) argued that the entire formation was deposited in the same basin as a whole unit. Thus, the Wilson Creek fault would have only a minor offset. On the other hand, Matti and others (1985) suggest that these rocks are actually two different formations juxtaposed by the Wilson Creek fault, based on different characteristics of the rocks such as color and depositional features on the two sides of the fault. If this is the case, the fault would need to have had a large displacement. Resolving this problem requires good age control and more detailed studies of these rocks.

Matti et al. (1985), and Weldon (personal communication, 1987, 1990) have proposed tentatively that the Mill Creek Formation may be the offset portion of the Punchbowl Formation at Devil's Punchbowl, and that they were separated by motion along the San Andreas fault. The arguments for this correlation include the similar character of rocks in these two formations, and similar age ranges. Furthermore, if the offset on the San Andreas fault was restored according to their models, these two formations would be at the same place. Age controls on the two formations again are critical for confirming this speculation.

Several questions need to be answered for the Mill Creek Formation. First, what is its depositional age? Like most of the late Cenozoic non-marine sedimentary rocks, age constraints are often difficult to provide for it. Although some Late Miocene plant fossils have been found from it, they were not good for more precise age constraints. A second question is whether or not the Mill Creek Formation is one unit with different depositional phases, or is actually two different formations that have been

brought together by the Mill Creek fault. Finally, have the Mill Creek rocks been rotated in response to displacement along strands of the San Andreas fault?

Originally, I attempted to resolve the above problems using paleomagnetic methods. Unfortunately, most of the Mill Creek sediments have proven to be magnetically unstable, making it nearly impossible to complete a magnetostratigraphic section. Therefore, in this chapter I concentrated only on rotations study and will not discuss stratigraphy further.

### PALEOMAGNETIC PROCEDURES

The Mill Creek Formation is exposed in Mill Creek Canyon on both sides of Highway 38 and the stream (Figure 1). It unconformably overlies crystalline basement rocks on the west, and is bounded by faults on the other sides (Sadler and Demirer, 1986). According to Sadler and Demirer (1986), the formation is folded gently into an east-west trending syncline. The main phase of the formation in middle of the fold is composed of fine-grained, green sandstones and siltstones, whereas the lateral facies at the edges of the two limbs consist of buff sandstones. The entire formation is well-exposed and very fresh because of quarrying for the highway.

At the beginning, thirty samples were collected from both flanks and near the axis of the syncline to conduct a fold test and to determine the magnetic stability of the rocks. Hence, stratigraphic distances between these samples were only measured approximately. Subsequently, another 48 samples were collected from the center of the fold near the axis where the rocks appeared more stable magnetically. At this locality, the beds of the Mill Creek Formation dip gently less than 5 degrees to the west, and are well-bedded and consolidated. The stratigraphic interval between samples averages

0.63 meters, with only a few large gaps, covering a 30 meter stratigraphic section. All samples were collected using a water-cooled gasoline-powered drill and oriented using standard methods. Declination measurements were confirmed by using a Sun-compass when possible. Processing and measurements of these samples are the same as those for samples from the Punchbowl Formation (see chapter 3, this thesis).

Magnetic properties of these samples vary greatly between those from near the axis of the syncline and those from near the edges of either flank. Samples collected from the center of the formation generally have very strong magnetization, the natural remanent magnetization (NRM) levels range from  $10^{-7}$  to  $10^{-6}$  A·M<sup>2</sup>. These samples behaved magnetically relatively well, with linear demagnetization trajectories pointing towards the origin in orthogonal projection (Figure 2). Samples collected from either flank of the fold have weak NRM ( $10^{-10}$  to  $10^{-8}$  A·M<sup>2</sup>), and some of them appear magnetically unstable (Figure 3). The demagnetization path for most of these samples is either jagged or random. A common feature of all Mill Creek samples, however, is that the natural remanent magnetization (NRM) drops sharply after 350°C. At higher temperatures, the demagnetization path of some samples became random (Figure 4).

Characteristic components were found using the principal component analysis technique of Kirschvink (1980) for each sample. Samples with obvious random demagnetization vectors were rejected, and only those with least-square error angles less than 10 degrees were accepted and used in further statistical calculations.

Figure 5 shows the results from the fold test on the Mill Creek samples. The Fisher (1953) precision parameter ( $\kappa$ ) improved from a value of 7.4 to 14.7 after tilt correction. With  $\kappa_1/\kappa_2$  ratio equals 2.0, it passes the fold test at the 95% confidence level (McElhinny, 1964), which is not bad for such a gentle fold. Hence, the magnetization probably pre-dates folding and the characteristic components isolated

**Figure 2. Orthogonal and equal-area plots of the typical demagnetization paths.**

LEFT - Orthogonal plot based on successive endpoints of demagnetization vectors. Solid circles are projected on a horizontal plane whereas open circles are on a vertical plane. Each division on axes represents remanent magnetization intensity of  $10^{-7} \text{ A}\cdot\text{M}^2$ .

RIGHT - Equal-area stereographic projection of the same demagnetization vectors as in left. Solid circles are the vectors in the lower hemisphere and open ones are plotted on the upper hemisphere.

All of these plots are based on bedding-corrected directions of magnetization. The AF demagnetizing field is in millitesla and temperatures are in degree Celsius.

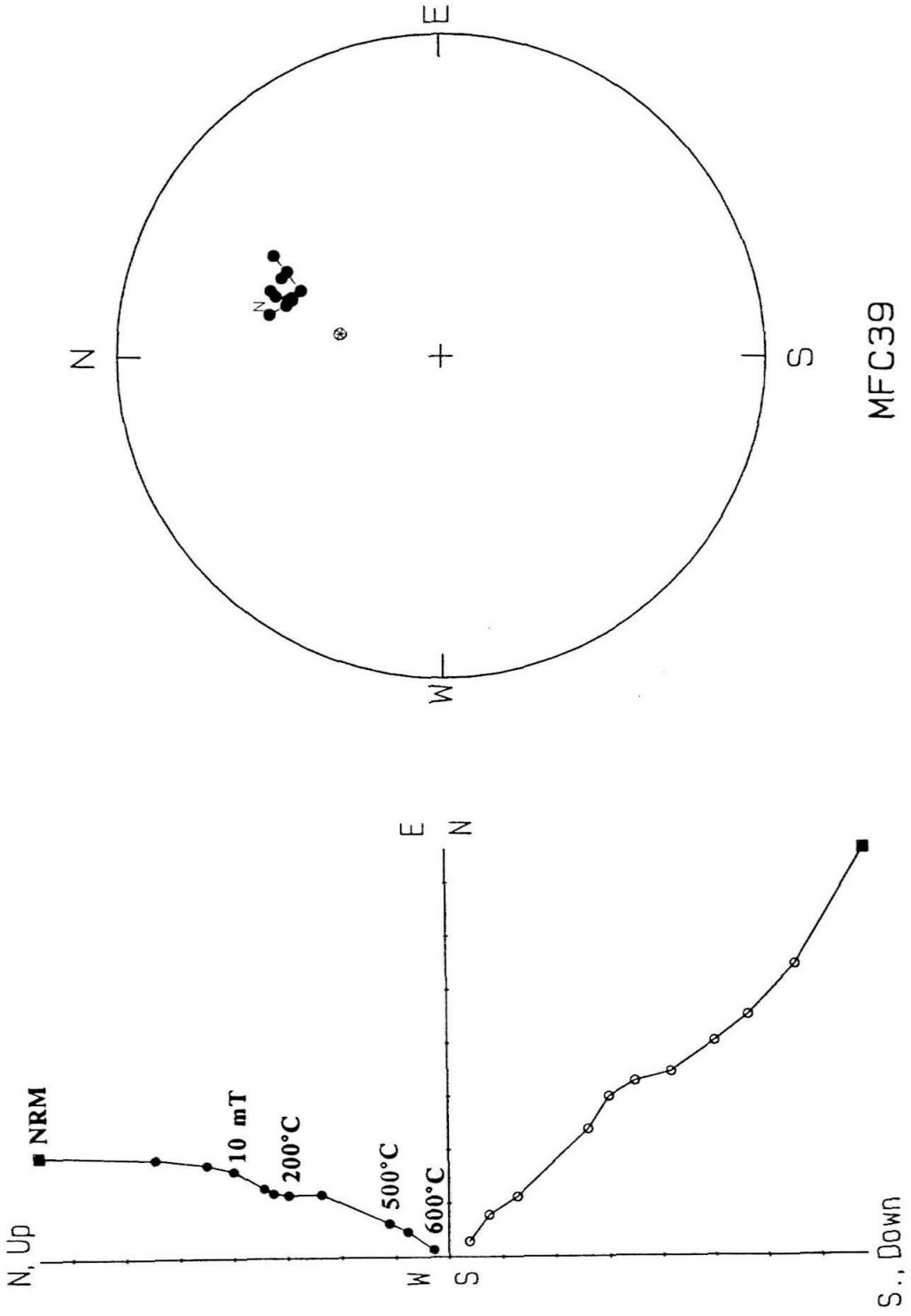
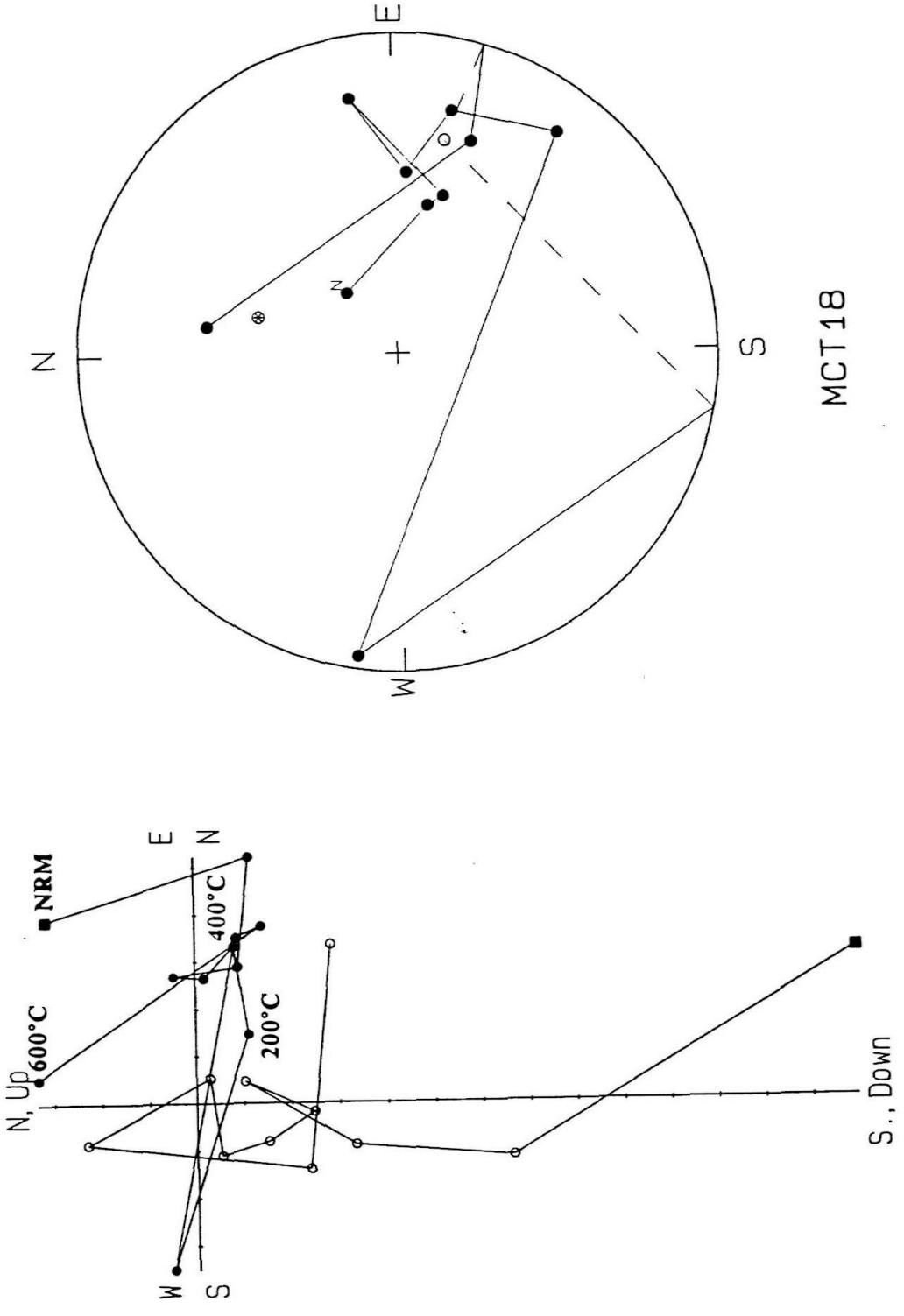


**Figure 3. Orthogonal and equal-area plots of the typical demagnetization paths.**

Plotting convention is the same as Figure 2. Each division on axes of the orthogonal plot represents remanent magnetization intensity of  $10^{-10}$  A·M<sup>2</sup>.

Sample was collected from edge of the basin.





MCT18

**Figure 4. Orthogonal and equal-area plots of the typical demagnetization paths.**

Plotting convention is the same as Figure 2. Sample was taken from near center of the basin.

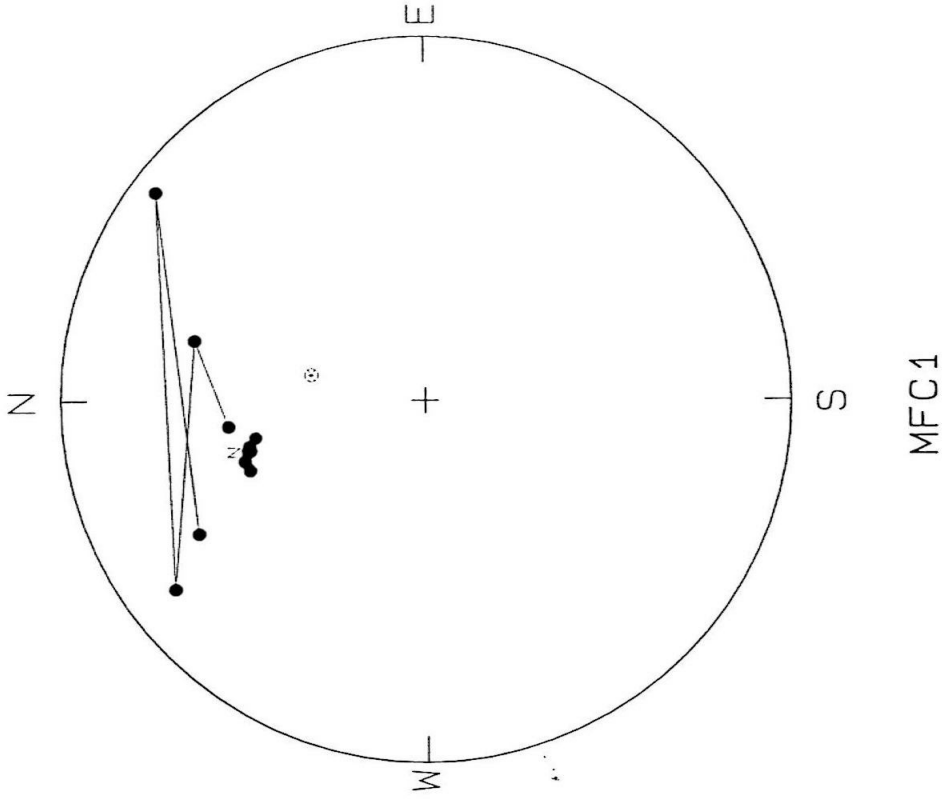
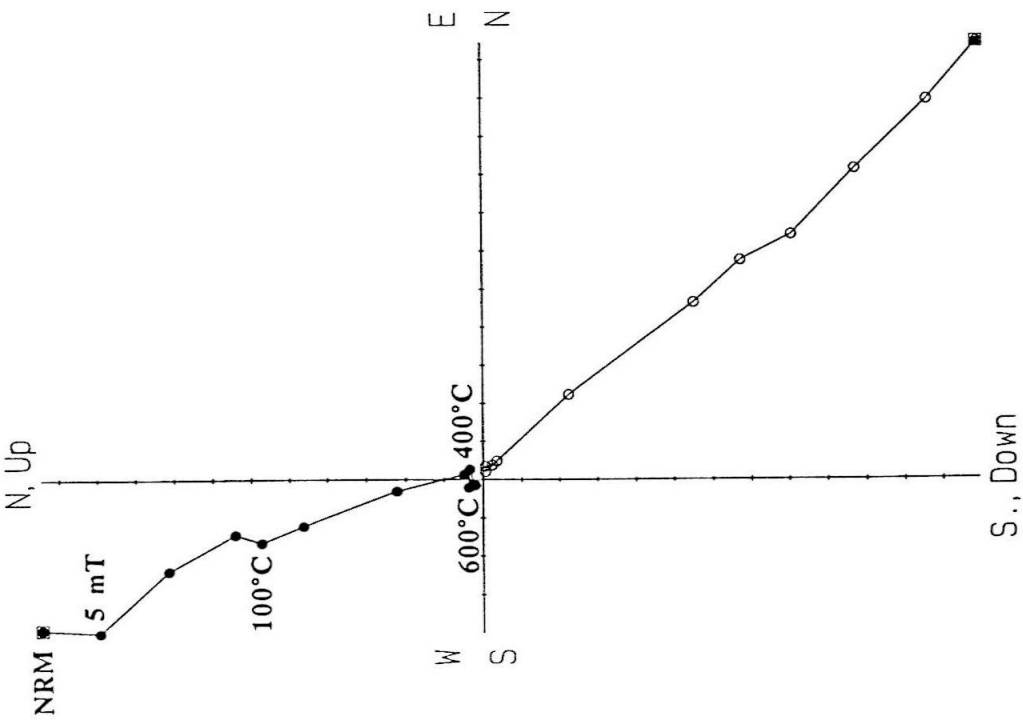


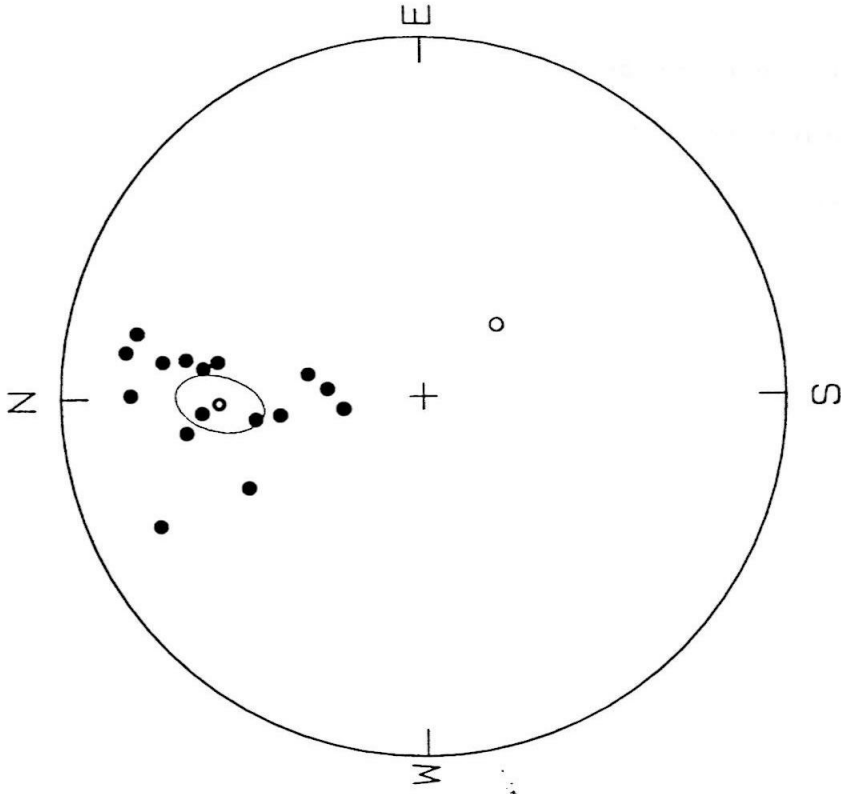
**Figure 5. Fold test of the Mill Creek samples.**

Averaged on samples collected from the center and both limbs of the Mill Creek syncline using Fisher (1953) and Bingham (1974) statistics.

LEFT -- results obtained before tilt correction of bedding;

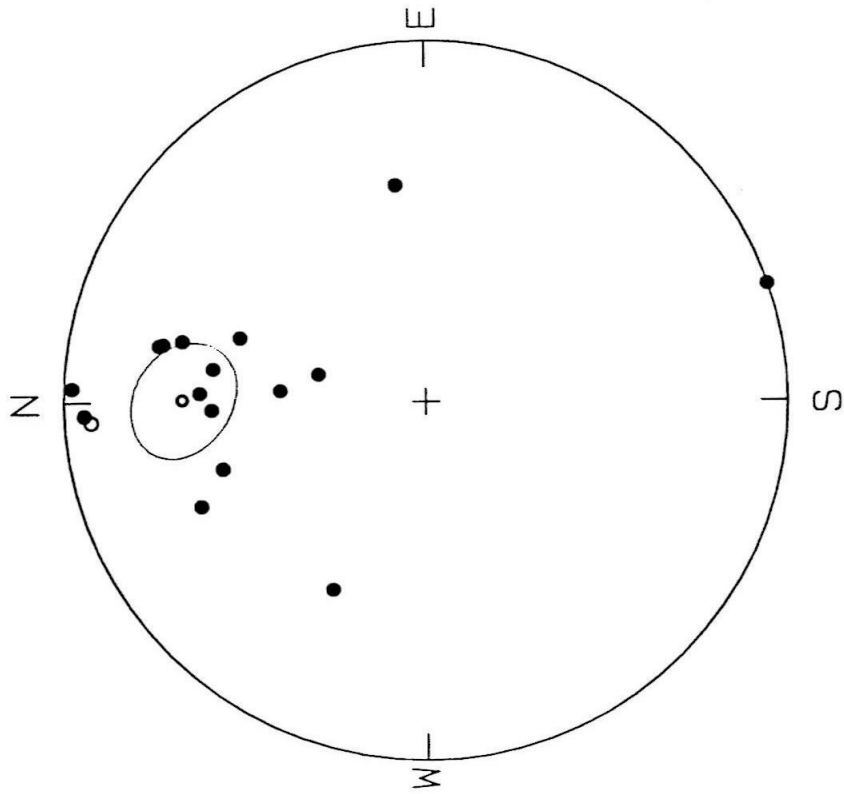
RIGHT -- results obtained after tilt correction of bedding.

Solid circle represents a vector directed onto the lower hemisphere, hollow circles represent vectors directed onto the upper hemisphere.



MILL CREEK FOLD TEST

Tilt Corrected



MILL CREEK FOLD TEST

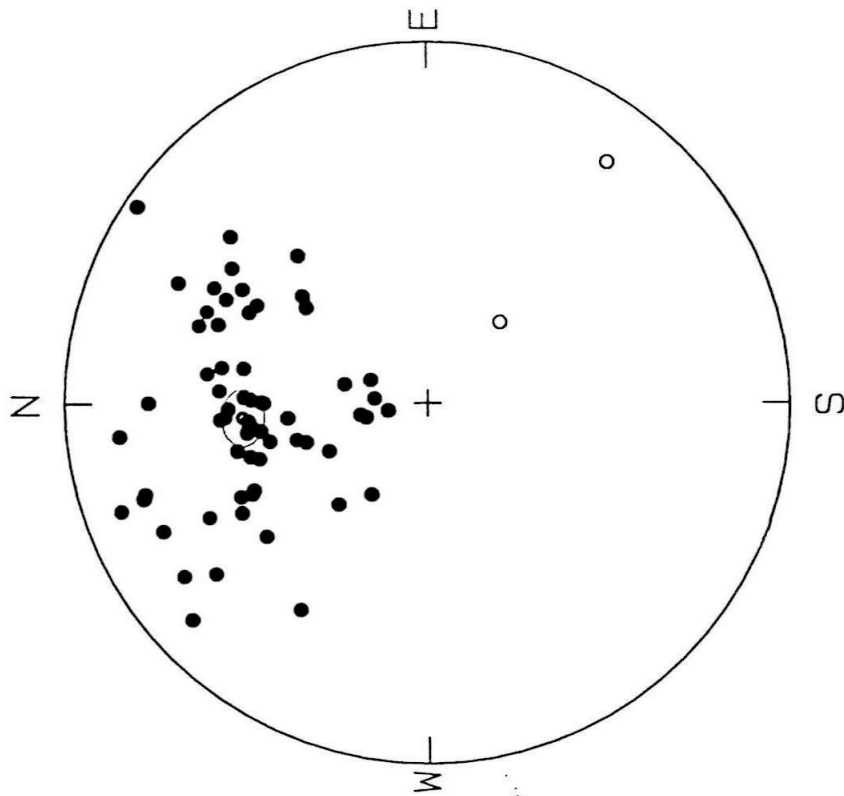
Geographic

from our samples are probably primary directions.

All these directions then were used to obtain an average direction for rocks of the Mill Creek Formation. Results of both Fisher and Bingham statistics are given in Table 1 and the Bingham oval of 95% confidence is shown on Figure 6. Because of small structural correction due to the shallow dip of the Mill Creek beds, the mean directions of the formation before and after tilt-correction of bedding are similar. As the mean declination of the Mill Creek Formation is  $355.3^\circ \pm 5.7^\circ$  (at the 95% confidence level), which does not differ significantly from the expected reference direction of North America ( $1.9^\circ \pm 3^\circ$ , Irving and Irving, 1982). I conclude that little or no rotation has occurred in the rocks of the Mill Creek Formation.

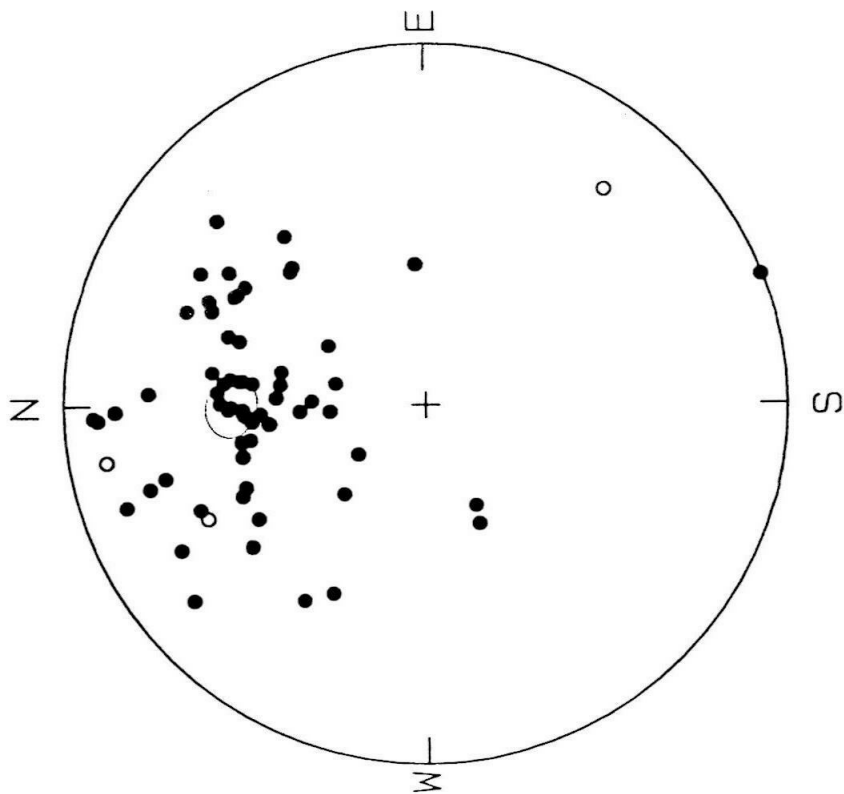
**Figure 6. Mean direction of the Mill Creek Formation.**

Averaged on all cleaned samples of the Mill Creek Formation using the Fisher (1953) and Bingham (1974) statistics. Plotting convention is the same as Figure 5.



MILL CREEK FORMATION

Tilt Corrected



MILL CREEK FORMATION

Geographic



## IMPLICATIONS

Although the sampled section is too short to conduct a magnetostratigraphic study of the formation, results of the Mill Creek Formation favor the speculation of Matti et al. (1985) and Weldon (personal communication, 1987, 1990) that the Mill Creek sediments were deposited in the same basin as the Punchbowl Formation at Devil's Punchbowl. The main argument for this suggestion is that the Mill Creek samples have mainly normal polarity, which may fit in one of the short normal magnetozones of the Punchbowl magnetostratigraphy (Liu et al., in preparation, this thesis, chapter 3). Unfortunately, the rocks on the north side of the Wilson Creek fault are not suitable for paleomagnetic study. Whether they were deposited in the same basin as rocks across the fault thus cannot be answered by this study.

Large crustal block rotations have been found usually in places associated with strike-slip faulting, so it is believed generally that large lateral displacements would be accompanied by rotations of the rigid blocks in-between the bounding faults. However, the Mill Creek Formation, which is between two strike-slip faults, does not show any significant tectonic rotation. If this result is correct, it suggests that blocks bounded by strike-slip faults may not necessarily rotate under the shear stress as suggested by the above models. The Mill Creek basin has an elongate shape outlined by the strands of the San Andreas fault and its long axis is parallel to the strike the San Andreas fault, i. e., it is parallel to the direction of the major lateral shear stress. Hence, it will not rotate under this shear.

In addition, the formation is at the southern front of the San Bernardino Mountains. The Crowder Formation at the western front of the same mountains (block) has not shown any significant rotations (Weldon et al., 1985; Weldon, 1986; Winston, 1985;

this thesis, chapter 2), the age of which may at least partially overlap with that of the Mill Creek Formation. This consistency appears to support the speculation that the San Bernardino Mountains and adjacent part of the Mojave block may not have been rotated since Miocene time. Also, if my interpretation for non-rotation of the Mill Creek block is correct, it implies that the San Andreas fault itself has not been rotated since late Miocene time.

### ACKNOWLEDGEMENTS

I am grateful to Ray Weldon who introduced this problem to me, and to Joe Kirschvink, both of whom provided help in both sampling and discussions. Peter Sadler's introduction of the geologic background of the Mill Creek area and his help with sampling were also appreciated. This study was supported by NSF grant EAR83-51370, by the Chevron Oil Field Research Company, by the Arco Foundation, and by equipment grants from the W. M. Keck and James Irving Foundations.

### REFERENCES

- Beck, M.E., Jr., 1976. Discordant paleomagnetic pole positions as evidence of regional shear in the western Cordillera of North America, *Am. J. Sci.*, v. 276, p. 694 - 712.
- Bingham, C., 1974. An antipodally symmetric distribution on the sphere: *Ann. Stat.*, v. 2, p. 1201 - 1225.
- Garfunkel, Z., 1974. Model for the late Cenozoic tectonic history of the Mojave Desert,

California, and its relation to adjacent regions: Geological Society of America Bulletin, v. 85, p. 1931 -1944.

Gibson, R.C., 1971. Non-marine turbidites and the San Andreas fault, San Bernardino Mountains, California: in W.A. Elders, ed., Geological excursions in southern California, Campus Museum Contributions number 1, Riverside, California, University of California, p. 167 - 181.

Fisher, R.A., 1953. Dispersion on a sphere: Proc. R. Soc. London Ser. A217, p. 295 - 305.

Irving, E., and Irving, G.A., 1982. Apparent polar wander paths carboniferous through Cenozoic and the assembly of Gondwana: Geophysical Surveys, v. 5, p. 141 - 188.

Kirschvink, J.L., 1980. The least-squares line and plane and the analysis of the paleomagnetic data: examples from Siberia and Morocco. Geophysical Journal of the Royal Astronomical Society, v. 62, p. 699-718.

Luyendyk, B.P., Kamerling, M.J., and Terres, R.R., 1980. Geometric models for Neogene crustal rotations in southern California. Geol. Soc. Amer. Bull., v. 91, p. 211-217.

Luyendyk, B.P., Kamerling, M.J., Terres R.R., and Hornafius, J.S., 1985. Simple shear of southern California during Neogene time suggested by paleomagnetic declinations. Jour. Geophys. Res., v.90, p. 12,454-12,466.

Matti, J.C., Morton, D.M., and Cox, B.F., 1985. Distribution and geological relations of fault systems in the vicinity of the central Transverse Ranges, southern California. U.S. Geol. Surv. Open File Report. 85-365, 37 p.

McElhinny, M.W., 1964. Statistical significance of the fold test in paleomagnetism. Geophys. J. R. Astr. Soc. v. 8, p. 338 - 340.

- McKenzie, D.P., and Jackson, J.A., 1983. The relationship between strain rates, crustal thickening, paleomagnetism, finite strain, and fault movement within a deforming zone: *Earth and Planet. Sci. Lett.*, v. 65, p. 184 - 202.
- Nur, A., Ron, H., and Scotti, O., 1986. Fault mechanics and the kinematics of block rotations. *Geology*, v. 14, p. 746 - 749.
- Owens, G.V., 1959. Sedimentary rocks of lower Mill Creek, San Bernardino Mountains, California: M. S. thesis, Claremont graduate school, 50 p.
- Sadler, P.M., and Demirer, A., 1986. Pelona schist clasts in the Cenozoic of the San Bernardino Mountains, southern California: in P. Ehlig, ed., *Neotectonics and faulting in southern California: Geological Society of America Cordilleran Section Meeting Guidebook*, Los Angeles, California, p. 129 -146.
- Weldon, R.J., Winston, D.S., Kirschvink, J.L., and Burbank, D.W., 1985. Magnetic stratigraphy of the Crowder Formation, Cajon Pass, so. California. *Abstracts with Programs, 97th Annual Meeting, Geol. Soc. Amer.*, Vol. 16, p. 689.
- Weldon, R.J., II, 1986. The late Cenozoic geology of Cajon Pass: Implications for tectonics and sedimentation along the San Andreas fault, Ph.D. thesis, California Institute of Technology, Pasadena, California. 400 p.
- Winston, D.S., 1985. Magnetic stratigraphy of the Crowder Formation, southern California, M. S. thesis, University of Southern California, Los Angeles, California, 100 p.

CHAPTER FIVE

**SUMMARY**

## Chapter 5

### Introduction

The Transverse Ranges and the bend in the San Andreas fault have long been a puzzle to geologists. This study provides some revisions and new constraints in the interpretation of the geological history of this area by improving age control on the Miocene sedimentary units and by measuring the magnitude of tectonic rotations in them. Most of the results and interpretations of my study have been presented in the last three chapters; this chapter thus serves to summarize the implications of my results in the general tectonic framework of the area. In particular, tectonic rotations in different senses and at different tectonic settings were combined in an attempt to better understand the tectonics and kinematics of crustal blocks and the relationship between them and their bounding faults.

### Magnetostratigraphy and its tectonic implications

As early as 1926 Noble proposed a correlation of Tertiary rocks in Cajon Pass with those in the Devil's Punchbowl, suggesting 10's of kilometers of right-lateral slip on the San Andreas fault. In the 1930's, Noble withdrew this suggestion due to intense criticism. As truly large scale slip (100's of kilometers) on the San Andreas fault was documented (beginning with Hill and Dibblee, 1953), this correlation was ignored, though not specifically disproved. Woodburne and Golz (1972) specifically addressed this correlation and based on age and lithology suggested that the correlation was invalid. However, they allowed that these two formations might have been deposited in

a large, continuous basin close to their present position based on their general similarity, and particularly, on the possibility of their overlap in age. This suggestion implied that a large offset along the San Andreas fault was not possible. While virtually no one believes these rocks correlate, uncertainties in their total age range remain and their age ranges provide critical insights into the timing of a number of faults in the San Andreas system. For this reason, and to determine tectonic rotations (discussed below), magnetostratigraphies of these critical units were established.

The magnetostratigraphy, presented in chapters 2 and 3 and summarized in Figure 14 of chapter 3 of this thesis, demonstrates that the "Cajon Facies" of Noble (1954) and the type Punchbowl span different time periods. Combined with the estimated age of fossils, the magnetostratigraphy of both formations can be unambiguously matched to the geomagnetic reversal time scale (Harland et al., 1982) (Figure 14 of chapter 3). The "Cajon Facies," here called the Cajon Formation, spans the period of time from at least 17 Ma to 12.7 Ma, whereas the type Punchbowl Formation has an age ranging from 12.5 Ma to 8.5 Ma. Also, the magnetic polarity patterns of the uppermost Cajon and the lowest Punchbowl are obviously different. Therefore, it can be concluded that these two formations do not overlap in age. Consequently, the 40 kilometer distance between the two formations might not be an indication of the offset along the San Andreas fault.

In conjunction with the magnetostratigraphy of another late Miocene sedimentary rock unit in Cajon Valley, the Crowder Formation (Weldon 1984, 1986; Winston 1985), the new age constraints on the Cajon Formation also yield some important implications for the structural and tectonic history of the Cajon Pass area. The Crowder magnetostratigraphy suggests that it was deposited in a distinctly different basin from that of the Cajon Formation in a period ranging from 17 Ma to 9.5 Ma

(Weldon, 1984; Winston, 1985; this thesis, chapter 2). Although deposition of the two formations might begin at roughly the same time (ca. 17 Ma), their youngest preserved sediments differ in age by about 4 Ma. Tectonic rotations in these two formations are also obviously different, with the Cajon having been rotated clockwise about 24° compared with zero for the Crowder. This also argues that the two formations were deposited in different basins, which have since undergone different tectonic processes. Considering the large size of the original basins where the two formations were deposited, my results also support the speculation that the Squaw Peak fault, which separates the two formations, must have large displacement at least on the order of tens of kilometers. In addition, the active periods of the Squaw Peak and Cajon Valley faults constrained by the Cajon, Crowder, and the Phelan (Weldon, 1984, 1986) formations are similar to that of the Liebre Mountain and San Gabriel faults, respectively. This supports the correlation between these faults, which suggests 150 kilometers of offset on the San Andreas fault since Pliocene time (Matti, 1985; Weldon, 1986; Weldon et al., 1990).

The age of the type Punchbowl Formation at Devil's Punchbowl has been constrained by my study as from 12.5 to 8.5 Ma (this thesis, chapter 3). It also provides a time constraint on the activity of the Punchbowl fault, which is an early strand of the San Andreas fault system (Ehlig, 1968; 1975; Weldon et al., 1990). As the basal breccia unit of the Punchbowl Formation forms an 11 km long, fault-sliced strip along the Punchbowl fault, and its extremely variable clast assemblage was derived from underlying slivers of different rocks in the fault zone, the fault probably formed "immediately before or during the deposition of the breccia" and also after the deposition of the Punchbowl Formation (Weldon et al., 1990). Our magnetostratigraphic section of the Punchbowl Formation started at the base of the breccia unit (this thesis,



chapter 3). Hence our results imply that the Punchbowl fault was active at least by about 12.5 million years ago and reactivated after 8.5 Ma.

### Tectonic Rotations

During the past decade, large paleodeclination anomalies were found in many places along the San Andreas fault system and other areas of strike-slip faulting, and various kinematic models have been invoked to explain them [e. g., Garfunkel (1974), Beck (1976), Luyendyk et al. (1980, 1985), and McKenzie and Jackson (1983)]. Most of these models relate azimuthal rotations to rigid crustal blocks bounded by secondary strike-slip faults which rotate together in response to lateral shear stress within major shear zones (Garfunkel, 1974; Beck, 1976; Ron et al., 1984; McKenzie and Jackson, 1983). Beck (1976) proposed a "ball-bearing" model in which discrete blocks between a set of parallel strike-slip faults rotate under a simple shear couple while the major bounding faults do not rotate. In this model, there must be gaps or circular bounding faults to accommodate the differential movements between the blocks, which are rarely observed in the field. Hence, this model has not been accepted by most people.

Many other geoscientists (Freund, 1974; Garfunkel 1974; Luyendyk and others, 1980, 1985; Ron et al., 1984; and McKenzie and Jackson, 1983) proposed generally similar "block rotation" models. In this type of proposed mechanism, the rigid, parallel blocks rotate, while maintaining the straight fault contacts between blocks, in response to lateral shear couple. Secondary bounding faults that are rotating with the blocks are necessary for accommodating rotations by strike-slip displacement along them. The model of Garfunkel (1974) and Ron et al. (1984) is slightly different, in which blocks rotate in order to maintain the close fault contact while these faults are slipping along

their strikes.

The Punchbowl, Cajon, Crowder, and Mill Creek formations included in this study are all bounded by large strike-slip faults, providing excellent tectonic sites for testing those various models and for better understanding these phenomena. These three blocks are either next to or within the modern San Andreas fault zone (Figure 1 of chapter 2, this thesis). Therefore, they are all under the influence of relative movement of the Pacific and North American plates (i. e., within the right-lateral shear zone). Our results, however, do not agree with the prediction of Luyendyk et al. (1980, 1985): the Punchbowl block shows about 28° counterclockwise rotation whereas the Crowder and Mill Creek formations appear to have little or no significant rotations. Only the Cajon block bounded by the Squaw Peak, Cajon Valley, and the San Andreas faults displays about 24 degree clockwise rotation. Although the rotation of the Cajon block might be explained partially by the model of Luyendyk et al. (1980, 1985) (see chapter 2 for details), these results generally do not support their models. Furthermore, if we assume that the lack of rotation in the Crowder and Mill Creek formations reflects that of the entire San Bernardino Mountains and adjacent part of the Mojave block, the prediction and model of Luyendyk et al. (1980, 1985) would not be valid for this area.

I have also tried to use other rotation models to explain our results but none of them fits our data and/or regional geologic data. Wells and Hillhouse (1989) and Ross et al. (1989) proposed that detachment faulting is an appropriate mechanism for rotations found in the Mojave Desert. Upper-plate tilt-blocks above the detachment fault were found to be rotated both clock- and counterclockwise, during gliding on local, low-angle faults above the detachment (Wells and Hillhouse, 1989). The sense of the rotation depends on the strike or geometry of the norm faults. Our results also

suggest that rotations may not always be related to the strike-slip (bounding) faults. Instead, thrust faulting can provide the appropriate mechanism for tectonic rotation. The rotations of the Cajon Formation can be explained best by uneven compression, caused by thrusting of the Squaw Peak system, exerted on the edge of the upper-plate blocks. This results in a local dextral shear that rotates the block clockwise (see discussion of chapter 2 for detail).

In the case of the Punchbowl Formation, the counterclockwise rotation is most likely due to the San Gabriel block rotating through the preexisting restraining geometry of the San Andreas fault in the central Transverse Ranges (Weldon and Humphreys, 1986; Terres and Luyendyk, 1985; this thesis, chapter 3). This result also supports the theory of Weldon and others that the Mojave block has acted as a "backstop" for the rotating San Gabriel block, and implies that the bend of the San Andreas fault has existed since the fault was formed.

Only the non-rotation of the Mill Creek Formation may be interpreted by the block rotation model. Nelson and Jones (1987) summarized several possible mechanisms of rotations in a shear zone. When the shearing occurs along the bounding faults parallel to the main shear zone, blocks between the bounding faults will not rotate at all. The Mill Creek result suggests that this is the case.

In summary, fault-bounded blocks within a lateral shear zone may not always rotate as suggested by those "block rotation" models. Sometimes, thrust and detachment faulting can be the mechanism for rotation of blocks bounded by faults. In addition, the geometry of the major fault along which rigid blocks are moving is responsible for the rotation, as is the case for the Punchbowl Formation. The geometry of normal and reverse faults in detachment and thrust faulting are also critical to produce the rotation and to determine the sense of the rotation (Wells and Hillhouse, 1989, Liu et al., in

preparation, this thesis, chapter 2). Our data also suggest that the San Bernardino Mountains and adjacent parts of the Mojave Desert have not rotated since the late Miocene, and the modern San Andreas fault has had its anomalous geometry probably since it formed 5 million years ago.

## REFERENCES

- Beck, M.E. Jr., 1976. Discordant paleomagnetic pole positions as evidence of regional shear in the western Cordillera of North America, *Am. J. Sci.*, v. 276, p. 694 - 712.
- Ehlig, P.L., 1968. Causes of distribution of Pelona, Rand, and Orocochia schists. *Proceedings of Conference on Geologic Problems of San Andreas fault system*; Stanford University, p. 294 - 306.
- Ehlig, P.L., 1975. Basement rocks of the San Gabriel Mountains, south of the San Andreas fault, southern California: in Crowell, J.C., ed., *San Andreas fault in southern California*, California Division of Mines and Geology, special report 118, p. 177 -186.
- Freund, R., 1974. Kinematics of transform and transcurrent faults: *Tectonophysics*, v. 21, p. 93 - 134.
- Garfunkel, Z., 1974. Model for the late Cenozoic tectonic history of the Mojave Desert, California, and its relation to adjacent regions: *Geological Society of American Bulletin*, v. 85, p. 1931 -1944.
- Garfunkel, Z., and Ron, H., 1985. Block rotation and deformation by strike-slip faults 2. the properties of a type of microscopic discontinuous deformation: *J. G. R.*,

v. 90, p. 8589 - 8602.

- Harland, W.B., Cox, A.V., Llewellyn, P.G., Pickton, C.A.G., Smith, A.G., and Walters, R., 1982. A Geological Time Scale. Cambridge Univ. Press, London/New York.
- Luyendyk, B.P., Kamerling, M.J., and Terres, R.R., 1980. Geometric models for Neogene crustal rotations in southern California. *Geol. Soc. Amer. Bull.*, v. 91, p. 211-217.
- Luyendyk, B.P., Kamerling, M.J., Terres R.R., and Hornafius, J.S., 1985. Simple shear of southern California during Neogene time suggested by paleomagnetic declinations. *Jour. Geophys. Res.*, v.90, p. 12,454-12,466.
- Matti, J.C., Morton, D.M., and Cox, B.F., 1985. Distribution and geological relations of fault systems in the vicinity of the central Transverse Ranges, southern California. U.S. Geol. Surv. Open File Report. 85-365, 37 p.
- McKenzie, D.P., and Jackson, J.A., 1983. The relationship between strain rates, crustal thickening, paleomagnetism, finite strain, and fault movement within a deforming zone: *Earth and Planet. Sci. Lett.*, v. 65, p. 184 - 202.
- Nelson, M.R., and Jones, C.H., 1987. Paleomagnetism and crustal rotations along a shear zone, Las Vegas Range, southern Nevada: *Tectonics*, v. 6, p. 13 -33.
- Noble, L.F., 1926. The San Andreas rift and some other active faults in the desert region of southeastern California. Carnegie Institute of Washington, Yearbook no. 25, p. 415-422.
- Noble, L.F., 1954 (a). Geology of the Valyermo Quadrangle and vicinity, California. U.S. Geological Survey Quadrangle Map Series, Washington D.C.
- Nur, A., Ron, H., and Scotti, O., 1986. Fault mechanics and the kinematics of block rotations. *Geology*, v. 14, p. 746 - 749.
- Ron, H., Freund, R., and Garfunkel, Z., 1984. Block rotation by strike-slip faulting:

Structural and paleomagnetic evidence, *J. G. R.*, v. 89, p. 6256 -6270.

Ross, T.M., Luyendyk, B.P., and Naston, R.B., 1988. Paleomagnetic evidence for Neogene clockwise tectonic rotations in the central Mojave Desert, California.

*Geology*, v. 17, p. 470 - 473.

Terres, R.R., and Luyendyk, B.P., 1985. Neogene tectonic rotation of the San Gabriel region, California, suggested by paleomagnetic vectors. *Journal of Geophysical Research*,

v. 90, p. 2467 - 2484.

Weldon, R.J., II, 1984. Implications of the age and distribution of the late Cenozoic stratigraphy in Cajon Pass, southern California: in *San Andreas fault -- Cajon Pass to Wrightwood*, Hester, R.L., and Hallinger, D.E., eds., *Pacific Sect., AAPG, Volume and Guidebook*, 55, p. 9-15.

Weldon, R.J., 1986. The late Cenozoic geology of Cajon Pass: Implications for tectonics and sedimentation along the San Andreas fault, Ph.D. thesis, California Institute of Technology, Pasadena, California. 400 p.

Weldon, R.J., 1986. The late Cenozoic geology of Cajon Pass: Implications for tectonics and sedimentation along the San Andreas fault, Ph.D. thesis, California Institute of Technology, Pasadena, California. 400 p.

Weldon, R.J., and Humphreys, E., 1986. A kinematic model of southern California.

*Tectonics*, v. 5, p. 33 - 48.

Weldon R.J., Meisling, K.E., and Alexander, J., 1990. A speculative history of the San

Andreas fault system in the central Transverse Ranges. In Powell, R.E., and Weldon, R.J., eds., *Palinspastic reconstruction of the San Andreas fault zone*,

*Geological Society of America Special Paper* (in press).

Wells, R.E., and Hillhouse, J.W., 1989. Paleomagnetism and tectonic rotation of the Lower Miocene Peach Springs Tuff: Colorado Plateau, Arizona, to Barstow,

California. *Geological Society of America Bulletin*, v. 101, p. 846 - 863.

Winston, D.S., 1985. Magnetic stratigraphy of the Crowder Formation, southern California, M.S. thesis, University of Southern California, Los Angeles,

California, 100 p.

Woodburne, M.O., and Golz, D., 1972. Stratigraphy of the Punchbowl Formation, Cajon Valley, southern California. University of California Publications in Geological Sciences, Vol. 92, 73 p.

Woodburne, M.O., 1975. Late Tertiary nonmarine rocks, Devil's Punchbowl and Cajon Valley, southern California: in Crowell, J.C., ed., San Andreas fault in southern California, California Division of Mines and Geology, special report 118, p. 187 - 196.